UNIVERSIDAD NACIONAL AUTÓNOMA DE MÉXICO

POSGRADO EN CIENCIAS BIOLÓGICAS

INSTITUTO DE GEOLOGÍA

REVISIÓN TAXONÓMICA DE LOS PECES FÓSILES DEL SUBORDEN ENCHODONTOIDEI DE MÉXICO Y SUS IMPLICACIONES EN LA SISTEMÁTICA, BIOGEOGRAFÍA Y EVOLUCIÓN DEL GRUPO

TESIS

QUE PARA OPTAR POR EL GRADO DE

DOCTOR EN CIENCIAS

PRESENTA:

JESÚS ALBERTO DÍAZ CRUZ

TUTOR PRINCIPAL: DR. JESÚS ALVARADO ORTEGA
INSTITUTO DE GEOLOGÍA, UNAM.
COMITÉ TUTOR: DRA. MARISOL MONTELLANO BALLESTEROS
INSTITUTO DE GEOLOGÍA, UNAM.
COMITÉ TUTOR: DR. VÍCTOR HUGO REYNOSO ROSALES
INSTITUTO DE BIOLOGÍA, UNAM.

CIUDAD UNIVERSITARIA, CD. MX., FEBRERO, 2022

UNIVERSIDAD NACIONAL AUTÓNOMA DE MÉXICO

POSGRADO EN CIENCIAS BIOLÓGICAS

INSTITUTO DE GEOLOGÍA

REVISIÓN TAXONÓMICA DE LOS PECES FÓSILES DEL SUBORDEN ENCHODONTOIDEI DE MÉXICO Y SUS IMPLICACIONES EN LA SISTEMÁTICA, BIOGEOGRAFÍA Y EVOLUCIÓN DEL GRUPO

TESIS

QUE PARA OPTAR POR EL GRADO DE

DOCTOR EN CIENCIAS

PRESENTA:

JESÚS ALBERTO DÍAZ CRUZ

TUTOR PRINCIPAL: DR. JESÚS ALVARADO ORTEGA
INSTITUTO DE GEOLOGÍA, UNAM.
COMITÉ TUTOR: DRA. MARISOL MONTELLANO BALLESTEROS
INSTITUTO DE GEOLOGÍA, UNAM.
COMITÉ TUTOR: DR. VÍCTOR HUGO REYNOSO ROSALES
INSTITUTO DE BIOLOGÍA, UNAM.

MÉXICO, CD. MX. FEBRERO, 2022

COORDINACIÓN DEL POSGRADO EN CIENCIAS BIOLÓGICAS

ENTIDAD INSTITUTO DE GEOLOGÍA

OFICIO CPCB/049/2022

ASUNTO: Oficio de Jurado

M. en C. Ivonne Ramírez Wence
Directora General de Administración Escolar, UNAM
P r e s e n t e

Me permito informar a usted que en la reunión ordinaria del Subcomité de Biología Evolutiva, Ecología, Manejo Integral de Ecosistemas y Sistemática del Posgrado en Ciencias Biológicas, celebrada el día **22 de noviembre de 2021** se aprobó el siguiente jurado para el examen de grado de **DOCTOR EN CIENCIAS** del estudiante **DÍAZ CRUZ JESÚS ALBERTO** con número de cuenta **517025891** con la tesis titulada **"REVISIÓN TAXONÓMICA DE LOS PECES FÓSILES DEL SUBORDEN ENCHODONTOIDEI DE MÉXICO Y SUS IMPLICACIONES EN LA SISTEMÁTICA, BIOGEOGRAFÍA Y EVOLUCIÓN DEL GRUPO",** realizada bajo la dirección del **DR. JESÚS ALVARADO ORTEGA**, quedando integrado de la siguiente manera:

Presidente:	DRA. HELGA OCHOTERENA BOOTH
Vocal:	DR. FRANCISCO SOUR TOVAR
Vocal:	DRA. KATIA ADRIANA GONZÁLEZ RODRÍGUEZ
Vocal:	DR. KLEYTON MAGNO CANTALICE SEVERIANO
Secretario:	DR. VÍCTOR HUGO REYNOSO ROSALES

Sin otro particular, me es grato enviarle un cordial saludo.

A T E N T A M E N T E
"POR MI RAZA HABLARÁ EL ESPÍRITU"
Ciudad Universitaria, Cd. Mx., a 17 de enero de 2022

COORDINADOR DEL PROGRAMA

POSGRADO EN CIENCIAS BIOLOGICAS
COORDINACIÓN

DR. ADOLFO GERARDO NAVARRO SIGÜENZA

AGRADECIMIENTOS INSTITUCIONALES

Al Posgrado en Ciencias Biológicas de la Universidad Nacional Autónoma de México (UNAM), por permitirme realizar mis estudios doctorales en su plan académico y por todo el apoyo académico y administrativo que se me fue otorgado hasta la conclusión de la presente tesis.

A los programas institucionales que brindaron apoyo para desarrollar mis actividades académicas. Al Consejo Nacional de Ciencia y Tecnología (CONACYT) por otorgarme la beca para estudios de Posgrado número 632640. Así como a la UNAM a través de su Programa de Apoyo a los Estudios de Posgrado (PAEP) y al Programa de Apoyo a Proyectos de Investigación e Innovación Tecnológica (PAPIIT) de la UNAM DGAPA-PAPIIT IN110920 a través del proyecto IN110920.

A los miembros de mi comité tutor: Dra. Marisol Montellano Ballesteros, Dr. Víctor Hugo Reynoso Rosales y Dr. Jesús Alvarado Ortega, cuyos comentarios, observaciones y sugerencias contribuyeron enormemente al desarrollo de este trabajo y a mi formación profesional.

AGRADECIMIENTOS A TÍTULO PERSONAL

Al Dr. Manuel Javier Avendaño Gil quien gracias a su práctica docente y dedicación me introdujo al maravilloso mundo de la paleontología.

Al equipo del Museo de Paleontología Eliseo Palacios Aguilera, quienes siempre fueron receptivos y me apoyaron durante mis primeros pasos como paleontólogo. Especialmente al Biol. Marco Antonio, al Dr. Gerardo Carbot, al M. en C. Luis Enrique y al M. en C. Bruno Andrés.

Agradezco profundamente a mi tutor de tesis, el Dr. Jesús Alvarado Ortega, por su paciencia, amistad y apoyo incondicional durante todos estos años de mi formación. Ha sido un camino largo desde la licenciatura hasta esta instancia, pero sin duda de mucho crecimiento personal y profesional.

A la Dra. Katya González, a la Dra. Helga Ochoterena, y al Dr. Francisco Sour Tovar, quienes se sumaron a este proyecto como sinodales y cuyas acertadas observaciones contribuyeron a mejorar una versión previa de este trabajo.

A Gerardo Álvarez y al Dr. Kleyton Cantalice, este último además de fungir como sinodal, brindaron apoyo y asesoramiento durante la preparación de material y toma de fotografías de algunos de los especímenes estudiados en la presente tesis.

A mis amigos del “Cubo”, Eli, Kathia y especialmente a David, Jair y Lalín, con quienes desarrollé un vínculo especial que traspasó los límites académicos.

A mis amigos de toda la vida: Cuauhtémoc, Jorge Enrique y Luis Carlos. Gracias por ser incondicionales y por apoyarme en etapas críticas de mi vida y crecimiento profesional.

A mi familia. A tía Chusita, a tía Nenita y tía Lupita, a mi tío Abraham y a mi papá, Beto. Gracias por apoyar esta inquietud mía por estudiar. Sin ustedes difícilmente habría conseguido llegar hasta aquí.

En memoria de:

Víctor Hugo López Bautista

(1989-2021)

Amigo y hermano

ÍNDICE

RESUMEN

El suborden Enchodontoidei es un grupo extinto de peces teleósteos del Cretácico Tardío—Paleoceno que habitaron los mares tropicales y subtropicales presentes en las regiones epicontinentales alrededor del mundo. Aunque este grupo es morfológicamente muy diverso, sus miembros se caracterizan por presentar cuerpos casi desnudos, pero con una serie de escudos dorsales, ubicados entre la cabeza y la base de la aleta dorsal, y un par de series de escamas laterales extendidas a lo largo del cuerpo recubriendo la línea lateral. Restos bien conservados de peces encodontoides han sido recientemente recuperados de numerosos afloramientos de diferentes edades del Cretácico de México, cubriendo la totalidad de las edades del Cretácico Superior, con excepción del Santoniano. En esta investigación se abordó el estudio sistemático de estos peces fósiles, se determinó su identidad taxonómica a nivel específico y se realizaron los análisis filogenéticos respectivos. Previo al presente trabajo, el registro de estos peces en México era escaso e incluía principalmente fósiles fragmentados e incompletos que difícilmente podían ser determinados. El estudio formal de los encodontoides recuperados en diversos afloramientos mexicanos revela una riqueza y diversidad sobresalientes para el extremo occidental del mar de Tetis. Como resultado de este trabajo se nombraron cuatro nuevos taxones: dos nuevos géneros y especies pertenecientes a Enchodontidae, *Vegrandichthys coitecus* y *Veridagon avendanoi*; y dos nuevas especies de Dercetidae, una nueva especie del género *Hastichthys, H. totonacus* así como una nueva especie del género *Apuliadercetis*, *A. gonzalezae*. Además, se evaluó el ajuste estratigráfico de la hipótesis filogenética de Enchodontidae y se exploraron las relaciones existentes entre configuraciones morfométricas de algunas de las estructuras osteológicas más variables en este grupo. La diversidad genérica de encodóntidos en los yacimientos del Cenomaniano temprano del sitio El Chango, en Chiapas es equiparable e incluso mayor a la diversidad observada en localidades de otras latitudes que han sido explotadas por décadas y que poseen una larga historia de estudios paleontológicos. La presencia de tres taxa de Enchodontidae exclusivos en la localidad paleontológica de El Chango, *Unicachichthys*, *Vegrandichthys* y *Veridagon*, hacen de este sitio el de mayor grado de endemismo a nivel genérico. Por otra parte, el estudio de los dercétidos mexicanos revela la presencia del género *Hastichthys* en los

sedimentos Turonianos de la cantera Huehuetla, Puebla y se concluye que *Rhynchodercetis regio,* previamente descrito de los estratos Turonianos de la cantera Vallecillo, Nuevo León, es parte de este género y es renombrado como *H. regio*. Asimismo, se reconoció la presencia de la primera especie americana de *Apuliadercetis* en estratos Campanianos de Ochuxhob, Tzimol, Chiapas. Adicionalmente, los resultados de este trabajo señalan que, la longitud corporal en Enchodontidae, incluidas las especies de otras latitudes, se ajusta a la ley de Cope o de incremento filético del tamaño corporal. El estudio preciso de los demás encodontoides mexicanos rebasan el esfuerzo y los alcances temporales de esta tesis; sin embargo, es claro que, México es poseedor de la mayor diversidad de estos peces en todo el continente americano. La evaluación del ajuste estratigráfico de sus filogenias y la peculiar variación morfológica identificada en los taxa mexicanos, sumada a la poca robustez de las hipótesis filogenéticas y a las hipótesis de homología primaria identificadas como redundantes, hacen necesario que estas últimas sean reevaluadas para las futuras reconstrucciones de las relaciones evolutivas de Enchodontoidei. Aunque algunas de esas hipótesis se han reinterpretado, un trabajo más detallado es requerido, sobre todo, considerando que hoy en día se poseen especímenes preparados, muy bien preservados, y considerados como potenciales taxones nuevos. En este contexto, el uso complementario de criterios de optimalidad como Inferencia Bayesiana o Máxima Parsimonia de Pesos Implicados para las reconstrucciones filogenéticas han ratificado la naturalidad de Enchodontidae, así como expuesto la poca robustez de la hipótesis filogenética de Enchodontoidei. Las evaluaciones de ajuste estratigráfico y morfometría geométrica rectifican y corroboran de manera estadística y objetiva aseveraciones evolutivas previamente sugeridas para Enchodontidae. Considerando la posición filogenética basal y la edad de los estratos donde fueron recuperados los encodóntidos de El Chango, Chiapas, se sugiere que el grupo pudo haber surgido en el extremo occidental del Tethys y a partir de esta región, migrar y especiar en otras latitudes. Para alcanzar esta distribución geográfica, la persistencia del corredor Hispánico hasta el Cretácico tardío parece haber sido crítica al permitir el intercambio paleoictiofaunístico entre los diferentes dominios del mar de Tethys. Los resultados de este trabajo revelan que el territorio mexicano desempeñó un papel preponderante para el hábitat, desarrollo y especiación de los encodontoides.

ABSTRACT

The suborder Enchodontoidei is an extinct group of Late Cretaceous—Paleocene teleost fish that inhabited the tropical and subtropical seas of epicontinental regions around the world. Although this group is morphologically diverse, its members are well characterized by almost naked bodies, but with a series of dorsal scutes between the occiput and the base of the dorsal fin, plus a pair of series of flank scales extended along the body protecting the lateral line. Recently, well-preserved remains of enchodontoids have been recovered from numerous Mexican Cretaceous deposits of different ages, except for the Santonian. In this research, the systematic study of these fossils was addressed, their taxonomic specific identities were determined, and the respective phylogenetic analyses were carried out. Prior to the present work, the Mexican record of these fishes was scarce and included mainly fragmented and incomplete fossils that could hardly be determined. The Mexican assemblage of this suborder reveals an outstanding richness and diversity for the western end of the Tethys Sea. As a result of this work, four new taxa were named: two new genera and species belonging to Enchodontidae, *Vegrandichthys coitecus* and *Veridagon avendanoi* as well as two new species of Dercetidae, a new species of the genus *Hastichthys, H. totonacus*, and a new species of the genus *Apuliadercetis, A. gonzalezae*. In addition, the stratigraphic fit of the phylogenetic hypothesis of Enchodontidae was evaluated and the relationships between morphometric configurations of some of the most variable osteological structures in this group were explored. The generic diversity of the early Cenomanian enchodontids from the El Chango site in Chiapas is comparable and even exceeds that observed in sites of other latitudes exploited and studied for many decades. The presence of three exclusive Enchodontidae taxa from the El Chango, including *Unicachichthys, Vegrandichthys,* and *Veridagon,* make this site, the one with the greatest endemism at the generic level. On the other hand, the study of the Mexican dercetids reveals the presence of the genus *Hastichthys* in the Turonian sediments of the Huehuetla quarry, Puebla and it is concluded that *Rhynchodercetis regio,* previously described from the Turonian strata of the Vallecillo quarry, Nuevo León, is part of this genus and is renamed as *H. regio.* Likewise, the presence of the first American species of *Apuliadercetis*

was recognized in Campanian strata of Ochuxhob, Tzimol, Chiapas. Additionally, the results of this work indicate that the body length in Enchodontidae, including species from other latitudes, obey the Cope's rule or phyletic increase in body size. The precise study of the other Mexican enchodontoids goes beyond the effort and temporal scope of this thesis; however, Mexico has the greatest diversity of these fishes in the entire American continent. The evaluation of the stratigraphic fit of its phylogenies and the peculiar morphological variation identified in the Mexican taxa, added to the lack of robustness of the phylogenetic hypotheses and the primary homology hypotheses identified as redundant, make it necessary for the latter to be reevaluated for future reconstructions of the evolutionary relations of Enchodontoidei. Although some of these hypotheses have been reinterpreted, more detailed work is required, especially considering that today there are prepared specimens, very well preserved, and considered as potential new taxa. In this context, the complementary use of optimality criteria such as Bayesian Inference or Implied-weights Parsimony for phylogenetic reconstructions has ratified the naturalness of Enchodontidae, as well as exposed the lack of robustness of the phylogenetic hypothesis of Enchodontoidei. Evaluations of stratigraphic fit and geometric morphometry statistically and objectively rectify and corroborate evolutionary assertions previously suggested for Enchodontidae. Regarding the basal phylogenetic position and the age of the strata where the enchodontids were recovered from the El Chango, Chiapas, it is suggested that the group may have emerged at the western end of the Tethys and from this region, migrate and speciate in other latitudes. To achieve this geographical distribution, the persistence of the Hispanic corridor until the late Cretaceous seems to have been critical in allowing paleoichthyofaunal exchange between the different domains of the Tethys Sea. The results of this work reveal that the Mexican territory played a preponderant role in the habitat, development, and enchodontoid speciation.

CAPÍTULO I: INTRODUCCIÓN

Generalidades sobre los grupos fósiles de Aulopiformes

Aulopiformes Rosen, 1994, es un grupo de peces comúnmente conocido como "peces lagartos". Actualmente se reconoce que este grupo contiene alrededor de 15 familias y aproximadamente 261 especies recientes; además, los grupos fósiles se incluyen en cinco familias y 21 géneros organizados en Alepisauroidei, Ichthyotringoidei y Halecoidei (Nelson, 2016). Para fines prácticos, en lo que sigue del presente trabajo, los Aulopiformes fósiles serán tratados como Enchodontoidei *sensu* Nelson (1994), bajo el entendido de que este tratamiento no refleja las últimas propuestas en la clasificación del grupo; sin embargo, esta nominación es útil para incluir a todos los Aulopiformes fósiles que actualmente se organizan en Alepisauroidei, Ichthyotringoidei y Halecoidei (consultar siguiente sección).

Enchodontoidei reúne a un grupo de peces fósiles morfológicamente muy diverso, en donde los cambios de longitud del cuerpo y el rostro son evidentes (Figura 1). Por ejemplo, los hay muy chatos como *Paraenchodus* hasta longirostrinos, como aquellos representantes de los géneros *Apateopholis* e *Ichthyotringa*. También existieron encodóntidos de cuerpo extremadamente alargado, como *Dercertis*, y de cuerpos cortos, semiredondos, y casi tan altos como largos, como el caso de *Parenchodus* (Goody, 1969; Raab y Chalifa, 1987). Las tallas de estos peces también fueron muy variadas; algunos sólo alcanzaban longitudes menores a diez centímetros, como en *Eurypholis boissieri*, mientras que otros posiblemente superaron el metro y medio, como el caso de *Cimolichthys nepaholica* (Goody, 1969; Goody, 1970).

Los peces de Enchodontoidei son interpretados como depredadores pelágicos eficientes. Se cree que este grupo teía un nado rápido y activo (*Enchodus* y *Palaeolycus*); pero también hay otros que se consideran depredadores de nado más lento, que pudieron vivir entre elementos arrecifales (*Parenchodus*) (Goody, 1970; Raab y Chalifa, 1987; Maisey, 2000). Se ha sugerido que peces como los *Enchodus* se alimentaban de cefalópodos o moluscos, haciendo uso de sus grandes dientes palatinos (Grandstaff y Parris, 1990). Evidencia directa de depredación en este grupo ha sido reportada para *Prionolepis catapbractus* y *Eurypholis boissieri*, en los que se ha reconocido contenido estomacal conformado de peces (Viohl, 1990). Los peces encodontoides fueron un componente ecológico importante de teleósteos

marinos del Cretácico Tardío (Newbrey y Konishi, 2015) al ser considerados normalmente como depredadores de la cadena alimenticia media (Fielitz, 2004). Sin embargo, otro contenido estomacal señala que estos peces también formaban parte del alimento de otros grupos de animales marinos, incluso de peces de mayor tamaño del mismo grupo (Stewart y Carpenter, 1990; Cavin, 1999), de cefalópodos (Stewart y Carpenter, 1990), mosasaurios (Newbrey y Konishi, 2015), y plesiosaurios (Cicimurri y Everhart, 2001).

Se reconocen a los encodontoides como habitantes de aguas marinas someras. Los reportes de estos peces normalmente provienen de afloramientos marinos depositados en o cerca de plataformas continentales, de ambientes marinos de agua clara y poco profunda, localidades de ambientes próximos a arrecifes o hasta de localidades con depósitos acumulados en lagunas o estuarios que tuvieron influencia ocasional de agua dulce (Forey et al., 2003; Vega et al., 2006; Friedman et al., 2015). Un ejemplo de este tipo de ambientes y con gran extensión geográfica es retratado en el Mar Interior de Norte América (Shimada y Fielitz, 2006).

Algunos de los congéneres actuales de los peces Enchodontoidei no presentan grandes diferencias de hábitat respecto a sus parientes fósiles. Los grupos recientes son encontrados en ambientes marinos o bénticos; en aguas tropicales, subtropicales o templadas, o bien habitando la plataforma continental externa y pendientes continentales superiores (Nelson, 2006). Sin embargo, otros grupos recientes relacionados con los encodontoides son peces que habitan aguas profundas y que exhiben una morfología diversa y peculiar con adaptaciones tales como bioluminiscencia, ojos tubulares o hermafroditismo sincrónico (Davis, 2010).

El rango temporal y de distribución geográfica de los encodontoides es amplio. El registro más antiguo de estos peces se remonta al Hauteriviano-Barremiano en el Cretácico temprano (Kriwet et al*.,* 2006); estos sobrevivieron hasta principios del Eoceno pero alcanzaron su máxima diversidad genérica en el Cenomaniano en el Cretásico Superior (Davis y Fielitz, 2010; Newbrey y Konishi, 2015; Silva y Gallo, 2016). Desde el punto de vista geográfico, los miembros de Enchodontoidei se han reportado prácticamente en todos los continentes, en afloramientos que alguna vez fueron mares epicontinentales (Davis y Fielitz, 2010; Silva y Gallo, 2011).

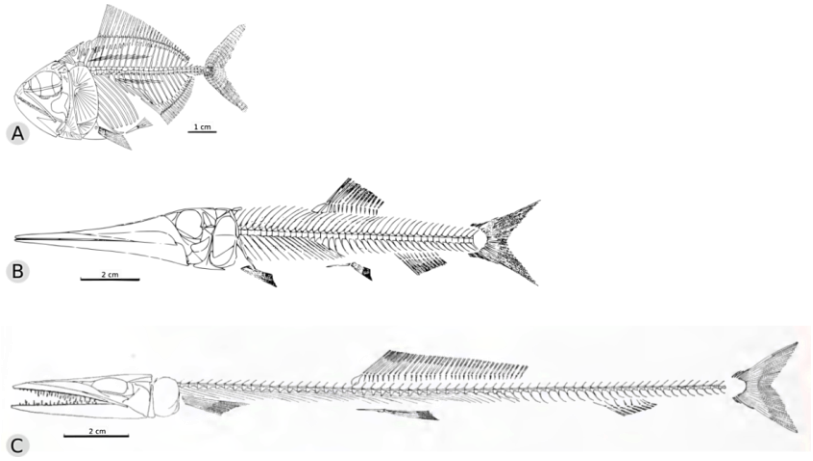

Figura 1. Reconstrucciones esquemáticas de algunos representantes de Enchodontoidei *sensu* Nelson (1994). A. *Parenchodus longipterygius* Raab y Chalifa*,* B. *Apateopholis laniatus* Davis*,* C. *Dercetis triqueter* Pictet*.* Imágenes modificadas de A: Raab y Chalifa (1987); B y C de Goody (1969).

Historia de las clasificaciones de Enchodontoidei

Las relaciones filogenéticas de Enchodontoidei son problemáticas, no solamente por la diversidad creciente de taxa fósiles a ser considerados, sino porque las relaciones entre los representantes fósiles y actuales de este grupo no son claras. El primer intento por agrupar a los encodontoides fue elaborado por Woodward (1901) quien incluyó ocho diferentes géneros en la Familia Enchodontidae, y a su vez, esta familia fue considerada como miembro del Suborden Isospondyli (Figura 2). Según Woodward (1901), Enchodontidae se divide en dos grupos, separados por la presencia o ausencia de un solo diente palatino terminal. Posteriormente, Goody (1969) estudió la relación existente entre varios grupos de peces cretácicos y presentó una hipótesis sobre la posición sistemática de los géneros de la familia Enchodontidae, Dercetidae y Scopelidae. Los miembros de estas familias fueron organizados bajo un contexto evolutivo en diferentes Órdenes, desde los más primitivos (Salmoniformes) a los más derivados (Ctenothrissiformes). Para Goody (1969), el Orden Salmoniformes estaba organizado en cuatro Subórdenes, Cimolichthyoidei, Enchodontoidei, Halecoidei e Ichthyotringoidei (Figura 2). Además, este autor seleccionó aquellos miembros de la Familia Enchodontidae *sensu* Woodward (1901) que poseían solo un diente palatino alargado y los ubicó como miembros del Suborden Enchodontoidei.

Poco tiempo después, Rosen (1973) erigió el Orden Aulopiformes, grupo que diagnosticó por la presencia de un proceso uncinado alargado sobre el segundo epibranquial (Figura 3). Quince familias de peces recientes y un grupo de 17 géneros fósiles fueron incluidos en este Orden. En la propuesta de Rosen (1973), los taxones fósiles considerados previamente por Goody (1969) son separados en dos grupos: el Suborden Alepisauroidei (15 géneros) y la Superfamila Synodontoidea (2 géneros) (ver Figura 2). El Suborden Alepisauroidei *sensu* Rosen (1973) incluye a *Apateodus, Apateopholis, Cimolichthys, Dercetis, Enchodus, Eurypholis, Halec, Hemisaurida, Ichthyotringa, Palaeolycus, Pelargorhynchus, Phylactocephalus*, *Prionolepis, Rhynchodercetis* y *Saurorhamphus*. A pesar del esfuerzo de este último autor, tal agrupación no tuvo un carácter sistemático y se basó solamente en similitudes morfológicas superficiales.

Nelson (1994), siguiendo los trabajos de Rosen (1973), Sulak (1977), Johnson (1982), Okiyama (1984) y Harrel y Stiassny (1986), propuso una clasificación de Aulopiformes en la que el Suborden Alepisauroidei sólo incluía a representantes recientes. Al mismo tiempo, este autor remueve los grupos fósiles que Goody (1969) ubicó en el Orden Salmoniformes, los considera como miembros de Orden Aulopiformes y del Suborden Enchodontoidei donde son agrupados en cuatro Superfamilias (Cimolichthyoidea, Enchodontoidea, Halecoidea e Ichthyotringoidea) (Figura 4).

Por otra parte, las relaciones de parentesco entre Aulopiformes recientes han sido evaluadas en repetidas ocasiones (Sulak, 1977; Johnson, 1982; Okiyama,1984; Patterson y Johnson 1995; Davis, 2010). La filogenia más incluyente del Orden fue elaboraron Baldwin y Johnson (1996) y se basó en análisis cladísticos considerando un amplio rango de datos morfológicos. En este trabajo, la monofilia del Orden Aulopiformes propuesta por Rosen (1973) fue corroborada y además se reconocieron nuevos caracteres diagnósticos para el grupo.

En la hipótesis filogenética de Baldwin y Johnson (1996) se incluyen aulopiformes que previamente mostraban afinidad incierta (*Chlorophthalmus*). Tras el reconocimiento la familia Paraulopidae por Sato y Nakabo (2002), la naturalidad del Orden Aulopiformes fue nuevamente evaluada; el resultado obtenido, aunque semejante al de Baldwin y Johnson (1996), difiere por la posición filogenética del género *Bathysauroides* (ver Sato y Nakabo, 2002:40, fig. 21). Un enfoque distinto para evaluar las relaciones de parentesco entre

Woodward (1901)

Order Actinopterygii
- Suborder Isospondyli
  - †Family Enchodontidae
    - †Genus *Enchodus*
    - †Genus *Eurypholis*
    - †Genus *Palaeolycus*
    - †Genus *Halec*
    - †Genus *Cymolichthys*
    - †Genus *Prionolepis*
    - †Genus *Leptecodon*
    - †Genus *Pantopholis*

Goody (1969):

Order Salmoniformes
- †Suborder Ichyotringoidei
  - †Family Ichthyotringidae
    - †Genus *Ichthyotringa*
  - Insertae sedis: †Genus *Apateodus*
  - †Family Apateopholidae
    - †Genus *Apateopholis*
- †Suborder Cimolichthyoidei
  - †Family Cimolichthydae
    - †Genus *Cimolichthys*
  - †Family Dercetidae
    - †Genus *Dercetis*
    - †Genus *Rhynchodercetis*
    - †Genus *Palargorhynchus*
- †Suborder Enchodontoidei*
  - †Family Enchodontidae
    - †Genus *Enchodus*
    - †Genus *Palaeolycus*
  - †Family Eurypholidae
    - †Genus *Eurypholis*
    - †Genus *Saurorhamphus*
- †Suborder Halecoidei
  - †Family Halecidae
    - †Genus *Halec*
    - †Genus *Pahylactocephalus*
    - †Genus *Hemisauridae*

Rosen (1973):

Order Aulopiformes, new name
- Suborder Aulopoidei, new name
  - Family Aulopidae
  - Family Bathysauridae
  - Family Bathypteroidae
  - Family Ipnopidae
  - Family Chlorophthalmidae
  - Family Notosudidae (=Scopelosauridae)
- †Suborder Alepisauroidei*
  - †Genus *Apateodus*
  - †Genus *Apateopholis*
  - †Genus *Cimolichthys*
  - †Genus *Dercetis*
  - †Genus *Enchodus*
  - †Genus *Eurypholis*
  - †Genus *Halec*
  - †Genus *Hemisaurida*
  - †Genus *Ichthyotringa*
  - †Genus *Palaeolycus*
  - †Genus *Pelargorhyncus*
  - †Genus *Phylactocephalus*
  - †Genus *Prionolepis*
  - †Genus *Rhynchodercetis*
  - †Genus *Saurorhamphus*
- †Superfamily Synodontoidea, new usage
  - Insertae sedis: †Genus *Sardinius*
  - Insertae sedis: †Genus *Volcichthys*
  - Family Synodontidae
  - Family Harpadontidae
  - Family Giganturidae (? + Rosauridae)
- Superfamily Alepisauroidea
  - Family Paralepididae
  - Family Omosudidae
  - Family Alepisauridae
  - Family Anotopteridae
  - Family Evermannellidae
  - Family Scopelarchidae

Figura 2. Diferentes propuestas en la clasificación de los encodontoides. *: Denota la ubicación de la mayoría de las formas fósiles relacionadas con las formas estudiadas en el presente trabajo. †: indica a un taxon extinto.

Aulopiformes recientes fue presentada por Davis (2010). Este autor recurre al uso de genes nucleares y mitocondriales de Aulopiformes que adiciona a las propuestas de homología primaria de Baldwin y Johnson (1996) en un ejercicio de reconstrucción filogenética empleando evidencia total. En la clasificación de Aulopiformes recientes propuesta por Davis

(2010), grupos sugeridos por Baldwin y Johnson (1996) son recategorizados, en tanto que la monofilia otros clados es ratificada.

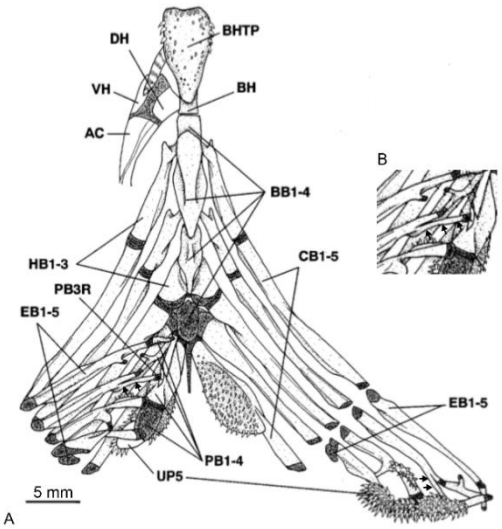

Figura 3. Arco branquial de *Paraulopus nigripinnis* Sato y Nakabo (2001), miembro de la familia Paraulopidae, suborden Aulopiformes. A) Arco completo y sus estructuras. B) Acercamiento al proceso uncinado del epibranquial 2, sinapomorfía del Orden Aulopiformes de acuerdo a Rosen (1973). Abreviaturas: **BB1–4**, basibranquial 1-4; **BH,** Basihyal; **CB1-5**, ceratobranquial 1-5; **EB1-1**; epibranquiales 1-3; hipobranquiales 1-3; PB1-4, faringobranquiales 1.4. **PB3R**, cresta dorsal del tercer faringobranquial. Fechas señalan al proceso uncinado. Imagen editada de Sato y Nakabo (2001).

Mientras que los trabajos señalados anteriormente abordan el estudio de las relaciones de parentesco entre Aulopiformes recientes, otros autores abordaron, aunque sin alcanzar consensos, las relaciones filogenéticas de Aulopiformes fósiles. Por ejemplo, Chalifa (1989) considera a la familia Dercetidae como grupo monofilético dentro del Suborden Cimolichthyoidei Goody, 1969. Taverne (1991) también exploró las relaciones entre dercétidos; originalmente los consideró como un clado miembro del Orden Stomiiformes, y posteriormente los reconoció como miembros del Suborden Enchodontoidei del Orden Aulopiformes (Taverne, 2006).

Para Gallo et al. (2005) la familia Dercetidae es monofilética y forma parte del Suborden Enchodontoidei Nelson, 1994. Por su parte, Taverne y Goolaerts (2015), describen nuevos miembros para la familia Dercetidae de estratos Maastrichtianos de Bélgica y posicionan a la familia como un grupo supeditado al Suborden Enchodontoidei, Berg 1937. En cambio, Díaz-Cruz et al. (2016) reconocieron un nuevo género miembro de la familia Enchodontidae de

estratos Cenomanianos de Chiapas al que no se le asignó directamente a algún Suborden, pero su posición filogenética fue evaluada tomando como referencia las propuestas de Fielitz (2004) y Silva y Gallo (2011). De manera similar, Vernygora et al. (2018), siguiendo la propuesta filogenética de Silva y Gallo (2011) y de Díaz-Cruz et al. (2016), describieron un nuevo taxón para la familia Dercetidae de estratos Turonianos de Colombia, trabajo en el cual tampoco existió una asignación explícita del nuevo taxón y de la familia Dercetidae a algún Suborden en particular, aunque sí reconocimiento como integrante del Orden Aulopiformes.

Ichthyotringoidei es otro grupo de Aulopiformes fósiles en el que también se han explorado las relaciones evolutivas de sus integrantes. Desafortunadamente hasta ahora, solamente se reconoce el trabajo elaborado por Fielitz y González-Rodríguez (2008), donde se determinó la posición filogenética de varias especies de Ichthyotringoidei. De manera similar a los trabajos de Dercetidae, estos autores se limitaron a estudiar interrelaciones de los integrantes de Ichthyotringoidei y no se profundizó en la discusión de las relaciones de este Suborden respecto a otros grupos de Aulopiformes fósiles.

Por otra parte, las relaciones filogenéticas de Enchodontidae, uno de los grupos más numerosos de Aulopiformes fósiles, han sido abordadas desde diferentes enfoques. Nelson (1994) siguiendo la propuesta de Rosen (1973) sobre la relación de las formas fósiles con los alepisauroides recientes, de-jerarquizó su posición dentro del Suborden Enchodontoidei, pasándolos de cuatro Subórdenes como señaló Goody (1969) a cuatro Superfamilias (Figura 2 y 4). En cambio, Fielitz (2004) evaluó la posición filogenética de Enchodontidae respecto a sus parientes recientes. Este autor tomó como base la propuesta evolutiva de los Aulopiformes recientes presentada por Baldwin y Johnson (1996) y encontró que la Superfamilia Enchodontoidea, compuesta por Cimolichthyidae y Enchodontidae, se recupera como un grupo monofilético (Fielitz, 2004, p. 627, fig. 2), al tiempo que esta Superfamilia representa el grupo hermano de la familia Alepisauridae.

La hipótesis filogenética de Fielitz (2004) exhibió reacomodos mínimos en la topología propuesta por Baldwin y Johnson (1996) y también recuperó la monofilia del Orden Aulopiformes. La clasificación presentada por este autor se centró exclusivamente en Enchodontidae, probablemente porque la monofilia de Enchodontoidea se sostiene exclusivamente por una combinación de caracteres homoplásicos (Fielitz, 2004, p. 632, tbl. 2; fig. 3). No obstante, esta evidencia fue suficiente para que Fielitz (2004) rechace formalmente

la propuesta de Goody (1969), en donde los encodóntidos se consideraban como integrantes del Orden Salmoniformes y se reafirmara su posición como integrantes de Aulopiformes.

A partir de la publicación del trabajo de Fielitz (2004), la clasificación del Orden Aulopiformes fue reestructurada. Nelson (2006) replanteó su propuesta de clasificación previamente publicada y señaló que los Aulopiformes incluyen seis Subórdenes: Alepisauroidei, Chlorophthalmoidei, Giganturoidei, Halecoidei, Ichthyotringoidei y Synodontoidei. En esta clasificación, Cimolichthyidae y Enchodontidae se consideran integrantes del Suborden Alepisauroidei en sintonía con los resultados presentados por Fielitz (2004).

En la propuesta asentada en evidencia total por Davis (2010), desafortunadamente no se consideró información morfológica de ningún grupo fósil; sin embargo, se discute brevemente la posición de algunos de estos grupos. Este autor señala que el parentesco entre los grupos de Aulopiformes recientes y los Subórdenes Ichthyotringoidei y Halecoidei son cuestionables, en tanto que las relaciones parentesco de Enchodontidae son presentadas tal y como fueron señaladas por Fielitz (2004) (Davis y Fielitz, 2010, p. 1196, fig. 1). De esta manera, para Davis y Fielitz (2010) la familia Enchodontidae es el grupo hermano de *Cimolichthys* (ver Fielitz, 2004, p. 627, fig. 2), y este clado, sin ninguna sinapomorfía, se recupera como grupo hermano de Alepisauridae (*Omosudis* + *Alepisaurus*) considerados en ese trabajo como integrantes de la Superfamilia Alepisauroidea. Estos autores reconocen la necesidad de elaborar estudios sistemáticos robustos para el grupo, y resaltan la proximidad que Enchodontidae mantiene con Alepisauridae como miembros de Alepisauroidea, Superfamilia con la misma composición de taxones que (Fielitz, 2004, p. 632, tbl. 2) consideró como Enchodontoidea. Con base en lo anterior, Enchodontoidea puede ser considerada como sinónimo de Alepisauroidea, teniendo en cuenta que, si los grupos fósiles son el principal objeto de estudio, entonces se ha preferido denominar al grupo como Enchodontoidea.

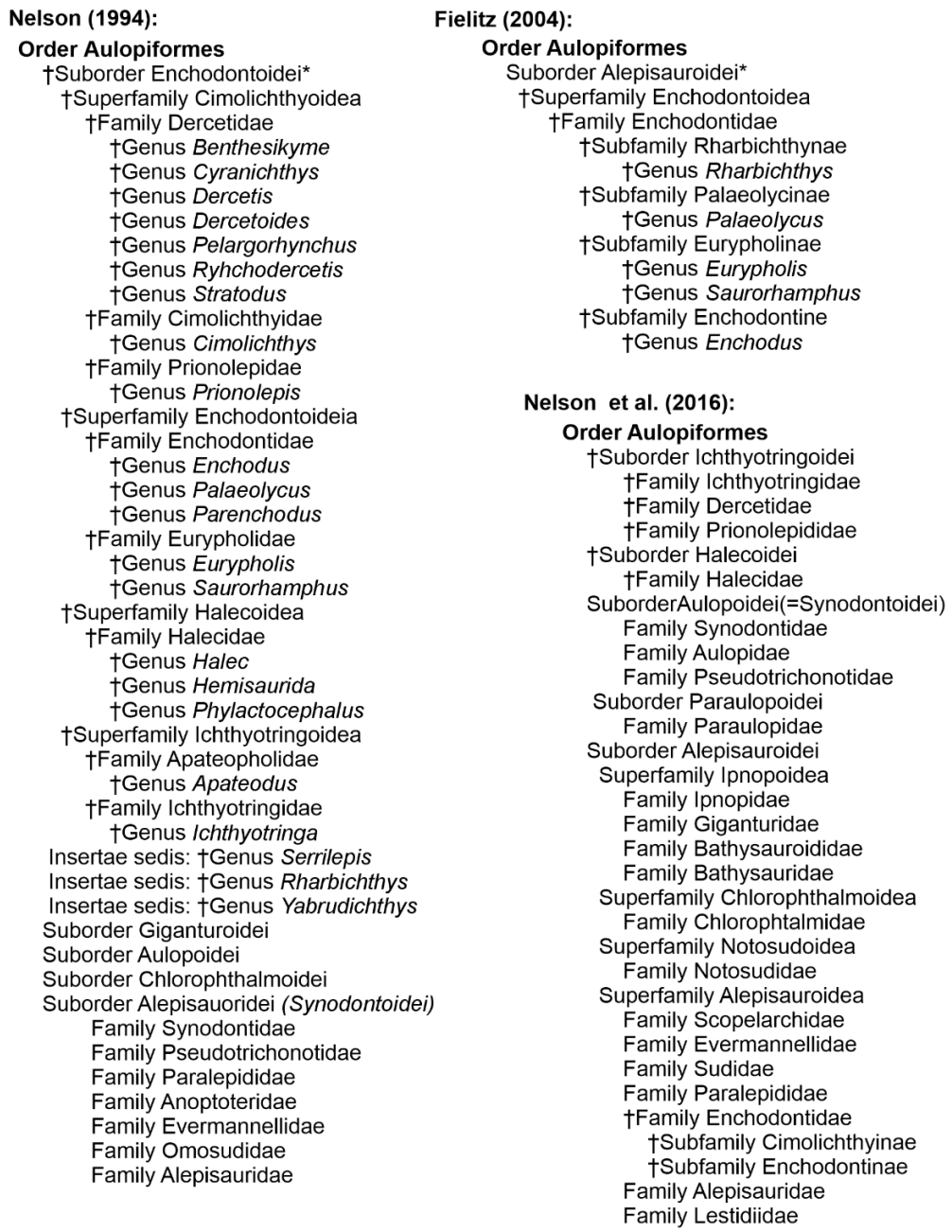

Figura 4. Propuestas adicionales para la clasificación de los encodontoides y sus congéneres. * Denota la ubicación de la mayoría de las formas fósiles relacionadas con el presente trabajo. †: señala a un taxon extinto.

A la fecha, la única propuesta filogenética elaborada con el objetivo de determinar exclusivamente las relaciones evolutivas entre los Aulopiformes fósiles fue elaborada por Silva y Gallo (2011). Estas autoras parten de la afinidad filogenética de estos grupos sugerida

por Goody (1969) y que Nelson (1994) reconoció como Enchodontoidei, a su vez integrante de Aulopiformes. En este trabajo, el más inclusivo del Suborden, Enchodontoidei se reconoció como un grupo parafilético, se reorganizaron familias como Apateopholidae y Halecidae, los géneros *Hemisaurida* y *Nardodex* se determinaron como *incertae sedis*, y se corroboraron clados monofiléticos como las familias Dercetidae y Enchodontidae. Estas dos últimas familias son cosmopolitas y representan los grupos más ampliamente estudiados del Suborden.

Por otra parte, una revisión de todos los géneros fósiles reconocidos como Aulopiformes fue elaborada por Newbrey y Konishi (2015). Este trabajo no fue situado bajo un contexto filogenético, pero resultó informativo porque recopiló un total de 37 géneros y señaló que al menos 26 de ellos son considerados como *incertae sedis*. Los géneros restantes fueron distribuidos en seis Subórdenes diferentes (Aulopoidei, Alepisauroidei, Chlorophthalmoidei, Halecoidei, Enchodontoidei e Ichthyotringoidei) (ver Cuadro 1).

Las investigaciones de Silva y Gallo (2011) y de Newbrey y Konishi (2015) se centraron únicamente en el estudio de grupos fósiles y es probable que por esta razón sus resultados no hayan sido considerados en la clasificación de Nelson et al. (2016). Estos últimos presentan una clasificación de Aulopiformes de acuerdo con sus relaciones filogenéticas. Nelson et al. (2016) toman como referencia a los trabajos de Fielitz (2004) y de Davis (2010) para proponer que los Aulopiformes se componen de cinco Subórdenes. De estos grupos, Ichthyotringoidei y Halecoidei están representados sólo por formas fósiles; otros dos grupos, Aulopoidei (=Synodontoidei) y Paraulopoidei, están integrados únicamente por peces recientes y, finalmente, el Suborden Alepisauroidei, donde se reflejan las relaciones evolutivas que mantienen los peces fósiles con algunos aulopiformes recientes (Superfamilia Alepisauroidea= Enchodontoidea).

Cuadro 1. Comparación de la composición de los diferentes Subórdenes fósiles de Aulopiformes. Algunos taxa se reconocen constantemente como integrantes del suborden Enchodontoidei o Halecoidei; sin embargo, otros géneros como *Pelargorhynchus*, se han considerado como miembros de diferentes Subórdenes. Entre paréntesis se coloca el número de especies reconocidas para cada género. *: tipo de trabajo elaborado.

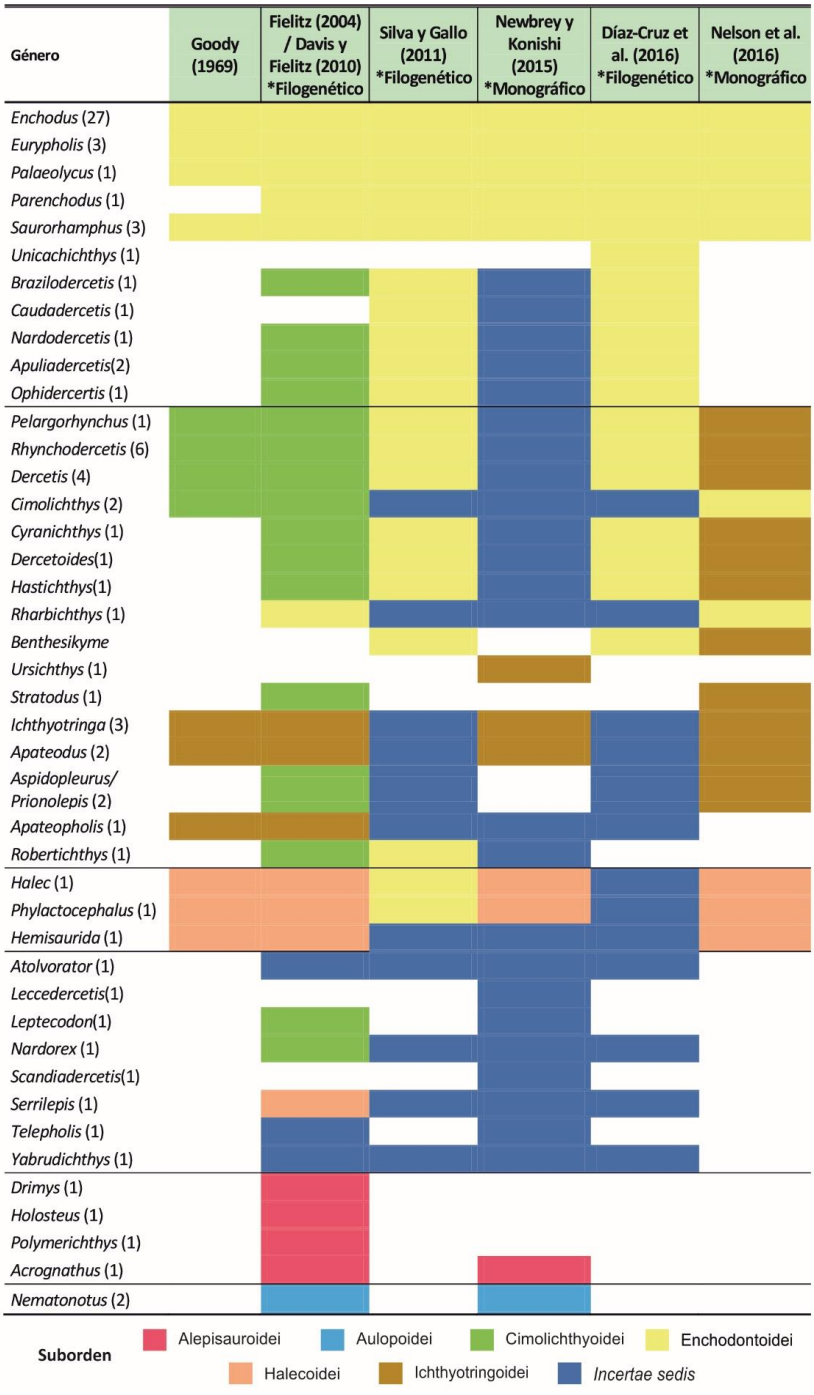

Nuevos taxones para Enchodontoidei

El suborden Enchodontoidei sin duda es un taxón problemático. Además, como indicado en la primera parte de este trabajo, salvo Enchodontidae, las relaciones filogenéticas entre los Aulopiformes fósiles con respecto a los Aulopiformes actuales no son claras (Nelson, 2006; Davis, 2010). Incluso entre Aulopiformes fósiles ha sido complicado corroborar su monofilia y demarcar la composición y los límites de las diferentes familias que lo integran (Nelson,1994; Silva y Gallo, 2011). Con las nuevas propuestas taxonómicas de los aulopiformes, junto con los recientes descubrimientos y descripciones de nuevos taxones, las hipótesis filogenéticas de Dercetidae (Gallo et al., 2005; Taverne, 2006), Enchodontidae (Fielitz, 2004; Silva y Gallo, 2011) e Ichthyotringoidei (Fielitz y González-Rodríguez, 2008) se han ido reajustado. Entre las modificaciones realizadas a las propuestas filogenéticas podemos encontrar adición, exclusión, y sustitución de taxones. Ejemplos de algunos de estos cambios son: la substitución de *Prionolepis* por *Aspidopleurus* en Alepisauroidei (Alvarado-Ortega y Porras-Múzquiz, 2012) y la exclusión *Robertichthys*, considerado ahora un integrante de Aspidorhynchidae (Aspidorhynchiformes) y no un encodóntido (Giersch, 2014).

La adición de taxones nuevos ha sido la práctica más común debido al descubrimiento de nuevos taxones tanto a nivel específico como a nivel genérico. Por ejemplo, *Apateodus busseni* de Kansas, Estados Unidos (Fielitz y Shimada, 2009), *Enchodus harranesis* de Jordania (Kaddumi, 2009) y *Enchodus mecoanalis* del Líbano (Forey et al., 2003), taxones a los que por sus remarcables características morfológicas se han determinado como encodontoides, pero a los que su posición filogenética no se ha determinado formalmente. Contrariamente, otros taxones en los que sí se ha explorado su posición filogenética corresponden a miembros de la familia Enchodontidae: *Enchodus zimapanensis* de Hidalgo, México (Fielitz y Gonzáles-Rodríguez, 2010), *E.* de Gavdos de Grecia (Cavin *et al*., 2012) y *E. tineidae* del desierto de Egipto (Holloway et al., 2016); y de la familia Dercetidae: *Candelarhynchus padillai*, del Turoniano de Colombia (Vernygora et al. 2018) y *Pelargorhynchus grandis* de estratos Maastrichtianos de Los Países Bajos (Wallaard et al. 2019). A nivel supragenérico también encontramos ejemplos de nuevos taxones, pero estos son menos comunes. Por ejemplo, el género monoespecífico *Unicachichthys* del Sur de México (Díaz-Cruz et al*.,* 2016) o *Ursichthys* del sur de Alberta, Canadá; taxones incluidos en

Enchodontidae y a una familia indeterminada (Ichthyotringoidei) respectivamente (Newbrey y Konishi, 2015).

Diversidad de encodontoides en el mundo

Si bien es cierto que los encodontoides exhiben un rango temporal amplio, la mayoría de ellos se han reportado de localidades con una edad restringida para el Cretácico superior. Son pocos los taxones que sobrepasan estos límites, entre ellos podemos encontrar a *Apateodus*, *Enchodus* o *Ichthyotringa* (Silva y Gallo, 2011, 2016; Newbrey y Konish, 2015). Durante comienzos del Cretácico superior, los encodontoides ya representaban un componente importante de las asociaciones fósiles de peces marinos dado su número relativamente alto de géneros y especies. Por ejemplo, los afloramientos de Hakel y Hajula en el Líbano, Komen, Eslovenia o Jbel Tselfat, Marruecos que cuentan con representantes de las familias Apateopholidae, Enchodontidae, Dercetidae, e Ichthyotringidae. La diversidad genérica para los Aulopiformes fósiles (encodontoides y otros taxones afines) alcanzó su máximo registro durante el Cenomaniano (100.5 - 93.9 Ma) (Newbrey y Konishi, 2015). Incluso, durante este periodo, el grupo se ha identificado como el más diversificado en algunos afloramientos, como evidenciado en localidades de Jerusalén, donde los Aulopiformes fósiles representan más del 50% de sus registros (Forey et al., 2003; Amalfitano et al., 2020).

Además de esta dominancia relativa, las asociaciones fósiles de los afloramientos más antiguos del Cretácico superior muestran cierto grado de similitud en su composición. Dicha similitud se atribuye potencialmente a proximidad geográfica de las localidades y a la semejanza en el ambiente de depósito (Amalfitano et al., 2020). Por otro lado, el dominio de Aulopiformes referente a la riqueza de individuos en los afloramientos fósiles se acentúa posteriormente (Santoniano-Campaniano 86.3 - 72.1 Ma) aunque con pocos taxones como sus representantes en localidades norteamericanas, principalmente de Estados Unidos (ver Allen y Shimada, 2021) y relativamente más diversificada pero igual de dominante en asociaciones del Mastrichtiano (72.1 – 66 Ma) en la meseta de fosfatos al poniente de Marruecos (Khalloufi et al., 2017). A pesar de que los estudios taxonómicos en varias localidades alrededor de mundo aún continúan, aparentemente el registro de encodontoides parece obedecer un aumento de su dominancia en las localidades a mediados del Cretácico tardío, seguido de un declive asociado a la extinción del Cretácico-Paleógeno (K-Pg) (Argyriou y Davesne, 2021). El estudio de las

faunas marinas fósiles durante este periodo contribuye a documentar mejor los impactos que la extinción del K-Pg tuvo en la diversidad de especies marinas del Cretácico superior.

Presencia de Enchodontoidei en México

Los peces del Suborden Enchodontoidei se han reportado para varios Estados de la República Mexicana; sin embargo, son un grupo parcialmente estudiado. Los primeros reportes de encodontoides datan de la década de los 50's para los Estados de San Luis Potosí y Tamaulipas (Turoniano; Maldonado-Koerdell, 1956), pero es hasta hace poco que el grupo se comenzó a reportar con mayor frecuencia. Actualmente se reconocen integrantes de Enchodontoidei para Vallecillo, Nuevo León (Turoniano; Blanco et al*.,* 2001); Muhi, Hidalgo (Albiano-Cenomaniano; González-Rodríguez y Applegate, 2000); diversas localidades cercanas a Múzquiz, Coahuila (Turoniano; Blanco-Piñón et al., 2004); Arroyo las Bocas, Guerrero (Turoniano; Alvarado-Ortega et al*.,* 2006a); El Espinal y El Chango, Chiapas; (Cenomaniano; Alvarado-Ortega et al., 2009) entre otros (Cuadro 2). A pesar de que la cantidad de registros de este grupo en México ha aumentado, son pocos los taxones que se han determinado a nivel específico.

Paralelamente al reconocimiento de los taxones mexicanos como miembros de Enchodontoidei, los trabajos de prospección y de rescate de peces fósiles en las localidades cretácicas de México continúan. El número de ejemplares resguardados en las colecciones científicas ha aumentado y en el presente trabajo comienzan a ser formalmente estudiados.

Varios de los ejemplares fósiles recientemente recuperados provienen de afloramientos previamente reconocidos, como El Chango en Chiapas o de localidades cercanas a Múzquiz, Coahuila. Adicionalmente a esto, también se han descubierto nuevas localidades fosilíferas, como las que se localizan en las cercanías de San Cristóbal de las Casas y Comitán, Chiapas o las ubicadas en el Estado de Puebla; en estos sitios se han reconocido grupos de peces afines a diversos grupos del Suborden Enchodontoidei (Alvarado-Ortega et al., 2019a,2019b, 2020). El reconocimiento de estas localidades y los ejemplares ahí recuperados cubren un vacío en la distribución de Enchodontoidei que anteriormente era desconocido para el dominio occidental del mar de Tethys y el sur del Mar Interior de América del Norte.

El registro fósil de México comienza a revelar elementos importantes que ayudan en la resolución de los conflictos taxonómicos de los peces encodontoides. Con el estudio detallado de los nuevos descubrimientos y su inclusión en los análisis filogenéticos del presente trabajo, se han construido hipótesis más incluyentes sobre la historia evolutiva de este grupo que servirán como base para interpretaciones biogeográficas y evolutivas más robustas. A la par, se trabaja en la revisión de encodontoides en diferentes colecciones científicas en México y en el extranjero, y se están redescribiendo taxones descritos hace décadas para documentar sus rasgos anatómicos e incrementar la variación morfológica que este grupo alcanzó.

Cuadro 2. Reportes de Enchodontoidei para México previos al presente trabajo. Muchos de ellos permanecen como taxa indeterminados y otros más se han reconocido hasta nivel de género. Familias de acuerdo con Silva y Gallo (2011) y Nelson et al. (2016).

Suborden	Género/Taxón	Reporte para México	Localidad	Edad	Autor
Alepisauroidei *sensu* Nelson, 2016	***Aspidopleurus***	*Aspidopleurus kickapoo*	La Mula, Coahuila	Turoniano	Alvarado-Ortega y Porras-Múzquiz (2012)
		Enchodus cf. venator	Vallecillo, Nuevo León	Turoniano	Giersch (2014)
		Enchodus. ferox	Los Reptiles, Chiapas	Maastrichtiano	Carbot-Chanona y Than-Marchese (2013)
		E. gladiolus	Rudista, Chiapas	Maastrichtiano	
		E. petrosus	Los Reptiles, Chiapas	Maastrichtiano	
		E. zimapanensis	Muhi, Hidalgo	Albiano-Cenomaniano	Fielitz y González-Rodríguez (2010)
	Enchodus	*Enchodus* sp	San José de las Rusias, Tamaulipas	Turoniano	Maldonado-Koerdell (1956)
		Enchodus sp	Xilitla, San Luis Potosí	Turoniano	Maldonado-Koerdell (1956)
		Enchodus sp	Vallecillo, Nuevo León	Turoniano	Blanco-Pinón (1998)
		Enchodus sp	Múzquiz, Coahuila	Turoniano-Coniaciano	Blanco-Piñón et al. (2004)
		Enchodus sp	Boquillas, Coahuila	Cenomaniano-Turoniano	González-Barba y Espinosa-Chávez, 2005
		Enchdous sp	El Chango, Chiapas	Cenomaniano	Díaz-Cruz et al. (2016)
		Enchodus sp	Arroyo las Bocas, Guerrero	Turoniano	Alvarado-Ortega et al. (2006a)
		Enchodus sp	Huehuetla, Puebla	Turoniano	Alvarado-Ortega et al. (2019)
		Enchodus sp	San José de Gracia, Puebla	Turoniano	Alvarado-Ortega et al. (2020a)
		Enchodus sp	Ochuxhob, Tzimol, Chiapas	Campaniano	Alvarado-Ortega et al. (2020b)
	Parenchodus	*Parenchodus* sp	Muhi, Hidalgo	Albiano-Cenomaniano	González-Rodríguez y Applegate (2000)
	Saurorhamphus	*Saurorhamphus* sp	El Chango y El Espinal, Chiapas	Cenomaniano	Alvarado-Ortega et al. (2009)
		Saurorhamphus sp	Vallecillo, Nuevo León	Turoniano	Alvarado-Ortega et al. (2006b)
	Unicachichthys	*Unicachichthys multidentata*	El Chango, Chiapas	Cenomaniano	Díaz-Cruz et al. (2016)
Cimolichthyoidei *sensu* Goody, 1969	***Apuliadercetis***	*Apuliadercetis* sp	Ochuxhob, Tzimol, Chiapas	Campaniano	Alvarado-Ortega et al. (2020b)
	Dercetis	*Dercetis* sp	Vallecillo, Nuevo León	Turoniano	Blanco-Piñón et al. (2001)
	Dercetis	*Dercetis* sp	San José de Gracia, Puel	Turoniano	Alvarado-Ortega et al. (2020a)
	Dercetoides	*Dercetoides* sp	Vallecillo, Nuevo León	Turoniano	Blanco-Piñón et al. (2001)
	Hastichthys	*Hastichthys* sp	Huehuetla, Puebla	Turoniano	Alvarado-Ortega et al. (2019)
	Rhynchodercetis* = *Hasticthhys	*Rhynchodercetis regio/ R. yovanovitchi*	Vallecillo, Nuevo León	Turoniano	Blanco-Piñón et al. (2001) Blanco-Piñón y Alvarado-Ortega (2006)/Giersch (2014)
		Rhynchodercetis sp	Arroyo las Bocas, Guerrero	Turoniano	Alvarado-Ortega et al. (2006b)
	Cimolichtidae	Formas aún no descritas	Vallecillo, Nuevo León	Turoniano	Alvarado-Ortega et al. (2006b)
Halecoidei *sensu* Goody, 1969	**Halecidae**	Formas aún no descritas	Múzquiz, Coahuila	Turoniano-Coniaciano	Alvarado-Ortega et al. (2006b)
Ichthyotringoidei *sensu* Goody, 1969	***Ichthyotringa***	*Ichthyotringa mexicana*	Muhi, Hidalgo	Albiano-Cenomaniano	Fielitz y González-Rodríguez (2008)

LITERATURA CITADA

Allen, J. y Shiamada, K. 2021 Fossil vertebrates from a unique marine bonebed of the Upper Cretaceous Niobrara Chalk, western Kansas, U.S.A.: new insights into the Niobrara vertebrate paleoecology. Manuscript submitted for publication.

Alvarado-Ortega, J. y Porras-Múzquiz, H.G. The first record of *Aspidopleurus* (Teleostei, Aulopiformes) in America, from the La Mula Quarry (Turonian), Coahuila, Mexico. *Revista Brasileira de Paleontologia*, 15, 3:251-263.

Alvarado-Ortega, J., Cantalice, K. M., Barrientos-Lara, J. I., Díaz-Cruz, J. A., Than-Marchese, B. A. 2019. The Huehuetla quarry, a Turonian deposit of marine vertebrates in the Sierra Norte of Puebla, central Mexico. *Palaeontologia Electronica*, 22(1).

Alvarado-Ortega, J., Cantalice, K. M., Díaz-Cruz, J. A., Castañeda-Posadas, C., Zavaleta-Villareal, V. 2020a. Vertebrate fossils from the San José de Gracia quarry, a new Late Cretaceous marine fossil site in Puebla, Mexico. *Boletín de la Sociedad Geológica Mexicana,* 72(1).

Alvarado-Ortega, J., Cantalice, K. M., Martínez-Melo, A., García-Barrera, P., Than-Marchese, B. A., Díaz-Cruz, J. A., Barrientos-Lara, J. I. 2020b. Tzimol, a Campanian marine paleontological site of the Angostura Formation near Comitán, Chiapas, southeastern Mexico. *Cretaceous Research*, 107, 104279.

Alvarado-Ortega, J., Garibay-Romero, L. M., Blanco-Piñón, A., González-Barba, G., Vega, F. J., y Centeno García, E. 2006a. Los peces fósiles de la Formación Mexcala (Cretácico Superior) en el Estado de Guerrero, México. *Revista Brasileira de Paleontologia*, 9(3), 261–272.

Alvarado-Ortega, J., González-Rodríguez, K.A., Blanco-Piñón, A., Espinosa-Arrubarrena, L. y Ovalles-Damián, E. 2006b. Mesozoic Osteichthyans of Mexico, in: Vega, F.J., Nyborg, T. G., Perrilliat, M.C., Montellano-Ballesteros, M., Cevallos-Ferriz. S.R.S., Quiroz-Barroso, S.A. (eds.), *Studies on Mexican Paleontology, Topics on Geobiology*, pp 169-207.

Alvarado-Ortega, J., Ovalles-Damián, E., Blanco-Piñón, A., 2009, The fossil fishes from the Sierra Madre Formation, Ocozocoautla, Chiapas, Southern Mexico: *Palaeontologia Electronica,* 12(2,4A), 1-22.

Baldwin, C.C., y Johnson, G.D., 1996. Aulopiform interrelationships. In: Stiassny, M.L.J., Parenti, L.R., Johnson, G.D. (Eds.), *Interrelationships of Fishes*. Academic Press, San Diego., pp. 355–404.

Berg, L. S. 1937. A classification of fish-like vertebrates. *Bulletin de l'Académie des Sciences de l'URSS*, 4, 1277-1280.

Berg, L., y Edwards, J. 1947. Classification of fishes both recent and fossil. Ann Arbor, 517 p.

Blanco, A., Stinnesbeck, W., López-oliva, J.G., Frey, E., Adatte, T., y González, A. H. 2001. Vallecillo, Nuevo León: una nueva localidad fosilífera del Cretácico Tardío en el noreste de México. *Revista Mexicana de Ciencias Geológicas*, 18, 186–199.

Blanco-Piñón, A. 1998. Vallecillo, Nuevo León: Yacimiento fosilífero del Noreste de México, Tesis de Mmaestría. Universidad Autónoma de Nuevo León.

Blanco-Piñón, A. y Alvarado-Ortega, J. 2006. *Rhynchodercetis regio*, sp. nov., a dercetid fish (Teleostei: Aulopiformes) from Vallecillo, Nuevo León State, Northeastern Mexico. *Journal of Vertebrate Paleontolgy*, 26(3), 552–558.

Blanco-Piñón, A., Porras, H., Vega-Vera, F., González-Rodríguez, K. A. y Alvarado-Ortega, J. 2004. Múzquiz, Coahuila: a new fossiliferous locality, northeastern Mexico, *IX Congreso Nacional de Paleontología*, Sociedad Mexicana de Paleontología, Libro de Resúmenes.

Cavin, L. 1999. Occurrence of a juvenile teleost, *Enchodus* sp., in a fish gut content from the Upper Cretaceous of Goulmima, Morocco. *Special Papers in Palaeontology*, 60, 57-72.

Cavin, L., Alexopoulos, A., y Piuz, A. 2012. Late Cretaceous (Maastrichtian) ray-finned fishes from the island of Gavdos, southern Greece, with comments on the evolutionary history of the aulopiform teleost Enchodus. *Bulletin de la Société géologique de France*, 183(6), 561-572.

Chalifa, Y., 1985. *Saurorhamphus judeaensis* (Salmoniformes: Enchodontidae), a new longirostrine fish from the Cenomanian of Ein-Yabrud, near Jerusalem. *Journal of Vertebrate Paleontology.* 5 (3), 181-193.

Chalifa, Y., 1989. New species of Enchodus (Pisces: Enchodontoidei) from the Lower Cenomanian of Ein-Yabrud, Israel. *Journal of Paleontology*. 63(3), 356-364.

Chalifa, Y., 1996. New species of *Enchodus* (Aulopiformes: Enchodontidae) from the Northern Negev, Israel, with comments on evolutionary trends in the Enchodontoidei. In: Arratia, G., Schultze, H.-P. (Eds.), *Mesozoic Fishes Systematics and Paleoecology.* Verlag Dr. Friedrich Pfeil, München, Germany, pp. 349-367.

Cicimurri, D.J. y Everhart, M.J. 2001. An elasmosaur with stomach contents and gastroliths from the Pierre Shale (Late Cretaceous) of Kansas. *Transactions of the Kansas Academy of Science*, 104(3), 129-143.

Davis, M.P. y Fielitz, C. 2010. Estimating divergence times of lizardfishes and their allies (Euteleostei: Aulopiformes) and the timing of deep-sea adaptations. *Molecular Phylogenetics and Evolution*, 57(3), 1194-1208.

Davis, M.P., 2010. Evolutionary relationships of the Aulopiformes (Euteleostei: Cyclosquamata): a molecular and total evidence approach. In: Nelson, J.S., Schultze, H.P., Wilson, M.V.H. (Eds.), *Origin and Phylogenetic Interrelationships of Teleosts*. Verlag Dr. F. Pfeil., München, pp. 431–470.

Díaz-Cruz, J.A., Alvarado-Ortega, J., y Carbot-Chanona, G. 2016. The Cenomanian short snout enchodontid fishes (Aulopifomes, Enchodontidae) from Sierra Madre Formation, Chiapas, southeastern Mexico. *Cretaceous Research*, 61, 136-150.

Fielitz, C. 2004. The phylogenetic relationships of the †Enchodontidae (Teleostei: Aulopiformes). *Recent Advances in the Origin and Early Radiation of Vertebrates*: Verlag Dr. Friedrich Pfeil, München, Germany, 619-634.

Fielitz, C. y González-Rodríguez, K. 2008. A new species of *Ichthyotringa* from the El Doctor Formation (Cretaceous), Hidalgo, Mexico. In: Arratia G., Schultze, H-P. y Wilson, M.V.H.

(Eds), *Mesozoic Fishes 4 – Homology and Phylogeny*, München: Verlag Dr. Friedrich Pfeil, p. 373–388.

Fielitz, C., y González-Rodríguez, K.A. 2010. A new species of *Enchodus* (Aulopiformes: Enchodontidae) from the Cretaceous (Albian to Cenomanian) of Zimapán, Hidalgo, México. *Journal of Vertebrate Paleontology*, 30(5), 1343-1351.

Fielitz, C., y Shimada, K. 2009. A New Species of *Apateodus* (Teleostei: Aulopiformes) from the Upper Cretaceous Niobrara Chalk of Western Kansas, USA. *Journal of Vertebrate Paleontology*, 29(3), 650-658.

Forey, P.L., Yi, L., Patterson, C., y Davies, C.E. 2003. Fossil fishes from the Cenomanian (Upper Cretaceous) of Namoura, Lebanon. *Journal of Systematic Palaeontology*, 1(4), 227.

Friedman, M., Beckett, H.T., Close, R.A., y Johanson, Z. 2015. The English chalk and London clay: Two remarkable British bony fish Lagerstätten. *Geological Society, London, Special Publications,* 430(1), 165-200.

Giersch, S., 2014. Die Knochenfische der Oberkreidezeit in Nordostmexiko: Beschreibung, Systematik, Vergesellschaftung, Paläobiogeographie und Paläoökologie. PhD Thesis, Ruprecht-Karls-Universität Heidelberg, Germany, 275 pp.

González-Barba, G. y Espinosa-Chavez, B. 2005. Cenomanian-Turonian fish fauna from the Boquillas Formation, North-West Coahuila, Mexico. *In: International Meeting on Mesozoic fishes, 4, 2005.* Extended Abstracts, UAM Ediciones, Madrid, p. 105-108.

González-Rodríguez, K.A. y Applegate, S.P. 2000. Muchi quarry, a new Cretaceous fish locality in Central Mexico, 60th *Annual Meeting, Soc. Vert. Paleonto., Abstracts,* p. 45A.

Goody, P.C. 1969. *The relationships of certain Upper Cretaceous teleosts with special reference to the myctophoids* (Vol. 7). British Museum (Natural History).

Goody, P.C. 1970. The Cretaceous teleostean fish Cimolichthys from the Niobrara Formation of Kansas and the Pierre Shale of Wyoming. *American Museum Novitates*, 2434, 29 pp.

Grandstaff, B.S., y Parris, D.C. 1990. Biostratigraphy of the fossil fish Enchodus Agassiz. *Journal of Vertebrate Paleontology*, 9(Suppl 3), 25A.

Holloway, W. L., Claeson, K. M., Sallam, H. M., El-Sayed, S., Kora, M., Sertich, J. J., and O'Connor, P. M. 2017. A new species of the neopterygian fish *Enchodus* from the Duwi Formation, Campanian, Late Cretaceous, Western Desert, central Egypt. *Acta Palaeontologica Polonica*, 62(2), 603-611.

Johnson, R.K. 1982. Fishes of the families Evermannellidae and Scopelarchidae: Systematics, morphology, interrelationships, and zoogeography. *Fieldiana*. *Zoology* (NS), 12, 1-252.

Kaddumi, H.F. 2009. Fossils of the Harrana Fauna and the adjacent areas. Publications of the Etrnal Rive Museum *of Natural History*, Amman. 324 pp.

Khalloufi, B., Brito, P. M. M., Cavin, L., Dutheil, D. B., Zouhri, S. 2017. Revue des ichthyofaunes mésozoïques et cénozoïques marocaines. *Paléontologie des vertébrés du Maroc: état des connaissances. Mémoires de la Société géologique de France, nouvelle série, Paris*, 180, 167-248.

Kriwet, J., Lirio, J.M., Nuñez, H.J., Puceat, E., y Lécuyer, C. 2006. Late Cretaceous Antarctic fish diversity. *Geological Society, London, Special Publications*, 258(1), 83-100.

Maisey J.G. 2000. *Discovering fossil fishes*. Henry Hold and Company. Canada. 223pp.

Maldonado-Koerdell, M. 1956, Peces fósiles de México III. Nota preliminar sobre peces del Turoniano Superior de Xilitla, San Luis Potosí, México. *Ciencia*, México, 16, 31-36.

Nelson, J.S. 1994. *Fishes of the World*, 3rd ed., New York: J Wiley and Sons, Inc., 600 p.

Nelson, J.S. 2006. *Fishes of the World*, fourth ed. John Wiley and Sons, New York. 624 p.

Nelson, J.S., Grande, T.C., y Wilson, M.V. 2016. *Fishes of the World*. John Wiley and Sons, Inc., 707 p.

Newbrey, M.G., y Konishi, T. 2015. A New Lizardfish (Teleostei, Aulopiformes) from the Late Cretaceous Bearpaw Formation of Alberta, Canada, with a Revised Diagnosis of *Apateodus* (Aulopiformes, Ichthyotringoidei). *Journal of Vertebrate Paleontology*, 35(3), e918042.

Okiyama, M. 1984. Myctophiformes: development. In: Moser, H.G., Richards, W.J., Cohen, D.M., Fahay, M.P., Kendall, A.W. Jr, Richardson, S.L. (eds) *Ontogeny and systematics of fishes.* Spec Publ 1. American Society of Ichthyologists and Herpetologists, Lawrence, 206–218 p.

Patterson, C., y Johnson, G.D., 1995. The intermuscular bones and ligaments of teleostean fishes. *Smithsonian Contributions to Zoology*. 559, 1–83.

Raab, M. y Chalifa, Y. 1987. A new enchodontid fish genus from the Upper Cenomanian of Jerusalem, Israel. *Palaeontology*, 30(4), 717-731.

Ronsen, D.E. 1973. Interrelationships of higher euteleostean fishes. In P.H. Greenwood, R. S. Miles y C. Patterson (Eds.), Interrelationships of fishes. *Journal of the Linnean Society (Zool).* 53:397-513. Suppl. A. Academic, New York.

Sato, T., y Nakabo, T. 2002. Paraulopidae and *Paraulopus*, a new family and genus of aulopiform fishes with revised relationships within the order. *Ichthyological Research*, 49(1), 25-46.

Shimada, K. y Fielitz, C. 2006. Annotated checklist of fossil fishes from the Smoky Hill Chalk of the Niobra Chalk (Upper Cretaceous) in Kansas. Bulletin of the New Mexico Museum of Natural History and Science, 35, 193-213.

Silva, H.M.A. y Gallo, V. 2011. Taxonomic review and phylogenetic analysis of Enchodontoidei (Teleostei: Aulopiformes). *Anais da Academia Brasileira de Ciências*, 83(2), 483–511.

Silva, H.M.A., 2007. Revisão taxonômica e filogenética dos peixes Enchodontoidei (*sensu* Nelson 1994) e considerações biogeográficas. Tesis del grado de Maestría. Programa de Pós-graduação em Ecologia e Evolução, Universidade do Estado do Rio de Janeiro, Brazil, 142 p.

Silva, H.M.A., y Gallo, V. 2016. Distributional patterns of enchodontoid fishes in the Late Cretaceous. *Cretaceous Research*, 65, 223-231.

Stewart, J.D. y Carpenter, K. 1990. Examples of vertebrate predation on cephalopods in the Late Cretaceous of the Western Interior. *Evolutionary Paleobiology of Behavior and Coevolution*. Elsevier, New York, 203-206.

Sulak, K. J. 1977. The systematics and biology of *Bathypterois* (Pisces,Chlorophthalmidae) with a revised classification of benthic myctophiform fishes. *Galathea Report*,14, 49–10.

Taverne, L., 1991. New considerations on the osteology and the phylogeny of the Cretaceous marine teleost family Dercetidae. *Biologisch Jaarboek Dodonaea*, 58(1990), 94-112.

Taverne L., 2006. Les poissons crétacés de Nardò. 24°. *Caudadercetis bannikovi* gen. et sp. nov. (Teleostei, Aulopiformes, Dercetidae). Considérations sur la phylogénie des Dercetidae. *Bolletino del Museo Civivo di Storia Naturale di Verona. Geologia Paleontogia Preistoria* 30: 27–48.

Taverne, L., y Goolaerts, S. 2015. The dercetid fishes (Teleostei, Aulopiformes) from the Maastrichtian (Late Cretaceous) of Belgium and The Netherlands. *Geologica Belgica*. 18: 21-30.

Vega, F.J., García-Barrera, P., Perrilliat, M. del C., Coutiño, M.A., y Mariño-Pérez, R. 2006. El Espinal, a new plattenkalk facies locality from the Lower Cretaceous Sierra Madre Formation, Chiapas, southeastern Mexico. *Revista Mexicana de Ciencias Geológicas*, 23(3):323-333.

Vernygora, O., Murray, A.M., Luque, J., Ruge, M.L.P., y Fonseca, M.E.P. 2017. A new Cretaceous dercetid fish (Neoteleostei: Aulopiformes) from the Turonian of Colombia. *Journal of Systematic Palaeontology*, 1-15.

Viohl, G. 1990. Piscivorous fishes of the Solnhofen Lithographic Limestone, in: Boucot A.J. (Ed*.), Evolutionary Paleobiology of Behavior and Coevolution*. Elsevier, Amsterdam, pp. 287-303.

Wallaard, J. J., Fraaije, R. H., Diependaal, H. J., Jagt, J. W. 2019. A new species of dercetid (Teleostei, Aulopiformes) from the type Maastrichtian of southern Limburg, the Netherlands. *Netherlands Journal of Geosciences*, 98.

CAPÍTULO II: *Dagon avendanoi* gen. and sp. nov. an Early Cenomanian Enchodontidae (Aulopiformes) fish from the El Chango quarry, Chiapas, southeastern Mexico

Journal of South American Earth Sciences 91 (2019) 272–284

Contents lists available at ScienceDirect

Journal of South American Earth Sciences

journal homepage: www.elsevier.com/locate/jsames

Dagon avendanoi gen. and sp. nov., an Early Cenomanian Enchodontidae (Aulopiformes) fish from the El Chango quarry, Chiapas, southeastern Mexico

Jesús Alberto Díaz-Cruz[a,b,*], Jesús Alvarado-Ortega[b], Gerardo Carbot-Chanona[c]

[a] Posgrado en Ciencias Biológicas, Unidad de Posgrado, Edificio A, 1° Piso, Circuito de Posgrados, Ciudad Universitaria, Coyoacán, C.P. 04510, Ciudad de México, Mexico
[b] Instituto de Geología, Universidad Nacional Autónoma de México; Circuito de la Investigación S/N, Ciudad Universitaria, Coyoacán, Ciudad de México, 04510, Mexico
[c] Museo de Paleontología Eliseo Palacios Aguilera, Dirección de Paleontología, Secretaría de Medio Ambiente e Historia Natural, Calzada de Los Hombres Ilustres S/N, Antiguo Parque Madero, Tuxtla Gutiérrez, Chiapas, Mexico

ARTICLE INFO

Keywords:
Dagon
Maximum parsimony
Bayesian inference
Cenomanian
Cintalapa
Mexico

ABSTRACT

Dagon avendanoi gen. and sp. nov. is described based on a single specimen from the Early Cenomanian marine deposits of the Cintalapa Formation at El Chango quarry, near Ocozocoautla de Espinosa, Chiapas, southeastern Mexico. This species is identified as a new member of Enchodontidae because it shows the predorsal scute series, a distinctive unique character of the family. Among enchodontids, *Dagon* is unique because its palatine bone has two large fang-like teeth longitudinally ordered; contrary, the palatine in other enchodontids has only one large terminal tooth (i.e. *Enchodus*) or many small teeth (i.e. *Unicachichthys*). The inclusion of the new genus within a phylogenetic analysis reveals that the family Enchodontidae is a natural group (*Unicachichthys* (*Dagon* (*Palaeolycus* (*Eurypholis* + *Saurorhamphus*) + (*Parenchodus* + *Enchodus*)))). This new fish represents the third enchodontid species described from Mexico; this, together with *Enchodus zimapanensis* and *Unicachichthys multidentata,* allows to recognize the early diversification of enchodontids during the lower limit of Late Cretaceous throughout the North American domain of the Tethys Sea.

1. Introduction

In 2004, Gerardo F. Carbot-Chanona and Ernesto Ovalles Damián, members of the paleontological staff of the Museum Eliseo Palacios Aguilera (MEPA), discovered a fossiliferous site now known as the El Chango quarry, near Ocozocoautla de Espinosa, Chiapas, southeastern Mexico (Fig. 1). Since then, the staff of this museum has driven an institutional project aimed to collect, study, and preserve the fossils from this quarry. Paleontologists and students from the Universidad de Ciencias y Artes de Chiapas and the Universidad Nacional Autónoma de México have been collaborating with MEPA in these tasks. Today, the MEPA collection includes more than 400 fossils from the El Chango quarry, making it the most important and emblematic paleontological site in southeastern Mexico.

The marine laminated limestone and dolomite strata of creamy-yellow color exposed in the El Chango quarry contain an abundant and diverse fossil biota. The assemblage recovered in this site up to now includes extraordinarily preserved specimens, proper of a true Konservat-Lagerstätte (Alvarado-Ortega et al., 2009). Although the fishes are the most abundant and diverse fossils in this site, other taxa are also relatively well represented, such as mollusks, crustaceans, insects, and plants (Ovalles-Damián et al., 2006; Vega et al., 2006, 2007; Alvarado-Ortega et al., 2009; Cevallos-Ferriz et al., 2012; Amaral et al., 2013; Garassino et al., 2013; González-Ramírez et al., 2013; and Guerrero-Márquez et al., 2013; among others).

The age of the fossil bearing strata of the El Chango quarry and a near coeval site, the El Espinal quarry, had been controversial. Shortly after being discovered, El Chango was reported as an outcrop of Albian or even Aptian age belonging to the Sierra Madre Formation (Ovalles-Damián et al., 2006; Vega et al., 2006, 2007; Huerta-Vergara et al., 2013); however, new accurate studies on its stratigraphy, regional geology, and fossil assemblage, reveal that it is a Cenomanian deposit of the Cintalapa Formation within the Sierra Madre Group (Alvarado-Ortega et al., 2009; Alvarado-Ortega and Than-Marchese, 2012, 2013). The occurrence of the ammonite *Graysonites* Young, 1958, indicate that this is an Early Cenomanian deposit (Moreno-Bedmar et al., 2014). The

* Corresponding author. Posgrado en Ciencias Biológicas, Unidad de Posgrado, Edificio A, 1° Piso, Circuito de Posgrados, Ciudad Universitaria, Coyoacán, C.P. 04510, Ciudad de México, Mexico.
E-mail address: vertebrata.j@gmail.com (J.A. Díaz-Cruz).

https://doi.org/10.1016/j.jsames.2019.01.014
Received 3 October 2018; Received in revised form 18 January 2019; Accepted 18 January 2019
Available online 22 February 2019

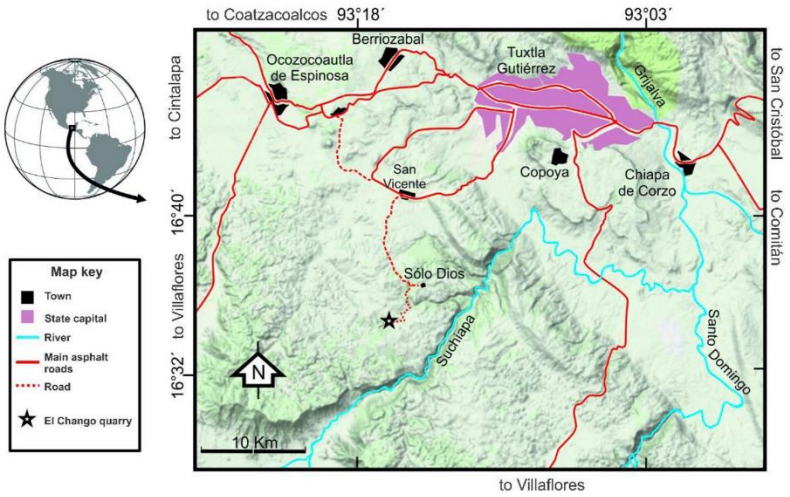

Fig. 1. Map of the El Chango quarry, near Ocozocoautla de Espinosa, Chiapas, México.

sedimentological sequences of these quarries were deposited into an estuarine or salty lagoon with ephemeral freshwater influence (Vega et al., 2006, 2007), under low energy and dysoxic/anoxic conditions, where the bioturbation or the establishment of bottom organisms were minimized (Moreno-Bedmar et al., 2014).

Among fossil fishes, representatives of the Enchodontidae are numerous in the El Chango quarry. This extinct teleostean family, firstly named by Woodward (1901), still is a somewhat problematic group. Although the enchodontids have been positioned in different taxonomic categories (Jordan, 1905; Berg, 1937; Arambourg, 1954; Goody, 1969; Rosen, 1973; Fielitz, 2004; Silva and Gallo, 2011; among others); currently, this family is placed within the marine order Aulopiformes. Genera already included in this family includes seven taxa: *Enchodus* Agassiz, 1833; *Saurorhamphus* Heckel, 1850; *Eurypholis* Pictet, 1850; *Palaeolycus* von der Marck, 1863; *Rharbichthys* Arambourg, 1954; *Parenchodus* Raab and Chalifa, 1987; and *Unicachichthys* Díaz-Cruz, Alvarado-Ortega, and Carbot-Chanona (2016) (i.e. Fielitz, 2004; Fielitz and González-Rodríguez, 2010; Silva, 2007; Silva and Gallo, 2011; Cavin et al., 2012; Holloway et al., 2017; among others).

Mexico possesses a rich fossil record of the family Enchodontidae; however, the taxonomical identities of many specimens are still uncertain (Díaz-Cruz and Alvarado-Ortega, 2017, 2018a, b; Díaz-Cruz et al., 2017). After the discovery of complete and well-preserved specimens of *Enchodus* and *Saurorhamphus* in the El Chango quarry (Alvarado-Ortega et al., 2009), the present authors realised the potential importance of the Mexican enchodontids; in 2011, we launched a research project to determine the taxonomic identity of these fossils and include them in appropriate phylogenetic and biogeographical context. Since then, five species have been formally identified in Mexico, including two new species. Based on isolated teeth from the Maastrichthian marine deposits of Chiapas, Carbot-Chanona and Than-Marchese (2013) identified specimens referred to *Enchodus petrosus* Cope (1874); *E. ferox* Leidy (1855); and *E. gladiolus* (Cope, 1872). *Unicachichthys multidentata* Díaz-Cruz et al. (2016), is a peculiar species from the El Chango quarry initally identified as a member of the genus *Enchodus* (Alvarado-Ortega et al., 2009). And, on behalf of another team of researchers, *Enchodus zimapanensis* Fielitz and González-Rodríguez (2010), was described from the Albian-Cenomanian deposits of the Muhi quarry, Hidalgo, central Mexico. Hence, the aim of this paper is to provide an accurate description of an enchodontid species from the El Chango quarry and explore its relationships within Enchodontidae.

2. Materials and methods

Preparation Methods. The fossil material was prepared combining chemical and mechanical procedures. The acid technique of Toombs and Rixon (1959) was used to dissolve the calcareous rocky matrix. Remaining patches of limestone were removed with pin vises and needles under binocular microscope. The fossil was photographed under white light and when necessary, it was coated with ammonium chloride and magnesium to get high contrast black and white photographs.

Anatomical Nomenclature. The osteological nomenclature and abbreviations used in this paper follow those used in similar publications on enchodontid fishes (Goody, 1969; Fielitz, 2004; and Cavin et al., 2012; among others).

Institutional Abbreviations. CME, Colección de Material Extranjero, a sub-collection of the Colección Nacional de Paleontología (IGM), Instituto de Geología, Universidad Nacional Autónoma de Mexico. BSPG, Bayerische Staatssammlung für Paläontologie und Geologie, München, Germany. IHNFG, Instituto de Historia Natural –Fósil, Geográfico–, Museo de Paleontología "Eliseo Palacios Aguilera", Chiapas, Mexico.

Comparative Materials Examined. The following specimens were studied with comparative proposes. *Enchodus* sp.: IHNFG-2989 and IHNFG-2653 from the Cenomanian deposits of the El Chango quarry, Chiapas, Mexico. *Eurypholis* sp.: CME 678, from the Cenomanian deposits of Heckel. *Eurypholis boissieri* Pictet (1850): BSPG 1988 XXV 374 and BSPG 1988 XXV 376, both from Cenomanian deposits of Hakel. *Unicachichthys multidentata*: IHNFG-2987 (holotype), IHNFG-2988, and IHNFG-4347, all from the early Cenomanian deposits of the El Chango quarry, Chiapas, Mexico.

Phylogenetic analyses. Two phylogenetic analyses were performed to assess the relationships of the new species described here.

Bayesian inference analysis was performed in the program MrBayes 3.2.6 (Ronquist et al., 2012). Specifications for the analysis were those outlined by Prieto-Márquez (2010) and Brusatte and Carr (2016). The dataset was analyzed using the Standard Discrete Model for morphology (Lewis, 2001) as implemented in MrBayes. Most settings were left as default: standard characters treated as unordered and all substitutions with the equal rates. The specified outgroup was *Diplophos* as used in previous phylogenetics analyses (Fielitz, 2004; Fielitz and González-Rodríguez, 2010).

We performed two sets of analyses using equal and variable amog

character rate variation; among character variation in the second analysis was specified using a gamma distribution with four discrete categories (rates = gamma, n = ngammacat = 4). Each seat of analyses had two independent runs and four chains (Nruns = 2 nchains = 4). The temperature parameter set to 0.01. For each run were set up 30,000,000 generations, a tree sampled every 1000 generations and 20 percent of samples discarded from the beginning of the chain. Generations were added until the standard deviation of split frequencies fell below 0.01. A 50% majority-rule consensus tree was obtained from each of these analyses. Bayes factor was calculated to know the significance of the harmonic means difference between analyses.

The second study performed to assess the relationships of the new species described in this work is a Maximum Parsimony Analysis. This is based on an updated version of dataset of Díaz-Cruz et al. (2016) (based on previous analyses published by Fielitz (2004), Fielitz and González-Rodríguez (2010), Silva and Gallo (2011), and Cavin et al. (2012)). In addition to the data of the new species described here, the new dataset includes information from Holloway et al. (2017) (see Appendix). A Maximum Parsimony analysis was performed using TNT 1.5 (Goloboff and Catalano, 2016) employing heuristic search "Traditional Search" with 1000 replicates and tree bisection reconnection (TRB) as swapping algorithm. Uninformative characters were deactivated and remaining were treated as non-additive. *Diplophos* was designated as outgroup according to previous phylogenetics proposals (Fielitz, 2004; Fielitz and González-Rodríguez, 2010). Consistency (CI) and retention (RI) indices of the strict consensus tree were calculated by using the script Stats for TNT.

3. Results

3.1. Systematic paleontology

Order Aulopiformes Rosen, 1973.
Family Enchodontidae Woodward, 1901.

Genus Dagon gen. nov

Type species. *Dagon avendanoi* sp. nov., see below.

Etimology. "Dagon" is the God-Fish of the Philistines and other Mesopotamian nations. Also "Dagon" deity revered for the Deep Ones from the story "Dagon" by H. P. Lovecraft

Diagnosis. As in the type species, see below.

Dagon avendanoi sp. nov

Holotype. IHNFG-5333, an almost complete individual exposing the left side of the body, in which large part of the head bones are dissolved, lost, or so fragmented that many bones of the right side are exposed showing their middle internal surface (Fig. 2).

Locality and age. Cenomanian laminated limestones deposits of the El Chango quarry; Cintalapa Formation, Ocozocoautla de Espinosa Municipality, Chiapas, southeastern Mexico (Alvarado-Ortega et al., 2009; Alvarado-Ortega and Than-Marchese, 2012, 2013).

Table 1
Body measurements and proportions of the specimen IHNFG-5333. The measurements are expressed in millimeters. Within single and double parentheses, the body proportions as % of the SL and HL respectively appear. Symbology: ≈, approximate measurement.

Total length (TL)	232
Standard length (SL)	189.5
Head length (HL)	54.5 (28.75)
Head height (HH)	41.5 (21.8)
Ocular diameter	11.9 ((21.8))
Maximum body height (MBH)	45.5 (24.01)
Caudal peduncle height (CPH)	10.8 (5.6)
Predorsal length (PDL)	84.4 (44.5)
Dorsal fin length (DFL)	29.9 (15.77)
Dorsal fin rays/pterygiophores	19/19
Pectoral fin rays	7
Prepelvic length (PPL)	75 (39.5)
Pelvic fin rays	8
Preanal length (PAL)	130.8 (69)
Anal fin length (AFL)	42.6 (22.48)
Anal fin rays/pterygiophores	25/25
Total/abdominal/caudal vertebrae	44/18/26

Etymology. The species epithet honors our friend and colleague, Manuel Javier Avendaño Gil, for his contributions to the development of paleontology in Chiapas.

Diagnosis. Enchodontid fish differing from others members of the family by the autapomorphy of a palatine bearing two large fang like teeth, as well as a combination of features, including the fusiform body with head length 25% of the standard length; premaxilla deep anteriorly with no ascending process; lower jaw three times longer than high; two rows of dentary teeth; dentary teeth behind to longest tooth decreasing in size posteriorly; ventral portion of preopercle broadens anteriorly and posteriorly; two postcleithra; three supraneurals; a complete series of ossified scales carrying the lateral line, in which the anterior ones small and the posteriors are larger.

3.2. Description

General features and proportions. Table 1 summarizes the body measurements and proportions of the IHNFG-5333, holotype and the only specimen known of *Dagon avendanoi* gen. and sp. nov. The overall body shape of this species is fusiform and robust; it resembles that of some other species of the genus *Enchodus*, e.g. *E. brevis* Chalifa (1989), and *E. marchesettii* (Kramberger, 1895). The total and standard lengths (TL and SL) are 232 and 189.5 mm respectively. The head is triangular and about 24% longer than high and its length is 28.75% of the SL. The

Fig. 2. *Dagon avendanoi* gen, and sp. nov. Holotype IHNFG-5333, from the early Cenomanian deposits of the El Chango quarry, Cintalapa Formation, Ocozocoautla de Espinosa, Chiapas, México.

orbit diameter is 28% of the head length. The dorsal border of the trunk is slightly inclined upward between the occipital and the dorsal fin base; hence, the middle part of the trunk is somewhat higher than the head. The maximum body height represents 24% of the SL and the predorsal length that is 44.5% of the SL. Both pectoral and pelvic fins are located on the ventral border of the body; the pelvic fins are subthoracic, located at 39.5% of SL, their origing is at level of vertebrae eight and nine and they are opposed to the middle of the predorsal part of the trunk. The dorsal and anal fins are triangular. The dorsal fin is relatively short; its length is 15.7% of the SL; originates at 44.5 and goes to 60.2% of the SL. Contrary, the anal fin length is 22.48% of the SL and is located far back on the body, between 69 and 91.48% of the SL, and it originates behind the dorsal fin. Behind the anal fin, the caudal peduncle is extended along the last six preural centra; its height is 5.6% of the SL. The fork of the caudal fin is deeper than the trunk than the trunk and consists of two deeply forked lobes of similar size.

Skull. The skull is triangular, longer than high. Although it is poorly preserved because the bones of its left side are almost entirely lost; its fragmentary bones show valuable data. The ethmoid, ocular, and otic-occipital sections of the skull show comparable lengths. In the ethmoid region, fragments of the mesethmoid show that this was a robust bone with a rounded and stout anterior process, wide lateral wings, and a flat rear overlapped by the frontals. There are fragments of an elongated and tubular nasal occupying the nasal capsule. The lateral ethmoid is a stout roughly rectangular bone located between the frontal and parasphenoid forming the posterior edge of the nasal capsule and the anterior edge of the orbit. The orbital section of the parasphenoid bone is a uniformly thin and toothless rod like structure. Anteriorly the parasphenoid is attached with the thickened and basal end of the lateral ethmoid bones before it reaches the vomer. It is impossible to define if the vomer is unique or paired.

The frontals are elongated bones that roof most of the skull, from the anterior edge of nasal capsule to beyond the orbit (Fig. 3). Anteriorly, the narrow anterior edges of frontals articulate with the mesethmoid; and posteriorly, they are laterally expanded and suture with the parietals, pterotic, and autosphenotic. Since the skull of IHNFG-5333 is laterally preserved, the suture between the frontals is unknown. It seems that the frontals are smooth bones except for a small posterior area, near the parietals, where they are ornamented with somewhat parallel short ridges. Due to bad preservation, it is unclear if the supraorbital sensory canal which runs along the frontals is enclosed by bone or exposed.

The small and rectangular parietal bones roof the posterior part of the skull but, it is unclear if they meet in the midline or are partially or totally separated by the supraoccipital bone. The supraoccipital bone is not preserved. The temporal foramen is present as a shallow dorsolateral depression in the skull that involves the posterior part of the frontal and all the parietal. Ventrally, the parietal sutures with the sphenotic and pterotic bones, which are poorly preserved to distinguish its limits.

Upper jaw. The premaxilla, maxilla, and a single supramaxilla form the upper jaw (Fig. 3). The left premaxilla is lost and the right one, preserved below the right palatine, exhibits large part of its inner surface; this is a laminar elongated wedge-shaped bone, three times longer than high. The alveolar border of the premaxilla is straight and occupies two thirds of the lower jaw length, its anterior edge i higher than the posterior and has a wide foramen for a large dentary fang. The premaxillary alveolar border carries a single row of eight conical teeth of decreasing size in anteroposterior order. The teeth are uniformly distributed and slightly curved backward. The premaxillary teeth are smaller than those of the lower jaw (Fig. 3).

Only fragments of the left maxilla are preserved; these reveal that this is a straight, flat, and smooth bone uniformly height. Although the length of this edentulous bone is about the half of the lower jaw; its anterior section is overlapped by the posterior premaxillar end. The supramaxilla is a smooth laminar elongated triangular bone that rests above the posterior section the maxilla.

Lower jaw. This jaw is a stout elongated triangular structure, about three times longer than high, with a short postarticular process, shallow symphysis, and poorly developed coronoid process is. The lower jaw extends backward beyond the orbit (Fig. 3). Although the outer surfaces of the lower jaw are strongly dissolved; it is possible to recognize that its bones are intensity ornamented with conspicuous longitudinal ridges.

The dentary bone constitutes 80% of the lower jaw length. The ventral border of the dentary is slightly convex, and the anterior tip displays a kind of chin consisting of four stout dental prongs. The dentary alveolar border is slightly sinuous and occupies two thirds of the lower jaw length. Just on the dentary alveolar border there is a row of at least ten stout and comparatively large teeth of variable size and shape. The teeth are slightly laterally compresses, curved backward and are uniformly distributed, including a very large anterior fang that occludes with the premaxillary tooth foramen and a posterior series of short and more conical teeth. A second row of dentary teeth includes small teeth that are scattered and preserved on an internal plane along the lower jaw.

The anguloarticular occupies the remaining 20% of the lower jaw length. The ascending posterior edge of this bone, above its short articular process, shows a thick band. The articular facet for the quadrate is present on the dorsal surface of the articular process, so the articulation of the lower jaw and the quadrate is laterally exposed. The retroarticular is a small triangular bone that occupies about a third of the lateral surface of the articular process.

Circumorbital bones. Fragments of laminar bones scattered around the orbit correspond to the circumorbital bones; their number and forms cannot be described. This fish does not have supraorbital bones. Remains of possible two semicircular and flimsy sclerotic bones occupy the eyeball.

Suspensorium. The left quadrate is only partially exposed; it seems to be a triangular structure with straight borders. The developed and ovoid head of this bone is projected downward showing an extensive joint surface, which extends from its anterior to posterior borders and fits with the deep articular facet on the postarticular process of the lower jaw. The joint surface in the articular facet is so extensive that includes part of the base of posterior ascending edge of anguloarticular bone. The anterior tip of the horizontal preopercular limb reaches the posterior edge of the quadrate. The articulation between the articular facet of lower jaw and the quadrate is laterally exposed. The sympletic is a flimsy and nail-shaped bone located in a deep notch.

Although metapterygoid and entopterygoid are very damaged, remains of these bones show that the first is extended and occupies large part of the cheek while the second is an small elongated flat bone placed in the ventral edge of the orbit below the parasphenoid. Only small part of the left hyomandibula is visible; the high and narrow ascending process of this bone runs parallel the ventral limb of the preopercle and joins the quadrate just in front of the anterior vertex of both preopercular limbs. The articular head of the hyomandibula is elongated and dorsally convex (Fig. 3).

The most striking bones in the suspensorium are the ectopterygoid and the palatine, which bear conspicuous teeth. The ectopterygoid is an elongated thick bone that bears five or six stout conical teeth, which are someway laterally compressed, of drecreasing size in anteroposterior order, and curved. The tips of posterior two ectopterygoid teeth are bent forward, two middle teeth of this bone are rather straight, and the two most anterior and largest ectopterygoid teeth are curved backward. The anterior edge of the ectopterygoid is deeply sinuous and forms a tight suture with the posterior palatine edge, below the ethmoid skull region. The palatine is a stout elongated bone that is higher than the ectopterygoid anterior edge. The ventral palatine edge bears two large fang-like teeth that also are somewhat laterally compressed; one is on anterior terminal position and the other in the middle of the bone (Fig. 3). The dorsal edge of this bone articulates with the vomer.

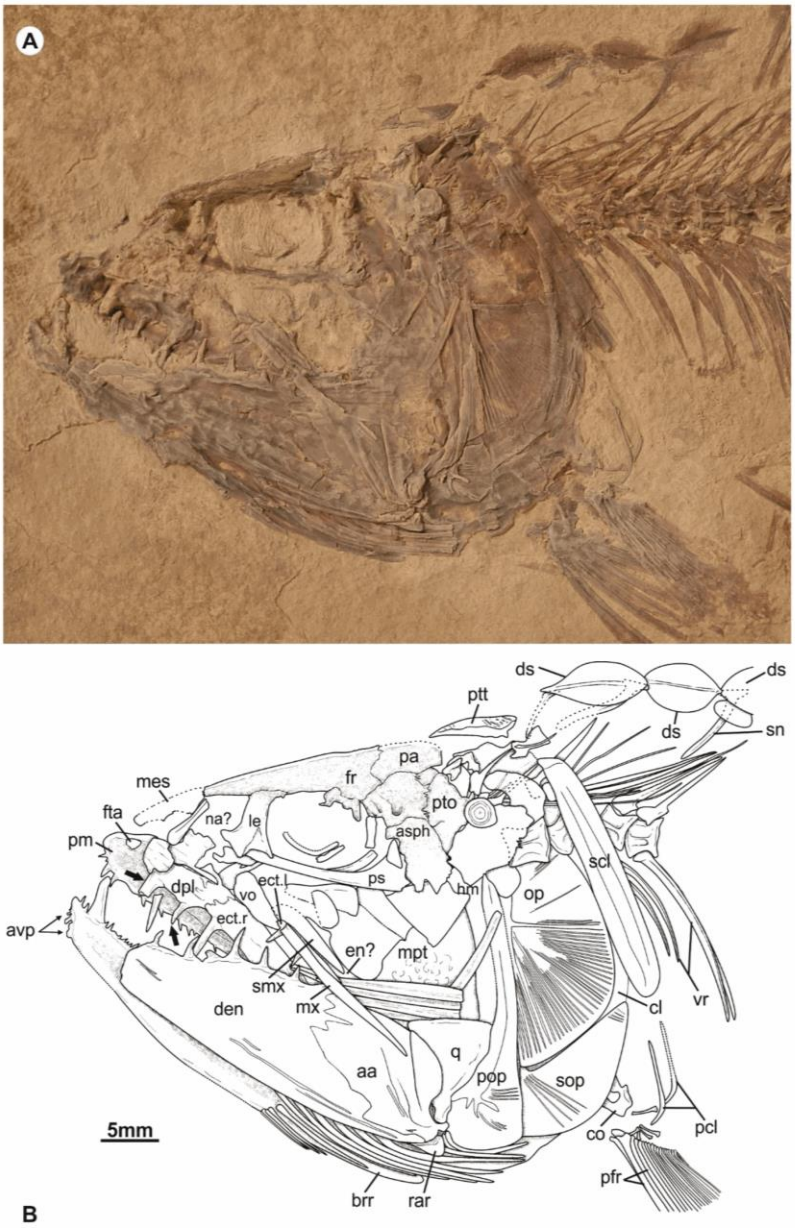

Fig. 3. *Dagon avendanoi* gen, and sp. nov. A) Lateral view of the head; B) Diagram of the head and pectoral girdle in lateral view. Abbreviations: aa, anguloarticular; asph, utosphenotic; avp, anteroventral prongs; brr, branchiostegal rays; cl, cleithrum; co, coracoid; den, dentary; dpl, dermopaltine; ds, dorsal scutes; ect, ectopterygoid; en, endopterygoid; fr, frontals; fta, fenestra; hm, hyomandibula; le, lateral ethmoid; mes, mesethmoid; mpt, metapterygoid; mx, maxilla; na, nasal; op, opercle; pa, parietals; pcl, postcleithrum; pfr, rays of the pectoral fin; pm, premaxilla; pop, preopercle; ps, parasphenoid; pto, pterotic; ptt, posttemporal; q, quadrate; rar, retroarticular; scl, supracleithrum; smx, supramaxilla; sn, supraneurals; sop, sobopercle; vr, s. Letter l, indicates left side. Arrows points out the lower posterior bar of the anguloarticular. Arrows point-out the palatine teeth.

Opercular bones and branchiostegal rays. The opercular series consists of three flat and laminar bones, the opercle, preopercle, and subopercle (Fig. 3). This fish does not have interopercle. The opercle is a kindey-shaped bone, about 1.5 times higher than wide, with its ventral region being slightly more expanded. The anterior edge of this bone is straight and thick. The hyomandibular articular facet is placed on the anterior edge and at the beginning of the upper quarter of this bone. The outer opercular surface is strongly ornamented with ridges and tubercles that radiate from the hyomandibular articular facet. A conspicuous straight longitudinal thick bar or strengthening ridge extends all along this bone.

The subopercle is a semicircular plate with the dorsal edge straight, two times longer than high, and as elongated as the ventral section of the opercle. This bone covers large part of the ventral section of the cleithrum. The anterior dorsal process of this bone is covered. The outer surface of ventral region of this bone is strongly ornamented with tubercles and ridges radiating from its anterior dorsal region.

The preopercle is a high flat bone with drop-like profile and probably as high as the opercle. In this bone, the vertical limb tapers upward forming a sharp dorsal tip, the posterior edge is practically straight, and its ventral region is expanded forward forming a rounded horizontal limb that meet with the posterior edge of the articular head of the quadrate bone. The preopercular sensory canal runs near the anterior edge of this bone and opens through three or four pores that are extended forming deep grooves that are curved backward. The outer surface of the ventral region of this bone is intensely ornamented with

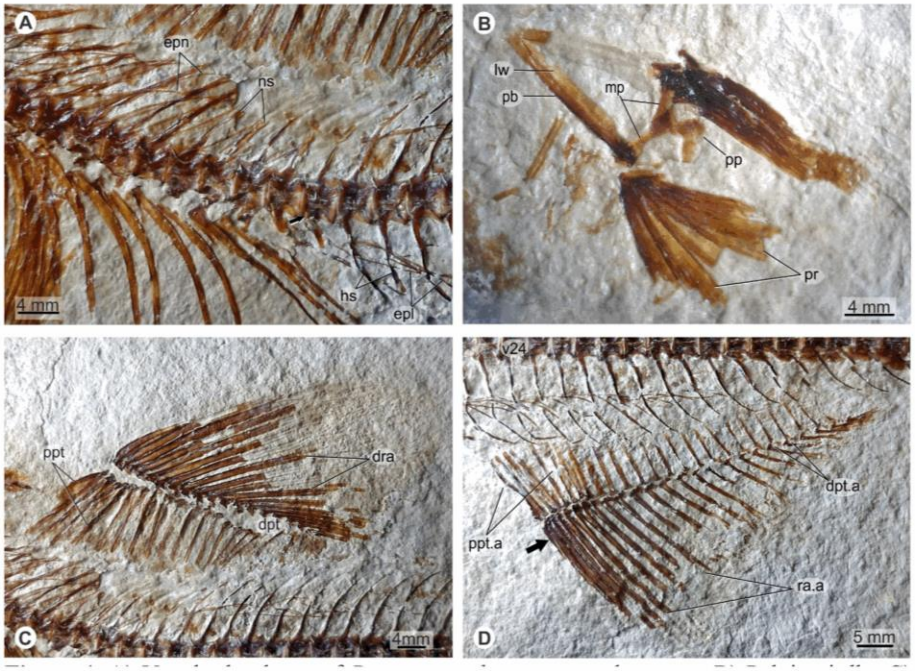

Fig. 4. A) Vertebral column of *Dagon avendanoi* gen, and sp. nov. B) Pelvic girdle, C) dorsal and D) anal fin. Abbreviations: dpt, distal pterygiophores; dpt.a, anal fin distal pterygiophores; dra, dorsal fin rays; epl, epipleurals; epn, epineurals; hs, haemal spine; lw, lateral wing; mp, medial process; ns; neural spine; pb, pelvic bone; pp, posterior process; ppt, proximal pterygiophores; ppt.a, anal fin proximal pterygiophores; pr, pelvic fin rays; ra.a, anal fin rays. Arrow points-out the spine-like first anal fin ray.

radiating ridges and tubercles, resembling those of the opercle and subopercle. In this species there are at least 14 elongated, flat, and curved branchiostegal rays extended from the middle part of the lower jaw to the anterior ventral tip of the cleithrum.

Vertebral column. IHNFG-5333 has 44 total vertebrae, including 18 abdominal, 24 caudal, and two ural centra. The centra are rectangular, slightly constricted in the center, and exhibit a middle longitudinal reinforcing ridge. The anterior centra are slightly longer than high; however, these progressively become shorter. Throughout the vertebral column, the neural and hemal arches are autogenous but, are tightly attached to the cavities or pits on the ventral and dorsal surfaces of the respective centra (Fig. 4A). Most anterior abdominal centra have ventrolateral pits to joint with the ribs; however, the last nine of these centra develop lateral paraphyses to joint with the expanded articular head of the ribs; these parapophyses are triangular and show increasing size in anterior-posterior order. There are preserved 14 pairs of elongated abdominal ribs so extended that enclose the upper three quarters of the abdominal cavity.

In the abdominal region, the anterior five of six centra are associated with neural arches composed of two unfussed halves that are upward enlarged formed a bifid neural spine. Remaining neural arches as well as all hemal arches and their respective neural and hemal spines are unpaired elements. The anterior half of the abdominal centra show neural spines straight and tilted backward; beyond these, all neural spines and all the hemal spines are rather curved backward. The hemal and neural spines of the posterior preural centra are progressively shorter. Both neural and hemal spines are not in contact nor placed between the dorsal or anal pterygiophores.

Along the trunk there are long and slender epineurals associated with the neural bone elements of all abdominal and the 13 anterior preural centra. Those epineurals associated with the most anterior abdominal centra have a tilted back position, are extended over five or six centra, and are attached to lateral surface of the respective centra. The size and position of these bones progressively change along the trunk; the last epineurals have a horizontal position, are extended over two preural centra, and are attached to the middle part of the respective neural spine.

Long and slender epipleurals are also present along the trunk. These bones are extended below three or four centra and associated with the last two abdominal centra and the anterior fourteen caudal centra. The position of these bones also changes from the anterior epipleurals inclined backward to those located at the end of the series that rest horizontally. The anterior tips of first two epipleurals rest on the parapophyses of abdominal centra while those of subsequent epipleurals rest on the respective hemal spines, occupying positions each farther from the respective hemal arch.

Although incomplete, it is possible to recognize three supraneurals (= predorsal bones) behind the occiput and separated from each other (Fig. 6A). These T shaped bones are about four times higher than long, in which the ventral limb is a stick curved forward, so ventrally elongated that the proximal end s is located into the space between the neural spines. The expanded and flat horizontal limb of these bones is extended along the dorsal edge of the trunk. The horizontal limbs of supraneurals seem intercalated with the dorsal scutes; the supraneural 1 contacts the anterior tip of dorsal scute 1, the supraneural 2 contacts the posterior tip of predorsal 1 and the anterior tip of predorsal 2, and so on.

Pectoral girdle and fin. Isolated remains of the left posttemporal are preserved in IHNFG 5333; these show that this bone is triangular and anteriorly tapered with a scratchy dorsal surface. The anterior dorsal process of this bone is long and projected forward; there are traces showing the shape and size of its small ventral process.

The posterior tip of the posttemporal covers the dorsal tip of supracleithrum. The latter is a trapezoidal and flat bone with an expanded

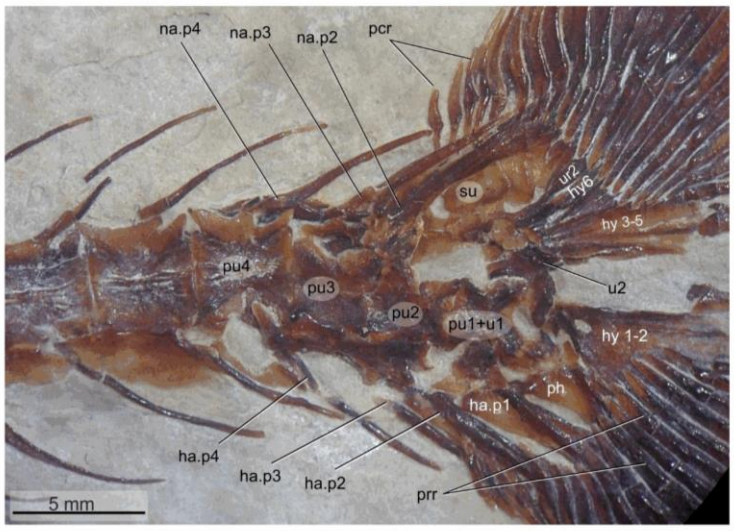

Fig. 5. The caudal skeleton of *Dagon avendanoi* gen, and sp. nov. Abbreviations: ha.p. haemal arch of the preural; hy, hypural; na.p. neural arch of the preural; pcr, procurrent rays; ph, parhypural; prr, principal rays; pu, preural; su, stegural; u, ural; ur, uroneural.

dorsal end; it is about six times higher than long. The supracleithrum rests on the lateral flank of the trunk, from the occiput up down the vertebral column, covering the upper middle part of the cleithrum and reaching the beginning of the abdominal cavity. The outer surface of the bone is ornamented with scarce blunt tubercles and dorsoventral grooves.

Although the subopercle and opercle cover a lot of the lateral outer surface of the cleithrum; the shape of this bone resembles a boomerang or an inverted C, evenly wide, and with an obtuse anterior concavity, in which the height of the vertical limb is two times the length of the horizontal one. The outer surface of the cleithrum is scarcely ornamented with blunt tubercles and dorsoventral ridges. The scapula and coracoid are partially covered by the ventral limb of the cleithrum. The coracoid shows its typical donut shape, pierced in the center. Two postcleithra are present; the dorsal one is ovoid, flat, and tilted backward while the ventral one is a small and thick rod-like structure distally curved (Fig. 3).

Since the trunk of this fish is practically nude, its left and right pectoral fins are exposed. At least three elongated and flat radial bones with wide ends support the proximal ends of pectoral rays and joint with the coracoid. Fifteen rays, distally segmented and branched, form the pectoral fin. The pectoral fins rays are progressively shorter in an anteroposterior direction; the anterior ones are the most conspicuous, as long as six abdominal centra and somewhat wider than the subsequent rays.

Pelvic girdle and fin. In IHNFG 5333, the pelvic fins are located in the anterior half of the abdominal cavity, below the centra 11 and 12; however, some ribs of this specimen are dislocated and piled up in the middle part of the abdomen, this suggests that the pelvic fin may also be dislocated from its life position.

The pelvic girdle is triangular and consists of two pelvic bones that meet medially only at their proximal and distal ends. Each pelvic bone is a rectangular structure (= central part of Stiassny and Moore, 1992), which is longitudinally supported with a thickened central axis and shows an inconspicuous internal wing. At its posterior end, the pelvic displays a stout median process, which forms an obtuse angle with the anterior part of this bone, sutures with its counterpart medially, and has a well-developed posterior process. The articular surface of pelvic bones is present in its lateral external corner, where a small lateral process protrudes outward. Eight flat, broaden, and distally segmented and branched rays constitute each pelvic fin, among which the larger ray is as long as four abdominal centra (Fig. 4B). No radial bones are recognized in these fins.

Dorsal fin. This relatively short and triangular fin consists of 19 rays, including the anterior one that is unsegmented and unbranched plus 18 rays distally branched and segmented. This fin is located above the vertebral centra 15–25 and opposed to the posterior half of the abdominal cavity. The length of the first branched dorsal fin ray equals that of three abdominal centra; the subsequent ray is about twice longer, and the third is the longest in the series being about two and a half times longer than the first ray. Posterior dorsal fin rays are progressively shorter. The last and first branched dorsal ray are equally long.

A series of 19 dorsal pterygiophores internally support the dorsal fin (Fig. 4C). The anterior proximal pterygiophores are stick-like bones with anterior and posterior wings and a widened proximal articular head; the last three pterygiophores lack these wings, and only in the first of these pterygiophores the anterior wing has an anterior thickening. The length of these bones is reduced along the series; hence, the last one is contained 2.5 times in the length of the first proximal dorsal pterygiophore. Between the proximal pterygiophores 8 to 11 there are some stout elongated middle pterygiophores having broadened ends, as well as somewhat oval distal pterygiophores.

Anal fin. This fin is relatively long and triangular; it is located far in the back of the trunk, opposite to the postdorsal section of the body, and below the preural centra 4 to 16. The anal fin consists of 26 anal rays including two short, unsegmented and unbranched, plus 24 long rays, distally branched and segmented. Among these, the second segmented ray is the longest of the fin and the posterior ones are progressively shorter.

Twenty-five stick-like proximal pterygiophores support the anal fin; anterior and posterior laminar projections or wings are present from the second to the tenth of these bones. The first anal proximal pterygiophore joints with the first short unsegmented ray, the second with the following two rays, and beyond proximal pterygiophores and anal fin rays have a relation one to one (Fig. 4D). The first six of these proximal pterygiophores are as long as four centra and the posterior proximal pterygiophores tend to be shorter. The posterior half of the anal fin is also supported by elongated medial pterygiophores and small oval distal pterygiophores.

Caudal fin. The expansion of this fin exceeds the maximum depth of the body; the fin is deeply furcated and consists of two equal triangular caudal lobes (Fig. 5). The caudal fin rays follow the caudal formula xi + I+9–8+I + xii, in which the dorsal lobe has 11 procurrent and 10 principal rays (including one segmented and unbranched plus nine segmented and branched) while the ventral lobe shows 12 procurrent and 9 principal rays (including (including one segmented and unbranched plus nine segmented and branched). The proximal tips of caudal fin rays are sharp except in the four innermost rays, two in the dorsal lobe and other two in the ventral one, in which these ends are rounded and broad.

The caudal fin is supported by the elements associated with four preural and two ural centra. Hemal and neural spines of these centra are curved backward reaching the level of anterior procurrent rays. Ural 1 and preural 1 are not well exposed in the specimen; however, probably these are fused forming a composite centrum. Ural 2 is relatively small in comparison the subsequente anterior preural centra. The hemal and neural arches of these centra are autogenous. Neural arch of the pleural 3 is robust and has a large spine; contrary, the neural arch of preural 2 is flat, wide, and triangular, and do not have a spine while the neural arch of the composed caudal centra (preural 1 + ural 1) is also flat, triangular, and fused with the single uroneural forming the stegural. At least two flat and oblong epural bones are present behind neural spine of preural 3 and above the stegural.

Hemal arch of preurals are stout and bears a complete elongated spine except in the preural 1. Hemal arche of preural 1, the parahypural, and a composed hypural plate (hypural 1 and 2 fused) joint with the composed caudal centra (preural 1 + ural 1); these arches are stout and have large spines that display an anterior wing extended from the base to the middle part of the spine. Probably a posterior, elongated, and laminar uroneural bone is present in this fish, resting on the posterior part of the stegural.

The proximal section of hypurals 1 and 2 are partially fused forming a wide triangular ventral hypural plate. Anteriorly, this plate shows a small fenestra that seems to be result of the incomplete fusion of these bones as well as a large ovoid fenestra previously observed on the hypural 1 of enchodontids with no hypural plate (i.e. Goody, 1969, Fig. 42). At least four rectangular hypurals of decreasing size joint with the ural 2. It seems that there is a conspicuous caudal hiatus between the hypural plate and hypural 3; however, probably this empty space is an artifact of the preservation. This observation is based on the presence of a deep groove along the ventral edge of the hypural 3, in which the dorsal edge of the ventral hypural plate may be fitted in life.

Scutes and scales. The trunk is practically nude except for the presence of three dorsal scutes covering entire anterior dorsal border, between the occiput and the dorsal fin base, and a flank row of scales enclosing the lateral line that is extended throughout the trunk, from the back of the fish to the base of caudal skeleton (Fig. 6).

The dorsal scutes are ovoid and have a middle longitudinal thickened axis that protrudes anteriorly and posteriorly forming sharp tips. The scutes are overlapping, the posterior tip of one scute rests on the anterior surface of the posterior subsequent one. Although in IHNFG 5333 these scutes expose their smooth internal surface; when these are moistened with water or alcohol, it is possible to see that the external and dorsal surface of these scutes is ornamented with lines of tubercles and ridges radiating from the scale center. The first predorsal scute is about 1.3 times longer than the posteriors (Fig. 6A).

A continuous series of smooth scales bearing a longitudinal central canal for the lateral line is preserved in each flank of the trunk. This scale series follows a sigmoid trajectory throughout the trunk; this rises in the rear of the supracleithrum, is abruptly curved downward in the middle of the abdominal region, reaching the vertebral column at the beginning of the caudal region of the trunk; these scale follow a straight trajectory covering the lateral surface of caudal centra; and near to the caudal skeleton these are located slightly below the centra. In the anterior part of the trunk, these scales are relatively small, elongated and somewhat square; those placed near and on the vertebral column are progressively larger, thicker, and became heart-shaped (cordiform) with a middle longitudinal external supporting ridge (Fig. 6).

3.3. Taxonomical remarks

In previous studies of the family Enchodontidae, the naturalness of this group was supported by at least four characters, the presence of a single terminal tooth in the palatine, dermopaltine bone same length or shorter than its tooth, the lack of interopercle, and the presence of middorsal scutes (Fielitz, 2004, Fig. 2; Fielitz and González-Rodríguez, 2010, Fig. 11; Silva, 2007, Fig. 9; Silva and Gallo, 2011, Fig. 1). The first character was recognized as not synapomorphic for the family, since this condition is also found in *Ophidercertis*, a genus of Decertidae (Taverne, 2005; Silva and Gallo, 2011).

Dagon avendanoi gen. and sp. nov shows the last two of these characters supporting its inclusion as a member of the family Enchodontidae. Recently, after the discovery of *Unicachichthys* the number of teeth on the palatine was revealed as a variable or multistate character among the enchodontids (Díaz-Cruz et al., 2016, Fig. 13); therefore, the synapomorphic or diagnostic status of the presence of a single terminal palatine tooth on Enchodontidae is indeed rejected. In fact, *Dagon* differs from all other enchodontids because it has two palatine teeth while *Unicachichthys* has a patch of many small palatine teeth, *Saurorhamphus* has a row of about ten palatine teeth, and other enchodontid genera have only one palatine tooth.

The enchodontid fishes show five main general body patterns resulting from deep skeletal modification. Among these *Saurorhamphus* is

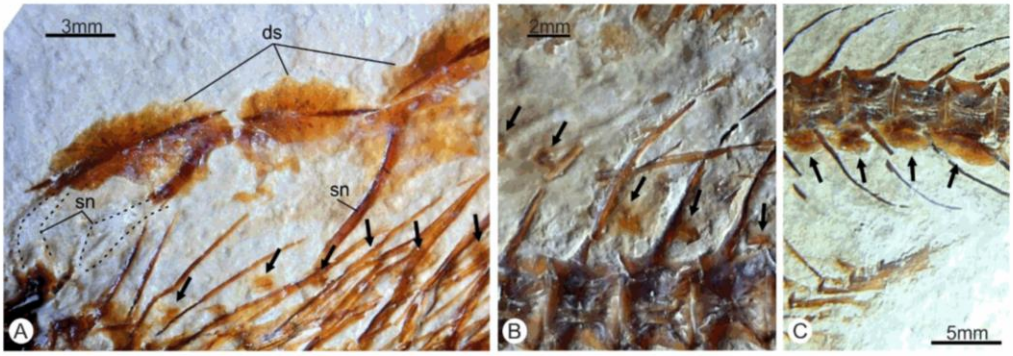

Fig. 6. A) Dorsal scutes of *Dagon avendanoi* gen, and sp. nov. and scales of the lateral line scales in the A) anterior, B) middle, and C) posterior regions of the trunk of *Dagon avendanoi* gen, and sp. nov. Arrows point-out scales in each region.

a fish with longirostrine head and elongated trunk; *Parenchodus* has a pug-nosed head with a peculiar high rounded trunk; *Palaeolycus* displays a pug-nosed head and an elongated body; *Enchodus* and *Unicachichthys* display a pug-nose head and pisciform trunk; and finally, *Eurypholis* is a fish with a moderate longirostrine head and pisciform trunk. IHNFG 5333 shares the pug-nose head and pisciform trunk with *Enchodus* and *Unicachichthys*.

Additionally, *Dagon avendanoi* gen. and sp. nov. has remarkable peculiar characteristics that make it easily differentiable from other enchodontids. *Eurypholis* and *Saurorhamphus* form the subfamily Eurypholinae that is supported on two peculiar characters, the articulation between the lower jaw and the quadrate is laterally covered and the opercle shows a middle acute angle or spine (at the end of the horizontal middle horizontal strengthening or bar of this bone). Contrary, in *Dagon* and all other enchodontids this articulation is laterally exposed and the posterior edge of the opercle is harmoniously rounded, with no spines or acute angles.

Palaeolycus and *Parenchodus* represent the extremes of body plasticity within Enchodotidae, and therefore, these are easily differentiable from *Dagon* gen. nov. and other enchodontids. *Palaeolycus* has an elongated trunk with 73 total centra, five predorsal scutes between the occipital and dorsal fin, and a high dentary symphysis (Goody, 1969, p. 95–98). Besides, *Parenchodus* has a high rounded trunk, with only 30 total vertebrae and only two predorsal scutes, and a shallow dentary symphysis (Raab and Chalifa, 1987, p. 724–729). In contrast, *Dagon* and other enchodontids have an intermediate number of total vertebral centra, which ranges between 38 and 45, three predorsal scutes, and a shallow dentary symphysis.

3.4. Phylogenetic analysis

The present phylogenetic study of family Enchodontidae is remarkable because it is based on the most comprehensive data set and provides two complementary phylogenetic hypotheses, one based on a Bayesian analysis and the other based on a Maximum Parsimony analysis. The Appendix of this work shows the complete descriptions and results of both phylogenetic analyses, which show that *Dagon avendanoi* gen. and sp. nov. represents a new member of the family Enchodontidae (Fig. 7).

The Bayesian analysis reveals that the enchodontids, now including *Dagon* gen. nov., have a high posterior probability to constitute a monophyletic group, the family Enchodontidae, which is the sister group of *Rharbichthys*, and together these constitute the sister group of *Cimolichthys* (Fig. 7A). Although within the family Enchodontidae, the relationships of *Enchodus*, *Parenchodus* and *Palaeolycus* are unclear; this result, shows that the two nominal enchodontid species from the El Chango quarry, *Dagon* and *Unicachichthys*, constitute a monophyletic group. This result agrees with previous studies, in which Enchodontidae and Cimolichthyidae are recovered as sister groups and part of the monophyletic Superfamily Enchodontoidea (Fielitz, 2004; Davis and Fielitz, 2010, Fig. 1:1196; Díaz-Cruz et al., 2016, appendix I, Figs. 1 and 2); however, the position of Cimolichthys as part of Echodontidae is refutable because recently, based on morphological data of the gill skeleton, Beckett et al. (2017) concluded that *Cimolichthys* as member of the family Notosudidae (the sister group of Alepisauroidea).

The results of the Maximum Parsimony analysis, performed in this work, show a strict consensus tree with better resolved relationships than that of the Bayesian Inference. The final result of the Maximum Pasimony analysis performed in this research show a strict consensus tree generated from six equally Most Parsimonious Trees (MPTs) (Fig. 3, Appendix). The consensus tree Total Length is 295 steps, the Consistency Index (CI) is 0.463, and the Retention Index (RI) is 0.690. In this phylogenetic hypothesis *Dagon avendanoi* gen. and sp. nov. is placed as a true member of the family Enchodontidae, between its basal member, *Unicachichthys*, and the more derived enchodontids (Fig. 7B). Contrary to Fielitz (2004), this result confirms that *Rharbichthys* does not belong to family Enchodontidae, as it was previously noted by Silva and Gallo (2011) and Díaz-Cruz et al. (2016). *Rharbichthys* does not have any longitudinal strengthening ridge along the opercle, whereas *Dagon avendanoi* and other enchodontids share the presence of an opercle with a middle longitudinal strengthening ridge or bar (see Appendix, character 47–1, Fig. 3).

In the present phylogenetic hypothesis, the family Enchodontidae, including *Dagon avendanoi* gen. and sp. nov., is supported by three synapomorphies (Fig. 7B, node C; Appendix, Fig. 3), including the lack of the supraorbital bone (character 43–1), the presence of a longitudinal strengthening bar or ridge along the opercle (character 47–1), and the opercle and subopercle bones ornamented with ridges and tubercles (character 50–2). Regarding this study, *Dagon* is an unquestionable member of this family because it has all these synapomorphies. Additionally, this family also show three homoplasies that include the presence of anteroventral prongs on dentary (character 36–1),

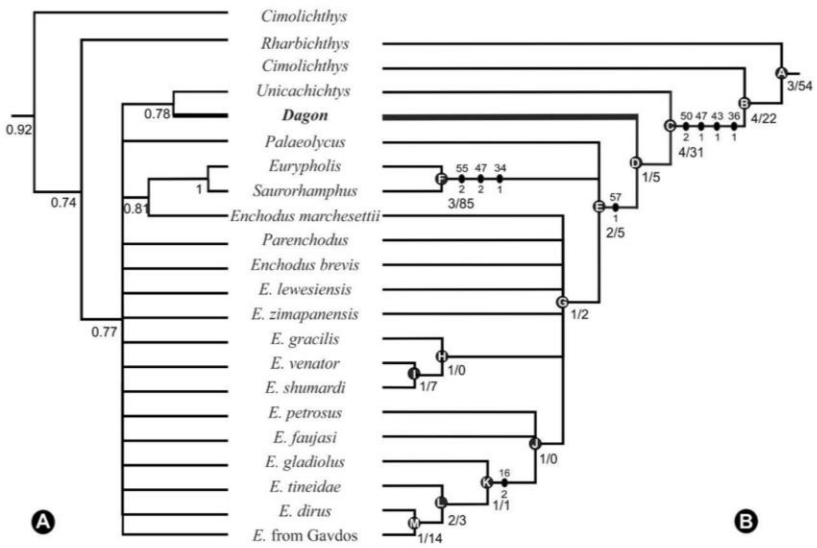

Fig. 7. Phylogenetic hypotheses of Enchodontidae obtained in this work. A) Bayesian Analysis (numbers by nodes indicate posterior probabilities supporting each clade). B) Consesnsus tree of six Most Parsimonious Trees generated in the Maximum Parsimony Analisis. Only the synapomorphies of Enchodontidae and its subtaxa are indicated B, see the complete description of these trees in the Appendix. Family Enchodontidae (Node C): 43–1, supraorbital bone absent; 47–1, opercular horizontal strengthening bar present; 50–2, opercular and subopercular dermal ornamented with tubercles along each ridge. Enchodontidae less *Unicachichthys* and *Dagon* (Node E): 57–1, only one postcleithrum. Subfamily Eurypholinae (Node F): 34–1, articulation between mandible-quadrate hidden or covered for the anguloarticular bone; 47–2, opercular horizontal strengthening bar overhang the posterior edge of this bone forming an acute angle or spine; 55–2, ventral portion of cleithrum widens anteriorly and posteriorly. Group of *Enchodus gladiolus-E.* sp. (Node K): 16–2, the dermopalatine tooth is sigmoidal in lateral view.

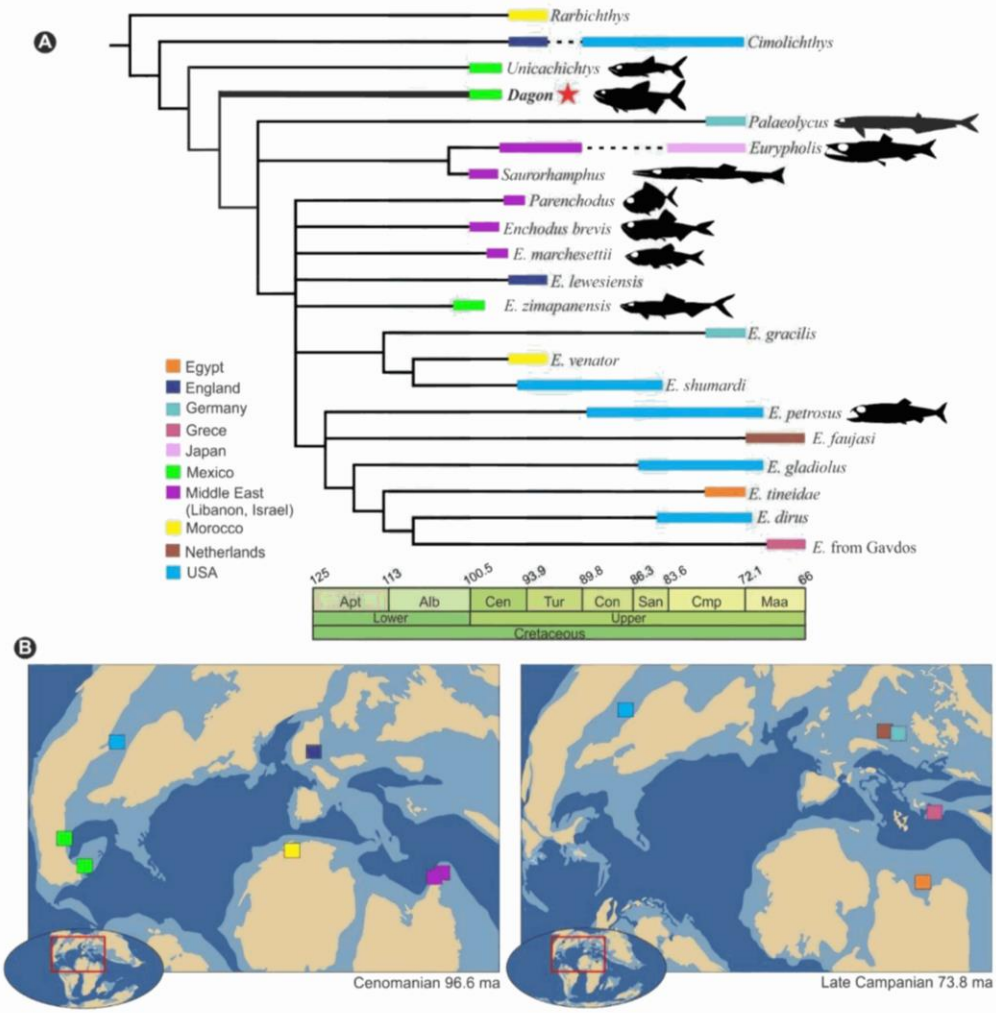

Fig. 8. Temporal and geographical distribution of enchodontid fishes based on data summarized in Table 2. A) Cladogram of the Enchodontidae obtained in the present study showing the temporal distribution of these fishes. B) Paleo-maps showing the geographical distribution of these fishes during the Cretaceous.

preopercle ornamented with ridges and tubercles (character 49–1), and mandibular sensory canal enclosed by bone (character 40–2), of which the first two are also present in *Dagon* (the dentary bone in IHNFG 5333 is superficially bad preserved making it impossible to recognize how the mandibular sensory canal is).

In our present phylogenetic hypothesis, the family Enchodontidae less *Unicachichthys*, is supported by three homoplasies (Fig. 7B, node D; Appendix, Fig. 3). In this group the dentary has two rows of teeth (character 37–1) and long anterior tooth, near to symphysis, that at least is 33% longer than the other posterior teeth of this bone (character 38–1), and the pelvic fin is located anterior to the dorsal fin (character 52–0). Although the pelvic fin probably is dislocated in the single specimen known of *Dagon avendanoi* gen. and sp. nov.; clearly, this Mexican fossil fish forms part of this enchodontid subgroup because it has both characters of dentary bone.

Another subgroup of the family Enchodontidae, which excludes *Unicachichthys* and *Dagon*, is also defined in the present analysis, and gathers *Enchodus, Parenchodus, Eurypholis, Saurorhamphus,* and *Palaeolycus* (Fig. 7B, node E; Appendix, Fig. 3). This is supported on a single synapomorphy, the presence of only one postcleithrum (character 57–1), and two homoplasies, the presence of two carinae in the palatine tooth (character 5–1) and the lack of supramaxilla (character 33–0). *Dagon* lacks these characters (contrary, it has two postcleithra, a supramaxilla, and no carinae in any of its two palatine teeth); such a situation, moves it away from other derived enchodontids, in which the relationships of *Paleolycus*, *Eurypholis* + *Saurorhamphus,* and *Parenchodus* + *Enchodus* are unresolved.

The close relationships of *Eurypholis* and *Saurorhamphus* were previously recognized; Goody (1969) included these genera within their own family, Eurypholidae; later Fielitz (2004) re-ranked this group, as subfamily Eurypholinae. In the present analysis, these fishes form the best supported group by sharing three synapomorphies (Fig. 7B, node F; Appendix, Fig. 3); the articulation between the lower jaw and the quadrate is hidden or covered below the anguloarticular and preopercle (character 34–1), the opercular horizontal strengthening bar overhang the posterior edge of this bone forming an acute angle or spine (character 47–2), and the ventral portion of cleithrum widens anteriorly and posteriorly (character 55–2). Additionally, *Eurypholis* and

Saurorhamphus share other homoplasies; the pectoral fin is located far from the edge of the body and it is located between the ventral edge of the trunk and the vertebral column (character 51–0); the hyomandibula facet of the skull is located in below the dilatator fossa (character 41–3), and tubercles cover the surface of the preopercle, opercle, subopercle, supracleithrum, frontal, and dentary bones (characters 54–2, 56–2, 3-3, 7–1; 49–3, 50–3, in Appendix).

Although the genus *Parenchodus*, known only by one species, is nested with the numerous species of *Enchodus*; this group is weakly supported by 11 homoplasies and lacks synapormorphies (Fig. 7B, node G; Appendix, Fig. 3). In these fishes the parasphenoid is wide beneath the orbit (character 9–1); the endopterygoid has teeth (character 11–0); in cross section, the palatine teeth is elliptical and has an anterior cutting edge (character 15–3); the mandibular canal is open (character 40–0); the lower jaw is ornamented with ridges and tubercles (character 41–2); there is a vertical bar in the posterior ascending edge of the anguloarticular bone (character 42–1); the ventral portion of preopercle broadens anteriorly and posteriorly (character 45–2); and the preopercle is ornamented with ridges and tubercles; the pelvic fin is located at or behind the dorsal fin (character 52–1); the cleithrum is ornamented with ridges (character 56–1); and the percentage of caudal vertebrae is more than 60% of total centra (character 65–2) (see Appendix).

Finally, the present phylogenetic analysis reveals that *Dagon* gen. nov. shows a combination of three homoplasies supporting its singularity. In this fish, the premaxilla is triangular, anteriorly deep and with no ascending process (31–2), dentary teeth of decreasing size are located behind a larger anterior tooth located near the symphysis (character 39–1), and the ventral section of the preopercle is anteriorly and posteriorly broad (character 45–2).

4. Discussion

Enchodus is the enchodontid genus more extensively studied, the most diverse, and with the widest geographical distribution. This is a common fish in marine deposits of Late Cretaceous in North America, Europe and Middle East; therefore, this genus has been a focus of different phylogenetical and biogeographical studies. Based on the occurrence of basal species of *Enchodus,* together with those of related genera as *Eurypholis*, *Saurorhamphus,* and *Parenchodus*, in middle Cenomanian sites of Middle East, Fielitz (2004) and later Cavin et al. (2012) suggested that this genus, and consequently the family, arose during the middle Cenomanian in the eastern domains of the Tethys Sea, in Middle East and Europe. According to these authors, these fishes arrived from this region to other continents (Fig. 8, Table 2), due to subsequent vicariants and dispersion events.

A series of evidence that contrast with the biogeographical hypotheses described above have appeared in Mexico. The reports of Mexican Cenomanian specimens of *Enchodus* and *Saurorhamphus* from the El Chango quarry and its close twin site, the El Espinal quarry, revealed the coeval existence of these genera all along the Tethys Sea, from Mexico to Middle East (Alvarado-Ortega et al., 2009). This first report of Mexican Cenomanian enchodontids gained relevance after discovering that the El Chango is rather an Early Cenomanian deposit (Moreno-Bedmar et al., 2014) and that these fossils include *Unicachichthys multidentata*, the most primitive enchodontid according to recent studies is present among these fish (Díaz-Cruz et al., 2016; Vernygora et al., 2018). A second blow to these hypotheses also comes from Mexico, where Fielitz and González-Rodríguez (2010) described the oldest enchodontid fish as *Enchodus zimapanensis*, discovered in the Albian-Cenomanian deposits of the Muhi quarry, Hidalgo.

Thus, the discoveries of Alvarado-Ortega et al. (2009) and Fielitz and González-Rodríguez (2010) grounded the previous biogeographical hypotheses of enchodontids, because these demonstrate that the Mexican territory possesses the basal and oldest enchodontids. Although the fossil record of Mexico has the oldest and the most primitive assemblageof enchodontids found so far, pointing out that the west of the Tethys Sea played a key role in the evolution of this group; this affirmation could be somewhat premature for at least two reasons: 1) although mostly resolved, the phylogenetic hypotheses of the family Enchodontidae draw an evolutionary pattern for disparity, in which it is hard to define the biogeographical history because practically all the enchodontid genera, except for *Palaeolycus,* appear in a short time during the Late Aptian and Middle Cenomanian in a wide region that includes the domains of the whole Tethyan Sea (Fig. 8). 2) A large number of enchodontids up to now recovered in Mexico still require

Table 2
Nominal species included in the phylogenetic analyses performed in this work.

Taxa	Locality and Age	References
Cimolichthys	Niobra Formation, Kansas; Coniacian-Santonian. Pierre Shale, Wyoming and Western Europe; Campanian. Chalk group, England; Cenomanian-Turonian boundary.	Goody (1970); Friedman et al. (2015).
E. marchesettii	Hakel, Lebanon; Middle Cenomanian.	Goody (1969); Fielitz (2004).
Enchodus brevis	Ein-Yabrud, Jerusalem; Lower Cenomanian.	Chalifa (1989).
E. dirus	Pierre-Shale group, South Dakota; Santonian-Maastrichtian.	Parris et al. (2007).
E. faujasi	NDA, Holland, and Jadet Petites Pyrénées, France; Maastrichtian.	Goody (1969); Breton et al., 1995.
E. sp. from Gavdos	Gavdos, Greece; Middle to Late Maastrichtian.	Cavin et al. (2012).
E. gladiolus	Pierre-Shale group, South Dakota; Santonian-Maastrichtian.	Parris et al. (2007).
E. gracilis	Sendenhorst, Westphalia, Germany; Upper Campanian.	Fielitz (2004),
E. lewesiensis	Chalk group, England; Cenomanian-Turonian boundary.	Friedman et al. (2015).
E. petrosus	Pierre-Shale group, South Dakota; Coniacian-Maastrichtian.	Parris et al. (2007).
E. shumardi	Pierre-Shale group, South Dakota; Cenomanian-Santonian.	Parris et al. (2007).
E. tineidae	Tineida, Dakhla Oasis, Egypt; Upper Campanian.	Holloway et al. (2017).
E. venator	Jbel Tselfat, Morocco; Cenomanian-Turonian boundary.	Khalloufi et al. (2010).
E. zimapanensis	Muhi, Mexico; Albian-Cenomanian.	Fielitz and González-Rodríguez (2010).
Eurypholis boissieri	Namoura, Hekel and Hajula; Lebanon; Middle Cenomanian.	Goody (1969); Forey et al. (2003).
Eurypholis pulchellus	Chalk group, England; Upper Cenomanian to Turonian	Friedman et al. (2015).
Eurypholis japonicus	Izumi Fm., Japan, Campanian	Yabumoto and Uyeno (1994).Uyeno and Minakawa, 1983.
Palaeolycus dreginensis	Sendenhorst, Westphalia, Germany; Upper Campanian	Fielitz (2004); Davis and Fielitz (2010).
Parenchodus longipterygius	Gival-Shaul, Jerusalem; Upper Cenomanian.	Raab and Chalifa (1987).
Rharbichthys ferox	Jbel Tselfat, Morocco; Cenomanian-Turonian.	Khalloufi et al. (2010).
Saurorhamphus judeaensis	Ein-Yabrud, Jerusalem; Lower Cenomanian.	Chalifa (1985).
S. freyeri	Trieste-Komen, Slovenia; Lower Cenomanian.	Goody (1969).
S. giorgiae	Nammoura, Lebanon; Middle Cenomanian.	Bannikov and Bacchia (2005).
Unicachichthys multidentata	El Chango, Chiapas, Mexico; Early Cenomanian.	Díaz-Cruz et al. (2016).
Dagon avendanoi	El Chango, Chiapas, Mexico; Early Cenomanian.	Present study.

study, 3) It is needed a major effort to recover a better resolved phylogenetic hypothesis of this family.

Recent studies show the considerable high diversity of the enchodontid fishes up to now recovered in Mexico (i.e. Alvarado-Ortega et al., 2006a; Alvarado-Ortega et al., 2006b, González-Rodríguez et al., 2016). In addition to those enchodontid species already identified from Chiapas and Hidalgo, the study of specimens of at least other three potential new species from the El Chango are in progress (Díaz-Cruz et al., 2013, 2016, 2017; and Díaz-Cruz and Alvarado-Ortega, 2018a and b); the same situation applies to many fossils from Turonian marine deposits that probably include different species and have been reported from the San José de las Rusias (Tamaulipas), Vallecillo quarry (Nuevo León), Xilitla (San Luis Potosí), Arroyo Las Bocas (Guerrero), as well as the Las Boquillas, La Mula, Los Pilotes, and Venustiano Carranza quarries (Coahuila) and the San José de Gracia site (Puebla) (Maldonado-Koerdell, 1956; Blanco-Piñón, 1998; González-Barba and Espinosa-Chávez, 2005; Porras-Múzquiz and Alvarado-Ortega, 2011; Romero-García, 2013; Giersch, 2014; Giersch et al., 2008).

The present result reveals that the anatomical features of *D. avendanoi* are congruent with the evolutionary history figured out in previous studies based on the data sets progressively updated from that constructed by Fielitz (2004), which has been proving to be reliable and robust. Although satisfactory, these results, should be considered partial because the taxonomic identity and relationships of other enchodontids of Mexico are under study.

4. Conclusions

The morphological data included in the description of *Dagon avendanoi* gen. and sp. nov. support its inclusion as a new member of the family Enchodontidae and also complement the understanding of the taxonomical and morphological diversity of these fishes. The study of the relationships of this species reveals new historical aspects on the early evolution of the family Enchodontidae. *Dagon* is added to other Mexican Cenomanian enchodontids, which show that at the dawn of the Late Cretaceous this family was already present in the western rim of the Tethys Sea, particularly in Mexico, where they found shallow and warm waters that favored their diversification.

The old age and basal phylogenetic position of Mexican enchodontids, mainly of those from the El Chango quarry, are important to reinterpreting the natural history of the family Enchodontidae; so, it this sense these fishes rival those of Europe and Middle East. This contribution is part of a series of works on the Mexican enchodontids that will be published in the near future and may reveal more details about the natural history of this family.

Acknowledgements

This manuscript represents a partial fulfillment of the requirements to obtain the degree of Doctor in Biological Sciences (Systematics) within the Posgrado en Ciencias Biológicas at Universidad Nacional Autónoma de México for the first author. We are in debt with the institutions and people that made this research possible; specially, authors recognize and thank the effort made by the team of the "Poyecto de prospección y resguardo del patrimonio paleontológico de Chiapas" who recovered the specimen herein studied. We also thank the reviewers thoughtful comments and suggestions towards improving this manuscript. UNAM provided the financial support for this research through out the DGAPA-PAPIIT subvention IN 209017. JADC has a personal PhD grant (632640) from CONACYT.

Appendix A. Supplementary data

Supplementary data to this article can be found online at https://doi.org/10.1016/j.jsames.2019.01.014.

References

Agassiz, L., 1833-1844. Recherches sur les Poissons Fossiles. 5 volumes plus supplement. pp. 1420 Neuchâtel, Petitpierre.

Alvarado-Ortega, J., Garibay-Romero, L.M., Blanco-Piñón, A., González-Barba, G., Vega, F.J., Centeno-García, E., 2006a. Los peces fósiles de la Formación Mexcala (Cretácico Superior) en el estado de Guerrero, México. Rev. Bras. Palaontol. 93 (3), 261–272.

Alvarado-Ortega, J., González Rodríguez, K.A., Blanco-Piñón, A., Espinosa-Arrubarrena, L., Ovalles-Damián, E., 2006b. Mesozoic osteichthyans of Mexico. In: In: Vega, F.J., Nyborg, T.G., Perrilliat, M.C., Montellano Ballesteros, M., Cevallos Ferriz, S.R.S., Quiroz Barroso, S.A. (Eds.), Studies on Mexican Paleontology, Topics on Geobiology, vol. 24. Springer, Dordrecht, The Netherlands, pp. 169–207.

Alvarado-Ortega, J., Ovalles-Damián, E., Blanco-Piñón, A., 2009. The fossil fishes from the Sierra Madre Formation, Ocozocoautla, Chiapas, southern Mexico. Palaeontol. Electron. 12 (2.4A), 1–22.

Alvarado-Ortega, J., Than-Marchese, B.A., 2012. A cenomanian aipichthyoid fish (teleostei, acanthomorpha) from America, *Zoqueichthys carolinae* gen. And sp. nov. From el Chango quarry (Cintalapa member, Sierra Madre Formation), Chiapas, Mexico. Rev. Mex. Ciencias Geol. 29 (3), 735–748.

Alvarado-Ortega, J., Than-Marchese, B.A., 2013. The first record of a North American Cenomanian Trachichthyidae fish (Acanthomorpha, Acanthopterygii), *Pepemkay maya*, gen. et sp. nov., from El Chango quarry (Sierra Madre Formation), Chiapas, Mexico. J. Vertebr. Paleontol. 33, 48–57.

Amaral, C.R., Alvarado-Ortega, J., Brito, P.M., 2013. *Sapperichthys* gen. nov., a new gonorynchid from the Cenomanian of Chiapas, Mexico. In: Arratia, G., Shultze, H.-P., Wilson, M.V.H. (Eds.), Mesozoic Fishes V –Global Diversity and Evolution-. Verlag Dr. Friedrich Pfiel, München, Germany, pp. 305–323.

Arambourg, C., 1954. Les Poissons crétacés du Jebel tselfat (maroc). Notes et Mémoires, Service des Mines et de la Carte Géologique du Maroc 118, 1–188.

Bannikov, A.F., Bacchia, F., 2005. New species of the Cenomanian Eurypterygii (Pisces, Teleostei) from Lebanon. Paleontol. J. 39 (5), 514–522 [Translated from the Russian, original version published in Paleontologicheskii Zhurnal, 5, 53–61.

Beckett, H., Giles, S., Friedman, M., 2017. Comparative anatomy of the gill skeleton of fossil Aulopiformes (Teleostei: eurypterygii). J. Syst. Palaeontol. 16 (14), 1221–1245.

Berg, L.S., 1937. A classification of fish-like vertebrates. Bulletin de l'Académie des Sciences de l'URSS 4, 1277–1280.

Blanco-Piñón, A., 1998. Vallecillo Nuevo León: yacimiento fosilífero del noreste de México. Master Thesis. Facultad de Ciencias de la Tierra, Universidad Autónoma de Nuevo León, Linares 148 pp.

Breton, G., Bilotte, M., Sigro, G., 1995. *Dipsacaster jadeti* sp. nov., Astropectinidae (Asteroidea, Echinodermata) du Maastrichtien des Petites Pyrénées (France). Bull. Trimestriel Soc. Geol. Normandie Amis Mus. Havre 82 (4), 35–42.

Brusatte, S.L., Carr, T.D., 2016. The phylogeny and evolutionary history of tyrannosauroid dinosaurs. Sci. Rep. 6, 1–8.

Carbot-Chanona, G., Than-Marchese, B.A., 2013. Presencia de *Enchodus* (Osteichthyes: Aulopiformes: Enchodontidae) en el Maastrichtiano (Cretácico tardío) de Chiapas, México. Paleontol. Mexic. 6 (1), 8–16.

Cavin, L., Alexopoulos, A., Piuz, A., 2012. Late Cretaceous (Maastrichtian) ray-finned fishes from the island of Gavdos, southern Greece, with comments on the evolutionary history of the aulopiform teleost *Enchodus*. Bull. Soc. Geol. Fr. 183 (6), 561–572.

Cevallos-Ferriz, S.R., González-Torres, E.A., Calvillo-Canadell, L., 2012. Perspectiva paleobotánica y geológica de la biodiversidad en México. Acta Bot. Mex. 100, 317–350.

Chalifa, Y., 1985. *Saurorhamphus judeaensis* (Salmoniformes: Enchodontidae), a new longirostrine fish from the cenomanian of ein-yabrud, near Jerusalem. J. Vertebr. Paleontol. 5 (3), 181–193.

Chalifa, Y., 1989. New species of *Enchodus* (Pisces: Enchodontoidei) from the lower Cenomanian of Ein-Yabrud, Israel. J. Paleontol. 63 (3), 356–364.

Cope, E.D., 1872. On the families of fishes of the Cretaceous formations of Kansas. Proc. Am. Phil. Soc. 12, 327–357.

Cope, E.D., 1874. Review of the vertebrata of the Cretaceous period found west of the Mississippi River. U.S. Geological Survey of the Territories Bulletin 1, 3–48.

Davis, M.P., Fielitz, C., 2010. Estimating divergence times of lizardfishes and their allies (Euteleostei: Aulopiformes) and the timing of deep-sea adaptations. Mol. Phylogenet. Evol. 57 (3), 1194–1208.

Díaz-Cruz, J.A., Alvarado-Ortega, J., 2017. Los peces enchodóntidos de México. In: XV Congreso Nacional de Paleontología, San Luis Potosí, México, Paleontología Mexicana, Volumen especial, vol. 2. pp. 37.

Díaz-Cruz, J.A., Alvarado-Ortega, J., 2018a. The late Cretaceous enchodontids (Enchodontidae: Aulopiformes) fishes from Mexico: new light into the evolution of Enchodontidae. In: 5th International Paleontological Congress. Abstract Book, Paris, France, pp. 1038.

Díaz-Cruz, J.A., Alvarado-Ortega, J., 2018b. A new enchodontid fish Enchodus-like from cenomanian deposits from the el Chango quarry (Cintalapa member, Sierra Madre Formation), Chiapas, Mexico. In: 78th Annual Meeting of the Society of Vertebrate Paleontology, Alburquerque, New Mexico, pp. xx.

Díaz-Cruz, J.A., Alvarado-Ortega, J., Carbot-Chanona, G., 2013. Nueva especie de pez del género *Enchodus* (Aulopiformes: Echodontidae) del Cenomaniano de Chiapas. In: Reynoso, V.H., Oseguera, B., Flores-Mejía, P. (Eds.), Programa y Resúmenes del VIII Congreso Latinoamericano de Paleontología y XIII Congreso Nacional de Paleontología. Universidad de Guanajuato. Guanajuato, México, pp. 45.

Díaz-Cruz, J.A., Alvarado-Ortega, J., Carbot-Chanona, G., 2016. The cenomanian short snout enchodontid fishes (aulopifomes, Enchodontidae) from Sierra Madre Formation, Chiapas, southeastern Mexico. Cretac. Res. 61, 136–150.

Díaz-Cruz, J.A., Porraz-Múzquiz, H.G., Alvarado-Ortega, J., 2017. Sobre la presencia de *Enchodus* (Enchodontidae: Aulopiformes) en los yacimientos marinos del Turoniano en el Norte de México. In: XV Congreso Nacional de Paleontología , San Luis Potosí, México; Paleontología Mexicana, Volumen especial, vol. 2. pp. 36.

Fielitz, C., 2004. The phylogenetic relationships of the †Enchodontidae (teleostei: Aulopiformes). In: Arratia, G., Wilson, M.V.H., Cloutier, R. (Eds.), Recent Advances in the Origin and Early Radiation of Vertebrates. Verlag Dr. Friedrich Pfeil, München, Germany, pp. 619–634.

Fielitz, C., González-Rodríguez, K.A., 2010. A new species of *Enchodus* (Aulopiformes: Enchodontidae) from the cretaceous (Albian to Cenomanian) of Zimapán, Hidalgo, México. J. Vertebr. Paleontol. 30 (5), 1343–1351.

Forey, P.L., Yi, L., Patterson, C., Davies, C.E., 2003. Fossil fishes from the Cenomanian (Upper Cretaceous) of Namoura, Lebanon. J. Syst. Palaeontol. 1 (4), 227–330.

Friedman, M., Beckett, H.T., Close, R.A., Johanson, Z., 2015. The English Chalk and London Clay: two remarkable British bony fish Lagerstätten. Geological Society, London, Special Publications 430, 165–200.

Garassino, A., Vega, F.J., Calvillo-Canadell, L., Cevallos-Ferriz, S.R., Coutiño, M.A., 2013. New decapod crustacean assemblage from the upper Cretaceous (Cenomanian) of Chiapas, Mexico. Neues Jahrbuch Geol. Palaontol. Abhand. 269 (3), 261–270.

Giersch, S., 2014. Die Knochenfische der Oberkreidezeit in Nordostmexiko: Beschreibung, Systematik, Vergesellschaftung, Paläobiogeographie und Paläoökologie. PhD. thesis. Ruprecht-Karls-Universität Heidelberg, Germany, pp. 275.

Giersch, S., Frey, E., Stinnesbeck, W., González-González, A.H., 2008. Fossil fish assemblages of northeastern Mexico: new evidence of mid Cretaceous Actinopterygian radiation. In: Krempaská, Z. (Ed.), 6th Meeting of the European Associat Ion of Vertebrate Paleontology, Museum of Spiš, Spišská Nová Ves, Slovak Republic, Volume of Abstracts, pp. 43–45.

Goloboff, P.A., Catalano, S.A., 2016. TNT version 1.5, including a full implementation of phylogenetic morphometrics. Cladistics 32, 221–238.

González-Barba, G., Espinosa-Chávez, B., 2005. Cenomanian-turonian fish fauna from the Boquillas Formation at Jaboncillos, north-west coahuila, Mexico. In: Poyato-Ariza, F.J. (Ed.), Fourth International Meeting on Mesozoic Fishes –Systematics, Homology, and Nomenclature–, Maraflores de la Sierra, Madrid, España. Extended Abstracts. Servicio de Publicaciones de la Universidad Autónoma de Madrid/UAM Ediciones, Spain, pp. 105–107.

González-Ramírez, I., Calvillo-Canadell, L., Cevallos-Ferriz, S.R.S., 2013. Coníferas cupresáceas fósiles de "El Chango", Chiapas (Aptiano). Palaontol. Mexic. 63, 26–31.

González-Rodríguez, K.A., Fielitz, C., Bravo-Cuevas, V.M., Baños-Rodríguez, R.E., 2016. Cretaceous osteichthyan fish assemblages from Mexico. New Mexico Museum of Natural History and Science Bulletin 71, 1–14.

Goody, P.C., 1969. The relationships of certain Upper Cretaceous teleosts with special reference to the myctophoids. Bull. Br. Mus. (Nat. Hist.) Geol. Suppl. 7, 1–225.

Goody, P.C., 1970. The cretaceous teleostean fish *Cimolichthys* from the Niobrara Formation of Kansas and the Pierre Shale of Wyoming. Am. Mus. Novit. 2434, 1–29.

Guerrero-Márquez, G., Calvillo-Canadell, L., Cevallos-Ferriz, S.R.S., Avendaño-Gil, J., 2013. Angiospermas cretácicas de la localidad "El Chango", Chiapas, México. Palaontol. Mexic. 2 (1), 32–39.

Heckel, J.J., 1850. Beitrage zur Kenntniss der fossilen Fische Osterreichs. Denkschriften der Kaiserlichen Akademie der Wissenschaften Mathematisch-Naturwissenschaftliche 1, 201–242 + 15 pls.

Holloway, W.L., Claeson, K.M., Sallam, H.M., El-Sayed, S., Kora, M., Sertich, J.J.-W., O'Connor, P.M., 2017. A new species of the neopterygian fish *Enchodus* from the Duwi Formation, Campanian, Late Cretaceous, Western Desert, central Egypt. Acta Palaeontol. Pol. 62 (3), 603–611.

Huerta-Vergara, A.R., Calvillo-Canadell, L., Cevallos-Ferriz, S.R.S., Silva-Pineda, A., 2013. Pinaceae en el Cetácico del norte y sur de México: complemento a su escaso registro fósil. Palaontol. Mexic. 2 (1), 66–78.

Jordan, D.S., 1905. A Guide to the Study of Fishes, vol. 1 H. Holt, New York.

Khalloufi, B., Ouarhache, D., Lelièvre, H., 2010. New paleontological and geological data about Jbel Tselfat (late Cretaceous of Morocco). Hist. Biol. 22 (1), 57–70.

Kramberger, K.G., 1895. De piscibus fossilibus Comeni, Mrzleci, Lesine et M. Libanonis. Djela Jugoslavenske Akademije Znanosti i Umjetnosti 16, 1–67 12 pls.

Leidy, J., 1855. Indications of twelve species of fossil fishes. Proc. Acad. Nat. Sci. Phila. 7, 395–397.

Lewis, P.O., 2001. A likelihood approach to estimating phylogeny from discrete morphological character data. Syst. Biol. 50, 913–925.

Maldonado-Koerdell, M., 1956. Peces fósiles de México, III. Nota preliminar sobre los peces del Turoniano Superior de Xilitla, San Luis Potosi (México). Ciencia 16, 31–35.

Marck, W. von der, 1863. Fossile Fische, Krebse und Pflanzen aus dem Plattenkalk der jüngsten Kreide in Westphalen. Palaeontographica 11, 1–83 + 14 pls.

Moreno-Bedmar, J.A., Latil, J.L., Villanueva-Amadoz, U., Calvillo-Canadell, L., Cevallos-Ferriz, S.R.S., 2014. Ammonite age-calibration of the EL Chango fossil-Lagerstätte, Chiapas state (SE Mexico). J. S. Am. Earth Sci. 56, 447–453.

Ovalles-Damián, E., Alvarado-Ortega, J., Blanco-Piñón, A., 2006. Los peces fósiles del Cretácico inferior de Ocozocoautla, Chiapas. In: Memoria X Congreso Nacional de Paleontología y libreto guía de la excursión a Tepexi de Rodríguez, Puebla. Publicación especial 5. Instituto de Geología, pp. 61.

Parris, D.C., Grandstaff, B.S., Gallagher, W.B., 2007. Fossil fish from the Pierre Shale group (late Cretaceous): clarifying the biostratigraphic record. Spec. Pap. Geol. Soc. Am. 427, 99.

Pictet, F.J., 1850. Description de quelque poissons fossiles du Mont Liban. Frick, J-G, Genève.

Porras-Múzquiz, H., Alvarado-Ortega, J., 2011. Sobre la ocurrencia de *Enchodus petrosus* Cope en el Cretácico Tardío de Múzquiz, Coahuila, México. In: XII Congreso Nacional de Paleontología; Sociedad Mexicana de Paleontología; Edificio Carolino. Benemérita Universidad Autónoma de Puebla; Libro de Resúmenes, pp. 113.

Prieto-Márquez, A., 2010. Global phylogeny of hadrosauridae (Dinosauria: ornithopoda) using parsimony and bayesian methods. Zool. J. Linn. Soc. 159 (2), 435–502.

Raab, M., Chalifa, Y., 1987. A new enchodontid fish genus from the upper Cenomanian of Jerusalem, Israel. Palaeontology 30, 717–731.

Romero-García, A.E., 2013. Descripción de los peces fósiles del género Enchodus Agassiz, 1835 (Teleostei, Aulopiformes), de La Cantera San José de Gracia (Cretácico, Turoniano), Molcaxac, Puebla. Tesis de Licenciatura, Facultad de Ciencias, Universidad Nacional Autónoma de México, pp. 68.

Ronquist, F., Teslenko, M., Van Der Mark, P., Ayres, D.L., Darling, A., Höhna, S., Huelsenbeck, J.P., 2012. Mrbayes 3.2: efficient bayesian phylogenetic inference and model choice across a large model space. Syst. Biol. 61 (3), 539–542.

Rosen, D.E., 1973. Interrelationships of higher euteleosteans fishes. In: Greenwood, P.H., Miles, R.S., Patterson, C. (Eds.), Interrelation of Fishes. Zoological Journal of the Linnean Society, London, pp. 397–513 Suppl. 1.

Silva, H.M.A., 2007. Revisão taxonômica e filogenética dos peixes Enchodontoidei (*sensu* Nelson, 1994) e considerações biogeográficas. Masters degree Thesis. Programa de Pós-graduação em Ecologia e Evolução, Universidade do Estado do Rio de Janeiro, Brazil, pp. 142.

Silva, H.M.A., Gallo, V., 2011. Taxonomic review and phylogenetic analysis of enchodontoidei (teleostei: Aulopiformes). An Acad. Bras Ciências 83 (2), 483–511.

Stiassny, M.L., Moore, J.A., 1992. A review of the pelvic girdle of acanthomorph fishes, with comments on hypotheses of acanthomorph intrarelationships. Zool. J. Linn. Soc. 104 (3), 209–242.

Taverne, L., 2005. Les Poissons crétacés de Nardò. 21°. *Ophidercetis* italiensis gen. et sp. nov. (Teleostei, Aulopiformes, Dercetidae). Une solution ostéologique au problème des genres *Dercetis* et *Benthesikyme* (= *Leptotrachelus*). Boll. del Mus. Civico Storia Nat. Verona Geol. Paleontol. Preistoria 29, 55–79.

Toombs, H.A., Rixon, A.E., 1959. The use of acids in the preparation of vertebrate fossils. Curator 2, 304–312.

Uyeno, T., Minakawa, T., 1983. A new enchodontoid fish of the genus *Eurypholis* from Cretaceous of Japan. Bull. Natl. Sci. Mus. Ser. C (Geol.) 9 (2), 79–83.

Vega, F.J., García-Barrera, P., Perrilliat, M.C., Coutiño, M.A., Mariño-Pérez, R., 2006. El Espinal, a new plattenkalk locality from the lower Cretaceous Sierra Madre Formation, Chiapas, southeastern Mexico. Rev. Mex. Ciencias Geol. 23 (3), 323–333.

Vega, F.J., Álvarez, F., Carbot-Chanona, G., 2007. Albian penaeoidea (Decapoda: Dendrobranchiata) from Chiapas, southern Mexico. 3rd symposium on mesozoic and cenozoic Decapoda Crustaceans, Museo di Storia Naturale di Milano. Mem. della Soc. Ital. Sci. Nat. del Mus. Civico Storia Nat. Milano 35 (2), 6–8.

Vernygora, O., Murray, A.M., Luque, J., Ruge, M.L.P., Fonseca, M.E.P., 2018. A new cretaceous dercetid fish (Neoteleostei: Aulopiformes) from the turonian of Colombia. J. Syst. Palaeontol. 16 (12), 1057–1071.

Woodward, A.S., 1901. Catalogue of the Fossil Fishes in the British Museum (Natural History), Part IV. British Museum (Natural History), London, pp. 636.

Yabumoto, Y., Uyeno, T., 1994. Late Mesozoic and Cenozoic fish faunas of Japan. Isl. Arc 3 (4), 255–269.

Young, K., 1958. *Graysonites*, a Cretaceous ammonite in Texas. J. Paleontol. 32, 171–182.

Corrigendum to "Dagon avendanoi gen. and sp. nov. an Early Cenomanian Enchodontidae (Aulopiformes) fish from the El Chango quarry, Chiapas, southeastern Mexico"

Journal of South American Earth Sciences 95 (2019) 102314

Contents lists available at ScienceDirect

Journal of South American Earth Sciences

journal homepage: www.elsevier.com/locate/jsames

Corrigendum to "Dagon avendanoi gen. and sp. nov., an Early Cenomanian Enchodontidae (Aulopiformes) fish from the El Chango quarry, Chiapas, southeastern Mexico" [J. South Am. Earth Sci. 91 (2019) 272–284]

Jesús Alberto Díaz-Cruz[a,b,*], Jesús Alvarado-Ortega[b], Gerardo Carbot-Chanona[c]

[a] Posgrado en Ciencias Biológicas, Unidad de Posgrado, Edificio A, 1° Piso, Circuito de Posgrados, Ciudad Universitaria, Coyoacán, C.P. 04510, Ciudad de México, Mexico
[b] Instituto de Geología, Universidad Nacional Autónoma de México, Circuito de la Investigación S/N, Ciudad Universitaria, Coyoacán, Ciudad de México, 04510, Mexico
[c] Museo de Paleontología Eliseo Palacios Aguilera, Dirección de Paleontología, Secretaría de Medio Ambiente e Historia Natural, Calzada de Los Hombres Ilustres S/N, Antiguo Parque Madero, Tuxtla Gutiérrez, Chiapas, Mexico

Recently, the authors of present corrigendum erected the name *Dagon avendanoi* Díaz-Cruz et al. (2019), family Enchodontidae (Aulopiformes) into pages of the Journal of South American Earth Sciences. Up to now, *Dagon avendanoi* is only known by the holotype, published with the catalog number IHNFG-5333, which was recovered from the Cenomanian deposits of the Cintalapa Formation, exploited in the El Chango quarry, near Ocozocoautla de Espinosa, Chiapas, southeastern Mexico (Díaz-Cruz et al., 2019, p. 274).

After the impression of the concerned article, we realized that this contained two important errors. On the one hand, the generic name "*Dagon*" was previously assigned to a group of butterfly species from South America by Higgins (1981). On the other hand, the mentioned catalog number, IHNFG-5333, was also preassigned to a specimen of the species *Icriobranchiocarcinus tzutzu* Vega et al. (2018, p. 336–337).

In order to obey the considerations of the principle of homonymy, set out in Chapter 12 and Article 52 of the current International Code of Zoological Nomenclature (International Commission on Zoological Nomenclature, 2000). Here we suggest changing the generic epithet of *Dagon*, in the species *Dagon avendanoi*, because this is a junior homonymous of the generic epithet assigned by Higgins (1981, p.108–110) to three South American butterfly species. The new name of *Dagon avendanoi* is *Veridagon avendanoi*, in which the generic epithet "*veri*" is derived from the Latin adjective *verus*, meaning "true or real"; together such generic names mean "the real Dagon". Finally, a new catalog number, IHNFG-5816, is now assigned to the holotype referred above to substitute the preoccupied number IHNFG-5333.

The authors would like to apologize for any inconvenience caused.

References

Comisión Internacional de Nomenclatura Zoológica, 2000. Código Internacional de Nomenclatura Zoológica. The International Commision on Zoological Nomenclature Editorial, versión en español de la 4° edición. Comisión Internacional de Nomenclatura Zoológica, Madrid 156 pp.

Díaz-Cruz, J.A., Alvarado-Ortega, J., Carbot-Chanona, G., 2019. Dagon avendanoi gen. And sp. nov., an Early Cenomanian Enchodontidae (Aulopiformes) fish from the El Chango quarry, Chiapas, southeastern Mexico. J. South Am. Earth Sci. 91, 272–284.

Higgins, L.G., 1981. A revision of Phyciodes Hübner and related genera, with a review of the classification of the Melitaeinae. Bull. Br. Mus. (Nat. Hist.) Ent. 43 (3), 77–243.

Vega, F.J., Charbonnier, S., Gómez-Pérez, L.E., Coutiño, M.A., Carbot-Chanona, G., de Araújo Távora, V., Serrano-Sánchez, M.L., Téodori, D., Hernández-Monzón, O., 2018. Review and additions to the Maastrichtian (late Cretaceous) crustacea from Chiapas, Mexico. J. South Am. Earth Sci. 85, 325–344.

DOI of original article: https://doi.org/10.1016/j.jsames.2019.01.014

* Corresponding author. Posgrado en Ciencias Biológicas, Unidad de Posgrado, Edificio A, 1° Piso, Circuito de Posgrados, Ciudad Universitaria, Coyoacán, C.P. 04510, Ciudad de México, Mexico.

E-mail address: vertebrata.j@gmail.com (J.A. Díaz-Cruz).

https://doi.org/10.1016/j.jsames.2019.102314

Available online 19 August 2019

CAPÍTULO III: A new long snout enchodontid (Aulopiformes: Enchodontidae) from early Cenomanian deposits of the el Chango quarry, Chiapas, Mexico: A multi-approach study

Palaeontologia Electronica
palaeo-electronica.org

A long snout enchodontid fish (Aulopiformes: Enchodontidae) from the Early Cretaceous deposits at the El Chango quarry, Chiapas, southeastern Mexico: A multi-approach study

Jesús Alberto Díaz-Cruz, Jesús Alvarado-Ortega, and Sam Giles

ABSTRACT

Vegrandichthys coitecus gen. et sp., nov., is described in this manuscript based on a single specimen from the Early Cenomanian marine deposits exposed in the El Chango quarry, Chiapas, Southern Mexico. Although this fish exhibits osteological features to support its insertion as a new member of the family Enchodontidae, it has a peculiar combination of characters that includes the presence of a relatively long and stout snout, lateral exposure of the quadrate and mandible articulation, a series of multiple anteroposterior strengthening bars along the opercle, the lateral line running into a series of complex scales, and the anal fin placed behind the dorsal fin. The phylogenetic position of *Vegrandichthys* was assessed with multiple approaches, namely Standard Maximum Parsimony (SMP), Implied Weighted Maximum Parsimony (IWMP), Phylogenetic Morphometrics (PM), and Bayesian Inference (IB). The single phylogenetic tree obtained from SMP shows the same topology as that resulting from IWMP: *Unicachichthys, Veridagon,* and *Palaeolycus* branch successively at the base of Enchodontidae, with the subfamilies Eurypholinae (comprising *Vegrandichthys, Eurypholis,* and *Saurorhamphus*) and Enchodontinae resolved as sister groups. The PM performed, including a landmark configuration of the preopercle, suggests that these data contain true phylogenetic signals. In IB, the phylogenetic hypothesis generated retains the clade Eurypholinae, but other taxa are located in a very different topology, which is presumably attributed to the data consistency. *Vegrandichthys* represents the first formally studied long-snout enchodontid from the Americas. It also was found that the stratigraphic fit of Enchodontidae decreases when *Enchodus zimapanensis* is included in the analysis.

Jesús Alberto Díaz-Cruz. Posgrado en Ciencias Biológicas, Unidad de Posgrado, Edificio A, 1° Piso, Circuito de Posgrados, Ciudad Universitaria, Coyoacán, Ciudad de México, 04510, México.
vertebrata.j@gmail.com
Jesús Alvarado-Ortega. Instituto de Geología, Universidad Nacional Autónoma de México, Circuito de la

http://zoobank.org/940BA81F-6E6E-427F-80B8-904C620A850E

Díaz-Cruz, Jesús Alberto, Alvarado-Ortega, Jesús, and Giles, Sam. 2020. A long snout enchodontid fish (Aulopiformes: Enchodontidae) from the Early Cretaceous deposits at the El Chango quarry, Chiapas, southeastern Mexico: A multi-approach study, 23(2):a30. https://doi.org/10.26879/1065
palaeo-electronica.org/content/2020/3063-a-long-snout-enchodontid-fish

Investigación S/N, Ciudad Universitaria, Delegación Coyoacán, Ciudad de México, 04510 México. alvarado@geologia.unam.mx
Sam Giles. Department of Earth Sciences, University of Oxford, South Parks Road, Oxford, OX1 3AN, UK. Current Address: School of Geography, Earth and Environmental Sciences, University of Birmingham, Edgbaston, B15 2TT, UK. s.giles.1@bham.ac.uk

Keywords: new genus; Eurypholinae; maximum parsimony; Bayesian inference; phylogenetic morphometrics

Submission: 9 February 2020. Acceptance: 4 June 2020

INTRODUCTION

The family Enchodontidae is a monophyletic group of extinct Cretaceous teleost fishes (Fielitz, 2004; Coelho, 2004; Silva and Gallo, 2011), which show a great morphological disparity in the shape of the trunk and snout, and range from between a few centimeters to over one and half meters in length (Díaz-Cruz and Alvarado-Ortega, 2017, 2018). These active and fast predatory fishes inhabited the mid-trophic level and were important components in the trophic chain in the Cretaceous seas, evidenced by their relatively common occurrence as well-preserved gut contents in larger fishes and other marine predators such as cephalopods and plesiosaurs (Stewart and Carpenter, 1990; Maisey, 1996; Cavin, 1999; Cicimurri and Everhart, 2001; Cavin et al., 2012; Porras-Múzquiz et al., 2019).

The enchodontids have been known since the first half of the nineteenth century (Agassiz, 1833); however, their comprehensive study only began in the second half of the 20th century. Prior the present, seven enchodontid genera have been identified (Díaz-Cruz et al., 2019b, table 2); these were inhabitants of marine shallow environments in the peripheral and epicontinental seas of northern Africa [Egypt and Morocco (Arambourg, 1954; Bardet et al., 2017; Holloway et al., 2017)], America [Argentina, Brazil, Peru, Mexico, and the United States (Silva-Santos and Salgado, 1969; Goody, 1976; Bogan and Agnolin, 2010; Schein et al., 2013; Gouiric-Cavalli et al., 2016)], Asia [Lebanon, Israel, Jordan and Japan (Uyeno and Minakawa, 1983; Yabumoto and Uyeno, 1994; Chalifa, 1996; Forey et al., 2003; Kaddumi, 2009)]; and Europe [Netherlands, Germany, United Kingdom, Greece, Italy (Goody, 1968, 1969; Cavin et al., 2012; Friedman et al., 2016)]. Goody (1969) explored the evolutionary relationships of enchodontids; however, the first phylogenetic hypothesis of the group was proposed by Fielitz (2004).

The fossil record of enchodontids is noticeably rich and diverse along the Tethys Sea, mainly in its North American and Middle Eastern realms. Silva and Gallo (2007) identified two areas of Cenomanian enchodontid endemism in this region, one located in North Africa and the other in the Middle East. Later, Cavin et al. (2012) claimed that the biogeography of enchodontids was dictated, in part, by vicariant events. In both studies, the origin of enchodontids is attributed to the central-western region of the Tethys Sea. Recently, Díaz-Cruz et al. (2019a,b) revealed intriguing data that contrasts with such an idea, specifically the presence of early-diverging enchodontid taxa in Mexico.

Although North American enchodontids have been long studied by numerous authors (e.g., Stewart, 1898; Hay, 1903; Green, 1913; Goody, 1976; Wilson and Chalifa, 1989) and their diversity from numerous sites in the United States of America and Canada is well known, Mexico has recently become a very important territory to study these fishes because they have been extracted in numerous paleontological sites ranging from Albian to Maastrichtian age. The first report of enchodontids from Mexico dates back to the 1950s when Maldonado-Koerdell (1956) found remains of these fishes in Turonian limestones exploited in Xilitla, San Luis Potosí, and inside a rocky core drilled near San José de las Rusias, Tamaulipas. In addition, these fishes have been reported from other sites including the Vallecillo quarry (Nuevo León), the Arroyo Las Bocas (Guerrero), the San Jose de Gracia quarry (Puebla), as well as the Las Boquillas, La Mula, Los Pilotes, and Venustiano Carranza quarries (Coahuila), the El Chango quarry and Tzimol (Chiapas), and the Muhi quarry (Hidalgo) (Blanco-Piñón, 1998; González-Barba and Espinosa-Chávez, 2005; Alvarado-Ortega et al., 2006a and b, 2009, 2019, 2020a and b; Giersch et al., 2008; Fielitz and González-Rodríguez, 2010; Porras-Múzquiz and Alvarado-Ortega, 2011; Carbot-Chanona and Than-Marchese, 2013; Romero-

García, 2013; Giersch, 2014; Díaz-Cruz et al., 2016, 2019ac; Díaz-Cruz and Alvarado-Ortega, 2017, 2018; among others). The nominal species of the Mexican enchodontids already described are noticeable, because they represent the most ancient record of this group in America, usually include relatively complete and well-preserved fossils, and are among the oldest enchodontids so far known from the Middle East and North Africa regions (Díaz-Cruz et al., 2019a-c). These Mexican enchodontids are *Enchodus zimapanensis* Fielitz and González-Rodríguez, 2010, from the Albian-Cenomanian deposits of the Muhi quarry, Hidalgo; *Unicachichthys multidentata* Díaz-Cruz et al., 2016, as well as *Veridagon avendanoi* (Díaz-Cruz et al., 2019b) from the early Cenomanian deposits of the El Chango quarry, Chiapas (Figure 1). Today, a great quantity of partially described specimens from Mexico is deposited in the paleontological collections of this country, waiting to be accurately studied.

The aim of this paper is to describe a new genus and species of enchodontid based on a single well-preserved specimen recovered from the early Cenomanian strata of the El Chango quarry, Chiapas, southern Mexico. In addition, the phylogenetic relationships of this new taxon are evaluated under different phylogenetic approaches and the stratigraphic congruence of the family is assessed.

The El Chango Quarry

El Chango quarry is a small outcrop of laminated limestones and dolomites with sporadic flint nodules located at 16º34'14.9" N and 93º16'12.7" W, within Ocozocoautla de Espinosa Municipality, and about 25 km to the southwestern of Tuxtla Gutiérrez, Chiapas, Mexico (Figure 2). According

FIGURE 1. Enchodontid species from the El Chango quarry, Chiapas, Mexico; A, IHNFG-2987, holotype of *Unicachichthys multidentata;* B, IHNFG-5816, holotype and single specimen of *Veridagon avendanoi.* Scale bar equals 1

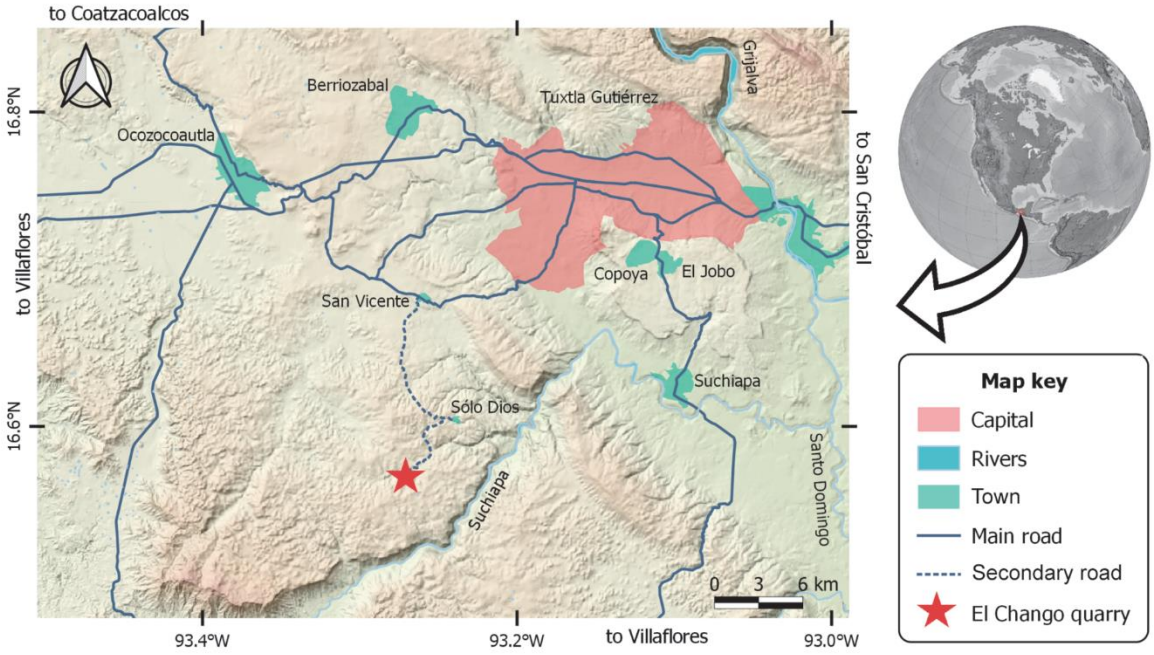

FIGURE 2. Geological map and geographical localization of the El Chango quarry, Chiapas, Mexico.

to Vega et al. (2007) these strata were accumulated in the bottom of an estuarine or salty lagoon with ephemeral freshwater influx during the late Albian; however, subsequently, Alvarado-Ortega et al. (2009) concluded that such age corresponds to the Cenomanian, and later Moreno-Bedmar et al. (2014) stated that this is rather early Cenomanian.

This quarry was opened in 2004 by members of the scientific staff of the Museo de Paleontología "Eliseo Palacios Aguilera" (Díaz-Cruz et al., 2019b). Since then, this institution has been in charge of collecting, studying, and preserving the fossils from this Lagerstätte. Today, the fossil collection from the El Chango housed in this museum contains more than 400 fossils, including mollusks, crustaceans, ammonites, insects, plants, and fishes (Ovalles-Damián et al., 2006; Vega et al., 2007; Alvarado-Ortega et al., 2009; Alvarado-Ortega and Than-Marchese, 2012, 2013; Amaral et al., 2013; Huerta-Vergara et al., 2013; Garassino et al., 2013; González-Ramírez et al., 2013; Guerrero-Márquez et al., 2013; Moreno-Bedmar et al., 2014; Carbot-Chanona, 2015; and Guinot et al., 2019; among others). Fishes are the best-preserved fossils at the El Chango; these are tightly laterally compressed, usually complete and articulated, and often show parts of soft tissues (muscles) and phosphatized stomach contents.

Böse (1905) described the "Cretaceous limestones with rudists" of the Central Chiapas depression, where the El Chango quarry is located, as a Cretaceous platform carbonate series of flint-bearing dolomites and limestones. Although Wiebe (1925) suggested this series as the San Cristóbal Formation; Nutall, in an unedited paper (in Salas, 1949), coined the Sierra Madre Formation name, and this is currently in use. Salas (1949) recognized a natural division of this formation into two units, an Albian–Cenomanian unit of limestones with a sugary aspect and apparently barren of fossils, and a Turonian unit of limestones bearing flints and abundant rudists. Later, González (1963) named these subunits as the Cantelhá and the Jolpabuchil members respectively. The discovery of microfossils during petroleum exploration contributed to re-ordering the units of the Sierra Madre limestones. Although some authors considered the Sierra Madre a single unit (Waite, 1986; Steele, 1986); others (e.g. Sánchez-Montes de Oca, 1969, 1973; Álvarez-Mena, 1975; Quezada-Muñetón, 1987) suggested that this geological sequence comprises three formations: the Cantelhá, Cintalapa, and Jolpabuchil formations. Alvarado-Ortega and Than-Marchese (2012) and Moreno-Bedmar et al. (2014) stated that the fossiliferous strata at El Chango quarry belong to the Cintalapa Formation.

MATERIALS AND METHODS

Preparation methods. The specimen studied here was transferred to polyester resin following the process described by Toombs and Rixon (1950, 1959). The bulk of the rocky matrix was mechanically removed using fine pneumatic air scribe; the fossil bones were then totally released from the remaining matrix, with the limestone dissolved through the application of intermittent baths in an acetic acid aqueous solution at 5% combined with baths in clean water. Pin vises and needles were used to remove the remaining rock residues from the fossil. The fossil was hardened with a light dissolution of plexigum in ethyl acetate applied with a fine brush.

Anatomical nomenclature. The osteological nomenclature and abbreviations used in this paper and its figures follow those used in similar previous publications on enchodontid fishes (Goody, 1969, 1976; Fielitz, 2004; among others).

Institutional abbreviations. IGM, Colección Nacional de Paleontología, Museo María del Carmen Perrilliat, Instituto de Geología, UNAM. **IHNFG**, Instituto de Historia Natural –Fósil, Geográfico–, housed in the Museo de Paleontología "Eliseo Palacios Aguilera", Chiapas, México. **MSNT**, Museo Civico di Storia Naturale, Trieste, Italy. **NHMUK**, Natural History Museum, London, United Kingdom. **GMWWU**, Geomuseum der WWU Münster. **UAHMP**, Museo de Paleontología, Centro de Investigaciones Biológicas, Universidad Autónoma del Estado de Hidalgo.

Comparative materials examined. The following specimens were studied for comparative purposes. *Cimolichthys lewesiensis* Leidy, 1857: NHMUK PV P1810 from the English Chalk, England. *Enchodus* sp.: IHNFG-2989 and IHNFG-2653 from the Cenomanian deposits of the El Chango quarry, Chiapas, Mexico. *Enchodus* sp.: IGM 11404 from the Campanian deposits of Ochuxhob, Tzimol, Chiapas, Mexico. *Enchodus gracilis* (von der Marck, 1858): GMWWU 8428, GMWWU 8429, GMWWU 8494, GMWWU 8498, and, GMWWU 8543 and NHMUK PV P.3848, all from the Upper-Senonian deposits of Sendenhorst, Warendorf, North Rhine-Westphalia, Germany. *Enchodus lewesiensis* (Mantell, 1822): GMWWU 950 from the Upper Campanian deposit of Darup, Coesfeld, North Rhine-Westphalia, Germany and NHMUK PV P.9249 and NHMUK PV P.73992, NHMUK PV P.9249, NHMUK PV P.5415, NHMUK PV P.4184 from the Cenomanian-Turonian deposits of Lewes, East Sussex, United Kingdom. *Enchodus macropterus* (von der Marck, 1858): GMWWU 8427 from the Upper Senonian deposits, Baumberge, Coesfeld, and GMWWU 8426, from the Upper Senonian deposits of Sendenhorst, Warendorf, both from North Rhine-Westphalia, Germany. *Enchodus major* (Davis, 1887) NHMUK PV P.4763 and NHMUK PV OR.49504 both from the Upper Santonian deposits of Sahel Alma, Lebanon. *Enchodus marchesettii* (Kramberger, 1895) NHMUK PV P.4748, NHMUK PV P.9250, NHMUK PV P.47315, NHMUK PV P.63181, all from the Cenomanian deposits of Hakel, Lebanon. *Enchodus mecoanalis* Forey et al., 2003: NHMUK PV P.62522 (holotype) and NHMUK PV P.63250 (paratype) both from the Middle Cenomanian deposits of Namoura, Lebanon. *Enchodus longidens* (Pictet, 1850): NHMUK PV P.4853 from the Upper Santonian deposits of Sahel Alma, Lebanon. *Enchodus petrosus* (Cope, 1874): NHMUK PV P. 9647 from the Upper Cretaceous deposits of Kansas, United States. *Enchodus zimapanensis* Fielitz and González-Rodríguez, 2010: UAHMP 679 (holotype) and UAHMP 678 from the Albian-Cenomanian deposits of Zimapán, Hidalgo, Mexico. *Eurypholis boissieri* Pictet, 1850: NHMUK PV P.63323, NHMUK P.73, and NHMUK PV P.47313, from the Middle Cenomanian deposits of Namoura, Lebanon. *Eurypholis pulchellus* (Woodward, 1901): NHMUK PV P.1703 (holotype) from the Cenomanian-Turonian deposits of Lewes, East Sussex, United Kingdom. *Palaeolycus dreginensis* von der Marck, 1863 GMWWU 808 and GMWWU 8438 (holotype) from the Upper-Senonian deposits of Sendenhorst, Warendorf, North Rhine-Westphalia, Germany. *Saurorhamphus freyeri* Heckel, 1850: MSNT 7804, MSNT 7805, MSNT 7806, MSNT 7807, MSNT 7809, MSNT 7810, MSNT 7811, and MSNT 7812 from the Middle-Upper Cenomanian deposits of Komen, Slovenia. *Unicachichthys multidentata* Díaz-Cruz et al., 2016: IHNFG-2987 (holotype), IHNFG-2988, and IHNFG-4347, all from the early Cenomanian deposits of the El Chango quarry, Chiapas, Mexico. *Veridagon avendanoi* (Díaz-Cruz et al., 2019b): IHNFG-5816 (holotype) from the early Cenomanian deposits of the El Chango quarry, Chiapas, Mexico.

Morphological data set. The assessment of the phylogenetic position of the new taxon described here is based on a morphological data matrix updated from Díaz-Cruz et al. (2019b). In turn, this incorporated data from Fielitz (2004), Fielitz and González-Rodríguez (2010), Cavin et al. (2012), Díaz-Cruz et al. (2016), and Holloway et al. (2017). Our resulting data matrix includes 96 characters and 32 taxa; the modifications implemented in this

matrix, as well as the detailed description of all the characters, are discussed in Appendix I and II. Our data matrix was generated using the software Mesquite: A modular system for evolutionary analysis v 3.61 (Maddison and Maddison, 2001).

Standard Maximum Parsimony (SMP). Our data matrix (Table 1, Appendix I) was analyzed using the protocols for the Standard Maximum Parsimony available in the program TNT v1.5 (Goloboff and Catalano, 2016). Uninformative characters were deactivated with the command *xinact* in order to obtain the shortest trees. Deactivated uninformative characters are listed in Appendix II. The outgroup taxon was set as *Diplophos* Günther, 1873, following Fielitz (2004). All characters were treated as nonadditive (Fitch, 1971). A traditional search (heuristic search) was used with the following parameters: memory up to the maximum number of trees (99999), 1,000 Wager trees as random seeds with 10,000 replications, Tree Bisection Reconnection (TBR) as swapping algorithm and 10 saved trees per replication.

Landmark data. Among enchodontid taxa, preopercle shape is extremely variable; therefore, sometimes this has been discretized in many different character states (e.g., Silva and Gallo, 2011), and incorporated in phylogenetic analyses (see Holloway et al., 2017; Díaz-Cruz et al., 2019b). Inclusion of the morphological variability present in the shape of this bone into phylogenetic analyses is a challenging task; therefore, characters 45 and 91 from the Díaz-Cruz et al. (2019b) related to the preopercle, were re-coded in the current analysis. In addition, a Phylogenetic Morphometrics analysis was conducted using landmark data of the preopercle and SMP analysis combining the landmark data with the morphological character matrix. These analyses are based on photographs directly obtained of the specimens referred above except for the following cases: a) *Enchodus dirus* (Leidy, 1857) and *E. gladiolus* (Cope, 1872) (photographs available in the Oceans of Kansas website maintained by Mike Everhart (http://oceansofkansas.com/Enchodus.html); b) *Parenchodus longipterygius* Raab and Chalifa, 1987 [Raab and Chalifa (1987, fig. 3:720)]; c) *Alepisaurus ferox* Lowe, 1833 [Goody (1969, fig. 79:172)].

A total of 20 type II and III landmarks [see Palci and Lee (2019) for further details] were obtained from the preopercle configuration using the program tpsDIG 2.16 and tpsUtil (Rohlf, 2005). The .tps file was then edited in Notepad, and taxa lacking preopercle information were filled with the corresponding number of missing entries. Then, the .tps file was imported into TNT 1.5 (Goloboff and Catalano, 2016) to create a readable file (see Table 2, Appendix I). Finally, the matrix was verified to see if the question marks corresponded with the taxa where the preopercle is partially preserved.

Phylogenetic Morphometrics (PM) analysis. The PM analysis was carried out exclusively with preopercle landmark data using the software TNT 1.5 (Goloboff and Catalano, 2016) (Table 2, Appendix I). Before running the analysis, the landmark information was standardized *(lmark rescale = *)*, and the standardization factor set to one *(lmark fact=1)* in order to calculate the score as the sum of landmark displacement for a single configuration. Then, landmarks were realigned; the method of resistant-fit-theta-rho analysis (RFTRA) for the superimposition of the landmark configuration was used, selecting *Cimolichthys* as the reference taxon *(lmreal rftra [1] /0).* Posteriorly, the size of the configurations was modified *(lmreal rftra [0]!).* The RFTRA method was chosen because, unlike other methods, it uses repeated medians, is less sensitive to the outliers, and accepts missing data in the configurations for the superimposition (Siegel and Benson, 1982; Catalano and Goloboff, 2012, 2018). In the analysis where only the preopercle configuration was analyzed, we verified that only individual landmarks were assessed *(lmark noconfsample)* to calculate the Bremer support and absolute frequencies for resampling. The rest of the landmark optimization options were left as default in TNT. The designated outgroup for this analysis was *Alepisaurus*, following Fielitz (2004) and Davis and Fielitz (2010). The strategy of search used in this analysis was the same as that designated for the SMP and IWMP analyses.

A SMP analysis was performed with a combined matrix of landmark and discretized morphological character data (See Table 3, Appendix I). As with the SMP analysis only considering discrete morphological characters, uninformative characters were deactivated *(xinact).* The outgroup was *Diplophos* as stated above. The deactivated characters were the same as those in the SMP analysis and can be accessed in the Appendix II. The parameters for the morphological characters were the same as in the SMP and IWMP analyses, and the parameters for landmarks followed those of the PM exclusively with landmarks, except for calculation of support values, which were calculated sampling the entire configuration (default option; *lmark confsample*). Although the landmark configuration mirrors the contour-line of the preopercle, no dis-

crete characters related to the preopercle were additionally deactivated or deleted. We made this exercise in order to explore the effect of landmark data addition to the discrete data set, being aware that an overemphasis and/or redundancy of characters might affect the tree topology.

Implied Weighted Maximum Parsimony (IWMP). This exercise uses the new matrix of only discrete characters herein proposed (Table 1, Appendix I). The analyses ran twice, evaluating two different constants: k=10 and k=100. Each analysis used a traditional search in TNT (heuristic search) with the parameters as described for the Standard Maximum Parsimony analysis.

Bayesian Inference analysis. The BI analysis was also based on the new matrix of discrete morphological character (Table 1, Appendix I). This analysis was performed using RevBayes v.1.0.10 (Höhna et al., 2016). The Mk script for tree inference with discrete morphology available at https://revbayes.github.io/tutorials/morph/ was selected. We chose this script as uninformative and invariant characters were left in the matrix (See Appendix II), so correction for ascertainment bias was not necessary. Some parameters of the script were modified to fit the data matrix: 1) the set-up outgroups were the taxa *Diplophos* and *Myctophum* as suggested by Fielitz (2004); 2) the binary morphological substitution model was modified to include a five states character Q-matrix, as this was the maximum number in the data set; and 3) the number of generations in the MCMC increased to 1,000,000. The posterior distribution of phylogenies was summarized computing the Maximum a Posteriori (MAP) phylogeny. The MAP tree, according to Höhna et al. (2017), is interpreted as the most probable tree to have been generated based on the observed data. Tracer v 1.7.1 (Rambaut et al., 2018) was used to analyze convergence as indicated by the Effective Sample Size (ESS).

Character mapping. The mapping of characters was carried-out exclusively with the results of the SMP analysis. In TNT 1.5 (Goloboff and Catalano, 2016) we mapped the common synapomorphies to the most parsimonious trees obtained (apo >), and then contrasted with the mapping of synapomorphies in Winclada-ASADO 1.61 (Nixon, 2002) using all characters as nonadditive and showing unambiguous changes only.

Stratigraphic congruence analysis. The stratigraphic congruence of Enchodontidae was assessed with the R package strap (Bell and Lloyd, 2015a). The ages for the stratigraphic calibrations were taken from Díaz-Cruz et al. (2019b:282). In this exercise, only the fossil taxa derived from the SMP analysis were considered, and *Cimolichthys* was designed as the outgroup because of its close relationship with Enchodontidae (Fielitz, 2004; Beckett et al., 2017). As noticed by Cavin et al. (2012), *Enchodus zimapanensis* has a derived position in Enchodontidae (see Fielitz and González-Rodríguez, 2010) but is one of the stratigraphically oldest species. Due to this, we analysed stratigraphic congruence twice: first including *E. zimapanensis,* and secondly excluding it. The number of input trees was one and 38, respectively. The stratigraphic congruence analysis consisted of 1000 permutations with random dates for the tips. Polytomies were treated as soft, tree shape topology as the input, with the same outgroup for all the random trees (hard=FALSE, randomly.sample.ages=TRUE, samp.perm=1000, rand.perm=1000, fix.topology=TRUE, fix.outgroup=TRUE). We chose the Stratigraphic Consistency Index (SCI) (Huelsenbeck, 1994) as stratigraphic fit measure for the input tree (best SCI) and plotted against the ICS 2019 (user-defined). Finally we printed the distribution histogram of the input and randomly generated trees with the SCI measurement (hist(X$rand.permutations[, "SCI"]). More detailed specifications are given in Bell and Lloyd (2015b). The second analysis ran with the same specifications.

RESULTS

Systematic Paleontology

Order Aulopiformes Rosen, 1973
Family ENCHODONTIDAE Woodward, 1901
Subfamily Eurypholinae Fielitz, 2004

Diagnosis (emended). The species included in this subfamily have slightly to very long bodies as well as slightly to very large snouts; ventral portion of the cleithrum widens anteriorly and posteriorly; cleithrum ornamented with tubercles; ventral border of the mandible straight up to the mandibular symphysis; trunk naked except for the predorsal scute series extended between the dorsal fin base and the occiput and a single lateral scale series that encloses the lateral line.

Genus *Vegrandichthys* gen. nov.

zoobank.org/E9C1E809-0BAC-4822-AD5F-A1F4A7CAA567

Type species. *Vegrandichthys coitecus* sp. nov., see below.

Etymology. The name is a combination of the Latin adjective ‘vegrandis’ that means small, and the Greek suffix ‘ichthys’ or fish.

Diagnosis. As for the type species, see below.

Vegrandichthys coitecus sp. nov.

zoobank.org/9CDD4D86-98BE-46BC-B19C-7018293E3350

Holotype. IHNFG 5927, an almost complete fish transferred to polyester resin, which exposes the left side of the body (Figures 3-6).

Locality and age. Early Cenomanian laminated limestones of the Cintalapa Formation exposed in the El Chango quarry, Ocozocoautla de Espinosa Municipality, Chiapas, southeastern Mexico.

Etymology. The species epithet is in reference to the word 'coiteco', which is the local given name to the people from Ocozocoautla de Espinosa Municipality.

Diagnosis. Long-snout fish with a moderately elongated trunk; head length almost one third of the body length; small stout ventroposterior spine on the preopercle; large ventroposterior spine on the cleithrum; articulation between the quadrate and mandible laterally exposed; many lateral thickened ridges on the opercle; tiny pelvic fin in subabdominal position; predorsal scutes series consisting of four large and ovoid scutes that are intensely ornamented with tubercles and bearing a medial longitudinal keel; and lateral line scales triangular, smooth, and bearing a prominent medial keel.

Description

Measurements and general proportions. IHNFG 5927, holotype and only known specimen of *Vegrandichthys coitecus* gen. et sp. nov. is a gracile, small, and almost complete specimen, in which the entire caudal fin and postanal preural vertebrae are missing (Figure 3A). Table 1 summarizes the measurements and body proportions of this specimen. The standard length in this fish is unknown; however, this feature can be estimated as the length of the preserved part in this fish is 50 mm and the postanal region of the trunk ranges between a fifth to a seventh of the standard length in other members of Eurypholinae, *Eurypholis*, and *Saurorhamphus* (see Goody, 1969, figs. 47 and 55). Based on these data, the estimated standard length of IHNFG 5927 is between 59 and 61 mm.

The head length (HL) is 19.6 mm and probably represents 32 to 33% of standard length. The orbital and postorbital regions of the skull show the same length and together represent 40% of the

FIGURE 3. A) Lateral view of *Vegrandichthys coitecus* gen. et sp. nov., IHNFG 5927 holotype transferred in plastic resin from Early Cenomanian deposits of the El Chango quarry, Chiapas, Mexico. B) Artistic reconstruction of *Vegrandichthys coitecus* gen. et sp. nov.

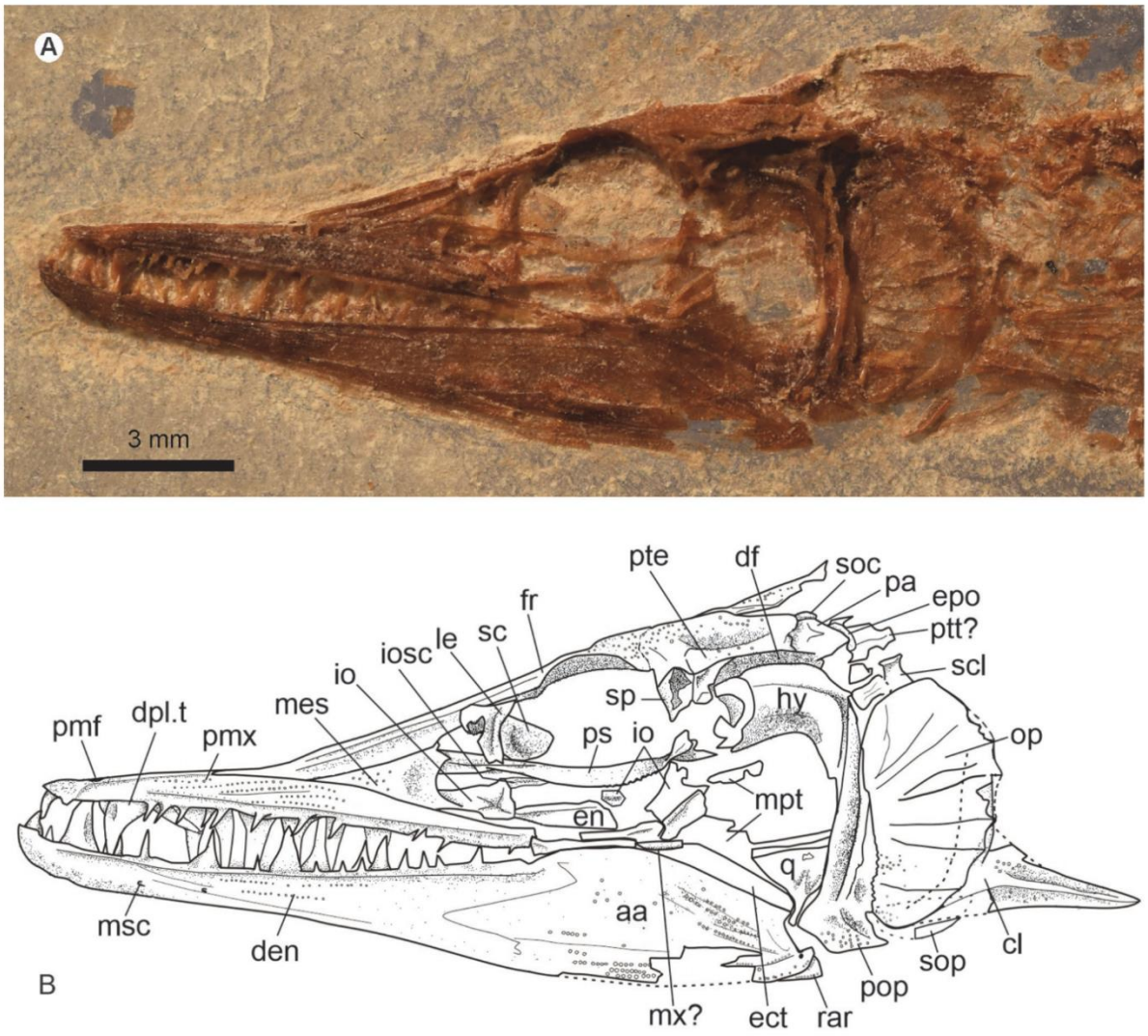

FIGURE 4. *Vegrandichthys coitecus* gen. et sp. nov. A) A close-up of the lateral view of the head; B) Drawing of the head and pectoral girdle in lateral view. Abbreviations: aa, anguloarticular; cl, cleithrum; den, dentary; df, dilatator fossa; dpl, dermopalatine, dpl.t, dermopaltine teeth; ect, ectopterygoid; en, endopterygoid; epo, epiotic; fr, frontals; hy, hyomandibula; io, infraorbital; iosc, infraorbital sensory canal; la, lacrimal; le, lateral ethmoid; mpt, metapterygoid; msc, mandibular sensory canal; mx, maxilla; op, opercle; pa, parietals; pmf, premaxillar fenestra; pmx, premaxilla; pop, preopercle; ps, parasphenoid; pte, pterotic; ptt, posttemporal; q, quadrate; rar, retroarticular; sc, sclerotic; scl, supracleithrum; soc, supraoccipital; sop, subopercle; sp, sphenotic.

skull length; the remaining 60% corresponds to the snout or preorbital region.

The body of IHNFG 5927 is shallow and fusiform. The head height (HH) is relatively shallow, representing a little less than 40% of the head length (HL) and is slightly less than the maximum body height that is present in the predorsal region of the trunk. The dorsal fin is short and placed in the posterior half of the abdominal cavity; the dorsal fin length and the predorsal length represent 25% and 150% of HL, respectively. The posterior end of the anal fin is unknown; however, it is longer than the dorsal fin and is located behind it. The anal fin base is at least 5.5 mm (28% of HL) and rises at 203% of HL. The pectoral fin is in the lateral surface of the trunk, a little closer to the abdominal edge than to the vertebral column. The small pelvic fin is in ventral position and located in the predorsal region of the trunk, at 136% of the HL. Behind the dorsal fin, the trunk progressively

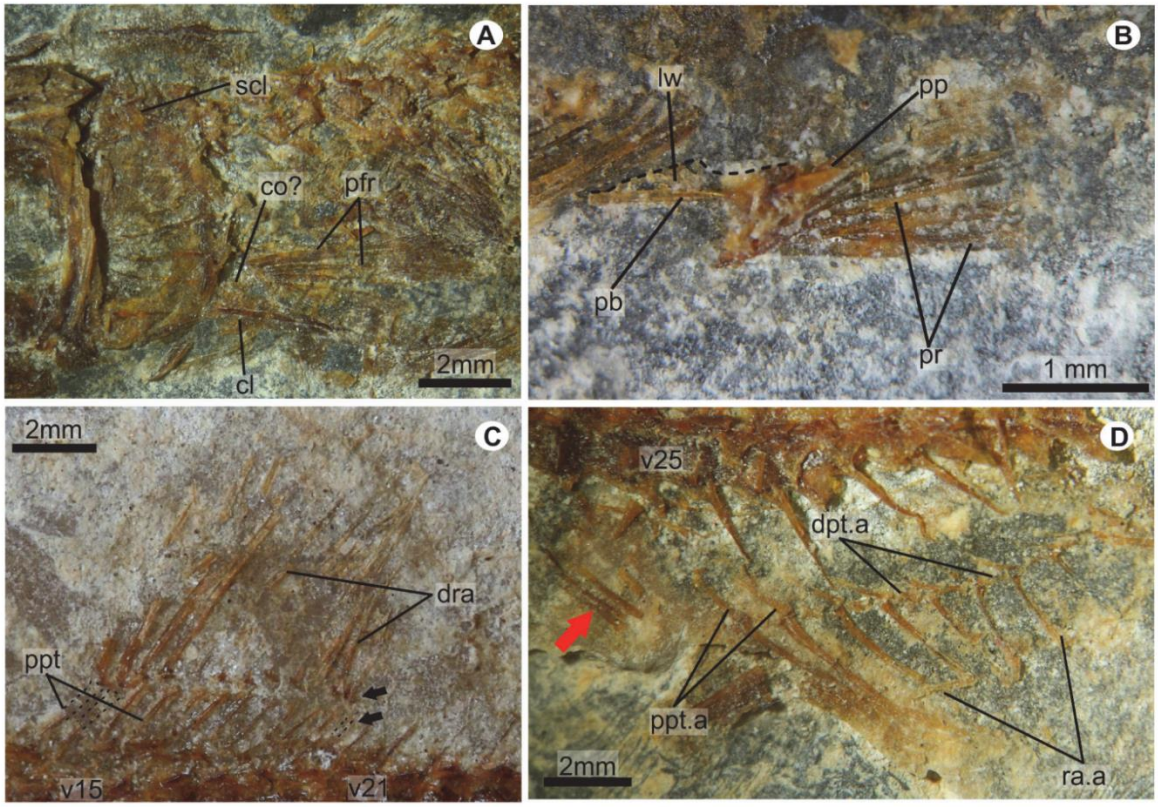

FIGURE 5. Close-up of different anatomical structures in the holotype of *Vegrandichthys coitecus* gen. et sp. nov. A) Pectoral girdle and fin, B) Pelvic girdle and fin, C) Dorsal fin and D) Anal fin. All anterior structures are laterally exposed. Abbreviations: cl, cleithrum; co, coracoid; dpt.a, anal fin distal pterygiophores; dra, dorsal fin rays; lw, lateral wing; pb, pelvic bone; pfr, pectoral fin rays; pp, posterior process; ppt.a, anal fin proximal pterygiophores; ppt, proximal pterygiophores; pr, pelvic rays; ra.a, anal fin rays; scl, supracleithrum; v, vertebra.

tapers and probably behind the anal fin forms a shallow caudal peduncle.

Skull. The skull is triangular, anteriorly tapered, and about three times longer than high (Figure 4). Although the contact of the mesethmoid with the anterior tips of the frontals is covered by the anterior dorsal ends of the premaxilla, the frontals are likely at least three-quarters the length of the skull roof. The left frontal is dorsally exposed showing its flat and triangular shape, anteriorly pointed, slightly wider behind the orbit, and rectangular in the postorbital region. Behind the orbit, each frontal is firmly sutured with four bones; laterally with the sphenotic and pterotic and posteriorly with the supraoccipital and parietal. The supraorbital sensory canal runs along the frontal, near its lateral edge, enclosed above the orbit and exposed in its preorbital region. The frontals are superficially smooth along the preorbital region; in contrast, behind the orbit the frontals and other bones are strongly ornamented with small tubercles. The parietals are short triangular bones at the back of the skull roof, expanded laterally, and medially separated by a small supraoccipital bone.

The sphenotic is a small and triangular bone bordering the dorsoposterior orbital region; the pterotic is an elongated rectangular bone that reaches the back of the skull (Figure 4). The posttemporal fossa is a small depression in the region where the frontal, pterotic, and sphenotic converge. The dilator fossa is a shallow elongated depression laterally extended along the posterior two thirds of the pterotic and roofed by the sphenotic. The parasphenoid is an elongated laminar and straight bar extended along the orbital and the ethmoid region of the skull, with a flat and smooth lateral surface bearing numerous micro-serrations along the ventral edge of its posterior half.

None of the bones of the posterior region of the skull are exposed except for the epiotic, which seems to be short and wide. Much of the lateral otic region of the skull is covered by the hyoman-

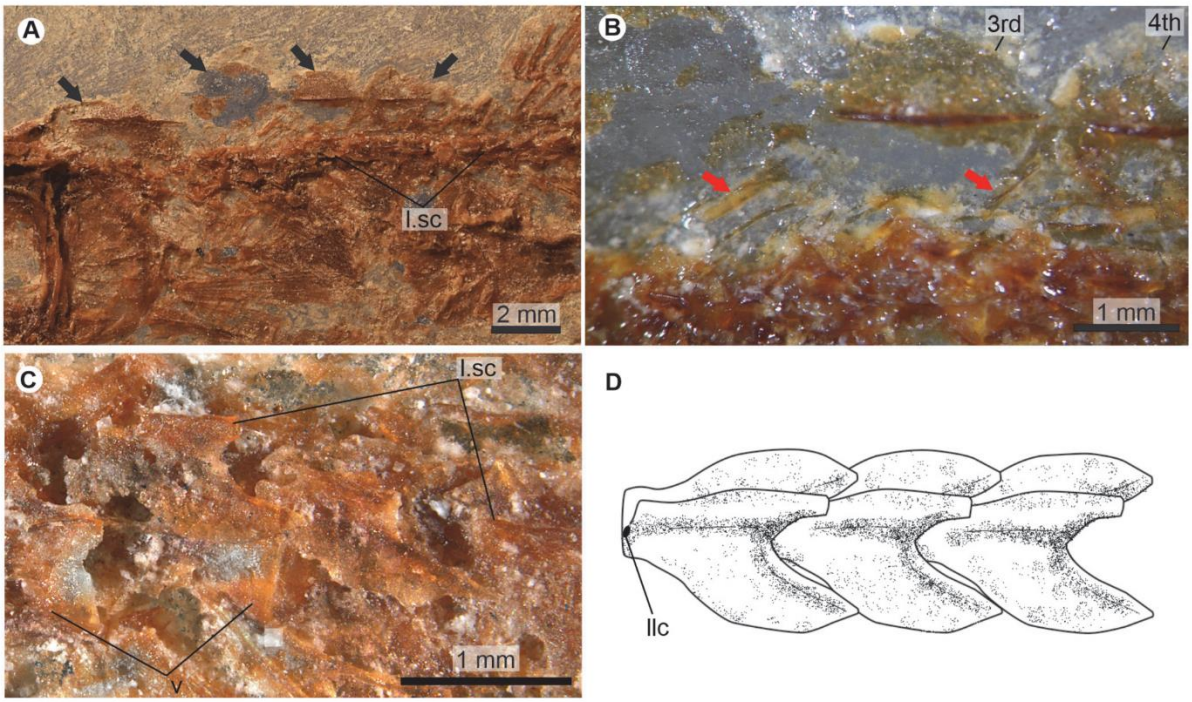

FIGURE 6. Scutes, scales and associated bones of *Vegrandichthys coitecus* gen. et sp. nov. A) Dorsal scutes series, B) close-up of the dorsal scutes region, C) close-up of the lateral line of scales, and D) drawing of the probable position and overlapping of the lateral line of scales. Abbreviations. llc, lateral lines canal; l.sc, lateral line scales; v, vertebrae. Ordinal numbers denote the number of dorsal scute. Black arrows point out each of the dorsal scutes. Red arrows point out the supraneurals.

TABLE 1. Measurements and body proportions of IHNFG-5927, holotype and single specimen of *Vegrandichthys coitecus* gen. et sp. nov. (all measurements are expressed in millimeters; + shows incomplete measurements and counts).

Measurements and counts		% of HL
Standard length (SL)	52+	?
Head length (HL)	19.6	100
Snout length (SL)	9.8	50
Head height (HH)	7.5	38.2
Maximum body height (MBH)	7.8	39.7
Predorsal length (PDL)	29.7	151.1
Preanal length (PAL)	39.7	202.5
Prepelvic length (PPL)	26.7	136.2
Dorsal fin length (DFL)	4.9	25
Anal fin length (AFL)	5.5+	?
Pectoral fin rays	6	
Dorsal fin rays/pterygiophores	12/11	
Anal fin rays/pterygiophores	13+/13+	
Pelvic fin rays	5	
Vertebrae (total/abdominal/caudal)	30+/21/9+	

dibula. In the preorbital region, the lateral ethmoid is a thick triangular and somewhat curved bone that separates the nasal capsule from the orbit, it sutures with the ventral inner surface of the frontal, and ventrally projects below the parasphenoid. The anterior edge of the nasal capsule is covered by the lateral process of the mesethmoid bone, which is an expanded triangular and flat structure that meets the lateral anterior end of the frontal and is covered by the dorsal edge of the premaxilla (Figure 4).

Circumorbital series. The circumorbital bones are poorly preserved (Figure 4). This is an open series, with no dorsal bones. Remains of flat, rectangular, and flimsy infraorbital bones from the left and right sides of the head are preserved below the nasal capsule and the middle orbit. All these bones show the infraorbital sensory canal running near to their respective orbital edges, as well as few ventral branches of this canal. A large semicircular and flat basal sclerotic bone occupies the orbit.

Suspensorium. Bones of the suspensorium or hyomandibular series are only partially exposed (Figure 4). The hyomandibula is a large T-shaped bone in which the descending process is curved forward and the head is broad with a sinuous articular surface. The central region of this bone is reinforced with apicobasal ridges.

The quadrate is a laminar triangular bone with a small stout ventral head that is inclined forward. The symplectic and the joint between the ventral tip of the hyomandibular and the quadrate are obscured. The ectopterygoid is a laminar and toothless bone that is only partially exposed; its anterior region lies below the lower jaw while its spatula-like posterior part is tilted backward to meet with the quadrate anterior edge. The metapterygoid is laminar and poorly preserved, contacting the concave anterior margin of the hyomandibula and the dorsal edge of the quadrate. Only fragmentary, laminar, and toothless remains of the endopterygoid are preserved.

Although the dermopalatine is entirely covered by the premaxilla, a large, robust dermopalatine tooth is visible. This tooth seems to be placed at the anterior end of the bone, has a stout base, and a conical crown slightly curved backward and projected downward. The dermopalatine appears to bear multiple teeth, but the smaller posterior teeth are difficult to distinguish with precision.

Upper jaw. The upper jaw consists of two bones, the premaxilla and maxilla (Figure 4). There is no indication of a supramaxilla. The premaxilla is a flat triangular bone, pointed posteriorly, and extends for three quarters of the jaw. This bone has a single row of small, conical, sharp teeth, which are of similar size and evenly separated, except for a series of progressively smaller teeth along the posterior quarter of the bone. The anteriormost maxillary tooth is peculiar because it is slightly larger and rather sigmoidal. The dorsal ends of both maxillae are bent inwards to form the roof of the anterior half of the snout. A small midline fenestra, near the tip of the snout, presumably accommodated two teeth from the lower jaws. The outer surface of the premaxilla is intensely ornamented with small tubercles. Fragments of the maxilla reveal that this toothless, smooth, and rod-like bone is extended below the orbit.

Lower jaw. Three bones of the lower jaw are exposed in IHNFG 5927: dentary, anguloarticular, and retroarticular (Figure 4). In lateral view, the lower jaw is elongate, extending below the orbit and the anterior half of the otic region of skull. The first two fifths of its length are shallow, and it becomes progressively deeper more posteriorly: its deepest point is four times the depth of its shallowest point. Both the alveolar and ventral border are somewhat sinuous, the symphysis is very shallow, and the coronoid process is hardly recognizable. At the base of its posterior edge, the jaw has a small posteriorly-directed postarticular process. The mandibular sensory canal runs close to the ventral edge of the lower jaw. It is enclosed by bone, and opens through six pores scattered along the dentary and the anguloarticular bones. The entire labial surface of this jaw is ornamented with numerous tubercles.

The dentary is a triangular bone, occupies a large part of the lower jaw, and has a posterior deep and acute concavity to suture tightly with the anguloarticular bone (Figure 4). The alveolar border of the dentary occupies about two thirds of the jaw and bears two rows of teeth. The labial tooth row includes conical teeth in two sets: groups of one to three small and gracile conical teeth intercalated with larger isolated teeth with thicker bases. The lingual dentary tooth row consists of at least four sharp laterally compressed teeth exposed in the middle of the alveolar border, which resemble the longer teeth on the labial teeth row but they are thinner. Of the labial dentary teeth, the second isolated tooth is so developed that, in life, its tip must have penetrated the premaxilla through its dental fenestra. Since the specimen has single premaxillary dental fenestra, it is possible that the anterior ends of both dentaries were either very close or met in a long symphysial contact.

Although the ventral anterior end of the dentary does not have osseous beards or dentary prongs (cf those of other enchodontids: *Enchodus*, Goody, 1969, figs. 36, 39; *Unicachichthys*, Díaz-Cruz et al., 2016, figs. 5, 6; *Veridagon*, Díaz-Cruz et al., 2019b, fig. 3), it does display a series of conspicuous bony lumps. At this point, it is not possible to decide whether these osseous lumps are a preservation artifact, an analogy, or a homology of the dentary prongs of other specimens. In the absence of additional fossils, the authors consider that *Vegrandichthys coitecus* gen. et sp. nov. lacks dentary prongs.

The anguloarticular occupies the posterior 40% of the lower jaw (Figure 4). This triangular bone bears the postarticular process in which the small and shallow articular facet for the quadrate is exposed in lateral or labio-lingual view. A tiny wedge-shaped retroarticular covers the postero-ventral corner of the postarticular process.

Opercular series. This series consists of three laminar bones, opercle, subopercle, and preopercle; the infraopercle is absent (Figure 4). The opercle is semicircular, about twice higher than long, and anteriorly straight and thick. An articular facet for the hyomandibular is borne near its anterior edge about a third of the way down. Seven thickened bars are present on the opercle, laterally exposed as longitudinal straight ridges; the central ridge is the most conspicuous. As the posterior edge of the opercle is very thin, it is not clear whether the bars form true spines or not. The lower third of the opercle is superficially ornamented with tubercles.

The preopercle is a triangular bone, about 2.5 times higher than long, dorsally pointed, ventrally convex, and expanded anteriorly and posteriorly (= “widens anterior and posteriorly” in Fielitz, 2004) (Figure 4). The anterior edge is thickened, slightly convex, and its base is expanded anteriorly; in contrast, the posterior edge of the preopercle is rather laminar, convex, bears small serrations, and its base forms a posterior thick and conspicuous spine. The preopercle is smooth except for small tubercles borne on its ventroposterior limb. The preopercular sensory canal is enclosed by bone and opens externally through two or three pores present in the ventroanterior preopercle limb.

Although the subopercle is poorly preserved and largely covered by the opercle, some remains of this laminar bone are preserved behind the preopercle and below the opercle. Apparently, the subopercle is ornamented with small tubercles (Figure 4).

Branchiostegal rays and gill arches. No element of the branchiostegal rays or the gill arches are exposed.

Vertebral column. Unfortunately, the specimen does not preserve the posterior part of the body; however, a large part of the vertebral column is exposed and consists of at least 30 total vertebrae, including 21 abdominal and at least nine caudal (Figures 3A, 5, 6A). All centra are hourglass-shaped bones and slightly constrained in the center. The centra in the middle of the body are about two times longer than high, while those placed in front and back are slightly and progressively shorter, and become about 1.5 times longer than high. Laterally, a couple of thick longitudinal ridges reinforce the centra. Along the vertebral column, the centra have no parapophyses or zygapophyses, and each centrum is fused with its respective dorsal and haemal arches and spines. The haemal and neural spines are uniformly thick, straight and inclined backward. In the abdominal centra, ribs are present as bars with a small articular head and a sharp distal tip.

At least two supraneurals are present below the predorsal scutes and between the occiput and the dorsal fin rays (Figure 6B). These spatula-like bones have a differentiated dorsal head that is anteriorly and posteriorly expanded, as well as an anteriorly directed elongated and straight ventral limb. Along the abdominal centra there are thread-like epineurals inclined backward that probably extended along three or four centra from the lateral surfaces of the neural arches. Remains of posteriorly directed thread-like epipleurals are present along the abdominal region.

Pectoral girdle and fin. Pectoral girdle bones are relatively poorly preserved or obscured (Figures 4, 5A). Only fragments of the left posttemporal bone are present behind the skull of the specimen. Most of the supracleithrum is covered by the opercle; only its dorsal end is exposed. The cleithrum is an inverted T-shaped bone in which the dorsal and anterior limbs are not completely observed. The posterior limb of the cleithrum forms a large spiny ventral process that projects posteriorly, and its longitudinal axis is reinforced by a conspicuous ridge. The cleithrum seems to be a smooth bone except for the posterior spine that is ornamented with small tubercles. No postcleitra are preserved.

The left pectoral fin is located above the ventral posterior spine of the cleithrum (Figure 5A). This fin consists of six distally branched and segmented rays. Only fragments of the coracoid are

preserved. The length of the pectoral fin equals four and a half abdominal vertebrae (Figure 3).

Pelvic girdle and fin. The pelvic fin is set on the anterior half of the abdomen on its ventral border and rises below the abdominal centrum 10. The length of the pelvic fin hardly equals that of two abdominal centra. This fin consists of five distally segmented and branched rays, which are supported on the posterior edge of the pelvic bone. This triangular bone has a laminated triangular lateral wing and a stout and short posterior process (Figure 5B).

Dorsal fin. The dorsal fin is contained within the posterior half of the abdominal cavity (Figure 3). It consists of 12 distally branched and segmented rays supported by 11 stick-like proximal pterygiophores (Figure 5C). This fin is rounded because the length of those rays in the middle of the fin equals the length of the base while those placed on the front and back are progressively shorter. The base of this fin is extended above the last six abdominal centrae (15-21). The dorsal fin rays are located close to the body because of the lack of distal pterygiophores.

Anal fin. The anal fin originates posteriorly to the dorsal fin (Figure 3). The posterior edge is not preserved, but there are 13 longitudinally grooved and distally segmented rays supported by 13 rod-like and straight proximal pterygiophores (Figure 5D). In the posterior two thirds of the anal fin, there are noticeably elongated distal pterygiophores causing the separation of the associated anal rays. Although the anterior anal fin rays are fragmented; it seems that the fin was roughly triangular in shape. The anal fin extends below the vertebrae 25 to 31; however, its first three proximal pterygiophores are projected into the space between the haemal spines of the first caudal centra (22 and 23).

Caudal skeleton and fin. The caudal fin is not preserved.

Squamation. The body is almost entirely naked (Figures 3A, 6A-D). However, the predorsal trunk edge bears a row of four predorsal scutes. The lateral line is enclosed by a single row of modified scales exposed along each body flank.

The predorsal scutes are ovoid structures, about two times longer than wide, forming a continuous row where the posterior end of one scute is in contact with the anterior tip of the subsequent scute (Figures 4, 6A-B). These scutes consist of a median longitudinal keel with a pointed posterior margin. Either side of the keel, a semi-ovoid lateral wing expands laterally to cover the predorsal edges of both body flanks. The entire outer surfaces of these scutes are intensely ornamented with numerous tubercles.

The modified flank scales of the lateral line are thin sinuous structures with rounded edges. A prominent keel is present on the midline, and either side of this is a posteriorly projecting subrectangular lobe (Figures 3, 6C-D). In the abdominal region these scales are rectangular, slightly higher than long, around two thirds the length of each vertebral centrum, and are placed slightly above the vertebral column. In contrast, the scales close to the caudal region are progressively smaller, shallower, and located at the level of the centra. The longitudinal axis of these scales encloses a tube that housed the lateral sensory canal. Additionally, above the canal, each scale has a conspicuous, laminar, and triangular keel that projects posteriorly.

Taxonomical Remarks

The family Enchodontidae has been studied by many authors (Fielitz, 2004; Silva, 2007; Fielitz and González-Rodríguez, 2010; Silva and Gallo, 2011; Cavin et al., 2012; Díaz-Cruz et al. 2016, 2019a), who agree on its monophyly but disagree over the inclusion of *Rharbichthys* and the composition of its subfamilies. *Vegrandichthys coitecus* gen. et sp. nov. exhibits some of the characters already included in the diagnosis of this family, such as the lack of interopercle and supraorbital, the presence of the horizontal strengthening bar on the opercle, tubercles ornamenting the opercle and subopercle, and a series of predorsal scutes between the occiput and the dorsal fin (Figures 3-6). Therefore, the inclusion of *Vegrandichthys* into the family Enchodontidae is strongly supported.

Additionally, *Vegrandichthys coitecus* gen. et sp. nov. possesses a peculiar combination of characters that is unique among enchodontid genera. Most enchodontids have preopercles with no posterior spines; however, *Vegrandichthys* and *Unicachichthys* share the presence of a posterior spine at the base of the preopercle. Such spine is short in *Vegrandichthys* (Figure 5) compared to that of *Unicachichthys* (Díaz-Cruz et al., 2016, fig.5).

Among enchodontids, as previously known, there are five different body patterns defined based on the different shapes of the snout and trunk: 1) a short snout and rather pisciform trunk as in *Enchodus, Unicachichthys,* and *Veridagon* [see Figure 1] ; 2) a short snout and rather rounded, short and high trunk, as in *Parenchodus*; 3) a short snout and

very long trunk as in *Palaeolycus*; 4) a moderately long snout and perciform trunk as in *Eurypholis*; 5) a long snout and very long trunk as in *Saurorhamphus*. The body pattern displayed by *Vegrandichthys* gen. nov. resembles that of *Eurypholis*; however, the length of the snout is intermediate between those seen in *Eurypholis* and *Saurorhamphus*.

Additionally, among enchodontids the articulation between the lower jaw and the quadrate shows two conditions. This articulation is laterally covered by a posterior extension of the anguloarticular bone in *Eurypholis* and *Saurorhamphus*, but laterally exposed in other enchodontids. *Vegrandichthys* gen. nov. shares the second condition with *Enchodus, Parenchodus, Unicachichthys, Veridagon,* and *Palaeolycus.*

Finally, among enchodontids, the opercle also shows two conditions. The posterior border of this bone is rounded and continuous in *Enchodus, Parenchodus, Unicachichthys, Veridagon,* and *Palaeolycus*. In contrast, in *Eurypholis* and *Saurorhamphus* the longitudinal crest in the middle of this bone is extended, forming a posterior spine. Again, in this case *Vegrandichthys* gen. nov. shows the first of the conditions; however, this new fish is unique because it has additional strengthening longitudinal crests in the preopercle.

Phylogenetic Results

The Standard Maximum Parsimony (SMP) analysis retained one most parsimonious tree of total length 316 steps (CI = 0.456 and RI = 0.693) (Figure 7). The SMP analysis resolves Enchodontidae as a monophyletic family comprising the genera *Enchodus, Eurypholis, Palaeolycus, Parenchodus, Saurorhamphus, Unicachichthys, Veridagon,* and the monospecific genus herein described, *Vegrandichthys*.

In this phylogenetic exercise, *Vegrandichthys coitecus* gen. et sp. nov. is supported as an enchodontid by the presence of four synapomorphies (Figure 5; node a): i) anteroventral prongs present; ii) supraorbital bone absent; iii) pelvic fin at or posterior to the dorsal fin; iv) opercular and subopercular dermal pattern as ridges with tubercles along each ridge. *Vegrandichthys* is placed in Eurypholinae as the sister taxon of the clade composed by *Eurypholis* + *Saurorhamphus*, on the basis of a single character: ventral portion of the cleithrum anterior and posteriorly widened (Figure 7; node d). Overall, in our phylogenetic analysis, the Bremer and bootstrap values across the retained tree are low.

The placement of *Vegrandichthys coitecus* gen. et sp. nov. as a member of Eurypholinae was also consistent in all the additional phylogenetic analyses carried out. The analysis based on Phylogenetic Morphometrics (PM) of the preopercle landmark configuration retained only one tree with best score = 0.04079. This phylogenetic hypothesis suggests, in addition, a close relationship between *Unicachichthys* and Eurypholinae (Figure 8A-B).

The phylogenetic analysis with Implied Weighted Maximum Parsimony (IWMP) recovered the same topology regardless of parameters (k=10 and k=100; Figure 8C). However, the best score was different for each analysis (k=100:1.6622; k=10; 12.9163). These results show the same phylogenetic relationships displayed in the analysis of SMP for all the taxa.

The phylogenetic hypothesis obtained with Bayesian Inference (BI) shows a very different topology with respect to those obtained with other methods (Figure 8D). Nevertheless, Eurypholinae keeps the same composition, and *Vegrandichthys* retains its phylogenetic placement in the subfamily.

The analysis combining morphological discrete data with the landmark configuration of the preopercle retained only one tree with tree length=316.04924, of which 0.04924 is the preopercle configuration contribution (Figure 8E). The phylogenetic position of the new taxon and the composition of Eurypholinae agree with the topology recovered with SMP, IWMP and BI.

In all the performed analyses the support values of the clades in the subfamily Eurypholinae, as well as their posterior probabilities, are among the highest values across the tree.

On the other hand, the stratigraphic fit analysis showed that the inclusion of *Enchodus zimapanensis* decreased the level of stratigraphic fit of Enchodontidae: stratigraphic fit is far more consistent in the analyses that excludes *E. zimapanensis* (Figure 9). Randomly generated ages in the first analysis improved slightly the stratigraphic fit, but in the second analysis they decreased it.

DISCUSSION

The monophyly of Enchodontidae has been repeatedly corroborated, as shown by Fielitz (2004), Silva and Gallo (2011), Díaz-Cruz et al. (2016, 2019b), and Vernygora et al. (2017); this finding is also supported in the present work. However, characters supporting the monophyly of the family differ from those reported in previous works. Originally, Fielitz (2004) found that the presence of

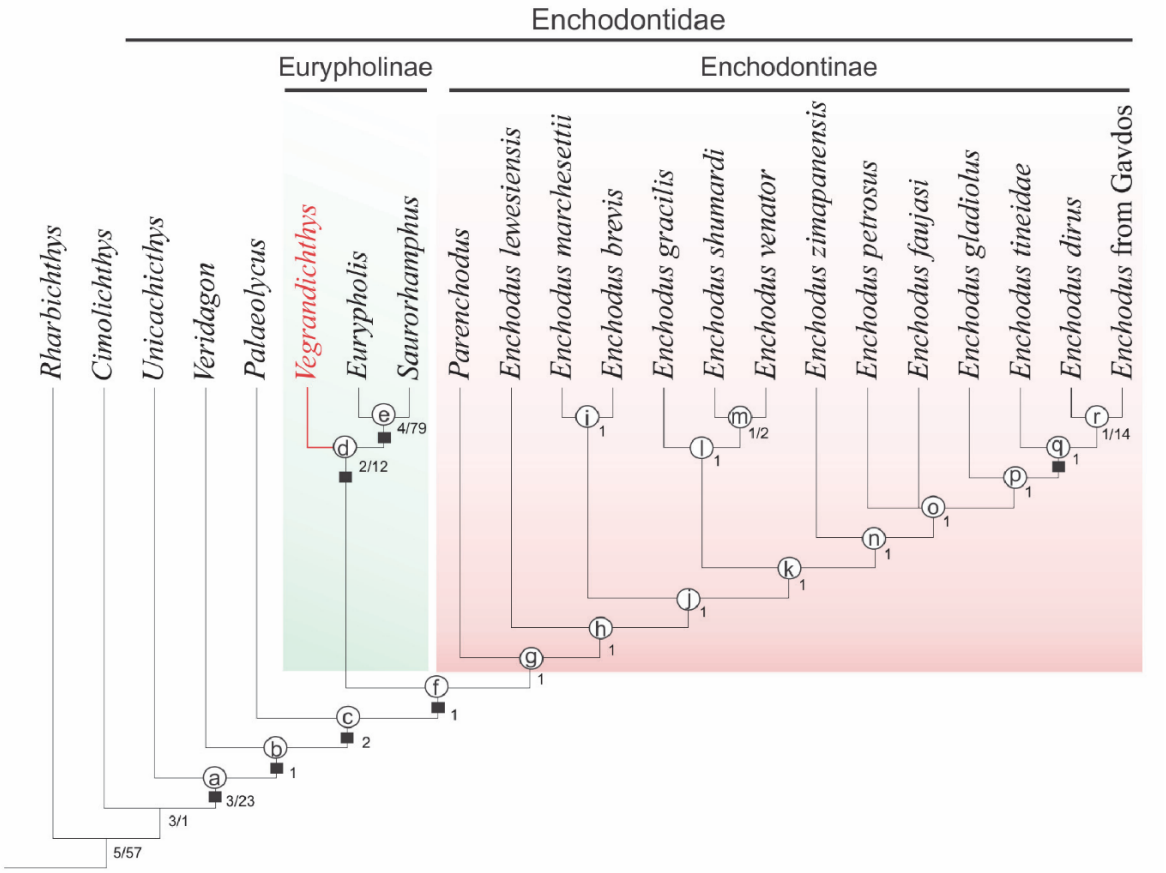

FIGURE 7. Phylogenetic relationships of Enchodontidae including *Vegrandichthys coitecus* gen. et sp. nov. obtained following the protocol described of the Standard of Maximum Parsimony (TL= 316, CI = 0.456, RI= 0.693). The subfamily Eurypholinae in green background and Enchodontinae in red background. Numbers by nodes indicate the supports values of Bremer/Bootstrap. Black squares indicate the presence of synapomorphic characters in Enchodontidae. Node a, Enchodontidae: presence of anteroventral prongs (36:1); absence of supraorbital bone (43:1); pelvic fin at or posterior to the dorsal fin in position (52:1); opercular and subopercular dermal pattern as tubercles (55:2). Node b: Laminar posterior limb in the ventral portion of the preopercle (50:0). Node c: Ectopterygoid teeth between six to eight teeth with the second tooth longest (12:2). Node d, Subfamily Eurypholinae: Ventral portion of cleithrum widens anteriorly and posteriorly (60:2). Node e: Laterally exposed articulation mandible-quadrate (34:1); Opercular horizontal strengthening ridge continues past posterior edge to form a spine (52:2). Node f: Mandibular dermal pattern as ridges with tubercles along each ridge (41:2); Preopercular dermal pattern as ridges with tubercles (54:2). Node q: Sigmoidal lateral view of dermopalatine teeth (16:2). Numbers by nodes show the Bremer/Bootstrap values. The subfamily Enchodontinae is only supported by homoplastic characters, therefore, we omitted them in the node description. Full description and character mapping are in Appendix II.

a single dermopalatine tooth, the dermopalatine bone same length or shorter than the tooth and the absence of interopercle were the diagnostic characters for Enchodontidae. This was modified by Silva and Gallo (2011), who proposed that the only synapomorphy for Enchodontidae is the presence of middorsal scutes. Díaz-Cruz et al. (2016:146) and Vernygora et al. (2017:12) recovered the same character as the single unique synapomorphy for Enchodontidae. However, the phylogenetic analysis of Enchodontidae performed by Díaz-Cruz et al. (2019b:280) challenged this hypothesis. These authors found that, after adding *Veridagon avendanoi* to the phylogeny, characters supporting the monophyly of Enchodontidae were: presence of anteroventral prongs, absence of supraorbital bone, dermal pattern on opercular and subopercular as ridges with tubercles along each ridge, and the presence of a horizontal bar on the opercular. The phylogenetic exercise presented here, partially

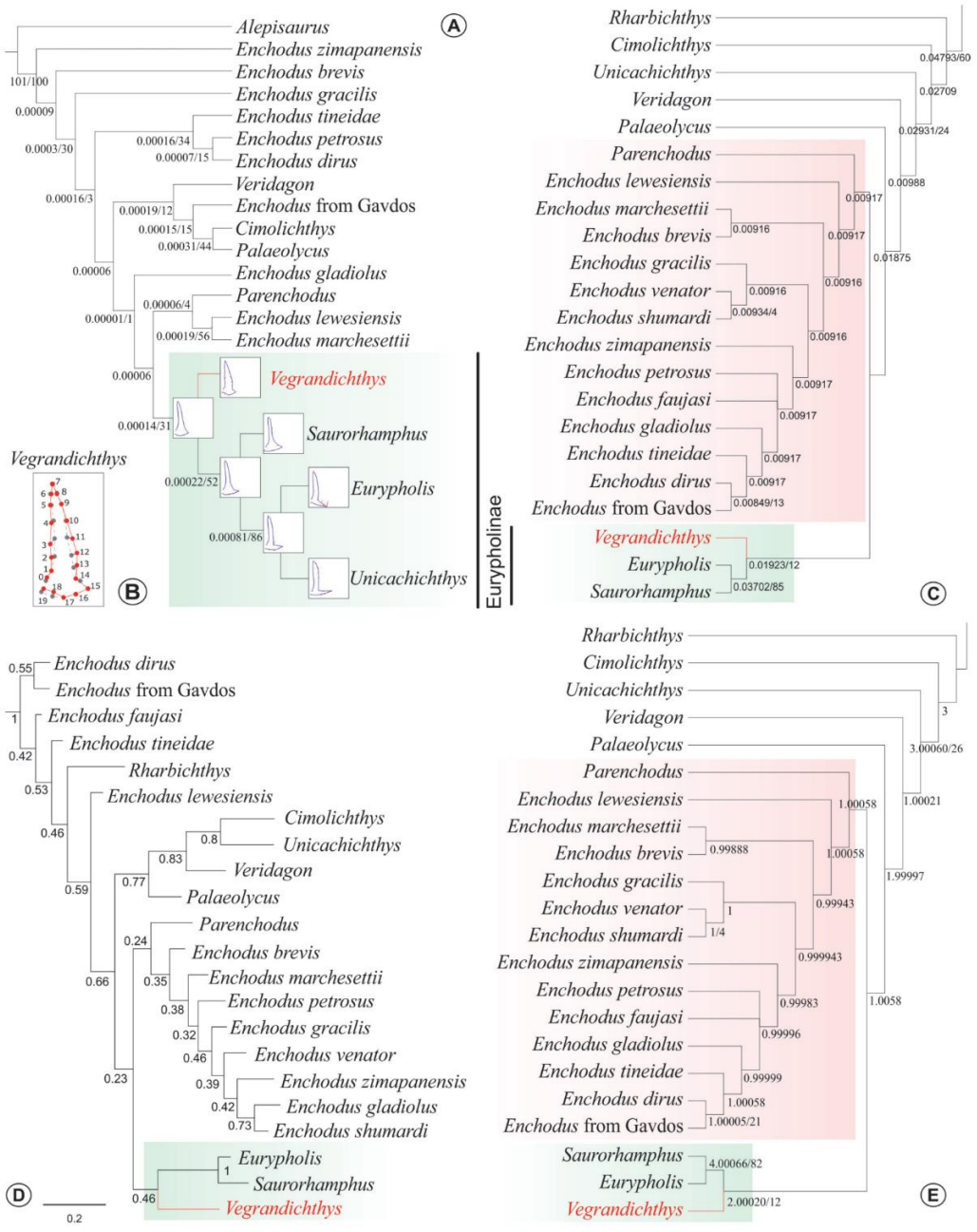

FIGURE 8. Results of the inclusion of *Vegrandichthys coitecus* gen. et sp. nov. in the phylogeny of Enchodontidae using multiple phylogenetic approaches. A) The one retained tree of Enchodontidae with the Phylogenetic Morphometrics (PM) method using only landmark data, the Best Score reached = 0.04079. B) Dots in red correspond to the landmark configuration of the preopercle used to run the PMA. C) Implied Weighted Maximum Parsimony (IWMP) tree (the same tree topology with K=10 and K=100) based exclusively on discrete morphological data. D) Maximum a Posteriori (MAP) phylogeny obtained with Bayesian Inference. E) Tree obtained with the combined matrix of morphological discrete data and the landmark configuration of the preopercle, using Standard Maximum Parsimony; Best score = 316.04924. In green background is the subfamily Eurypholinae, except in A that includes *Unicachichthys*. Background in red is the clade formed by *Parenchodus* + *Enchodus* species. In all the phylogenetic analyses *Vegrandichthys coitecus* gen. et sp. nov. new is recovered as a member of the subfamily Eurypholinae along with *Eurypholis* and *Saurorhamphus*. Numbers by nodes indicate Bremmer / bootstrap (when present) values except in D, where numbers indicate the posterior probability. Full phylogenetic hypotheses and their description can be accessed in Appendix II.

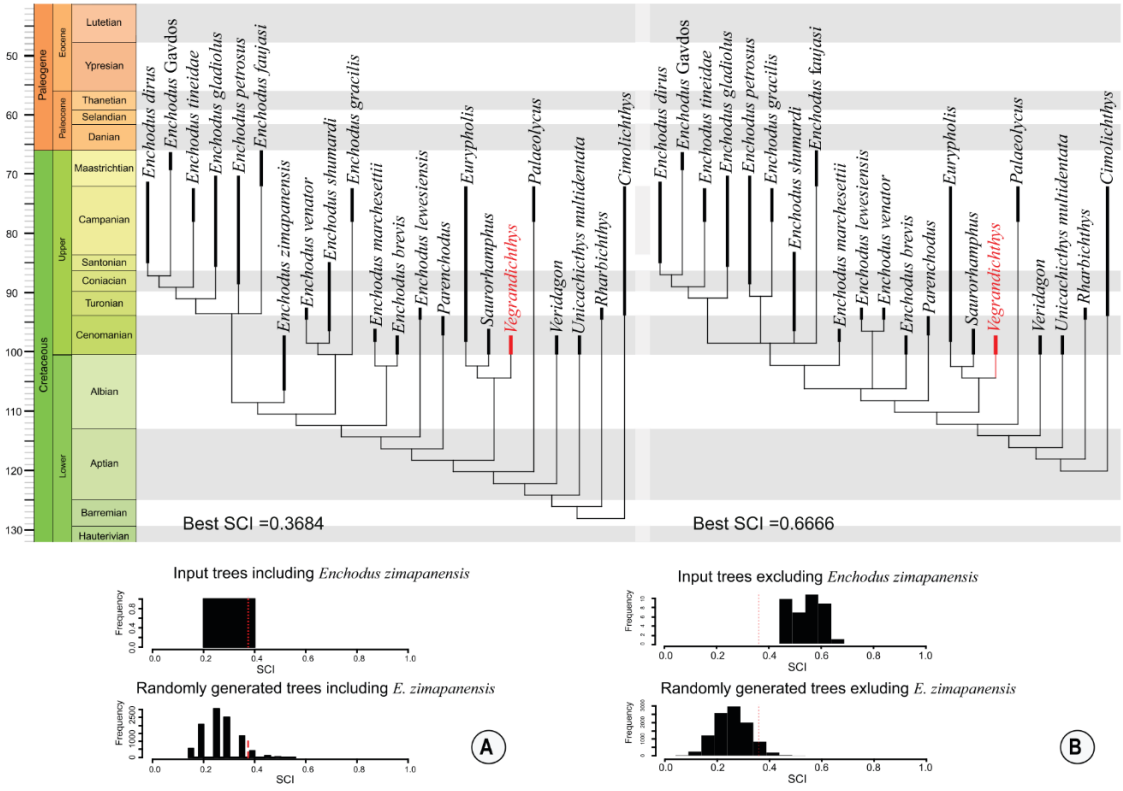

FIGURE 9. Assessment of the stratigraphic congruence in Enchodontidae. A) Phylogeny including *Enchodus zimapanensis* and B) phylogeny excluding it. Both phylogenies time-calibrated and plotted against the ICS 2019 data. Red branch points out the phylogenetic position of *Vegrandichthys coitecus* gen. et sp. nov. Below each tree, there are the histograms of the SCI for the input and randomly generated topologies.

agrees with the results described by Díaz-Cruz et al. (2019b), also recovering the first three characters, but additionally finding the pelvic fin at or posterior to the dorsal fin in position (52:1) as a synapomorphy. Moreover, in the work of Díaz-Cruz et al. (2019b) as well as the present work, *Rharbichthys* is excluded from Enchodontidae.

It is important to highlight that the phylogenetic analysis of Silva and Gallo (2011) is aimed at understanding phylogenetic relationships within the suborder Enchodontoidei, and included Dercetidae and other *incertae sedis* taxa [see Silva and Gallo (2011) and Vernygora et al. (2017)] in addition to Enchodontidae. Because of this different focus, the morphological characters and formulations of primary homology vary from those used in this manuscript. In contrast, the data matrix employed by Fielitz (2004) focuses on the relationships between enchodontids and extant forms, and therefore serves as a backbone for our study. The character pertaining to dorsal bony scutes (c.78 in Fielitz 2004; c.83 in the present work) also captures information relating to dermal ornament, which may not be independent (Simões et al., 2017). Furthermore, compound characters such as this are recognized to be problematic (Brazeau, 2011; Simões et al., 2017), and this may account for the presence of dorsal scutes not being recovered as a synapomorphy for the family.

Time calibrated phylogenies of Enchodontidae show that most taxa are restricted to the earliest period of the Late Cretaceous, suggesting a Cenomanian 'explosion' for the group. However, inclusion of *Enchodus zimapanensis* decreases the stratigraphic fit of the family, suggesting that the evolutionary history of Enchodontidae is far from complete. Recent work by Díaz-Cruz et al. (2019a) reporting additional *Enchodus* species from the Middle East supports this, but the full implications of these findings on enchodontid phylogeny are not yet known. Isolated teeth with enchodontid affinity have also been reported from

lower Barremian strata of Alcaine, Spain (Kriwet, 2003), and specimens referred to *Enchodus* sp. are known from the early Aptian-late Barremian of Morro de Chaves formation, Alagoas, Brazil (Coelho, 2004; García et al., 2018). Unfortunately, due the incompleteness of these records, and their uncertain taxonomical affinity, it is not possible for us to include them in our analysis. In the meantime, the finding and formal description of *Vegrandichthys,* the first Eurypholinae from the Americas, strengthens the importance of this territory for better understanding Enchodontidae evolution.

Multi-approach Study in Enchodontidae

Although the main objective of this manuscript is not the assessment of the "best" phylogenetic method, the use of multiple criteria to reconstruct phylogenetic relationships with an empirical data set revealed some interesting results.

First, the topology of the single shortest tree recovered using Standard Maximum Parsimony criterium did not differ from those topologies obtained with Implied Weighted Maximum Parsimony. Goloboff et al. (2018) stated that implied weights, in general, outperforms equal weights parsimony even in the presence of missing entries. However, our results are consistent and there is no discrepancy among the groups found by each variant of parsimony.

Our Phylogenetic Morphometrics (PM) analysis of the landmark configuration of the opercle also appears to carry a reliable phylogenetic signal, despite not including information for all taxa in the analysis. Catalano et al. (2014) found that Phylogenetic Morphometrics only retrieve some clades found by other source of data, and that it is necessary to consider multiple landmark configurations in order to improve correspondence of results (Catalano and Torres, 2016). In this manuscript, we only assessed the landmark configuration of the preopercle, a bone that exhibits a high morphological variation. However, employing the searching algorithm in TNT that minimize the displacement of the landmark sum (Catalano et al., 2010) was effective to find true phylogenetic signal. Future work will include landmark configurations on other bones, including those with a variable shape (e.g. the preopercle) on which homologous points are difficult to identify.

Moreover, it is known that the combination of landmark with discrete data might produce data redundancy if the landmark configuration is also considered by discrete characters (Palci and Lee, 2018). The results of our combined analysis show that the inclusion of the landmark configuration in the discrete data set does not modify the topology retrieved by the SMP analysis (see Figure 5) even though, discrete characters of the preopercle shape remained in the data matrix. We ascribe these results to the very low contribution of the landmark data as well as to the increase in the length of discrete characters that avoided the examination of landmarks (Goloboff and Catalano, 2016:226) producing, in the combined data analysis, lower computing time and a topology markedly different from that analyzing exclusively landmark data.

Additionally, as a result of analyzing and discretizing the data related to the preopercle in our data set, we observed that special attention should be paid when dealing with landmark combined with discrete data for two main reasons. First, when analyzed as a whole, a landmark configuration tries to equal the weight of a discrete character (e.g shape of a given bone). However, there are some conditions that cannot be covered by a 2D landmark configuration, such as the thickness of the bone. Second, the shape of a bone can be distilled into several discrete characters, thus, the contribution sum of multiple discrete characters may be higher than that of the landmark configuration, unless extra weight is put to the landmark character. In our combined exercise, landmark information can be seen as a complementary source of information rather than a substitute of discrete characters as previously described by other authors (Perrard et al., 2015; Palci and Lee, 2018), but further analyses in this regard are required.

Finally, according to our results, Bayesian Inference analysis (BI) seems to be more sensitive to the quality of the data than parsimony analyses. The comparison of the tree topology obtained with Bayesian Inference with that of the Standard Maximum Parsimony (SMP) shows a great difference in the branch arrangement. However, many of the internal nodes in the parsimony analyses are poorly supported (Figure 5), with low support values and few synapomorphic characters. In general, this phylogeny shows that the CI of the data set is 0.456. Puttick et al. (2018) found that if the dataset contains consistent characters and its CI is about 0.5 or higher, then the method used to infer relationships is irrelevant, with similar results recovered across different analyses. SMP resolves a high level of homoplasy in our dataset, which may account for topological differences between parsimony and Bayesian analyses. However, the phylogenetic position of *Vegrandichthys* gen. nov. and

composition of Eurypholinae are consistent across our analyses, likely due to the relatively high support for this clade, and indicating a high level of support for the accuracy of this result (Goloboff et al., 2018). To more completely assess these first impressions in BI with Enchodontidae, it will be necessary to conduct a thoughtful revision of character reformulations.

CONCLUSIONS

Vegrandichthys coitecus is recognized as a new member of the family Enchodontidae, as indicated by multiple phylogenetic approaches. Its phylogenetic position as an early-diverging member of the subfamily Eurypholinae is also well-supported. While our analyses recover enchodontid monophyly, the synapomorphies upholding this vary from some previous works.

Although the stratigraphic fit of Enchodontidae decreases when *Enchodus zimapanensis* is included in the analysis, there is no doubt about the importance of the inclusion of enchodontids with temporal record earlier to the Cenomanian, in terms of both the origin of the family and its palaeobiogeographical distribution. Future work focusing on stratigraphically older members of the group is vital to understand its origins.

Congruence of results across multiple phylogenetic analyses indicates the robustness of our results. Phylogenetic Morphometrics is an excellent tool for exploratory analyses of shape variation; it can be used as a first approach to study anatomical change of an entire bone under parsimony criteria. Fossil preservation bias and specimen incompleteness limits the use of this kind of tool, but even partially preserved elements can be incorporated to some extent. The contribution of a single landmark configuration may be too little to influence topology, and future work should consider multiple landmark configurations in combined analyses, while also taking into account potential data redundancy. In this sense, we recommend performing analyses separately as well as in a combined approach in order to examine the influence of different kinds of data.

Bayesian Inference appears to be more sensitive to data consistency, and future work should test the influence of states of character frequency. A reformulation of anatomical characters, in particular to consider primary homologies and avoid compound characters, may also be necessary to fully understand the evolutionary history of Enchodontidae.

ACKNOWLEDGMENTS

This manuscript represents a partial fulfillment of the requirements to obtain the degree of Doctor in Biological Sciences (Systematics) within the Posgrado en Ciencias Biológicas at Universidad Nacional Autónoma de México for the first author. The authors thank all the paleontologists, students, and volunteers involved in the collection of fossils from the El Chango quarry, mainly to the staff of the Museum of Paleontology “Eliseo Palacios Aguilera” (MEPA) who is in charge of the “Poyecto de prospección y resguardo del patrimonio paleontológico de Chiapas” and the Instituto de Geología, Universidad Nacional Autónoma de Mexico. The preparation of the specimen was performed by B.A. Than-Marchese. Dr. M. Bertling, Dr. T. Smith, and Dr. A. Folie from Geomuseum der WWU and the Royal Belgian Institute of Natural Science provided valuable historical references of Enchodontidae. Authors are also deeply grateful with all the curators of the paleontological collections that kindly gave us access to review and borrow fossils material herein reviewed especially to MSc. G. Carbot-Chanona from the MEPA, Chiapas, Mexico; Dr. K. González-Rodríguez from the Museo de Paleontología, UAEH, Mexico; Dr. D. Arbulla from the Museo Civico di Storia Naturale di Trieste, Italy; Dr. E. Bernard and Dr. M. Richter from Natural History Museum, UK; Dr. M. Bertling from the Geomuseum der WWU, Münster, Germany. Likewise, to Dr. C. Fielitz for the comments and discussion on Enchodontidae held in the SVP Albuquerque 2018. This manuscript was improved with valuable suggestions provided by Dr. K. Cantalice and two anonymous reviewers. The development of this project is supported with Financial found provided by the UNAM through the grant from DGAPA-PAPIIT IN207314 and the individual postgraduate grant number 632640 given to JADC from CONACyT (Mexico) as well as support from the University of Birmingham and Royal Society Dorothy Hodgkin Research Fellowship to SG.

REFERENCES

Agassiz, J.L.R. 1833. *Recherches sur les poisons fossils,* Volume 1 (preface dated in 1833). Neuchâtel et Soleure, Petitpierre.

Alvarado-Ortega, J., Cantalice, K.M., Barrientos-Lara, J.I., Díaz-Cruz, J.A., and Than-Marchese, B.A. 2019. The Huehuetla quarry, a Turonian deposit of marine vertebrates in the Sierra Norte of Puebla, Central Mexico. *Palaeontologia Electronica*, 22.1.13:1–20. https://doi.org/10.26879/921

Alvarado-Ortega, J., Cantalice, K.M., Díaz-Cruz, J.A., Castañeda-Posadas, C., and Zavaleta-Villareal, V. 2020a. Vertebrate fossils from the San José de Gracia quarry, a new Late Cretaceous marine fossil site in Puebla, Mexico. *Boletín de la Sociedad Geológica Mexicana*, 72(1):1–21. https://doi.org/10.18268/BSGM2020v72n1a160819

Alvarado-Ortega, J., Cantalice, K.M., Martínez-Melo, A., García-Barrera, P., Than-Marchese, B.A., Díaz-Cruz, J.A., and Barrientos-Lara, J.I. 2020b. Tzimol, a Campanian marine paleontological site of the Angostura Formation near Comitán, Chiapas, southeastern Mexico. *Cretaceous Research*, 107:1–16. https://doi.org/10.1016/j.cretres.2019.104279

Alvarado-Ortega, J., Garibay-Romero, L.M., Blanco-Piñón, A., González-Barba. G., Vega-Vera. F.J., and Centeno-García, E. 2006a. Los peces fósiles de la Formación Mexcala (Cretácico Superior) en el Estado de Guerrero, México. *Revista Brasileira de Paleontologia*, 93(3):261–272.

Alvarado-Ortega, J., González Rodríguez, K.A., Blanco-Piñón, A., Espinosa-Arrubarrena, L., and Ovalles-Damián, E. 2006b. Mesozoic osteichthyans of Mexico, p. 169–207. In Vega, F.J., Nyborg, T.G., Perrilliat, M.C., Montellano Ballesteros, M., Cevallos Ferriz, S.R.S., and Quiroz Barroso, S.A. (eds.), *Studies on Mexican Paleontology. Topics in Geobiology*, 24. Springer, Dordrecht, the Netherlands.

Alvarado-Ortega, J., Ovalles-Damián, E., and Blanco-Piñón, A. 2009. The fossil fishes from the Sierra Madre Formation, Ocozocoautla, Chiapas, southern Mexico. *Palaeontologia Electronica*, 12.2.4A:1–22. palaeo-electronica.org/2009_2/168/index.html

Alvarado-Ortega, J. and Than-Marchese, B.A. 2012. A Cenomanian aipichthyoid fish (Teleostei, Acanthomorpha) from America*, Zoqueichthys carolinae* gen. and sp. nov. from El Chango quarry (Cintalapa Member, Sierra Madre Formation), Chiapas, Mexico. *Revista Mexicana de Ciencias Geológicas*, 29(3):735-748.

Alvarado-Ortega, J. and Than-Marchese, B.A. 2013. The first record of a North American Cenomanian Trachichthyidae fish (Acanthomorpha, Acanthopterygii), *Pepemkay maya*, gen. et sp. nov., from El Chango quarry (Sierra Madre Formation), Chiapas, Mexico. *Journal of Vertebrate Paleontology*, 33(1):48-57. https://doi.org/10.1080/02724634.2012.712585

Álvarez-Mena, A. 1975. *Estratigrafía del Cretácico de la Región Central de Chiapas*. Bachelor's Thesis, Instituto Politécnico Nacional, Escuela Superior de Ingeniería y Arquitectura, México.

Amaral, C.R., Alvarado-Ortega, J., and Brito, P.M. 2013. *Sapperichthys* gen. nov., a new gonorynchid from the Cenomanian of Chiapas, Mexico, p. 305–323. In Arratia, G., Shultze, H.-P., and Wilson, M.V.H. (eds.), *Mesozoic Fishes V –Global Diversity and Evolution*. Verlag Dr. Friedrich Pfiel, Munchen, Germany.

Arambourg, C. 1954. Les poissons crétacés du Jebel Tselfat (Maroc). *Notes et Mémoires du Service Géologique,* 118:1-188.

Bardet, N., Gheerbrant, E., Noubhani, A., Henri, C., Jouve, S., Bourdon, E., Pereda Suberbiola, X., Jalil, N.-E., Vincent, P., Houssaye, A., Sole, F., El Houssani Darif, K., Adnet, S., Rage, J.-C., De Lapparent de Broin, F., Sudre, J., Bouya, B., Amaghzaz, M., and Meslouh, S. 2017. Les vertébrés des phosphates crétacés-paléogènes (72,1-47,8 Ma) du Maroc, p. 351–452. In Zourhi, S. (ed.), *Paléontologie des Vertébrés du Maroc: état des connaissances. Mémoires de la Société Géologique de France,* 180.

Beckett, H., Giles, S., and Friedman, M. 2017. Comparative anatomy of the gill skeleton of fossil Aulopiformes (Teleostei: Eurypterygii). *Journal of Systematic Palaeontology*, 16(14):1221-1245. https://doi.org/10.1080/14772019.2017.1387184

Bell, M.A. and Lloyd, G.T. 2015a. Strap: An R package for plotting phylogenies against stratigraphy and assessing their stratigraphic congruence. *Palaeontology*, 58(2):379–389. https://doi.org/10.1111/pala.12142

Bell, M.A. and Lloyd, G.T. 2015b. Strap: An R package for plotting phylogenies against stratigraphy and assessing their stratigraphic congruence: A tutorial. *Palaeontology*, 58(2):379–389. https://doi.org/10.1111/pala.12142

Blanco-Piñón, A. 1998. *Vallecillo Nuevo León: Yacimiento Fosilífero del Noreste de México*. Master's Thesis. Facultad de Ciencias de la Tierra, Universidad Autónoma de Nuevo León, Linares.

Bogan, S. and Agnolin, F.L. 2010. Primera ictiofauna marina del Cretácico Superior (Formación Jaguel, Maastrichtiano) de la provincia de Río Negro, Argentina. *Papéis Avulsos de Zoologia*, 50(12):175–188. https://doi.org/10.1590/S0031-10492010001200001

Böse, E. 1905. Reseña acerca de la geología de Chiapas y Tabasco. Instituto Geológico de México, *Boletín*, 20:1-113.

Brazeau, M.D. 2011. Problematic character coding methods in morphology and their effects. *Biological Journal of the Linnean Society*, 104(3):489–498. https://doi.org/10.1111/j.1095-8312.2011.01755.x

Carbot-Chanona, G. 2015. La Colección Paleontológica de la SEMAHN: análisis preliminar. *Lacandonia*, 9(2):43-54.

Carbot-Chanona, G. and Than-Marchese, B.A. 2013. Presencia de *Enchodus* (Osteichthyes: Aulopiformes: Enchodontidae) en el Maastrichtiano (Cretácico tardío) de Chiapas, México. *Paleontología Mexicana,* 63(1):8–16.

Catalano, S.A., Ercoli, M.D., and Prevosti, F.J. 2014. The more, the better: the use of multiple landmark configurations to solve the phylogenetic relationships in musteloids. *Systematic Biology*, 64(2):294–306. https://doi.org/10.1093/sysbio/syu107

Catalano, S.A. and Goloboff, P.A. 2012. Simultaneously mapping and superimposing landmark configurations with parsimony as optimality criterion. *Systematic Biology*, 61(3):392–400. https://doi.org/10.1093/sysbio/syr119

Catalano, S.A. and Goloboff, P.A. 2018. A guide for the analysis of continuous and landmark characters in TNT (Tree Analysis using New Technologies). https://doi.org/10.13140/RG.2.2.23797.27360

Catalano, S.A., Goloboff, P.A., and Giannini, N.P. 2010. Phylogenetic morphometrics (I): the use of landmark data in a phylogenetic framework. *Cladistics*, 26(5):539–549. https://doi.org/10.1111/j.1096-0031.2010.00302.x

Catalano, S.A. and Torres, A. 2016. Phylogenetic inference based on landmark data in 41 empirical data sets. *Zoologica Scripta*, 46(1):1–11. https://doi.org/10.1111/zsc.12186

Cavin, L. 1999. Occurrence of a juvenile teleost, *Enchodus* sp., in a fish gut content from the upper Cretaceous of Goulmima, Morocco. *Special Papers in Palaeontology*, 60:57–72.

Cavin, L., Alexopoulos, A., and Piuz, A. 2012. Late Cretaceous (Maastrichtian) ray-finned fishes from the island of Gavdos, southern Greece, with comments on the evolutionary history of the aulopiform teleost *Enchodus*. *Bulletin de la Societe Geologique de France*, 183(6):561–572. https://doi.org/10.2113/gssgfbull.183.6.561

Chalifa, Y. 1996. New species of *Enchodus* (Aulopiformes: Enchodontidae) from the Northern Negev, Israel, with comments on evolutionary trends in the Enchodontoidei, p. 349–367. In Arratia, G. and Schultze, H.-P. (eds.), *Mesozoic Fishes—Systematics and Paleoecology*. Verlag Dr. Friedrich Pfeil, München, Germany.

Cicimurri, D.J. and Everhart, M.J. 2001. An elasmosaur with stomach contents and gastroliths from the Pierre Shale (Late Cretaceous) of Kansas. *Transactions of the Kansas Academy of Science*, 104(3):129–143. https://doi.org/10.1660/0022-8443(2001)104[0129:AEWSCA]2.0.CO;2

Coelho, P.M. 2004. *Revisão Sistemática dos Enchodontidae (Euteleostei: Aulopiformes) do Brasil*. M.Sc.Thesis. Universidade Federal do Rio de Janeiro, Rio de Janeiro, Brasil.

Cope, E.D. 1872. On the families of fishes of the Cretaceous formation of Kansas. *Proceedings of the American Philosophical Society*, 12(86):327–357.

Cope, E.D. 1874. Review of the Vertebrata of the Cretaceous Period found west of Mississippi River. *Bulletin of the U.S. Geological and Geographical Survey, Territories*, 1(2):3–48.

Davis, J.W. 1887. The fossil fishes of the Chalk of Mount Lebanon in Syria. *Scientific Transactions of the Royal Dublin Society*, 3:457–636.

Davis, M.P. and Fielitz, C. 2010. Estimating divergence times of lizardfishes and their allies (Euteleostei: Aulopiformes) and the timing of deep-sea adaptations. *Molecular Phylogenetics and Evolution*, 57(3):1194–1208. https://doi.org/10.1016/j.ympev.2010.09.003

Díaz-Cruz, J.A. and Alvarado-Ortega, J. 2017. Los peces enchodóntidos de México. *Paleontología Mexicana*, 2:37.

Díaz-Cruz, J.A. and Alvarado-Ortega, J. 2018. The Late Cretaceous enchodontids (Enchodontidae: Aulopiformes) fishes from Mexico: new light into the evolution of Enchodontidae. *5th International Palaeontological Congress*, *Paris, France*, p. 1038.

Díaz-Cruz, J.A., Alvarado-Ortega, J., and Bernard, E. 2019a. Phylogenetic implications of two enchodontids species (Enchodontidae: Aulopiformes) from the Middle East: researching on the global evolutive patterns of the enchodontid fishes. *Paleontologia Mexicana*, 5:24.

Díaz-Cruz, J.A., Alvarado-Ortega, J., and Carbot-Chanona, G. 2016. The Cenomanian short snout enchodontid fishes (Aulopifomes, Enchodontidae) from Sierra Madre Formation, Chiapas, southeastern Mexico. *Cretaceous Research*, 61:136–150. https://doi.org/10.1016/j.cretres.2015.12.026

Díaz-Cruz, J.A., Alvarado-Ortega, J., and Carbot-Chanona, G. 2019b. *Dagon avendanoi* gen. and sp. nov., an Early Cenomanian Enchodontidae (Aulopiformes) fish from the El Chango quarry, Chiapas, southeastern Mexico. *Journal of South American Earth Sciences*, 91:272–284. https://doi.org/10.1016/j.jsames.2019.01.014

Díaz-Cruz, J.A., Alvarado-Ortega, J., and Carbot-Chanona, G. 2019c. Corrigendum to "*Dagon avendanoi* gen. and sp. nov., an Early Cenomanian Enchodontidae (Aulopiformes) fish from the El Chango quarry, Chiapas, southeastern Mexico." *Journal of South American Earth Sciences*, 91:272–284. https://www.sciencedirect.com/science/article/pii/S0895981119304183

Fielitz, C. 2004. The phylogenetic relationships of the †Enchodontidae (Teleostei: Aulopiformes), p. 619–634. In Arratia, G., Wilson, M.V.H., and Cloutier, R. (eds.), *Recent Advances in the Origin and Early Radiation of Vertebrates*. Verlag Dr. Friedrich Pfeil, München.

Fielitz, C. and González-Rodríguez, K.A. 2010. A New Species of *Enchodus* (Aulopiformes: Enchodontidae) from the Cretaceous (Albian to Cenomanian) of Zimapán, Hidalgo, México. *Journal of Vertebrate Paleontology*, 30(5):1343–1351. https://doi.org/10.1080/02724634.2010.501438

Fitch, W. 1971. Toward defining the course of evolution: minimal change for a specific tree topology. *Systematic Zoology*, 20:406–416.

Forey, P.L., Yi, L., Patterson, C., and Davies, C.E. 2003. Fossil fishes from the Cenomanian (Upper Cretaceous) of Namoura, Lebanon. *Journal of Systematic Palaeontology*, 1(4):227–330. https://doi.org/10.1017/S147720190300107X

Friedman, M., Beckett, H.T., Close, R.A., and Johanson, Z. 2016. The English Chalk and London Clay: Two remarkable British bony fish lagerstätten. *Geological Society Special Publication*, 430(1):165–200. https://doi.org/10.1144/SP430.18

Garcia, G.G., Garcia, A.J.V., and Henriques, M.H.P. 2018. Palynology of the Morro do Chaves Formation (Lower Cretaceous), Sergipe Alagoas Basin, NE Brazil: paleoenvironmental implications for the early history of the South Atlantic. *Cretaceous Research*, 90:7–20. https://doi.org/10.1016/j.cretres.2018.03.029

Giersch, S. 2014. *Die Knochenfische der Oberkreidezeit in Nordostmexiko: Beschreibung, Systematik, Vergesellschaftung, Paläobiogeographie und Paläoökologie*. PhD Thesis, Ruprecht-Karls-Universität Heidelberg, Germany.

Giersch, S., Frey, E., Stinnesbeck, W., and González-González, A.H. 2008. Fossil fish assemblages of northeastern Mexico: new evidence of mid Cretaceous Actinopterygian radiation, p. 43–45. In Krempaská, Z. (ed.), *6th Meeting of the European Association of Vertebrate Paleontology*, Museum of Spiš, Spišská Nová Ves, Slovak Republic.

Goloboff, P.A. and Catalano, S.A. 2016. TNT version 1.5, including a full implementation of phylogenetic morphometrics. *Cladistics*, 32(3):221–238.

Goloboff, P.A., Torres, A., and Arias, J.S. 2018. Weighted parsimony outperforms other methods of phylogenetic inference under models appropriate for morphology. *Cladistics*, 34(4):407–437. https://doi.org/10.1111/cla.12205

González, A.J. 1963. Levantamiento del Área San Cristóbal-Bachajón. *Petróleos Mexicanos, Zona Sur, Informe Geológico*, 498:1–59. (unpublished report)

González-Barba, G. and Espinosa-Chávez, B. 2005. Cenomanian-Turonian fish fauna from the Boquillas Formation at Jaboncillos, north-west Coahuila, Mexico, p. 105–107. In Poyato-Ariza, F.J. (ed.), *Fourth International Meeting on Mesozoic Fishes – Systematics, Homology, and Nomenclature, Maraflores de la Sierra, Madrid, España. Extended Abstracts*. Servicio de Publicaciones de la Universidad Autónoma de Madrid/UAM Ediciones, Spain.

González-Ramírez, I., Calvillo-Canadell, L., and Cevallos-Ferriz, S.R.S. 2013. Coníferas cupresaceas fósiles de El Chango, Chiapas (Aptiano). *Paleontología Mexicana*, 63(1):26–31.

González-Rodríguez, K.A., Fielitz, C., Bravo-Cuevas, V.M., and Baños-Rodríguez, R.E. 2016. Cretaceous osteichthyan fish assemblages from Mexico. *New Mexico Museum of Natural History and Science Bulletin*, 71:1–14.

Goody, P.C. 1968. The skull of *Enchodus faujasi* from the Maastricht of southern Holland. *Proceedings of the Koninklijke Nederlandse Akademie van Wetenschappen*, B71:209–231.

Goody, P.C. 1969. The relationships of certain Upper Cretaceous teleosts, with special reference to the myctophoids. *Bulletin of the British Museum (Natural History) Geology Supplement*, 7:1–255.

Goody, P.C. 1976. *Enchodus* (Teleostei: Enchodontidae) from the Upper Cretaceous Pierre Shale of Wyoming and South Dakota with an evaluation of the North American enchodontid species. *Palaeontographica Abteilung*, A152:91–112.

Gouiric-Cavalli, S., Cione, A.L., Pérez, L.M., Iribarme, M., Allcca, M., and Poiré, D.G. 2016. Primer Registro del pez cretácico *Enchodus*. *XVIII Congreso Peruano de Geología*, Lima, Perú, p. 1–3.

Green, W.R. 1913. A description of the specimens of the teleostean genus *Enchodus* in the University of Kansas Museum. *Kansas University Science Bulletin*, 7(2):71–107.

Guerrero-Márquez, G., Calvillo-Canadell, L., Cevallos-Ferriz, S. R., and Avendaño Gil, J. 2013. Angiospermas cretácicas de la localidad “El Chango”, Chiapas, México. *Paleontología Mexicana*, 63(1):32-39.

Guinot, D., Carbot-Chanona, G., and Vega, F.J. 2019. Archaeochiapasidae n. fam., a new early Cenomanian brachyuran family from Chiapas, Mexico, new insights on Lecythocaridae Schweitzer & Feldmann, 2009, and phylogenetic implications. *Geodiversitas*, 41(7):285-322. https://doi.org/10.5252/geodiversitas2019v41a7

Günther, A. 1873. XXXI.—Report on a collection of fishes from China. *Journal of Natural History*, 12(69):239-250.

Hay, O.P. 1903. On certain genera and species of North American Cretaceous actinopterous fishes. *Bulletin of the American Museum of Natural History*, 19(1):1–9.

Heckel, J.J. 1850. Beiträge zur Kenntniss der fossilen Fische Oesterreichs. *Denkschriften der kaiserlichen Akademie der Wissenschaften, math.-naturwiss. Classe,* 1:201–242.

Höhna, S., Landis, M.J., and Heath, T.A. 2017. Phylogenetic inference using RevBayes. *Current Protocols in Bioinformatics*, 57(1):6-16. https://doi.org/10.1002/cpbi.22

Höhna, S., Landis, M.J., Heath, T.A., Boussau, B., Lartillot, N., Moore, B.R., Huelsenbeck, J.P., and Ronquist, F. 2016. RevBayes: Bayesian phylogenetic inference using graphical models and an interactive model-specification language. *Systematic Biology*, 65(4):726–736. https://doi.org/10.1093/sysbio/syw021

Holloway, W.L., Claeson, K.M., Sallam, H.M., El-Sayed, S., Kora, M., Sertich, J.J.-W., and O’Connor, P.M. 2017. A new species of the neopterygian fish *Enchodus* from the Duwi Formation, Campanian, Late Cretaceous, Western Desert, central Egypt. *Acta Palaeontologica Polonica*, 62(3):603–611. https://doi.org/10.4202/app.00331.2016

Huelsenbeck, J.P. 1994. Comparing the stratigraphic record to estimates of phylogeny. *Paleobiology*, 20(4):470–483.

Huerta-Vergara, A.R., Calvillo-Canadell, L., Cevallos-Ferriz, S.R.S., and Silva-Pineda, A. 2013. Pinaceae en el Cretácico del norte y sur de México: complemento a su escaso registro fósil. *Paleontología Mexicana*, 63(1):66–78.

Kaddumi, H.F. 2009. A new species of large *Enchodus* fishes (Aulopiformes: Enchodontidae) from the late Maastrichtian of Harrana, p. 204–214. In Kaddumi, H.F., *Fossils of the Harrana Fauna and the Adjacent Areas. Eternal River Museum of Natural History, Amman, Jordan.*

Kramberger, D.G. 1895. De piscibus fossilibus Comeni, Mrzleci, Lesinae et M. Libanonis. *Djela Jugoslavenska Akademija Znanosti, I Umjetnosti, Zagreb*, 16:1–67.

Kriwet, J. 2003. Lancetfish teeth (Neoteleostei, Alepisauroidei) from the Early Cretaceous of Alcaine, NE Spain. *Lethaia,* 36(4):323–332. https://doi.org/10.1080/00241160310006484

Leidy, J. 1857. Notices of some remains of extinct fishes. *Proceedings of the Academy of Natural Sciences of Philadelphia*, 1857:167–168.

Lowe, R.T. 1833. Description of *Alepisaurus*, a new genus of fishes. *Proceedings of the Zoological Society of London*, 1:104.

Maddison, W.P. and Maddison, D.R. 2001. *Mesquite: a Modular System for Evolutionary Analysis*, Version 3.61. https://www.mesquiteproject.org/

Maisey, J.G. 1996. *Discovering Fossil Fishes*. Henry Holt and Company, New York.

Maldonado-Koerdell, M. 1956. Peces fósiles de México, III. Nota preliminar sobre los peces del Turoniano Superior de Xilitla, San Luis Potosi (México). *Ciencia*, 19:1–9.

Mantell, G. 1822. *The Fossils of the South Downs; or Illustrations of the Geology of Sussex*. Lupton Relfe, London.

Moreno-Bedmar, J.A., Latil, J.-L., Villanueva-Amadoz, U., Calvillo-Canadell, L., and Cevallos-Ferriz, S.R.S. 2014. Ammonite age-calibration of the El Chango Fossil-Lagerstätte, Chiapas state (SE Mexico). *Journal of South American Earth Sciences*, 56:447–453. https://doi.org/10.1016/j.jsames.2014.09.022

Nixon, K.C. 2002. *Winclada-ASADO 1.61. Computer Software and Documentation.*

Ovalles-Damián, E., Alvarado-Ortega, J., and Blanco-Piñón, A. 2006. Los peces fósiles del Cretácico inferior de Ocozocoautla, Chiapas. *Memorias del X Congreso Nacional de Paleontología, Sociedad Mexicana de Paleontología, México*, p. 6.

Palci, A. and Lee, M.S.Y. 2018. Geometric morphometrics, homology and cladistics: review and recommendations. *Cladistics*, 35(2):230–242. https://doi.org/10.1111/cla.12340

Perrard, A., López-Osorio, F., and Carpenter, J.M. 2015. Phylogeny, landmark analysis and the use of wing venation to study the evolution of social wasps (Hymenoptera: Vespidae: Vespinae). *Cladistics*, 32(4):406–425. https://doi.org/10.1111/cla.12138

Pictet, F.J. 1850. *Description de Guelques Poissons Fossiles du Mont Liban*. J-K Fick, Geneve.

Porras-Múzquiz, H. and Alvarado-Ortega, J. 2011. Sobre la ocurrencia de *Enchodus petrosus* Cope en el Cretácico tardío de Múzquiz, Coahuila, México. *XII Congreso Nacional de Paleontología, Sociedad Mexicana de Paleontología, Benemérita Universidad Autónoma de Puebla*, p. 113.

Porras-Múzquiz, H.G., Díaz-Cruz, J.A., Alvarado-Ortega, J., and Cantalice, K.M. 2019. Evidencia de interacción depredador-presa en peces del género *Enchodus* (Enchodontidae: Aulopiformes) de localidades del Cretácico Superior Coahuila, Norte de México Porras-Múzquiz. *Paleontología Mexicana*, 5:116.

Puttick, M.N., O'Reilly, J.E., Pisani, D., and Donoghue, P.C.J. 2018. Probabilistic methods outperform parsimony in the phylogenetic analysis of data simulated without a probabilistic model. *Palaeontology*, 62(1):1–17. https://doi.org/10.1111/pala.12388

Quezada-Muñetón, J.Q. 1987. El Cretácico medio-Superior y el límite Cretácico Superior-Terciario inferior en la Sierra de Chiapas. *Boletín de la Asociación Mexicana de Geologos Petroleros*, 39(1):1–98.

Raab, M. and Chalifa, Y. 1987. A new enchodontid fish genus from the upper Cenomanian of Jerusalem, Israel. *Palaentology*, 30:717–731.

Rambaut, A., Drummond, A.J., Xie, D., Baele, G., and Suchard, M.A. 2018. Posterior summarization in Bayesian phylogenetics using Tracer 1.7. *Systematic Biology*, 67(5):901–904. https://doi.org/10.1093/sysbio/syy032

Rohlf, F.J. 2005. *tpsDig, digitize landmarks and outlines*. Department of Ecology and Evolution, State University of New York at Stony Brook, Stony Brook, New York.

Rosen, D.E. 1973. Interrelationships of higher euteleostean fishes, p. 397–513. In Greenwood, P.H., Miles, R.S., and Patterson, C. (eds.), *Interrelationships of Fishes*. Zoological Journal of the Linnean Society Supplement 1.

Salas, G.P. 1949. El Cretácico de la Cuenca de Macuspana y su correlación. *Boletín de la Sociedad Geológica Mexicana*, 14:47-65.

Sánchez-Montes de Oca, R. 1969. Estratigrafía y paleogeografía del Mesozoico de la Sierra del Sur: Instituto Mexicano del Petróleo. *Seminario Sobre Exploración Petrolera, Mesa 4, Capítulo 5*.

Sánchez-Montes de Oca, R. 1973. Proyecto Mesozoico Arrecifal, Sierra de Chiapas: México, Petróleos Mexicanos, Zona Sur. *Informe Geológico* 581. (unpublished report)

Schein, J.P., Parris, D.C., Poole, J.C., and Lacovara, K.J. 2013. A nearly complete skull of *Enchodus ferox* (Actinopterygii, Aulopiformes) from the Upper Cretaceous Ripley Formation of Lowndes County, Alabama. *Bulletin of the Alabama Museum of Natural History*, 31(1):78–83.

Siegel, F.A. and Benson, R.H. 1982. A robust comparison of biological shapes. *Biometrics*, 38(2):341–350.

Silva-Santos, R. and Salgado, S. 1969. *Enchodus longipectoralis* (Schaeffer), um Teleostei do Cretáceo de Sergipe. *Anais da Academia Brasileira de Ciências*, 41(3):381–392.

Silva, H.M.A. and Gallo, V. 2007. Parsimony analysis of endemicity of enchodontoid fishes from the Cenomanian. *Carnets de Géologie*, 1:1–8.

Silva, H.M.A. and Gallo, V. 2011. Taxonomic review and phylogenetic analysis of Enchodontoidei (Teleostei: Aulopiformes). *Anais da Academia Brasileira de Ciencias*, 83(2):483–511. https://doi.org/10.1590/S0001-37652011000200010

Simões, T.R., Caldwell, M.W., Palci, A., and Nydam, R.L. 2017. Giant taxon-character matrices: quality of character constructions remains critical regardless of size. *Cladistics*, 33(2):198–219. https://doi.org/10.1111/cla.12163

Steele, D.R. 1986. Contributions to the stratigraphy of Sierra Madre Limestone (Cretaceous) of Chiapas, Part 1. Physical stratigraphy and petrology of the Cretaceous Sierra Madre Limestone, westcentral Chiapas: *Instituto de Geología, Boletín*, 102:1-101.

Stewart, A. 1898. A preliminary description of seven new species of fish from the Cretaceous of Kansas. *Kansas University Quarterly*, 7:189–196.

Stewart, J.D. and Carpenter, K. 1990. Examples of vertebrate predation on cephalopods in the Late Cretaceous of the Western Interior, p. 203–206. In Boucot, A.J. (ed.), *Evolutionary Paleobiology of Behavior and Coevolution*. Elsevier, Amsterdam.

Toombs, H.A. and Rixon, A.E. 1950. The use of plastics in the “Transfer Method” of preparing fossils. *The Museums Journal*, 50(5):105–107.

Toombs, H.A. and Rixon, A.E. 1959. The use of acids in the preparation of vertebrate fossils. *Curator: The Museum Journal*, 2(4):304–312.

Uyeno, T. and Minakawa, T. 1983. A new enchodontoid fish of the genus *Eurypholis* from Cretaceous of Japan. *Bulletin of the National Science Museum. Series C*, 9(2):79–83.

Vega, F.J., Álvarez, F., and Carbot-Chanona, G. 2007. Albian penaeoidea [sic] (Decapoda: Dendrobranchiata) from Chiapas, Southern Mexico. *Memorie della Societá Italiana di Scienze Naturali e del Museo Civico di Storia Naturale di Milano*, 35(2):6–8.

Vernygora, O., Murray, A.M., Luque, J., Ruge, M.L.P., and Fonseca, M.E.P. 2017. A new Cretaceous dercetid fish (Neoteleostei: Aulopiformes) from the Turonian of Colombia. *Journal of Systematic Palaeontology*, 16(12):1057–1071. https://doi.org/10.1080/14772019.2017.1391884

von der Marck, W. 1858. Ueber einige Wirbelthiere, Crustaceen und Cephalopoden der westfälishcen Kreide. *Zeitschrift der deutschen geologischen Gesellschaft, Berlin,* 10:231–271.

von der Marck, W. 1863. Fossile Fische, Krebse und Pflanzen aus dem Plattenkalk der jüngsten Kreide in Westphalen. *Palaeontographica*, 11:1–83.

Waite, L.E. 1986, Contributions to the stratigraphy of Sierra Madre Limestone (Cretaceous) of Chiapas, Part 2, Biostratigraphy and paleoenvironmental analysis of the Sierra Madre Limestone (Cretaceous), Chiapas. *Instituto de Geología, Boletín*, 102:103–245.

Wiebe, W.A. 1925, Geology of southern Mexico oil fields. *Pan-American Geologist*, 94:121–138.

Wilson, M.V. and Chalifa, Y. 1989. Fossil marine actinopterygian fishes from the Kaskapau Formation (Upper Cretaceous: Turonian) near Watino, Alberta. *Canadian Journal of Earth Sciences*, 26(12):2604-2620. https://doi.org/10.1139/e89-222

Woodward, A.S. 1901. Catalogue of the fossil fishes in the British Museum (Natural History). Part IV. Containing the actinopteryigian Teleostomi of the suborders Isospondyli (in part), *Ostariophysi, Apodes, Percesoces, Hemibranchii, Acanthopterygii, and Anacanthini*. British Museum (Natural History), London.

Yabumoto, Y., Uyeno, T. 1994. Late Mesozoic and Cenozoic fish faunas of Japan. *The Island Arc*, 3(4):255–269.

APPENDIX I

This appendix contains all the data matrices used in the phylogenetic study of *Vegrandichthys coitecus* gen. et sp. nov. Here, we present the matrices in the order they appear in the main manuscript. (PDF file available for zipped download at https://palaeo-electronica.org/content/2020/3063-a-long-snout-enchodontid-fish.)

APPENDIX II

This appendix presents the modifications made to some characters reported in previous works, it also shows the complete list of the characters used in the phylogenetic analyses, highlighting those that were not considered or included due to be phylogenetically uninformative (autoapomorphic or invariant). Also, it is possible to find the matrices employed in the phylogenetic exercises and the complete phylogenies obtained. (PDF file available for zipped download at https://palaeo-electronica.org/content/2020/3063-a-long-snout-enchodontid-fish.)

CAPÍTULO IV: *Hastichthys totonacus* sp. nov., a North American Turonian dercetid fish from the Huehuetla quarry, Puebla, Mexico

Journal of South American Earth Sciences 105 (2021) 102900

Contents lists available at ScienceDirect

Journal of South American Earth Sciences

journal homepage: www.elsevier.com/locate/jsames

Hastichthys totonacus sp. nov., a North American Turonian dercetid fish (Teleostei, Aulopiformes) from the Huehuetla quarry, Puebla, Mexico

Jesús Alvarado-Ortega [a], Jesús Alberto Díaz-Cruz [b,*]

[a] *Instituto de Geología, Universidad Nacional Autónoma de México, Circuito de la Investigación S/N, Ciudad Universitaria, Delegación Coyoacán, Ciudad de México, 04510 Mexico*

[b] *Posgrado en Ciencias Biológicas, Universidad Nacional Autónoma de México, Circuito de la Investigación S/N, Ciudad Universitaria, Delegación Coyoacán, Ciudad de México, 04510 Mexico*

ARTICLE INFO

Keywords:
New species
Phylogeny
Taxonomical reassignment
Enchodontoidei
Fossil fishes
Late cretaceous

ABSTRACT

A new fossil needlefish species is named in this work as *Hastichthys totonacus,* based on specimens from the marine Turonian deposits of the Agua Nueva Formation, exposed in the Huehuetla quarry, into the Sierra Norte region of Puebla, Mexico. The osteology of this new species shows a diagnostic character of the order Aulopiformes, the occurrence of epipleurals bones associated with abdominal centra, at least from the centrum 2. This new species also shows the most distinctive features of the family Dercetidae and genus *Hastichthys*, including the longirostrine head; the elongated body; two pairs of triangular and expanded transverse processes in the abdominal centra; the low and elongated neural arches on abdominal centra bearing short neural spines; a row of triradiate scutes on each body flak; and the anterior part of maxilla and dentary bones are ornamented with longitudinal and parallel ridges. *Hastichthys totonacus* is the second species in the genus and differs from the type species, *H. gracilis*, in having a relatively shorter body with 59 total centra, the head length is about 38% of the standard length, the dorsal fin has seven rays, and the anal fin has eight rays. The inclusion of this new species in different phylogenetic analyses reveals that the interrelationships of the Dercetidae family are poorly resolved and that *H. totonacus* sp. nov. and *H. gracilis* form a monophyletic group. Additionally, the species *Rhynchodercetis regio,* from the Turonian sediments of the Agua Nueva Formation, exploited in the Vallecillo quarry, Nuevo León, northern Mexico, is also placed into the genus *Hastichthys* because it has the most prominent character of this genus, the tips of rostrum and mandible are ornamented with longitudinal and parallel striae and ridges. The occurrence of these two Mexican Turonian species extends the temporal and geographical distribution of the genus *Hastichthys*, from the Cenomanian deposits of the western Tethys Sea realm preserved in the Middle East toward the Turonian deposits of eastern Mexico, at the southern end of North America.

1. Introduction

The genus *Hastichthys* Taverne, 1991, was erected to include *Hastichthys gracilis* (Chalifa, 1989), originally described as part of the genus *Rhynchodercetis* Arambourg, 1943. This fish belongs to the family Dercetidae, an extinct Cenomanian-Danian (Late Cretaceous-Early Paleocene) needlefish clade that forms part of the order Aulopiformes (Vernygora et al., 2018). Remains of these fishes have been recovered in marine deposits of northern Africa, North and South America, Middle East, as well as Europe (Goody, 1969; Gallo et al., 2005; Blanco and Alvarado-Ortega, 2006; Blanco et al., 2008; Taverne, 1991, 2006a; Vernygora et al., 2018; Alvarado-Ortega et al., 2020a, b; among others). Before the present paper, the temporal and geographical distributions of *Hastichthys* were extremely restricted to the Lower Cenomanian marine deposits of the Amminadav Formation, in Ein-Yabrud, Cisjordania, Palestine. Other potential specimens of *H. gracilis* from the Middle Cenomanian of Namoura deposit, Lebanon, were reported by Forey et al. (2003), as cf. *Rhynchodercetis gracilis*.

Today the family Dercetidae consists of at least 35 valid nominal species gathered in 17 genera (Table 1). This group has complex taxonomical and nomenclatural histories. Although the erection of this family is constantly attributed to Pictet (1850); Woodward (1901) named it for the first time to include different species of the genus *Dercetis* Munster and Agassiz, 1833 (in Agassiz, 1833 (not 1837 as it was

* Corresponding author.
E-mail addresses: alvarado@geologia.unam.mx (J. Alvarado-Ortega), vertebrata.j@gmail.com (J.A. Díaz-Cruz).

https://doi.org/10.1016/j.jsames.2020.102900
Received 16 August 2020; Received in revised form 11 September 2020; Accepted 12 September 2020
Available online 7 October 2020
0895-9811/

Table 1
Nominal species of the family Dercetidae (this is an updated list based on the lists provided by Silva and Gallo (2011, p. 485). * shows the type species and ** indicates species that today are not considered part of the family Dercetidae.

Species	Temporal and geographic distribution
Apuliadercetis tyleri Taverne (2006a).*	Campanian-Maastrichtian. Nardò, Italy.
Apuliadercetis indeherbergei Taverne and Goolaerts, 2015.	Upper Maastrichtian, Gulpen Fm. CBR Lische quarry, near Eben-Emael, Belgium.
Benthesikyme armatus (von der Marck, 1863).*	Campanian, Sendenhorst, Westphalia, Germany.
Benthesikyme gracilis (Davis, 1887).	Upper Senonian, Sahel Alma, Lebanon.
Benthesikyme rostralis (Signeux, 1954).	Upper Senonian, Sahel Alma, Lebanon.
Benthesikyme triqueter (Pictet, 1850).	Upper Senonian, Sahel Alma, Lebanon.
Benthesikyme serpentina (Hay, 1903).	Middle Cenomanian, Hakel and Hadjula, Lebanon.
Benthesikyme elongatus (Agassiz, 1835, p. 493).	Senonian and Turonian, southeastern, England.
Braziloderceti longirostris Figueiredo and Gallo (2006).*	Early Turonian. Atlantida Fm., the Pelotas Basin, southern Brazil.
Candelarhynchus padillai Vernygora et al., 2018.*	Lower–middle Turonian deposits of the San Rafael Formation, Colombia.
Caudadercetis bannikovi Taverne (2006b).*	Campanan-Maastrichtian limit, Portoselvaggio, near Nardò, Apulia, Italy.
Dercetis congolensis Casier (1965).	Cenomanian, Kipala Fm., Kwango, Zaire.
Dercetis sagittatus (von der Marck, 1863).	Campanian, Sendenhorst, Westphalia, Germany.
Dercetis scutatus Agassiz (1833) (not 1843).*	Senonian, Baumberg, Westphalia, Germany.
*Dercetis tenuis*Pictet (1850).	Upper Senonian, Sahel Alma, Lebanon.
Dercetoides venator Chalifa (1989).*	Lower Cenomanian, Amminadav Fm., Ein-Yabrud, Cisjordania, Palestine.
Cyranichthys ornatissimus (Casier, 1965).*	Cenomanian, Kipala Fm., Kwango, Zaire.
Cyranichthys jagti Taverne (1987).	Maastricthian, Maastricht Fm. Belgium and Netherlands.
Hastichthys gracilis (Chalifa, 1989).*	Lower Cenomanian, Amminadav Fm., Ein-Yabrud, Cisjordania, Palestine.
Hastichthys regio (Blanco and Alvarado-Ortega, 2006). (see the discussion section in this work).	Lower Turonian, Agua Nueva Fm. Vallecillo quarry, Nuevo León, Mexico.
Hastichthys totonacus Alvarado-Ortega, Díaz-Cruz. (present work).	Turonian, Agua Nueva Fm., Huehuetla quarry, Puebla, Mexico.
Kwangodercetis verbeeki Casier (1965).*	Cenomanian, Kipala Fm., Kwango, Zaire.
Leccedercetis longirostris Taverne (2008).*	Campanan-Maastrichtian limit, Portoselvaggio, near Nardò, Apulia, Italy.
Nardodercetis vandewallei Taverne, 2005a.*	Campanian-Maastrichtian, Nardò, Italy.
Nardocercetis garganoi Taverne (2013).	Late Santonian, Promontoire de Gargano, Apricena, Italy.
Ophidercetis italiensis Taverne (2005b).*	Campanian-Maastrichtian, Nardò, Italy.
Paradercetis kipalaensis Casier (1965).*	Cenomanian, Kipala Fm., Kwango, Zaire.
Pelargorhynchus dercetiformis von der Marck (1858).*	Upper Senonian, Sendenhorst, Westphalia, Germany.
*Pelargorhynchus grandis*Wallaard et al. (2019).	Maastrichtian. Maastricht Fm. 't Rooth quarry, near Bemelen, Netherlands.
Rhynchodercetis gortanii (d'Erasmo, 1946).	Lower Cenomanian, Comen, Trieste, Slovenia-
*Rhynchodercetis yovanovitchi*Arambourg (1943).*	Lower Cenomanian, Tjebel Tselfat, Morocco. Cenomanian, Floresta, Sicily, Italy.
Rhynchodercetis hakelensis (Pictet and Humbert, 1866).	Middle Cenomanian, Hakel, Lebanon.
Robertichthys riograndensis Blanco-Piñón, Alvarado-Ortega (2005).**	Lower Turonian, Agua Nueva Fm., Vallecillo quarry, Nuevo León, Mexico.
Scandiadercetis limhamnensis (Davis, 1890).*	Danian, Saltholm Limestone, near Malmö, Schonen, Sweden.

noted by Woodward (1901) and Bücker (1835)), *Pelargorhynchus*, von der Marck (1858), and *Leptotrachelus* von der Marck (1863) (also see Arambourg, 1954; Taverne, 1991, 2006a, b; Baldwin and Johnson, 1996; Gallo et al., 2005; Silva and Gallo, 2011; Nelson, 1994; among others). Nowadays, species of the genus *Leptotrachelus* are included in the genus *Benthesikyme* White and Moy-Thomas, 1940, because the name "Leptotrachelus" was preoccupied with a carabid coleopter described by Latreille (1829). Later, Woodward (1903) suggested that dercetids are related to families Halosauridae and Notacanthidae, the spiny eels, which today are included within Elopomorpha. Contrary, Jordan (1905) pointed out that dercetids are related to extinct members of Alepisauroidei, the lancetfishes, grouped into the order Iniomi described by Gosline et al. (1966). Subsequently, Goody (1969) regarded that the order Salmoniformes includes other 10 extinct genera (placed in the suborders: Ichthyotringoidei, Enchodontoidei, Halecoidei) as well as the Woodward's dercetids, which were grouped into the Suborder Cimolichthyoidei that also includes *Cimolichthys* Leidy, 1857 and *Aspidopleurus* Pictet and Humbert, 1866. Alvarado-Ortega and Porras-Múzquiz (2012) demonstrated that *Aspidopleurus* was erroneously synonymized with *Prionolepis* Egerton, 1850 (in Dixon, 1850).

Afterward, Rosen (1973) resumed Jordan's idea, he erected the order Aulopiformes comprising the non-ctenosquamate eurypterygians that corresponds to the order Isumi minus the families Myctophidae and Neoscopelidae and includes the suborders Aulopoidei plus Alepisauroidae. Additionally, Rosen (1973) suggested that Alepisauroide includes two living superfamilies (Synodontoidea, and Alepisauroidea) plus the Goody's salmoniform extinct genera. More recently, Nelson (1994) placed the extinct alepisauroids in the suborder Enchodontoidei, previously suggested by Berg (1937), simply to re-rank the family Enchodontidae, previously created by Woodward (1901), to include only the species of *Enchodus* and its Late Cretaceous allies. In the last twenty years, different authors have been working to discover the genealogical relationships of the family Dercetidae (Taverne, 1991, 2006b; Blanco et al., 2008; Gallo et al., 2005; Silva and Gallo, 2011; Vernygora et al., 2018).

In 2017, the authors of this work launched a research project to recover and study the fossils of enchodontoid fishes from paleontological sites in Mexico. Up to now, the Mexican dercetids include a specimen of the *Dercetis* from the Turonian deposits of the San José de Gracia quarry, in Puebla (Alvarado-Ortega et al., 2020a); numerous specimens of the genus *Apuliadercetis* Taverne, 2006, from the Campanian deposits of the Tzimol quarry, in Chiapas (Alvarado-Ortega et al., 2020b); and different unidentified dercetids from Turonian strata exploited in the Arroyo las Bocas, in Guerrero (Alvarado-Ortega et al., 2006), Xilitla quarry, in San Luis Potosí (Blanco-Piñón et al., 2006), and Vallecillo quarry, in Nuevo León (Blanco-Piñón, 2003; Blanco et al., 2001). The dercetid specimens from the Vallecillo quarry already identified belong to three species, *Rhynchodercetis yovanovitchi* Arambourg (1943) (see Giersch, 2014), *Rhynchodercetis regio* Blanco and Alvarado-Ortega (2006), and *Robertichthys riograndensis*, Blanco-Piñón and Alvarado-Ortega (2005). Among these species, Giersch (2014:65) and Díaz-Cruz et al. (2016) considered that *Robertichthys riograndensis* is not a dercetid nor enchodontoidei. Finally, Alvarado-Ortega et al. (2019) reported the youngest and first record of *Hastichthys* in America, based on almost complete and fragmentary specimens from the Turonian deposits of Huehuetla quarry, in Puebla. Therefore, the present work aims are to provide an accurate description of these *Hastichthys* specimens from Huehuetla, to support their inclusion into a new species, and to explore its relationships.

The Huehuetla quarry is a Turonian marine vertebrate site

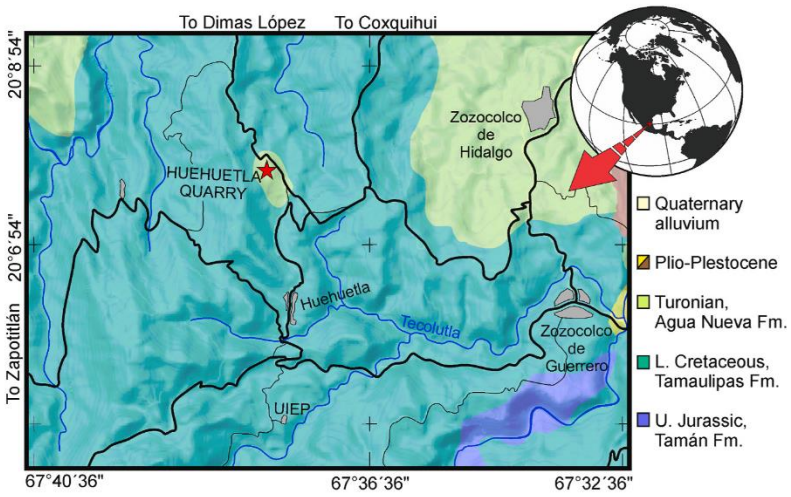

Fig. 1. Geological map of the Huehuetla quarry, near Huehuetla town, Puebla, Mexico (based on Alvarado-Ortega et al., 2019, fig. 1).

discovered in 2017 (Alvarado-Ortega et al., 2019). This small and shallow fossiliferous quarry located between the coordinates 20°7′45.9″ N and 97°37′48.3″ W exposes jet-black marine sediments belonging to the Agua Nueva Formation. This site takes its name from the near Huehuetla town that also is the political center of the homonymous municipality, into the Sierra Norte Region, Puebla, Mexico (Fig. 1). This small site is exploited by local people to extract beautiful jet-black slabs that are commercialized to cover floors or walls. The fossiliferous strata of Huehuetla consist of parallel and finely laminated carbonated shales that are strongly rotten, bituminous, and oily. These marly layers are interbedded with scarce millimetric horizons of black flint and some thin layers of bentonite. When weathered, these rocks become dark gray. Within this lithological sequence, nodules are scarce, and the crystals of pyrite are randomly scattered within these hard-carbonated rocks and over the fossils.

Besides *Hastichthys*, the macrofossil assemblage already identified from the Huehuetla quarry includes some bivalves as well as numerous fishes and some other remains of mosasaurs not yet identified. Fishes are the most abundant, best preserved, and more diverse fossils in Huehuetla quarry; these include *Tselfatia formosa* Arambourg (1943); *Goulmimichthys roberti* Blanco and Cavin (2003); *Enchodus* Agassiz, 1835 (not 1843); specimens referable to *Nursallia tethysensis* Capasso et al., 2009; and others belonging to Clupeidae (Alvarado-Ortega et al., 2019).

2. Materials and Methods

Preparation methods. Fossils were mechanically prepared with needles and odontological devices under a stereoscopic microscope. When necessary, the fossils were glued with cyanoacrylate; they were hardened with a weak solution of plexigum diluted in methacrylate acetate applied with a fine brush. As noted in the figures of this work, the specimens were photographed under dry and wet conditions, white light, and before and after being coated with ammonium citrate.

Anatomical nomenclature and abbreviations. The taxonomic identification of fossil taxa, as well as the anatomical nomenclature and abbreviations used here are based on similar publications (Goody, 1969; Taverne, 1991; among others).

Institutional abbreviations. Fossils from the Huehuetla quarry are deposited and catalogued under the acronym IGM that correspond to the Colección Nacional de Paleontología, housed into the Museo María del Carmen Perrilliat at the Instituto de Geología, UNAM.

Phylogenetic analysis. The phylogenetic reconstructions presented in this work are based on the data set proposed by Silva and Gallo (2011) aimed to understand the phylogenetic relationships among Enchodontoidei. This matrix in turn has been modified and new taxa have been added (see Díaz-Cruz et al., 2016, 2019a; 2019b, 2020; Vernygora et al., 2018). To assess the phylogenetic position of the taxon herein described, we incorporated it into the data matrix and conducted four phylogenic analyses. Two of them using Standard Maximum Parsimony and Implied Weighted Parsimony and the rest ran under the Bayesian Inference approach.

The Maximum Parsimony analyses were performed in TNT 1.5 (Goloboff and Catalano, 2016); for Standard Maximum Parsimony, all the characters were treated as non-additive (unordered) and equally weighted. Silva and Gallo (2011) proposed the outgroup comprising *Protostomias* Arambourg, 1943 (Stomiiformes), *Trachinocephalus* Gill, 1861 (Aulopiformes), and *Sardinioides* von der Marck (1858) (Myctophiformes), of which the first two taxa were recovered as members of the ingroup even though they belong to different orders. As our objective was to assess the phylogenetic position of the taxon herein described, we decided to keep those taxa and only use *Sardinioides* as outgroup without forcing the monophyly of the suborder. The search strategy consisted of a traditional search using Random Addition Sequences (RAS) as starting trees, Tree Bisection Reconnection (TBR) as branch swapping algorithm, holding 1 tree per replication and running for 50,000 replications (mult = ras tbr hold 1 rep 50,000). As some replications overflowed, additional TBR was applied to the trees kept in memory. The Implied Weighted Maximum Parsimony analysis ran with k = 10 and the rest of the settings as those implemented in the Standard Maximum Parsimony analysis.

The Bayesian Inference analyses were performed using MrBayes v3.2.6 (Ronquist et al., 2012). The phylogenetic exercises considered all the morphological characters as unordered of standard type. The outgroup was *Sardinioides*, with no constraints to the topology. The analysis ran 10,000,000 generations with six independent simultaneous analyses and 12 chains. The percentage of samples discarded was 20%. One analysis assumed variable rates of character change and other equal rates, except for this modification, the settings for the second analysis remaining the same. At the end of both analyses, a majority-rule consensus tree was calculated. To optimize the computing time, the Beagle library (Ayres et al., 2012) was activated and used. Posterior samples of the Bayesian Inference analyses were visualized with Tracer 1.7 (Rambaut et al., 2018) to evaluate convergence.

Character mapping was performed using the results of the Standard

Maximum Parsimony. The supporting characters of clades were mapping for all the Most Parsimonious Trees in TNT 1.5 (Goloboff and Catalano, 2016) using the command *apo* >, which also shows the state transformations. To compare the tree topologies resulting from the phylogenetic analyses, we created a tanglegram using the R packages dendextend (Galili, 2015), phylogram (Wilkinson and Davy, 2018), and treeio (Wang et al., 2020).

. Results

.1. Systematic paleontology

Order Aulopiformes Rosen, 1973.
Family Dercetidae Woodward, 1901.
Genus Hastichthys Taverne, 1991.

Species included. The type species, *Hastichthys gracilis* (Chalifa, 989), from the Lower Cenomanian, Amminadav Fm., Ein-Yabrud, near amallah; Cisjordania, Palestine. Two Turonian Mexican species omprising *Hastichthys totonacus* sp. nov. described below, plus *Hastichthys regio* (Blanco and Alvarado-Ortega, 2006), from Turonian deposits of the Agua Nueva Formation, Vallecillo quarry, Nuevo León, Mexico, previously described as *Rynchodercetis regio* are here placed into this genus (see discussion section).

Hastichthys *totonacus* sp. nov.
(Figs. 2–9, Table 2).
LSID Urn:lsid:zoobank.org:pub:26EF06C1-C9E2-4B7C-AF1C-99FC17625BE8

Holotype. IGM 7969, complete articulated specimen exposing the left side with 129 mm of SL (Fig. 2A, 5B, 9) (also see Alvarado-Ortega et al., 2019, figs. 5.1 and 5.4).

Paratypes. IGM 7970, head exposing the skull roof and the pectoral girdle (Fig. 3B) (also see Alvarado-Ortega et al., 2019, Figs. 5.2 and 5.3). IGM 11518, incomplete specimen with no rostrum nor caudal fin, exposing the lateral right side of the body (Figs. 6 and 8). IGM 11519, incomplete specimen exposing the left lateral side of the trunk with no caudal region (Fig. 2B, 5C). IGM 11520, incomplete specimen exposing the left lateral side of the trunk without snout tip nor caudal region (Fig. 2C, 4). IGM 11521, incomplete specimen exposing the dorsal

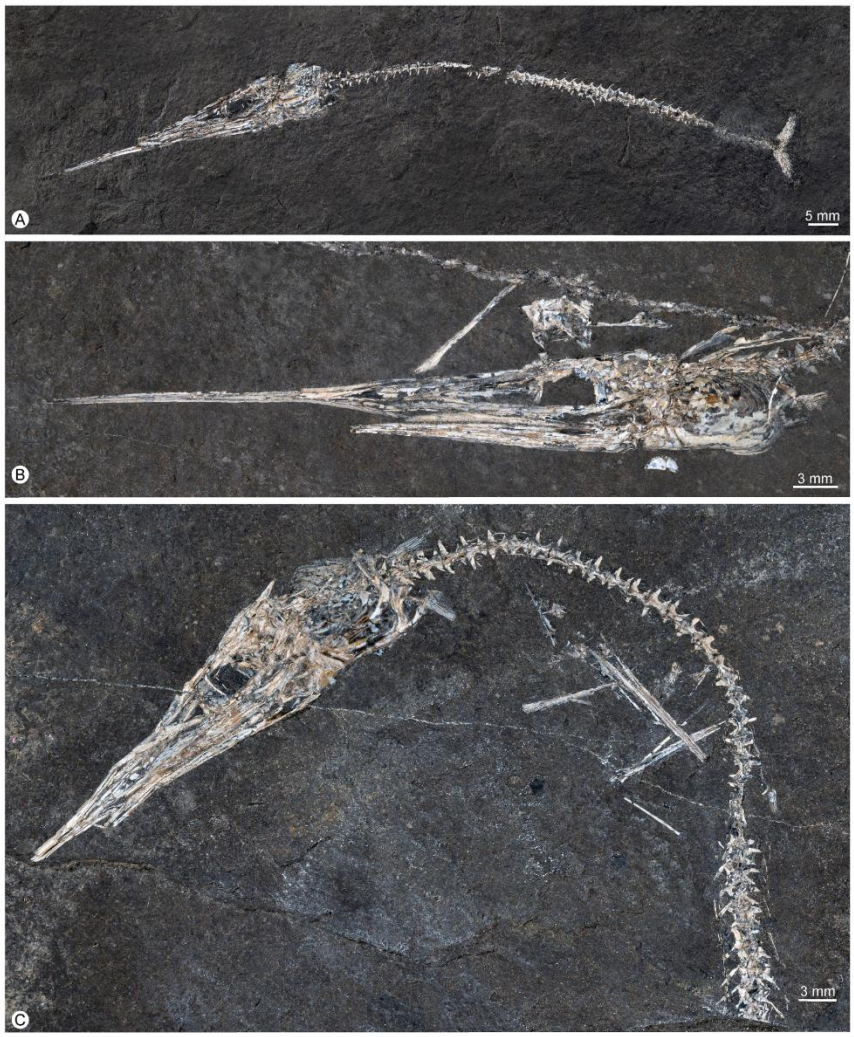

ig. 2. Specimens of the type series of *Hastichthys totonacus* sp. nov. from the Huehuetla quarry, Puebla, México. A) IGM 7969, holotype and most complete specimen s far known. B) IGM 11519, paratype. C) IGM 11520, paratype.

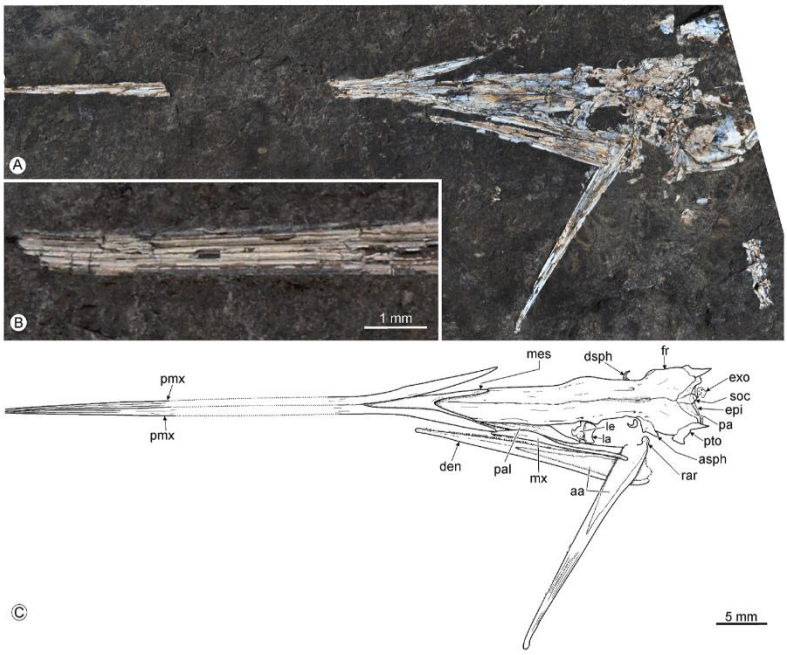

Fig. 3. Head of *Hastichthys totonacus* sp. nov. from the Huehuetla quarry, Puebla, México. A) General view of IGM 7970, paratype. B) Close-up of the rostrum of IGM 11528 b, paratype, which shows longitudinal and parallel striae and ridges ornamenting the outer surface of the upper jaw. C) Simplified and idealized line drawing based on A. Abbreviations: aa, anguloarticular; asph, autosphenotic; den, dentary; dsph, dermosphenotic; epi, epiotic; exo, exoccipital; fr, frontal; la, lachrymal; le, lateral ethmoid; mes, mesethmoid; mx, maxilla; pa, parietal; pal, palatine; pmx, premaxilla; pto, pterotic; rar, retroarticular; soc, supraoccipital.

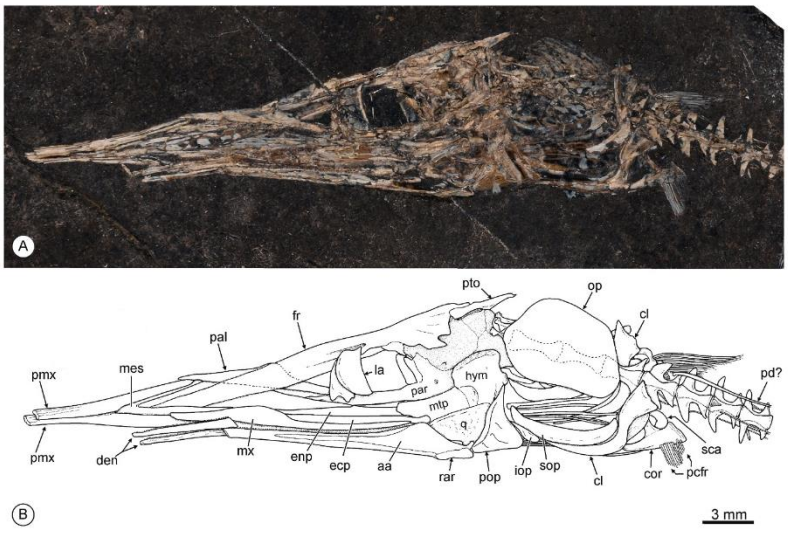

Fig. 4. Head of *Hastichthys totonacus* sp. nov. from the Huehuetla quarry, Puebla, México. A) General view of IGM 11520, paratype. B) Simplified line drawing of the skull based on A. Abbreviations: aa, anguloarticular; cl, cleithrum; cor, coracoid; den, dentary; ect, ectopterygoid; enp, endopterygoid; fr, frontal; hym, hyomandibular; iop, infraopercle; la, lachrymal; mes, mesethmoid; mtp, metapterygoid; mx, maxilla; op, opercle; pal, palatine; par, parasphenoid; pd, predorsal; pmx, premaxilla; pcfr, pectoral-fin rays; pd, predorsal; pop, preopercle; pto, pterotic; q, quadrate; rar, retroarticular; sca, scapula; sop, subopercle. The dotted lines on the opercle correspond to vertebrae 1, 2, and part of the 3.

surface of the head and part of the abdominal region, without the snout tip nor large part of the trunk. IGM 11522, isolated head exposing the lateral right view. IGM 11523, isolated bad preserved head showing part of the skull ventral surface, without the snout tip. IGM 11524, part of the abdominal region and all caudal region of the trunk exposing the left side. IGM 11525, part of the trunk between the occiput and the pelvic fin, ventrally exposed (Fig. 7). IGM 11526 a and b, incomplete specimen preserved in part (a) and counterpart (b), with the head and some abdominal vertebrae. IGM 11527, isolated and scattered bones of the jaws (Fig. 5D). IGM 11528 a and b (part and counterpart), a fragment of the snout preserved in part (a) and counterpart (b) (Fig. 3A). IGM 11529, caudal fin and ten precaudal centra. IGM 11530, a badly preserved fragment of the head exposing its left side (Fig. 5A).

Etymology. The species name derives from the "Totonaca" or the "people of the hot land place" in Náhuatl language, which was a prehispanic civilization that inhabited the region of Huehuetla town and other regions of Puebla, Veracruz, and Hidalgo.

Age and distribution. All specimens come from a superficial sequence of jet-black bituminous marls, no more than 30 cm thick, once extracted from the Huehuetla quarry, Sierra Norte Region, Puebla, Mexico (Fig. 1). This site is formerly cataloged as IGM-loc 3889. Strata exploited in the Huehuetla quarry belong to the Turonian section of the

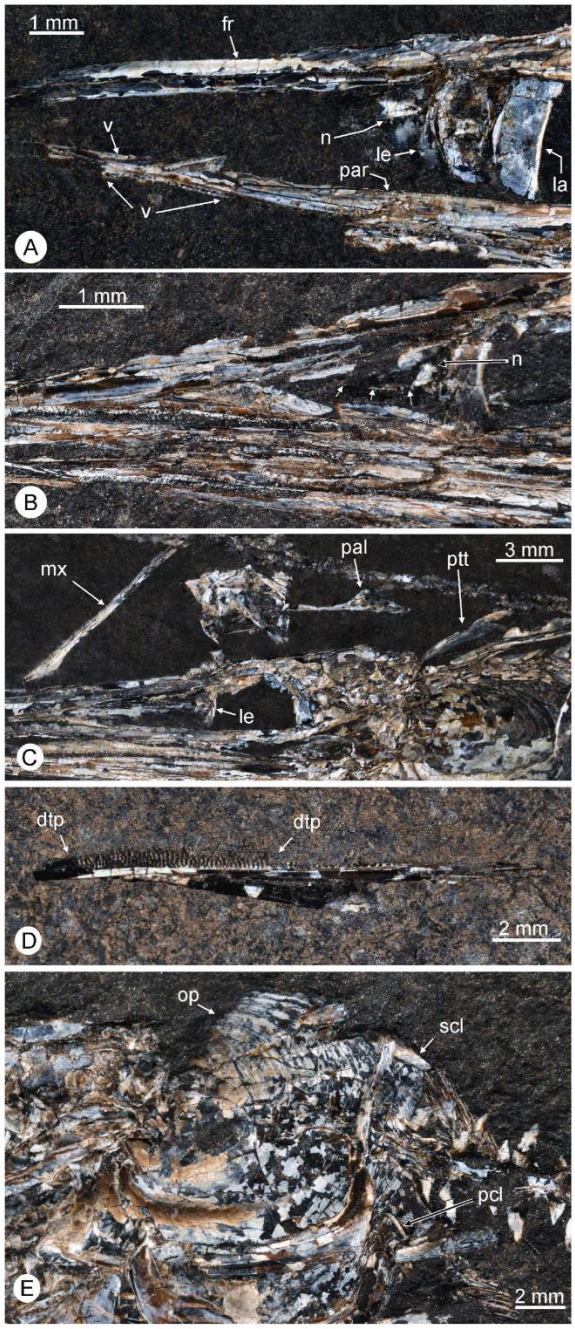

Fig. 5. Osteological details of *Hastichthys totonacus* sp. nov. from the Huehuetla quarry, Puebla, México. A) Close-up of the skull ethmoid region in IGM 11530, paratype. B) Close-up of the skull ethmoid region in IGM 7969, holotype. C) Close-up of the skull of IGM 11519, paratype. D) Anterior part of the dentary bone of IGM 11527, paratype. E) Close-up of the pectoral girdle region in IGM 7969, holotype. Abbreviations: dtp, dentary tooth patch; fr, frontal; la, lachrymal; le, lateral ethmoid; mx, maxilla; na, nasal (associated arrows on the nasal show the thread-like anterior projection of this bone); op, opercle; pal, palatine; par, parasphenoid; ptt, posttemporal; pcl, poscleithrum; scl, supracleithrum; v, vomer.

Agua Nueva Formation (Alvarado-Ortega et al., 2019).

Diagnosis. Species of *Hastichthys* that differs from its allied species, *H. gracilis* and *H. regio,* in the following set of postcranial characters, the trunk is relatively short and consists of 59 total centra, including 32 abdominal, 25 caudal preural, and two urals (versus 71 total centra, including 44 abdominal, 25 caudal preural, and two urals observed in *H. gracilis*; and those 61 total centra of *H. regio*); seven dorsal fin rays (versus 9 of *H. gracilis*); eight anal fin rays (versus at least 10 to 19 of *H. gracilis* and *H. regio*).

3.2. Description

Body shape and general proportions. Measurements and body proportions of *Hastichthys totonacus* sp. nov. are summarized in Table 2. Unfortunately, only the holotype represents a complete specimen (Fig. 2A); therefore, the body features described below are based on IGM 7969. Regarding the head length, the largest specimen of this species is IGM 7970, which was about 1.5 times larger than the holotype.

Hastichthys totonacus sp. nov. is a serpentiform and longirostrine small fish that probably did not exceed 300 mm in total length. The body shallow and practically uniform throughout the preanal region of the trunk; beyond, the height of the body gradually decreases up to the inconspicuous caudal peduncle. The elongated head is triangular, shallow, and including the opercle it occupies about 37.9% of the standard length (SL). The rostrum and the mandibles are about 29.4% of SL and 67.4% of the head length while the latter represents about 57% of the preorbital length. The pelvic fin seems to be triangular and about as long as the centra 4 and 5; its base is placed in the midpoint between the spine and the ventral edge of the body. The fins are small. The dorsal fin is triangular and placed behind the middle of the body, between 61.2 and 63.5% of SL. The pelvic fins are triangular and in opposition with the middle part of the dorsal fin. The anal fin is triangular and located far back in the body between 86.8 and 89% of SL. The caudal fin is short, high, and consists of two triangular, equally sized, and deeply forked lobes.

Skull. In this longirostrine fish, the skull is triangular, very elongated, and anteriorly tapered. The skull is about 10 times longer than high. The rostrum is slender, straight, and ends in an acute tip. Here, the orbital and postorbital regions are equally high and long, and together occupy the posterior 25% of the skull length (Figs. 2–4).

The frontals are the largest bones in the skull (Figs. 3–5). The interfrontal suture is straight and extends along the entire length of these bones, from the ethmoid region to near the posterior edge of the skull. There is a shallow interfrontal depression extended above the orbit and part of the postorbital region. Each frontal is a long and roughly triangular bone, anteriorly narrow, laterally notched above the orbit, strongly expanded posteriorly covering part of the lateral surface of the skull, and have a posterolateral process that almost separates the parietal from the pterotic. The posterolateral processes of the frontals extend far back toward the occiput, their tilted medial edges enclose a couple of parietals and the minute supraoccipital bone. Laterally and behind the orbit, each of these processes borders the autosphentic and prootic bones as well as the conspicuous and spiny pterotic posterior process. The lateral expansion of frontal bone roofs the posttemporal fossa. In front of the orbit, the frontals are laterally straight except for a small triangular lateral process located just in front of the orbit that is associated with the supraorbital canal path, from the frontal to nasal bone. Together, the anterior ends of frontal bones penetrate the middle posterior fork of the mesethmoid bone. The frontals are practically smooth except for some scarce and longitudinal ridges alongside their lateral edges that enclose the supraorbital sensory canal as well as some scarce inconspicuous longitudinal grooves present in its expanded postorbital region. Along the frontal bones, the supraorbital sensory canal is fully enclosed by bone and only opens through some pores present around the orbit and the ethmoidal region.

The parietals are small and smooth ovoid bones located far back on

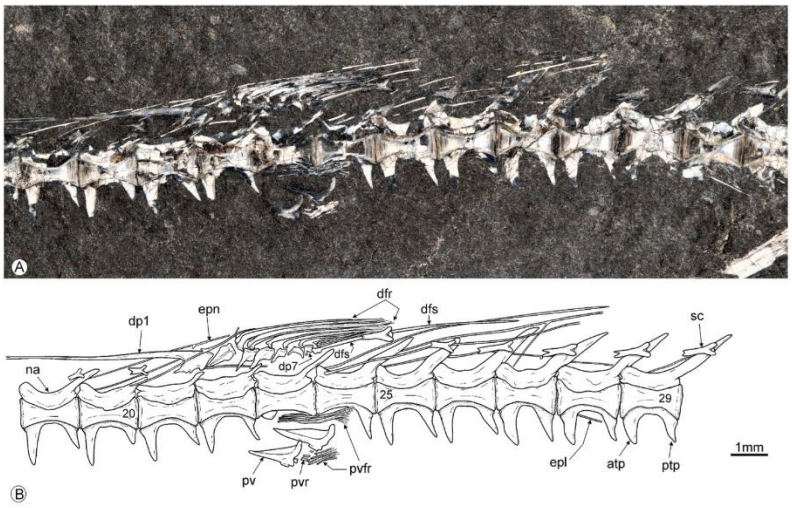

Fig. 6. Dorsal fin region of the trunk of *Hastichthys totonacus* sp. nov., from the Huehuetla quarry, Puebla, Mexico. A) Close-up of the dorsal fin region of IGM 11518, paratype. B) Simplified line drawing based on A. Abbreviations: atp, anterior transverse process; dfr, dorsal-fin rays; dfs, dorsal fin stay; dp, dorsal proximal pterygiophore; epl, epipleural; epn, epineural; na, neural arch; ptp, posterior transverse process; pv, pelvic bones; pvfr, pelvic fin ray; pvr, pelvic fin radial; sc, scutes. Numbers on centra indicate their position.

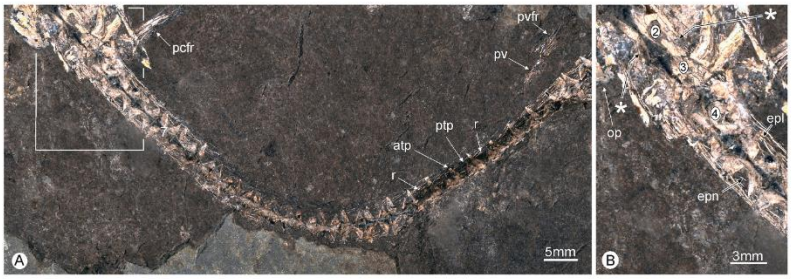

Fig. 7. Distribution of epineural and epipleural bones in *Hastichthys* totonacus sp. nov., from the Huehuetla quarry, Puebla, Mexico. A) IGM 11525, exposing the ventral surface of the trunk and posterior part of the head. B) Close-up of first abdominal centra of IGM 11528 (rectangle on A). Abbreviations: atp, anterior transverse process; epl, epipleural; epn, epineural; op, opercle; pcfr, pectoral fin ray; ptp, posterior transverse process; pv, pelvic bone; pvfr, pelvic fin ray; r, rib; Numbers on centra indicate their position; *, epipleural on abdominal centrum 2.

the skull roof, near the posterior margin of the skull (Fig. 3). The medial edges of these bones are in contact each other anteriorly, between the frontals and the supraoccipital bone, whereas posteriorly they are separated by the supraoccipital bone. The medial edge of each parietal sutures the lateral process of the frontal and a reduced part of the pterotic middle edge. Posteriorly, the parietals suture the small, short, and wide dorsal components of the respective epiotic bones, and together these four bones dorsally enclose the small supraoccipital bone that rather lacks posterior crest.

The pterotic is an elongated bone that has a noticeable acute posterior process extended beyond the occiput region (Figs. 3 and 4). Dorsally this bone shows an elongated, flat, and curved surface that is entirely smooth. Laterally, the pterotic is rather triangular, projected downward along the posterior half of the skull, and exhibits an elongated hyomandibular facet below a small shelf alongside the skull top.

IGM 6970 exhibits the left exoccipital disarticulated behind the skull (Fig. 3). This bone is roughly rectangular, about two times higher than wide, and is pierced for a large foramen for the occipital nerve. The dorsal half of its medial edge has a deep concave notch that represents half of the foramen magnum.

Unfortunately, the available specimens do not show the skull back surface and the lateral surfaces of their postorbital regions are strongly fractured and compressed. Therefore, it is not possible to provide an accurate description of the bones of this skull regions. The orbit seems to be internally bordered by basisphenoid bones, which are projected inward forming the orbit posterior walls that are slightly curved and convex.

The parasphenoid is a complex bone with an elongated, smooth, untoothed, and stout bar projected along the ethmoid and orbital skull regions, which is slightly dorsoventrally compressed (Figs. 4 and 5A). The postorbital part of the parasphenoid is stout and expands to cover the basal half and about the anterior two-thirds of the postorbital surface of the skull. In the ventral edge of this bone, there is an obtuse angle between its postorbital and orbital regions because the postorbital part slightly tilts upwards.

The ethmoid skull region shows a large triangular nasal cavity largely covered by the palatine bone (Figs. 3–5A-C). On either side of the skull, this cavity is bordered by the frontal dorsally, the parasphenoid and vomer ventrally, and the lateral ethmoid posteriorly. The lateral ethmoid is a stout rectangular bone tightly sutured to the ventral surface of the respective frontal bone and projected downward without reaching the dorsal edge of the parasphenoid. Just behind the anterior corner formed by the frontal and lateral ethmoid bones, there is a small rectangular nasal bone with a thread-like process projected forward. The mesethmoid is a V-shaped bone, pointed anteriorly and posteriorly forked, which separates the premaxilla from frontal bones at the level of the anterior tip of the lower jaw.

In IGM 11530, the bones that border the nasal capsule are exposed (Fig. 5A). It is difficult to distinguish if the vomers are fused or not. The vomers are attached to the anterior end of the parasphenoid bone that penetrates the forked rear of the vomer (or between the vomers). There is a triangular and laminar small ascending process in the middle of the vomer(s).

Circumorbital bones. There are no traces of infraorbital, antorbital, or supraorbital bones in any of the available specimens (Figs. 3–5). Both the left and right sickle-shaped dermosphenotic bones are preserved in

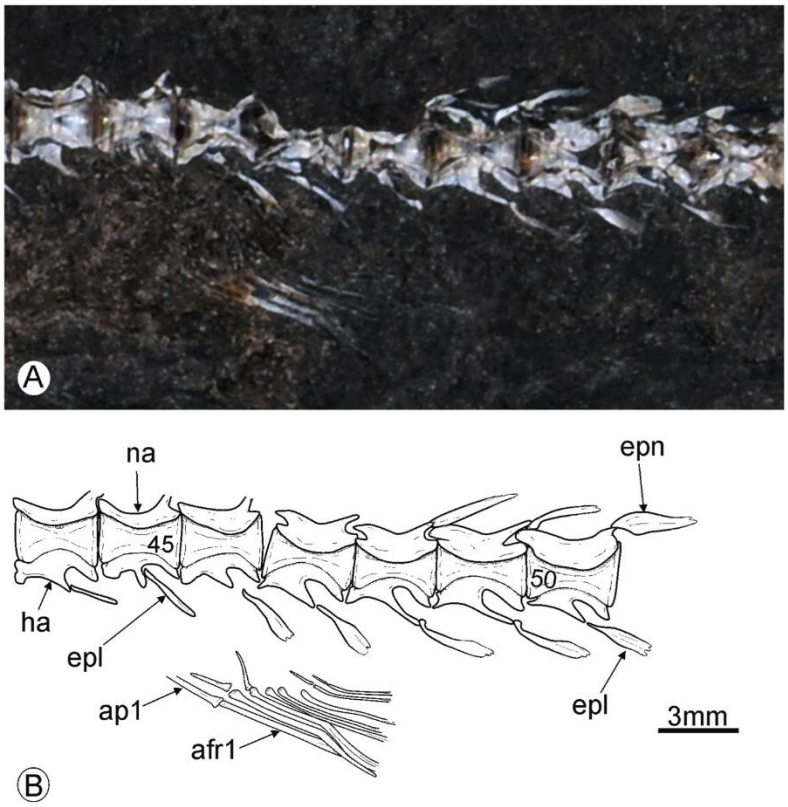

Fig. 8. Anal fin region of *Hastichthys totonacus* sp. nov. from the Huehuetla quarry, Puebla, Mexico. A) Close up of caudal fin of IGM 11518, paratype, under wet conditions. B) Simplified and idealized line drawing based on A. Abbreviations: afr, anal-fin ray; ap, anal pterygiophore; epl, epipleural; epn, epineural; ha, haemal arch; na, neural arch. The numbers on centra show the relative position of each centrum into the vertebral column.

IGM 7970. The lateral ethmoid bones are covered with a large semicircular, thin, and flat, lachrymal bone. No sclerotic bones are observed within the orbital cavity.

Upper jaw. The upper jaw consists of the premaxilla and maxilla; there is no supramaxilla (Figs. 3–5C). The premaxillae are long, narrow, and toothless bones that form the anterior part of the rostrum. The anterior 75% of these bones are semicylindrical structures tightly sutured each other medially forming a slender straight beak of the rostrum. Further posteriorly, these bones are lateromedially forked to embrace the tip of the mesethmoid bone up to the level of the first third of the lower jaw. The anterior surface of these bones is ornamented with large, longitudinal, and parallel striae and ridges.

The maxilla is a shallow, very elongated, smooth, and lateromedially compressed bone extended from the posterior orbit to the anterior tip of frontal bones (Figs. 3–5C). The contact between the maxilla and premaxilla is weak, the anterior tip of the former contacts only the posterior tip of the latter. In the maxilla, both anterior and posterior ends are tapered, its posterior half is evenly tall, and its anterior third shows a triangular anterodorsal process. The maxilla ventral edge is straight and densely occupied with a row of numerous small conical teeth with sharp tips and somewhat curved in and backward. Throughout the alveolar border, the density, size, and shape of teeth are uniform.

Lower jaw. The lower jaw is an elongate and shallow triangular structure that consists of the dentary, anguloarticular, and retroarticular bones (Figs. 3 and 4). This jaw is noticeably shorter than the rostrum, the articulation between the lower jaw and the quadrate is below the middle of the postorbital skull region, and so, its length represents 56.2% of the preorbital length of the skull.

The dentary is an elongated triangular bone with the extremely low symphysis, no coronoid process, and deeply forked posteriorly (Figs. 3 and 4). The dorsal and ventral borders of this bone are straight except in the anterior quarter, in which the dentary is tilted downward. The alveolar border occupies at least the anterior four-fifths of the bone and shows a single tooth row of small teeth; however, the lingual surface of the bone shows a rugose alveolar patch where two to four tooth rows are placed near to the anterior end (Fig. 5D). The size, shape, and distribution of dentary teeth resemble those of the maxilla. The anterior third of the dentary lateral surface is ornamented with long and parallel striae and ridges; beyond, this bone is rather smooth. The anguloarticular is triangular, occupies the posterior third of the lower jaw, and forms the large part of the mandibular postarticular process. The articulation between the lower jaw and the quadrate is located below the middle postorbital region of the skull. The ventral part of the postarticular process includes an elongated and triangular retroarticular bone. The mandibular sensory canal is enclosed, opening only through some pores near the dentary ventral border.

Suspensorium and branchial arch. The hyomandibular is a broad and robust bone with a single articular dorsal head, a rounded anterior flange, and a short shaft vertically oriented. The opercular condyle is stout and protrudes backward from the middle of the hyomandibular posterior edge (Fig. 4). A low, elongated, and triangular quadrate possesses a stout and wide articular head. The articulation of the quadrate and lower jaw is laterally exposed. The symplectic bone and part of the quadrate are covered by the anterior expansion of preopercle and cannot

Fig. 9. Caudal fin of *Hastichthys totonacus* sp. nov. from the Huehuetla quarry, Puebla, Mexico. A) Close-up of the caudal fin in IGM 7969, holotype, under wet conditions. B) Simplified and idealized line drawings based on A (haemal arches and spines on preural centra 2 and 3 are based on IGM 11524). Abbreviations: csut, convolute suture between hypurals 2 and 3; ep, epural; hapu, haemal arch (and fused spine) of preural centrum; hy, hypural; napu, neural arch (and fused spine) of preural centrum; php, parhypural; pu, preural centrum; u, ural centrum; un, uroneural. Black arrows enclose the first principal caudal ray on dorsal and lower caudal lobes.

be identified in any of the specimens. The metapterygoid is roughly subrectangular, elongate, and broad; it seems to have a sinuous suture with the hyomandibular.

The ectopterygoid and endopterygoid are elongated bones placed below the orbit and part of the skull preorbital region (Fig. 4). The ventral edge of the ectopterygoid bone bears small teeth that resemble those on the maxilla. It is unclear if the ventral edge of the endopterygoid is also toothed. The palatine is an elongated triangular bone in which both anterior and posterior extremes are acute, and the middle dorsal triangular wing covers the anterior region of the nasal capsule. Some inconspicuous longitudinal grooves cover the palatine outer surface. The ventral edge of the palatine is entirely toothed with small teeth that resemble those of the maxilla, except for the presence of some slightly larger teeth in the middle of the bone.

The branchial skeleton is almost obscured in all available specimens; however, some curved branchiostegal rays are exposed below the opercular series. Although the number of branchiostegal rays cannot be determined; the anterior ones are long thread-like and become more expanded posteriorly.

Opercular bones. The opercular series consists of the opercle, subopercle, preopercle, and interopercle (Fig. 4). The opercle is an elongated ovoid bone, about 1.3 times longer than high; it is smooth and flat. The opercle shows concentric bone growth bands. In the opercle, the hyomandibular facet is in the middle of its anterior edge. The subopercle is a semicircular, flat, and strongly curved bone located below the opercle that has an expanded triangular anterior ascending process.

The preopercle is a triangular bone, about 1.5 higher than long, slightly concave anteriorly, straight posteriorly, and has scarce openings of the preopercular sensory canal on its lateral surface. The tall and smooth wedge-shaped interopercle is located between the preopercle and the subopercle.

Axial skeleton. Among the referred specimens, IGM 7969 and IGM 11518 show the most complete axial skeleton. The former has 59 total centra, including 32 abdominal, 25 caudal, plus two urals. The preural 1 and ural 1 are fused into the caudal skeleton (Fig. 2A, 9). IGM 11518 has 58 cent ra preserved, including 32 abdominal and 24 unfused caudal centra. Probably this specimen only lost the composed caudal centra (pu1+u1) and ural 2. Overall, the centra are hourglass-shaped, strongly constricted in the middle (Figs. 2, 4–9). The first two centra are elongated, at least 2.5 times longer than tall. Beyond, other centra become progressively shorter at such a degree that the posterior preural centra are almost square.

Each centrum is fused with their respective neural arch (Figs. 2, 4–9). These arches are overall rectangular, low, slightly longer than the centrum, and with the anterior end slightly overhanging the centra and tilted forward and upward [= prezygapophyses of Goody (1969)]. Each neural arch bears a stick-like neural spine that is projected backward resting on the dorsal edge of the subsequent neural arch. In the abdominal region, the neural spines are relatively short because these are extended only over the anterior half of the subsequent neural arch. Beyond, in the caudal centra, the neural arches became longer. Short and slender ribs articulate with the ventral surfaces of the anterior transverse processes of the abdominal centra. The haemal arches are relatively small, noticeably shorter than the respective centra, and carry a haemal spine that has practically the same size and inclination of the associated neural spine.

In the abdominal region, the centra has a pair of large triangular transverse processes projected laterally and downward (Figs. 2, 4–7). The anterior process is always larger than the posterior process. In the caudal region, the anterior transverse processes become smaller, projected more vertically, and probably meet each other medially forming haemal arches, in which small zygapophyses are present. Above the pelvic girdle, the centra 23 and 24 have no transverse processes in IGM 11518 and these processes are normal-sized in other specimens (Figs. 6 and 7).

Most of the centra are associated with intermuscular bones, which

Table 2
Measurements and proportions of specimens of *Hastichthys totonacus sp. nov.* from the Huehuetla quarry. Abbreviations, -, character obscured or not preserved; ?, character questionable; +, incomplete observation.

	IGM 7969	IGM 7970	IGM 11518	IGM 11519	IGM 11520	IGM 11521	IGM 11524	IGM 11525	IGM 11526	IGM 11589	
		Measurements (in mm) and proportions									Avg, (Range)
Total length	136	–	–	–	–	–	–	–	–	–	–
Standard length (SL)	129	–	130+	102+	96+	45+	53+	81+	41.7+	11+	130+ max.
Head length (HL)	49	79	26+	49	36+	40+	–	–	32.3	–	(32–79)
%SL	37.9	–	–	–	–	–	–	–	–	–	37.9
Preorbital length	32	58	12+	32	20+	24+	–	–	21.2	–	(21.2–59)
(POL)	29.4	–	–	–	–	–	–	–	–	–	29.4
% SL	65.3	73.4	–	65.3	–	–	–	–	65.6	–	67.4
%HL											(65.3–73.4)
Mandibular length	18	28+	18+	18.5	21+	–	–	–	9.9+	–	(18–28+)
% SL	13.9	–	–	–	–	–	–	–	–	–	13.9
%HL	36.7	–	–	37.7	–	–	–	–	–	–	37.2
%POL	56.2	–	–	57.8	–	–	–	–	–	–	(36.7–37.7)
											57 (56.2–57.8)
Predorsal length	79	–	63+	–	75?	–	–	–	–	–	79
% SL	61.2	–	–	–	–	–	–	–	–	–	61.2
Dorsal fin length	3	–	3	–	–	–	2.5	–	–	–	(2.5–3)
% SL	2.3	–	–	–	–	–	–	–	–	–	2.3
Preanal length	112	–	103+	–	–	–	–	–	–	–	(112)
% SL	86.8	–	–	–	–	–	–	–	–	–	86.8
Anal fin length	1+	–	2+	–	–	–	2.2	–	–	–	(2.2)
% SL	0.8+	–	–	–	–	–	–	–	–	–	0.8+
Prepelvic length	84?	–	35+	–	76	–	–	75+	–	–	(76–84?)
% SL	65.1?	–	–	–	–	–	–	–	–	–	65.1?
		Accounts									Mode (Range)
Total vertebrae	59	–	–	–	–	–	–	–	–	–	59
Abdominal	32	3+	32	32	32?	14+	16+	28+	12+	–	32 (32)
Caudal	25	–	24+	17+	14+	–	25	–	–	11+	25 (25)
Urals	2	–	–	–	–	–	2	–	–	2	2 (2)
Pair of ribs	?	–	6+	–	10	–	5+	15+	2+	–	–
Dorsal-fin rays	7	–	7	–	1+	–	7	–	–	–	7 (7)
Anal-fin rays	6+	–	8	–	–	–	8	–	–	–	8 (8)
Pectoral rays	9+	–	–	11	11	–	–	9+	–	–	11 (11)
Pelvic rays	6+	–	5+	–	8	–	–	8	–	–	8 (8)

probably do not include epicentrals (Figs. 6–8). The centrum 2 and all posterior abdominal centra have long thread-like epineurals and epipleurals bones that in some cases are extended along 6 centra. The anterior epineurals are forked near to the tip while the epineurals near to the dorsal fin are more deeply forked or Y-shaped. Beyond, the epineurals are shorter and not forked. The abdominal centra, including the second, and most of the caudal centra are associated with epipleurals. The epineurals and epipleurals associated with the tip of haemal and neural spines of those centra located above and behind the anal fin are oval, short, and expanded bones. The epineurals and epipleural bones are absent in the posterior six or seven preural centra.

In the anterior part of the trunk, there are some long and flat bones posteriorly extended up near the dorsal fin base. These bones are unpaired and noticeable wider than the intermuscular bones. Against Goody (1969), who thought that these bones could be median intermuscular bones or ossified dorsal ligament; we suggest these are hypertrophied predorsal bones (=supraneurals) (Fig. 4).

Pectoral girdle and fin. The posttemporal bone is an oval, flat, and smooth bone that lies above and along the opercle. This has a sinuous dorsoposterior edge and two anterior processes of the same length, of which the ventral process is thin while the dorsal process is broad (Fig. 5C). The supracleithrum is rectangular, slightly tilted back and downward, and rests on the dorsal end of the cleithrum, above of the vertebral column (Fig. 5E).

In the lateral view, the cleithrum is S-shaped and consists of two sections separated by a middle tightening (Fig. 4). In this bone, the dorsal section is triangular, expanded dorsally, and ends in a dorsoanterior acute tip while the ventral section is a low thorn-like projection that lies below the posterior two-thirds of the subopercle. Parallel growth bands are present in the dorsal section of the cleithrum. The single postcleithrum is a stick-like bone (Fig. 5E).

The coracoid is a spatula-shaped bone anteriorly tapered, with a sinuous posterior edge and its anterior tip inserted below the base of the middle tightening part of the cleithrum (Fig. 4). This bone has a dorsal process protruding on its middle part and reaches the ventral end of the scapula. Posteriorly, the coracoid is expanded and so elongated that overhangs the posterior tip of the cleithrum dorsal section. The scapula is a small somewhat rectangular bone attached to the posterior angle of the cleithrum. The proximal ends of at least four rectangular radials articulate with the small posterior edge of scapula; distally, these bones support the pectoral fin rays.

The pectoral fin seems to be triangular, short, and probably its length equals that of two abdominal centra (Fig. 4). The articulation between the pectoral fin radials and pectoral rays is vertically oriented. This fin is inserted at half the abdominal cavity height, equally spaced from the ventral edge and the vertebral column. Al least 11 thin, elongated, and distally branched and segmented rays form the pectoral fin.

Pelvic girdle and fin. The pelvic girdle consists of two triangular pelvic bones located in opposition to the dorsal fin base. The bones lie below the centra 23 and 24; in IGM 11518, these centra have no transverse processes while in other specimens such processes are of normal size (Figs. 6 and 7). The pelvic bone is triangular, about two times longer than wide, tapered anteriorly and expanded posteriorly that shows a short medial process bearing a small posterior process. The pelvic bone length is about that of centrum 23. The medial processes of both pelvic bones are slightly irregular; therefore, presumably in life, these bones were medially attached by cartilage. The pelvic fin seems to be triangular and is about as long as two centra. The pelvic fin consists of only eight thin and distally segmented and branched rays, which are proximally supported on at least four small radial bones.

Dorsal fin. This fin is triangular, short, anteriorly high, and is located at the beginning of the second third of the trunk, above the abdominal centra 23 and 24, in opposition to the pelvic fin (Fig. 6). The fin consists of seven thin and distally branched and segmented rays; among which, the first tree equals the length of centra 23 and 24. Posteriorly dorsal fin rays become shorter.

Seven proximal pterygiophores support the dorsal fin, which are projected within the interneural space between the neural spines and are so long that almost contact the neural arches located below (Fig. 6). The articular ends of these pterygiophores are noticeably expanded; hence, no medial or distal pterygiophores are present. The first proximal dorsal pterygiophore has a flat, thin and, hypertrophied anterior triangular expansion extended up to the eighth anterior abdominal centra (abdominal centra 15–22). Posterior to these pterygiophores, there is a dorsal fin stay with an expanded anterior head and an elongated, flat and belt-shaped process that rests above five centra.

Anal fin. This short triangular fin is located far back in the trunk, below the centra 46 and 47 (= preurals 12 and 11) (Fig. 8). Eight distally segmented and branched rays form this fin. Among these, the second anal-fin ray is the larger and its length equals that of centra 46 and 47. The anterior and posterior rays are progressively shorter. This fin is internally supported on eight anal proximal pterygiophores that have expanded articular heads and are progressively smaller.

Caudal skeleton. The caudal fin consists of 15 procurrent and 19 principal rays ordered following the formula vii + I+9–8+I + viii. The haemal and neural spines of posterior three preural centra are comparatively thick and are tilted backward supporting the elements of the caudal fin (Fig. 9).

The caudal skeleton is complex and consists of a composed centrum that results from the fusion of ural 1, preural 1, the proximal ends of parhypural, hypurals 1 and 2, and the tip of the dorsal hypural plate resulting from the total fusion of hypurals 3 and 4 (Fig. 9). Above the ural 2 and hypural 5 are fused. There is no caudal diastema between hypurals 2 and 3; contrary, these bones are strongly attached to each other throughout a deeply sinuous or convolute suture. There is a small spiny neural arch on preural 1, a single, thin, and stick-like epural, and two stout uroneurals.

Scutes. The body is naked except for one row of thin scutes extended along each flank of the body, slightly above the vertebral column (Fig. 6). These scutes are delicate and therefore patchy preserved. The scutes are flat and Y-shaped, with a rectangular horizontal limb elongated and anteriorly forked plus two symmetrical limbs that are short, thin, and tilted about 45° downward and upward. Here, the horizontal limb is rostrocaudal perforated by the lateral line. Although these scutes are similarly shaped and sized along the trunk, near the tail these become more triangular because the lower posterior limbs are shorter. The scutes are smooth and have no external longitudinal ridges.

4. Discussion

4.1. Taxonomical remarks

Nowadays, the order Aulopiformes is diagnosed with seven features, including 1) the epibranchial 2 has an elongate uncinate process bridging the gap between the posterolaterally displaced pharyngobranchial 2 and the pharyngobranchial 3 (Rosen, 1973); 2) the absence of cartilaginous condyle on pharyngobranchial 3 for articulation with epibranchial 2 (Johnson, 1992); 3) the epipleural series is anteriorly developed from at least the abdominal centrum 2 (Patterson and Johnson, 1995); 4) the larvae have peritoneal pigmentation (Johnson, 1982); 5) one or more of the anterior epipleurals are dorsally displaced into the horizontal septum (Patterson and Johnson, 1995); 6) the lack of swim bladder (Johnson, 1982); and 7) the medial processes of the pelvic girdle are joined medially by cartilage (Baldwin and Johnson, 1996). Among these features, only the first four are synapomorphies (Baldwin and Johnson, 1996, p. 396). In the specimens of *Hastichthys totonacus* sp. nov., the pelvic bones show conspicuous medial processes that in life, were probably attached with cartilage (Fig. 6). Additionally, these Mexican specimens have long epipleural (and epineural) bones associated with almost all centra, at least from the abdominal centrum 2 (Fig. 7). The presence of these two characters supports the inclusion of *H. totonacus* as a new member of the order Aulopiformes.

Different authors have indicated numerous diagnostic characters of the family Dercetidae (e.g. Woodward, 1901; Chalifa, 1989, tbl. 1; Taverne, 1991, Taverne, 2005a,b; 2006b; Gallo et al., 2005). *Hastichthys totonacus* sp. nov. is an irrefutable member of this family because its specimens show all the following distinctive characters of the family (continuing with the numbering initiated in the previous paragraph): 8) the trunk is shallow and long (Fig. 3A); 9) the longirostrine and low shape of the head, in which the orbital and postorbital sections of the skull are noticeably short; 10) the presence of a single tooth row on the maxilla; 11) lack of the supraorbital (Fig. 3B, 4, 5); 12) lack of supramaxilla (Figs. 4 and 5); 13) the first two vertebrae are elongated, at least 2.5 times longer than wide (Fig. 4); 14) there are one or two pairs of transverse processes projected ventrolaterally in each centra, well developed in the abdominal centra (Figs. 4, 6 and 7); 15) the neural arches are shallow, elongated, and cover the entire dorsal edge of the centra (Figs. 4, 6–8); 16) in the abdominal and the most anterior caudal centra, the neural spines are extremely small, and its length is less than the half of the respective centrum (Figs. 6 and 8) [Gallo et al. (2005) and Vernygora et al. (2018) suggested that this is synapormorphy of Dercetidae]; 17) the trunk shows one or two rows of triradiate (Y-shaped) scutes covering the flanks of the trunk (Fig. 6).

Hastichthys totonacus sp. nov. forms part of a more exclusive dercetid subgroup, which includes *Pelargorhynchus* von der Marck (1858); *Rhynchodercetis* Arambourg, 1943; *Dercetoides* Chalifa, 1989; *Hastichthys* Taverne, 1991; *Nardodercetis* Taverne, 2005a,b; *Caudadercetis* Taverne, 2006b; and *Candelarhynchus* Vernygora et al., 2018. The members of this unnamed subgroup are recognized by different authors as derived taxa (e.g. Chalifa, 1989; Taverne, 1991, 2006b; Gallo et al., 2005; and Vernygora et al., 2018). The characters shared by these dercetids are (continuing with the numbering of previous paragraphs): 18) the mesethmoid is bifid (Fig. 3); 19) the skull displays a mesoparietal condition (the parietals are in contact medially and separates the supraoccipital bone from the frontals) (Fig. 3); 20) the suture between hypurals 2 and 3 is deeply sinuous or convolute (Fig. 9); 21) the parietals are comparatively small and displaced far in the back of the skull because the frontals are noticeable extended backward (Fig. 3). 22) The preural 1 and ural 1 are fused (Fig. 9).

Regarding the anterior group of putative derived dercetid taxa, *Hastichthys totonacus* sp. nov. also forms part of a more exclusive subgroup that consists of *Nardodercetis*, *Rhynchodercetis, Candelarhynchus*, and *Hastichthys*. These genera share at least two highlight features: 23) The premaxilla is toothless (Fig. 3) and 24) the mandible length is comparatively shorter than the snout (Fig. 3). Among these genera, *Candelarhynchus* and *Hastichthys* share the presence of a noticeable character that is also present in *H. totonacus* sp. nov.: 25) the longitudinal and parallel striae and ridges ornamenting the anterior parts of the rostrum and mandibles (Figs. 3, 4 and 10).

Before the present manuscript, *Hastichthys* and *Candelarhynchus* were monospecific genera and each nominal species was only known by a single fossil. *H. gracilis* is represented by a complete and well-preserved specimen while *C. padillai* is documented from the impression of an incomplete fish without the posterior half of the trunk and the rostrum anterior end (Chalifa, 1989; Vernygora et al., 2018). Although these fishes share the peculiar ornamentation on the rostrum and mandible, the incomplete preservation of *C. padillai* does not allow for an accurate comparative study; nonetheless, these genera display more differences than common characters. Here, *Hastichthys totonacus* sp. nov. is placed into the genus *Hastichthys* because it is morphologically more like *H. gracilis* than to *C. padillai*. In both *H. gracilis* and *H. totonacus* sp. nov. the centra have two transverse processes, the pterotic bone has a long

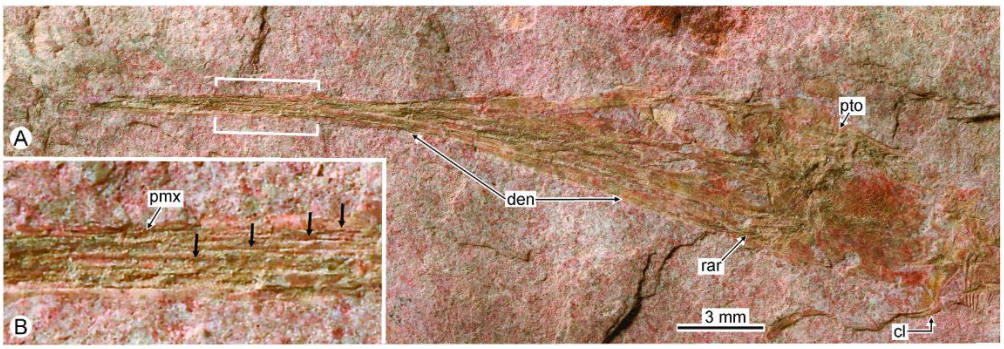

Fig. 10. IGM 11531, *Hastichthys* sp. from the Turonian deposits of the Mexcala Formation exploited in the Arroyo las Bocas, near Taxco, Guerrero, southern Mexico. A) General photograph under white light. B) Close-up of the rostrum (rectangle on A). Abbreviations: den, dentary (tip of this bone); pmx, premaxilla; pto, pterotic bone (the posterior process of this bone); rar, retroarticular; black arrows in B shows the longitudinal and parallel striae and ridges on the outer surface of the premaxilla.

posterior process that overhangs the occiput, and the frontals are extended far backward near the nape (Figs. 3–5; Chalifa (1989, Figs. 2 and 3); otherwise, in *C. padillai* the centra only have the anterior of these processes, the pterotic posterior process is not developed, and the frontals are comparatively shorter and only cover the anterior half of the skull postorbital region (Vernygora et al., 2018, Figs. 4 and 6).

In this work, the species *Rhynchodercetis regio* is recognized as a species of the genus *Hastichthys*, as *Hastichthys regio* (Blanco and Alvarado-Ortega, 2006) (Table 3). This species, named based on three bad preserved fossils from the Turonian deposits of the Agua Nueva Formation exploited in the Vallecillo quarry, near Vallecillo town, Nuevo León, Mexico (Blanco-Piñón, 2003; Blanco et al., 2001), was recently suggested by Giersch (2014) as a junior synonymous with the type species of *Rhynchodercetis*, *R. yovanovitchy* Arambourg, 1943. The Giersch's assumption, not yet formally published, reveals that the number of centra and fin rays, as well as the morphometric proportions of the body, head, and jaws of *R. regio* and other *Rhynchodercetis* specimens from Vallecillo, overlap with those recorded in *R. yovanovitchy*. In this work, *R. regio* is renamed as *H. regio* because this Mexican species present the features shared by *H. gracilis* and *H. totonacus* sp. nov. previously mentioned (see Blanco and Alvarado-Ortega, 2006).

Table 3 summarizes the morphological comparison between the nominal species of both dercetid genera reported in Mexico, *Rhynchodercetis* and *Hastichthys*, including those of dubious affinity as *Hastichthys regio,* from the Vallecillo quarry, and the specimens conferred to *Hastichthys gracilis,* from Namoura, originally included into the genus *Rhynchodercetis* (Blanco and Alvarado-Ortega, 2006; Forey et al., 2003). A general glance at this data suggests that some proportions of the body, head, and snout change ontogenetically, as Giersch (2014) noticed in *R. yovanovitchy*; however, to define the range of variation of these proportions it is necessary to study a large fossil sample, a requirement that at the moment is not met in several of the species considered. As Forey et al. (2003) concluded, the values of the characters considered on the single specimen of *H. gracilis* are remarkably close with their corresponding deviations observed in specimens of cf. *Rynchodercetis gracilis* from Namoura. Therefore, it is congruent to consider that these specimens belong to *H. gracilis*; however, it is still necessary to confirm that the specimens from Namoura have the rostrum and mandible ornamented, as it is in *Hastichthys*.

Based on a morphological comparison (Table 3), here it is recognized

Table 3
Comparison among the species of *Hastichthys* (based on data from Goody, 1969; Chalifa, 1989, tbl. 3; Forey et al., 2003, tbl. 63; Blanco and Alvarado-Ortega, 2006, tbl. 1; and the present work).

	Hastichthys totonacus sp.nov.	*Hastichthys regio*	*Hastichthys gracilis*	cf. *H. gracilis* from Namoura (cf. *R. gracilis* in Forey et al., 2003)	*Rynchodercetis yovanovitchi*	*Rynchodercetis hakelensis*	*Rynchodercetis gortanii*
Maximum Standard length	130+	300	370	258	145	100	220
Head length as % SL	37.9	35	28.1	32 (28–35)	39–50	25	25–30
Preorbital length as % SL	29.4	–	19.7	22.9 (19.2–24.8)	28.9	–	–
Preorbital length as % HL	67.4 (65.3–73.4)	75–80	70.1	71.2 (70–80)	60–70	70	–
Mandibular length as % SL	13.9	–	13.5	13.6 (11.8–15.2)	–	–	–
Mandibular length as % HL	37.2 (36.7–37.7)	–	48	41.2 (34.1–48)	–	–	–
First dorsal pterygiophore hypertrophied	Yes	?	Yes	Yes	No	No	No
Interopercle (Present)	Yes	Yes	Yes	Yes	Yes	No	No
Premaxilla and dentary anteriorly ornamented	Yes	Yes	Yes	?	No	No	No
Total vertebrae	59	65	71	73–76	65–67	60	78–80
Abdominal	32	–	44	43–46	–	28	–
(Preural) Caudal	25	–	25	–	25–26	30	≈30
Pectoral rays	11	?	11	10–13	10	10+	10
Pelvic rays	8	?	9	6–7	7–8	7+	8
Dorsal rays	7	?	9	7–10	8	7	8
Anal rays	8	10+	18–19	18–19	6–7	8	16–20

that *Rynchodercetis* and *Hastichthys*, including *H. regio* and *H. totonacus* sp. nov., clearly differ from each other in at least two features. In *Rhynchodercetis* the first dorsal pterygiophore does not have a noticeable anterior extension while in *Hastichthys* this pterygiophore shows a long anterior tape-like expansion (Chalifa, 1989). The opercle series of *Hastichthys* and *Rynchodercetis yovanovitchi* includes the interopercle; contrary, in other species of *Rynchodercetis* this bone is absent. Probably, because of convergent evolution, both genera include short, moderately long, and long species, in which the length of the anal fin also varies. *Hastichthys gracilis* and *R. gortani* have a long trunk with many centra (71–76 and 78–80, respectively) and elongated anal fin (18–19 and 16–20 anal rays respectively). Otherwise, *H. regio* and *R. yovanovitchi* have trunks of intermediate length (with 65 and 35–38 centra, respectively), the last species definitively has a short anal fin with only 6–7 rays while in the first has a longer anal fin with at least 10 rays. Finally, *Hastichthys totonacus* sp. nov. and *R. hakelensis* have the shortest trunks with a low number of total centra (59 and 60, respectively) and short anal fins (with 8 rays).

In the present context, *Hastichthys totonacus* sp. nov. is distinguishable from the other species of *Hastichthys*. After the taxonomical reassignment of *H. regio*, *Hastichthys* is recognized as a diverse fish of the Mexican Late Cretaceous marine deposits. Those dercetid fishes from the Turonian deposits exploited in the Arroyo Las Bocas in Guerrero, southern Mexico, belonging to the Mexcala Formation (Alvarado-Ortega et al., 2006), are extremely fragmentary; however, they can be identified as *Hastichthys* sp. because they exhibit the diagnostic features of *Hastichthys*, such as the rostrum and mandible are anteriorly covered with longitudinal and parallel striae and ridges, presence of a prominent posterior process of the pterotic, the mandible is about 50% of the length of the rostrum, the toothed premaxilla, and the cleithrum has a dorsal triangular section (Fig. 10).

4.2. Phylogenetic results

In this research, the relationships of *Hastichthys totonacus* sp. nov. are explored through four analyses that include the suborder Enchodontoidei (Figs. 11 and 12) and were performed as described in the Materials and Methods section (also see Supplements A, B, C). Although all analyses are based on the same data set, one of these essays does not allow to obtain a suitable phylogenetic solution while the other three support the naturalness of the family Dercetidae and the inclusion of this new species within the genus *Hastichthys*, together with its type species *H. gracilis*.

The Standard Maximum Parsimony Analysis (SMPA) is a strict consensus tree of 730 steps obtained from 170 Most Parsimonious Trees (MPTs), which individually have a Total Length (TL) of 465 steps, its

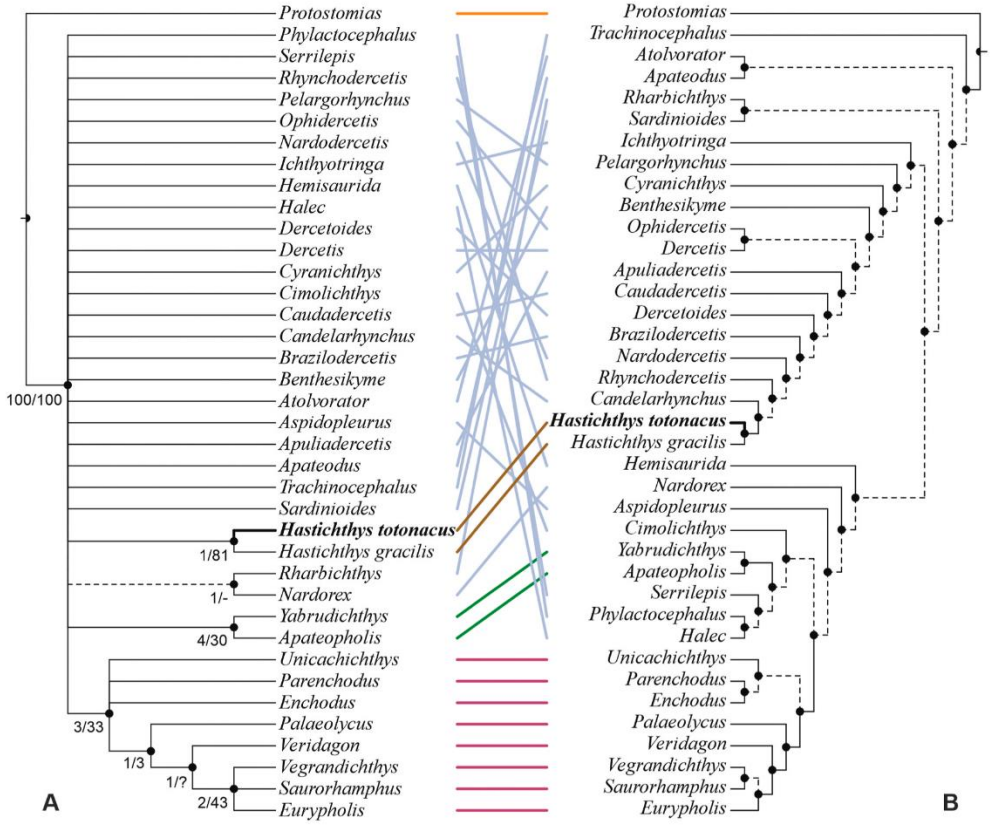

Fig. 11. Tanglegram of the phylogenetic hypotheses of Enchodontoidei. A) Phylogenetic hypothesis of 730 steps of Total Length (TL) obtained from a Strict Consensus of 170 Most Parsimonious Trees (MPTs) resulting from a Standard Maximum Parsimony protocol. B) Phylogenetic hypothesis resulting as a single tree with the Best Score of 22.93615 obtained under Implied Weighted Maximum Parsimony protocol with k = 10. Colored linking lines correspond to the common subtrees found in each reconstruction. Dotted branches show different edges between trees. Red branches show the phylogenetic position of *Hastichthys totonacus* sp. nov. Numbers in each node indicate Bremer/Bootstrap support values.

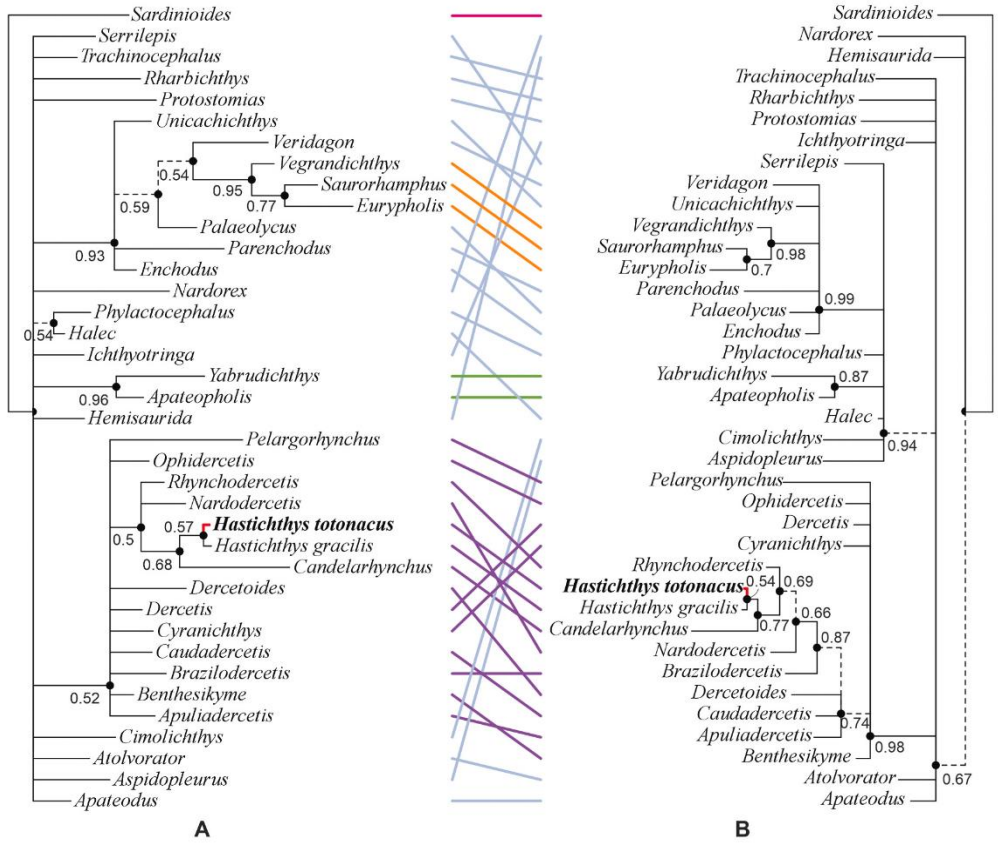

Fig. 12. Tanglegram of the majority rule consensus trees of Enchodontoidei obtained in the Bayesian Inference approach performed in this research. A) Phylogenetic Hypothesis with Equal Rate of character change. B) Phylogenetic Hypothesis with Variable Rate of character change. Colored linking lines correspond to the common subtrees found in each reconstruction. Dotted branches show different edges between trees. Red branches show the phylogenetic position of *Hastichthys totonacus* sp. nov. Numbers by nodes indicate posterior probabilities support values.

Consistency Index (CI) is 0.183, and Retention Index (RI) is 0.144 (Fig. 11A). Supplement C shows a complete description and character mapping of the strict consensus tree based on the common synapomorphies present in all the MPTs. This hypothesis suggests the unnatural condition of the order Enchodontoidei, in which there are three monophyletic groups (*Rharbichthys* + *Nardorex*, *Yabrudichthys* + *Apateopholis,* and family Enchodontidae) are ordered into a huge polytomy that involves all the putative members of the family Dercetidae, other taxa previously excluded from these families (i.e. *Ichthyotringa*, *Aspidopleurus*, *Halec*, *Serrilepis*, *Apatheopholis*, *Cimolichthys*), plus members of the outgroup considered by Silva and Gallo (2011). Here, the family Enchodontidae is supported on an unambiguous synapomorphy, the presence of middorsal scutes between on the predorsal edge of the body (87: 1), as it was previously observed by Vernygora et al. (2018, fig. 9). Although this result challenges the naturalness of the family Dercetidae; we consider this as a mere artifact of the addition of an increasing number of dercetid genera described in the last two decades (8 of those 17 genera in Table 1) within a dataset that has barely incorporated new characters, as well as, the low phylogenetic significance of many of the data included in this and previous phylogenetic essays. This result uncovers the urgent need to review the anatomy of many dercetids and allies.

The single tree generated in the Implied Weighted Maximum Parsimony Analysis (IWMPA) (under k = 10, and Best Score of 22.93615) (Fig. 11B) shows the monophyly Enchodontoidei including *Trachinicephalus* and *Protostomias* and recovers the families Enchodontidae and Dercetidae, in which *Rharbichthys* is the basal member, *Trachinicephalus* + *Protostomias* and *Apateodus* + *Altovorator* constitute an intermediate group, while the most derived group include Dercetidae + *Ichthyotringa* on the one side plus *Hemisaurida*+ (*Nardorex* + *Aspidopleurus*) + (Enchodontidae + the *Cimolichthys-Halec* group). In this hypothesis, the monophyly of the family Dercetidae, including *Pelargorhynchus* as the basal member, could be supported on the presence of the convoluted suture between hypurals 2 and 3 (char. 83:1), as it was previously suggested by Vernygora et al. (2018, Fig. 9); however, such possible synapomorphy is highly ambiguous because the contact between the hypurals 2 and 3 are unknown in different dercetid taxa (i. e. *Candelarhynchus*, *Ophidercetis*, and *Pelargorhynchus*, among others) (see Suppl. C). Contrary to the phylogenetic hypothesis published by Vernygora et al. (2018), in which the character 71-1, presence of reduced neural spines, represents a synapomorphy of Dercetidae plus *Trachinicephalus*, *Protostomias, Apateodus,* and *Altovorator*; in the present IWMPA hypothesis, this character is considered homoplasic after the inclusion of *Ichthyothringa* as the sister group of all dercetids.

Finally, the Bayesian Inference under Equal Rate (BIA-ER) and

Variable Rate of character change (BIA-VR) protocols after reach convergency had a standard deviation of split frequencies of 0.0052 and 0.0054, respectively. These phylogenetic hypotheses have similar majority rule consensus topologies (Fig. 12), which also resemble that of IWMPA. Among these two analyses, the BIA-VR shows higher posterior probabilities support values (Fig. 12A). The probabilistic methods displayed a better performance analyzing a highly homoplasic empirical data set as noted by other authors (Puttick et al., 2019); however, the best-resolved topology (completely dichotomized) correspond to that retrieved by the IWMPA. It is known that this approach normally outperforms the SMPA in different metrics, but it also may find a larger proportion of incorrect groups (Goloboff et al., 2018). In the present study, both IWMPA and the Bayesian Inference analyses are rather in agreement regarding finding Enchodontidae and Dercetidae as monophyletic groups.

5. Conclusions

The present study reveals the unexpected presence of the dercetid genus *Hastichthys* in America, after the description of *Hastichthys totonacus* sp. nov. from the Huehuetla quarry (Figs. 2–9), the generic relocation of *H. regio*, from the Vallecillo quarry that was erected as part of the genus *Rhynchodercetis* (Blanco and Alvarado-Ortega, 2006), and the superficial observation of the one incomplete specimen from the Arroyo Las Bocas quarry (Fig. 10). The fossils studied here exhibit the most outstanding features included in the diagnosis of the genus *Hastichthys* (Taverne, 1991), revealing that during the Turonian the genus *Hastichthys* was a diverse and widespread group of fishes in the epicontinental sea at the southern and tropical region of North America, nowadays Mexico.

According to Giersch (2014) *Rhynchodercetis regio*, here considered as *Hastichthys regio,* is a junior synonymous with *Rhynchodercetis yovanovitchi,* mainly because the proportions of the head, mandible, and rostrum of the former species reported by Blanco and Alvarado-Ortega (2006) are included within the ontogenetical variability observed in the latter. Unfortunately, such a Giersch's idea has not yet been formally published, and currently, it is inconclusive because is based on a few data and unidentified specimens. Today, *Hastichthys* and *Rhynchodercetis* are morphologically remarkably similar and their relationships deserve a deep review, in which the individual and ontogenetical variability of each nominal species must be explored to avoid the possible overestimation of the taxonomic diversity of these fish. Based on the actual knowledge of these genera, *Hastichthys totonacus* sp. nov. displays enough distinctive features to be considered as a new species.

The phylogenetic analyses previously published by Gallo et al. (2005), Silva and Gallo (2011) and later by Vernygora et al. (2018) already showed weakly supported results, which to some degree contrast with those obtained in the present investigation. Although the Standard Maximum Parsimony Analysis performed here yields unexpected results, where the family Dercetidae turns out to be an unnatural clade (Fig. 11A); a deeper exploration of the morphological data is available, through the Implied Weighted Maximum Parsimony and Bayesian Inference Analyses (Figs. 11B and 12), which recognizes the monophyly of this family with *Hastichthys totonacus* sp. nov. included. These results are an urgent call to review all the species now considered as part of the family Dercetidae, to generate a robust hypothesis. Aware of this situation, the authors of this work are working on the recovery and studying of Mexican fossil fishes of the suborder Enchodontoidei.

Author statement

Jesus Alvarado-Ortega and Jesús Alberto Díaz-Cruz. Both authors contributed equally to this work: conceptualization, material preparation, methodology, formal analyses, resources, writing and review-editing.

Declaration of competing interest

The authors declare that they have no known competing financial interests or personal relationships that could have appeared to influence the work reported in this paper.

Acknowledgments

The authors thank Félix Aranguthy and his father Ranulfo, who kindly donated the fossils studied here. Juan Miguel Contreras and Kleyton Cantalice help us with the photographs of this work. Kleyton Cantalice, Oksana Vernygora, and an anonymous reviewer gave us valuable observations that deeply improved this work. UNAM provided the financial support for this manuscript through the grant DGAPA-PAPIIT IN110920. CONACyT provided additional financial support through the individual grant 632640 to JADC.

Appendix A. Supplementary data

Supplementary data related to this article can be found at https://doi.org/10.1016/j.jsames.2020.102900.

References

Agassiz, L., 1833. *Recherches sur les Poissons fossils.* Tomes II, Neuchâtel et Soleure, Petitpierre [this work has traditionally been cited as part of a collection of five volumes dated as "1833-1843", or individually as "1843" based on the preface signed 1843; however, according to own author, pp. 281–304 the Tome II of this collection appeared in 1833 and the version published in 1843 only differs in the inclusion of the section "Additions et corrections" between.

Agassiz, L., 1835. Recherches sur les Poissons fossils. Tome V. Petitpierre, Neuchâtel and Soleure (dated as 1833-1843, with a preface of 1843). [Traditionally, this work has been cited as part of a collection with five-volumes dated as "1833-1843". Also, this work has been individually dated as "1843", based on the preface signed by L. Agassiz in 1843; however, Woodward, (1901, p. 190) cites this book as "Poiss. Foss., Feuill. 1835" and Bücker, p. 538.

Alvarado-Ortega, J., Porras-Múzquiz, H.G., 2012. The first American record of *Aspidopleurus* (Teleostei, Aulopiformes), from La Mula quarry (Turonian), Coahuila state, Mexico. Rev. Bras. Palaontol. 15 (3), 251–263.

Alvarado-Ortega, J., Cantalice, S.K.M., Barrientos-Lara, J.I., Díaz-Cruz, J.A., Than-Marchese, B.A., 2019. The Huehuetla quarry, a Turonian deposit of marine vertebrates in the Sierra Norte of Puebla, central Mexico. Palaeontol. Electron. 22 (1), 1–20. https://doi.org/10.26879/921.

Alvarado-Ortega, J., Cantalice, K.M., Díaz-Cruz, J.A., Castañeda-Posadas, C., Zavaleta-Villareal, V., 2020a. Vertebrate fossils from the San José de Gracia quarry, a new Late Cretaceous marine fossil site in Puebla, Mexico. Bol. Soc. Geol. Mex. 72 (1), 1–21. https://doi.org/10.18268/BSGM2020v72n1a160819.

Alvarado-Ortega, J., Cantalice, K.M., Martínez-Melo, A., García-Barrera, P., Than-Marchese, B.A., Díaz-Cruz, J.A., Barrientos-Lara, J.I., 2020b. Tzimol, a Campanian marine paleontological site of the angostura formation near Comitán, Chiapas, southeastern Mexico. Cretac. Res. 107, 104279. https://doi.org/10.1016/j.cretres.2019.104279.

Alvarado-Ortega, J., Garibay-Romero, L.M., Blanco-Piñón, A., González-Barba, G., Vega-Vera, F.J., Centeno-García, E., 2006. Los peces fósiles de la Formación Mexcala (Cretácico Superior) en el Estado de Guerrero, México. Rev. Bras. Palaontol. 9, 261–272.

Arambourg, C., 1943. Note préliminaire sur quelques Poissons fossiles nouveaux. Bull. Soc. Geol. Fr. 5, 281–288.

Arambourg, C., 1954. Les Poissons cretaces du Jebel Tselfat (Maroc). Notes et Memoires, Service des Mines et de la Carte Geologique du Maroc 118, 1–188.

Ayres, D.L., Darling, A., Zwickl, D.J., Beerli, P., Holder, M.T., Lewis, P.O., Huelsenbeck, J.P., Ronquist, F., Swofford, D.L., Cummings, M.P., Rambaut, A., Suchard, M.A., 2012. BEAGLE: an application programming interface and high-performance computing library for statistical phylogenetics. Syst. Biol. 61 (1), 170–173.

Baldwin, C.C., Johnson, G.D., 1996. Interrelationships of Aulopiformes. In: Stiassny, M. L., Parenti, L.R., Johnson, G.D. (Eds.), Interrelationships of Fishes. Academic Press, pp. 255–404.

Berg, L.S., 1937. A classification of fish-like vertebrates. Bulletin de l'Académie des Sciences de l'URSS, Classe des Sciences mathématiques et naturelles 4, 1277–1280.

Blanco, A., Alvarado-Ortega, J., 2006. *Rhynchodercetis regio*, sp. nov., a dercetid fish (Teleostei: Aulopiformes) from Vallecillo, Nuevo León state, northeastern Mexico. J. Vertebr. Paleontol. 26 (3), 552–558.

Blanco, A., Cavin, L., 2003. New Teleostei from the Agua Nueva Formation (Turonian), Vallecillo (NE Mexico). Comptes Rendus Palevol 2, 299–306. https://doi.org/10.1016/S1631-0683(03)00064-2.

Blanco, A., Alvarado-Ortega, J., Gallo, V., 2008. *Robertichthys riograndensis* from the lower Turonian (Upper Cretaceous) Vallecillo lagerstätte, NE-Mexico: description and relationships. In: Arratia, G., Schultze, H.-P., Wilson, M.V.H. (Eds.), Mesozoic

Fishes 4 – Homology and Phylogeny. Verlag Dr. Friedrich Pfeil, Munich, pp. 389–397.
Blanco, A., Stinnesbeck, W., López-Oliva, J.G., Frey, E., Adatte, T., González, A.H., 2001. Vallecillo, Nuevo León: una nueva localidad fosilífera del Cretácico Tardío en el noreste de México. Rev. Mex. Ciencias Geol. 18, 186–199.
Blanco-Piñón, A., 2003. Peces Fósiles de la Formación Agua Nueva (Turoniano) en el Municipio de Vallecillo, Nuevo León, NE-México. Unpublished PhD Thesis, Universidad Autónoma de Nuevo León, Linares, Nuevo León, México.
Blanco-Piñón, A., Alvarado-Ortega, J., 2005. New dercetid fish (Aulopiformes: Teleostei) from the early Turonian of Vallecillo, NE Mexico. In: Poyato-Ariza, J. (Ed.), Fourth International Meeting on Mesozoic Fishes – Systematics, Homology, and Nomenclature. Miraflores de la Sierra, Madrid, pp. 43–46.
Blanco-Piñón, A., Alvarado-Ortega, J., Rojas-León, A., Camargo-Cruz, T., 2006. Xilitla, una asociación fosilífera del Cretácico Superior (Turoniano), San Luis Potosí, Mexico Central, X Congreso de la Sociedad Mexicana de Paleontología. México, Ciudad de México, Instituto de Geología, Publicación Especial 5, Universidad Nacional Autónoma de México. Memoria del X Congreso Nacional de Paleontología y libreto guía excursión a Tepexi de Rodríguez, Puebla, p. 25.
Bücker, A., 1835. Neueste literatur. Neues Jahrbuch für Mineralogie, Geognosie, Geologie und Petrefaktenkunde 1835, 538–539.
Capasso, L.L., Abi Saad, P., Taverne, L., 2009. Nursallia tethysensis sp. nov., a new pycnodont fish (Neopterygii: Halecostomi) from the Cenomanian of Lebanon. Bull. Inst. R. Sci. Nat. Belg. Sci. Terre 79, 117–136.
Casier, E., 1965. Poissons fossiles de la serie du Kwango (Congo), vol. 50. Musee Royal de L'Afrique Centrale - Tervuren, Belgique -, pp. 1–64. Annales - Serie IN-8 - Sciences Geologiques.
Chalifa, Y., 1989. Two new species of longirostrine fishes from the early Cenomanian (late Cretaceous) of Ein-Yabrud, Israel, with comments on the phylogeny of the Dercetidae. J. Vertebr. Paleontol. 9, 314–328. https://doi.org/10.1080/02724634.1989.10011765.
Davis, J.W., 1887. The fossil fishes of the Chalk of Mount Lebanon in Syria. Sci. Trans. R. Dublin Soc. 3, 457–636.
Davis, J., 1890. On the Fossil Cretaceous Formation of Scandinavia, vol. 4. Scientifical Transaction Royal Dublin Society, 2ème série, pp. 391–434 (+ plts. xxxviii-xliv).
d'Erasmo, G., 1946. L'ittiofauna cretacea dei dintorni di Comeno nel Carso Triestino. Atti della Regia Accademia delle Scienze fisiche e matematiche della Societ a Reale di Napoli, Serie 3 (8), 1–134.
Díaz-Cruz, J.A., Alvarado-Ortega, J., Carbot-Chanona, G., 2016. The Cenomanian short snout enchodontid fishes (aulopifomes, Enchodontidae) from Sierra Madre formation, Chiapas, southeastern Mexico. Cretac. Res. 65, 136–150. https://doi.org/10.1016/j.cretres.2015.12.026.
Díaz-Cruz, J.A., Alvarado-Ortega, J., Carbot-Chanona, G., 2019a. *Dagon avendanoi* gen. And sp. nov., an early Cenomanian Enchodontidae (Aulopiformes) fish from the el Chango quarry, Chiapas, southeastern Mexico. J. S. Am. Earth Sci. 91, 272–284.
Díaz-Cruz, J.A., Alvarado-Ortega, J., Carbot-Chanona, G., 2019b. Corrigendum to" *Dagon avendanoi* gen. And sp. nov., an early Cenomanian Enchodontidae (Aulopiformes) fish from the el Chango quarry, Chiapas, southeastern Mexico"[J. South Am. Earth Sci. 91 (2019) 272-284]. J. S. Am. Earth Sci. 95, 102314.
Díaz-Cruz, J.A., Alvarado-Ortega, J., Giles, S., 2020. A long snout enchodontid fish (Aulopiformes: Enchodontidae) from the Early Cretaceous deposits at the El Chango quarry, Chiapas, southeastern Mexico: a multi-approach study. Palaeontol. Electron. 23 (2), a30. https://doi.org/10.26879/1065.
Dixon, F, 1850. The Geology and Fossils of the Tertiary and Cretaceous Formations of Sussex.. Longman, Brown, Green and Longmans, p. 422.
Figueiredo, F. J. de, Gallo, V., 2006. A new dercetid fish (Neoteloesti: Aulopiformes) from the Turonian of the pelotas basin, southern Brazil. Palaeontology 49, 445–456.
Forey, P.L., Yi, L., Patterson, C., Davies, C.E., 2003. Fossil fishes from the Cenomanian (upper Cretaceous) of Namoura, Lebanon. J. Syst. Palaeontol. 1, 1–227. https://doi.org/10.1017/S147720190300107X.
Gallo, V., Figueiredo, F.D., Silva, H.D., 2005. Análise Filogenética Dos Dercetidae (Teleostei, Aulopiformes), vol. 63. Arquivos do Museu Nacional, Rio de Janeiro, pp. 329–352.
Galili, T., 2015. Dendextend: an R package for visualizing, adjusting and comparing trees of hierarchical clustering. Bioinformatics 31 (22), 3718–3720. https://doi.org/10.1093/bioinformatics/btv428.
Gill, T., 1861. Catalogue of the fishes of the eastern coast of North America, from Greenland to Georgia. Proc. Acad. Nat. Sci. Phila. 13, 1–63.
Giersch, S., 2014. Die Knochenfische der Oberkreidezeit in Nordostmexiko: Beschreibung, Systematik, Vergesellschaftung, Paläobiogeographie und Paläoökologie. Doctoral dissertation, Ruprecht-Karls-Universität Heidelberg, Heidelberg, Germany.
Goloboff, P.A., Catalano, S.A., 2016. TNT version 1.5, including a full implementation of phylogenetic morphometrics. Cladistics 32, 221–238. https://doi.org/10.1111/cla.12160.
Goloboff, P.A., Torres, A., Arias, J.S., 2018. Weighted parsimony outperforms other methods of phylogenetic inference under models appropriate for morphology. Cladistics 34 (4), 407–437. https://doi.org/10.1111/cla.12205.
Goody, P.C., 1969. The relationships of certain Upper Cretaceous Teleosts with special reference to the Myctophids. Bull. Br. Mus. Nat. Hist. Hist. 7, 1–255.
Gosline, W.A., Marshall, N.B., Mead, G.W., 1966. Iniomi: characters and synopsis of families. Volume 5, part 1. In: Böhlke, E. (Ed.), Fishes of the Western Atlantic. Memoirs of the Sears Foundation for Marine Research. Sears Foundation for Marine Research, New Haven, pp. 1–18.
Hay, O.P., 1903. On a collection of Upper Cretaceous fishes from Mount Lebanon, Syria, with description of four new genera and nineteen new species. Bull. Am. Mus. Nat. Hist. 19, 395–452.
Johnson, R.K., 1982. Fishes of the families Evermannellidae and Scopelarchidae: systematics, morphology, interrelationships, and zoogeography. Fieldiana - Zool. 12, 1–252.
Johnson, G.D., 1992. Monophyly of the euteleostean clades: Neoteleostei, Eurypterygii, and Ctenosquamata. Copeia 8–25.
Jordan, D.S., 1905. A Guide to the Study of Fishes, vol. 2. Henry Holt and Company, New York.
Latreille, P.A., 1829. Tome V. Suite et fin des insectes. In: Cuvier, G. (Ed.), Le règne animal distribué d'après son organisation, pour servir de base à l'histoire naturelle des animaux et d'introduction à l'anatomie comparée, avec figures dessinées d'après nature. Nouvelle édition, revue et augmentée. Déterville, Paris, pp. 17–20.
Leidy, J., 1857. Remarks on *saurocephalus* and its allies. Trans. Am. Phil. Soc. 11, 91–95.
Nelson, J.S., 1994. Fishes of the World. Wiley & Sons, New York John.
Patterson, C., Johnson, G.D., 1995. The intermuscular bones and ligaments of teleostean fishes. Smithsonian Contrib. Zool. 559, 1–85.
Pictet, F.-J., 1850. Description de quelques Poissons fossiles du Mont Liban. Jules-Guillaume Fick, Genève, p. 59.
Pictet, F.-J., Humbert, A., 1866. Nouvelles recherches sur les poissons fossiles du Mont Liban. Chez Georg, Paris, p. 114.
Puttick, M.N., O'Reilly, J.E., Pisani, D., Donoghue, P.C., 2019. Probabilistic methods outperform parsimony in the phylogenetic analysis of data simulated without a probabilistic model. Palaeontology 62 (1), 1–17. https://doi.org/10.1111/pala.12388.
Rambaut, A., Drummond, A.J., Xie, D., Baele, G., Suchard, M.A., 2018. Posterior summarization in Bayesian phylogenetics using Tracer 1.7. Syst. Biol. 67 (5), 901–904. https://doi.org/10.1093/sysbio/syy032.
Ronquist, F., Teslenko, M., Van Der Mark, P., Ayres, D.L., Darling, A., Hohna, S., Huelsenbeck, J.P., 2012. MrBayes 3.2: efficient bayesian phylogenetic inference and model choice across a large model space. Syst. Biol. 61 (3), 539–542. https://doi.org/10.1093/sysbio/sys029.
Rosen, D.E., 1973. Interrelationships of higher euteleosteans fishes. In: Greenwood, P.H., Miles, R.S., Patterson, C. (Eds.), Interrelation of Fishes. Zoological Journal of the Linnean Society, London, pp. 397–513.
Signeux, J., 1954. - Notes paléoichthyologiques (suite). IV. *Leptotrachelus nouveau* du Sénonien de Sahel alma (liban). Bulletin du Muséum national d'Histoire naturelle, série 2, fasc 5 (26), 642–645.
Silva, H.M.A., Gallo, V., 2011. Taxonomic review and phylogenetic analysis of enchodontoidei (Teleostei: Aulopiformes). An. Acad. Bras. Cienc. 83 (2), 483–511. https://doi.org/10.1590/S0001-37652011000200010.
Taverne, L., 1987. Ostéologie de *Cyranichthys ornatissimus* nov. gen. du Cénomanien du Zaire et de *Rhynchodercetis yovanovitchi* du Cénomanien de l'Afrique du Nord. Les relations intergeneriques et la position systématique de la famille neocrétacique marine des Dercetidae (Pisces, Teleostei). Annales du Musée Royal de l'Afrique Centrale, Tervuren, Rapport Annuel 93–112.
Taverne, L., 1991. New considerations on the osteology and phylogeny of the Cretaceous marine teleost family Dercetidae. Biol. Jaarb. Dodonaea 58, 94–112.
Taverne, L., 2005a. Les Poissons crétacés de Nardò. 22°. *Nardodercetis vaudewallei* gen. et sp. nov. (Teleostei, Aulopiformes, Dercetidae). Boll. del Mus. Civico Storia Nat. Verona Geol. Paleontol. Preistoria 29, 81–93.
Taverne, L., 2005b. Les Poissons crétacés de Nardò. 21°. *Ophidercetis italiensis* gen. et sp. nov. (Teleostei, Aulopiformes, Dercetidae). Une solution ostéologique au problème des genres *Dercetis* et *Benthesikyme* (= *Leptotrachelus*). Boll. del Mus. Civico Storia Nat. Verona Geol. Paleontol. Preistoria 29, 55–79.
Taverne, L., 2006a. Les Poissons crétacés de Nardò. 23°. *Apuliadercetis tyleri* gen. et sp. nov. (Teleostei, Aulopiformes, Dercetidae). Boll. del Mus. Civico Storia Nat. Verona Geol. Paleontol. Preistoria 30, 11–27.
Taverne, L., 2006b. Les Poissons crétacés de Nardò. 24°. *Caudadercetis bannikovi* gen. et sp. nov. (Teleostei, Aulopiformes, Dercetidae). Considérations sur la phylogénie des Dercetida. Boll. del Mus. Civico Storia Nat. Verona Geol. Paleontol. Preistoria 30, 27–48.
Taverne, L., 2008. Les Poissons crétacés de Nardò. 27°. *Leccedercetis longirostris* gen. et sp. nov. (Teleostei, Aulopiformes, Dercetidae). Boll. del Mus. Civico Storia Nat. Verona Geol. Paleontol. Preistoria 32, 3–8.
Taverne, L., 2013. Les Poissons du Santonien (Crétacé supérieur) d'Apricena (Italie du Sud). 5. *Nardodercetis garganoi* sp. nov. (Teleostei, Aulopiformes, Dercetidae). Boll. del Mus. Civico Storia Nat. Verona Geol. Paleontol. Preistoria 37, 67–72.
Taverne, L., Goolaerts, S., 2015. The dercetid fishes (Teleostei, Aulopiformes) from the Maastrichtian (late Cretaceous) of Belgium and The Netherlands. Geol. Belg. 18, 21–30.
Vernygora, O., Murray, A.M., Luque, J., Ruge, M.L.P., Fonseca, M.E.P., 2018. A new Cretaceous dercetid fish (Neoteleostei: Aulopiformes) from the Turonian of Colombia. J. Syst. Palaeontol. 16 (12), 1057–1071. https://doi.org/10.1080/14772019.2017.1391884.
von der Marck, W., 1858. Über einige Wirbeltiere, Kruster und Cephalopoden der westfälischen Kreide. Z. Dtsch. Geol. Ges. 10, 231–271.
von der Marck, W., 1863. Fossile Fische, Krebse und Pflanzen aus dem Plattenkalk der jüngsten Kreide aus Westphalen. Palaeontographica 11, 1–83.
Wallaard, J.J.W., Fraaije, R.H.B., Diependaal, H.J., Jagt, J.W.M., 2019. A new species of dercetid (Teleostei, Aulopiformes) from the type Maastrichtian of southern Limburg, The Netherlands. Neth. J. Geosci. 98, e2. https://doi.org/10.1017/njg.2019.1.
Wang, L.-G., Lam, T.T.-Y., Xu, S., Dai, Z., Zhou, L., Feng, T., Guo, P., Dunn, C.W., Jones, B.R., Bradley, T., Zhu, H., Guan, Y., Jiang, Y., Yu, G., 2020. Treeio: an R package for phylogenetic tree input and output with richly annotated and associated data. Mol. Biol. Evol. 37 (2), 599–603. https://doi.org/10.1093/molbev/msz240.
White, E.I., Moy-Thomas, J.A., 1940. Notes on the nomenclature of fossil fishes—Part II, Homonyms D–L. Ann. Mag. Nat. Hist. 11 (6), 98–103.

Wilkinson, S.P., Davy, S.K., 2018. Phylogram: an R package for phylogenetic analysis with nested lists. J. Open Source Software 3 (26), 790. https://doi.org/10.21105/joss.00790.

Woodward, A.S., 1901. Catalogue of the Fossil Fishes in the British Museum (Natural History), Part IV. British Museum (Natural History), London, p. 636. https://doi.org/10.5962/bhl.title.61854.

Woodward, A.S., 1903. The fossil fishes of the English Chalk. Part II. Monogr. Palaeontogr. Soc. 57 (266), 57–96 (+ Plates XIV–XX).

CAPÍTULO V: Phylogenetic Morphometrics, Geometric Morphometrics and the Mexican fossils to understand evolutionary trends of Enchodontid fishes

Journal of South American Earth Sciences 111 (2021) 103492

Contents lists available at ScienceDirect

Journal of South American Earth Sciences

journal homepage: www.elsevier.com/locate/jsames

Phylogenetic morphometrics, geometric morphometrics and the Mexican fossils to understand evolutionary trends of enchodontid fishes

Jesús Alberto Díaz-Cruz [a,b,*], Jesús Alvarado-Ortega [b], Marcia M. Ramírez-Sánchez [c], Emma Louise Bernard [d], Lu Allington-Jones [d], Mark Graham [e]

[a] Posgrado en Ciencias Biológicas, Universidad Nacional Autónoma de México, Circuito de la Investigación S/N, Ciudad Universitaria, Delegación Coyoacán, Ciudad de México, 04510, Mexico
[b] Instituto de Geología, Universidad Nacional Autónoma de México, Circuito de la Investigación S/N, Ciudad Universitaria, Delegación Coyoacán, Ciudad de México, 04510, Mexico
[c] Facultad de Ciencias, Universidad Nacional Autónoma de México, Coyoacán, Ciudad de México, 04510, Mexico
[d] Curator Fossil Fish, Department of Earth Sciences. The Natural History Museum, Cromwell Road, London, SW7 5BD, United Kingdom
[e] The Conservation Centre, Core Research Laboratories, The Natural History Museum, Cromwell Road, London, SW7 5BD, United Kingdom

ARTICLE INFO

Keywords:
Fossil aulopiformes
Paleobiogeography
Cope's rule
Phylogeny
Tethys sea

ABSTRACT

Enchodontids were a diverse and abundant fish marine clade that during the Upper Cretaceous became common inhabitants of temperate coastal environments around the world. The recent studies on Mexican enchodontid species have contributed to better understand their evolutionary relationships; however, the phylogenetic significance of the morphological variability of some bones in these fishes is unclear. Here, we explore the morphological variation and the phylogenetic implications that the preopercle, and lower jaw have throughout the geological time; these bones were selected because usually are well-preserved in fossils belonging to the group. Our results indicate that temporally, the enchodontid species herein studied can be divided into two main groups, one present in the early-Upper Cretaceous group and the other in the late-Upper Cretaceous. Additionally, our results indicate that body size in Enchodontidae seems to adjust to the phyletic increase of size or Cope's rule. The shapes of the preopercle and lower jaw of enchodontids are highly variable that it is hard to use these as supra-specific distinctive features. Among these fishes, the most differentiated shapes correspond to those that developed an elongated and shallow lower jaw, and those with preopercles that bear a posteroventral well-developed spine, as in Eurypholinae and *Unicachichthys*. The phylogenetic relationships of enchodontid fishes defined by the configurations of these two skeletal structures provide a glimpse of the biogeographical relationships of the family; however, these patterns should be analyzed considering a most complete and inclusive phylogeny.

1. Introduction

Enchodontids comprise a very diversified group of teleost fishes mainly restricted to the Late Cretaceous. Currently, members of the family Enchodontidae are often distinguished by the possession of some or all of the following characteristics: a row of dorsal scutes placed between the occiput and the origin of the dorsal fin, the presence of anteroventral prongs on lower jaw, and a horizontal strengthening bar on the opercle (Fielitz, 2004; Silva and Gallo, 2011; Vernygora et al., 2018; Díaz-Cruz et al., 2020). From the Barremian up to early Eocene, it is possible to find isolated teeth and fragmentary material, potentially assigned to enchodontids (Rana, 1990; Kriwet, 2003; Coelho, 2004; Rana et al., 2004; Tewari et al., 2010). However, most complete and exquisitely preserved specimens are commonly found in Upper Cretaceous localities from all over the world (Silva and Gallo, 2011; Cavin et al., 2012; Díaz-Cruz et al., 2019a).

The morphological variation of Enchodontids is extensive and includes species with short and deep bodies, others rather pisciform, and some serpentiform (e.g. Goody, 1969). Chalifa (1996) suggested that the bodies of these fishes were part of two evolutionary trends developed from the pisciform body-plan. In the first tendency, the body becomes shorter as it is seen among Old World species such as *Enchodus lewesiensis*

* Corresponding author. Posgrado en Ciencias Biológicas, Universidad Nacional Autónoma de México, Circuito de la Investigación S/N, Ciudad Universitaria, Delegación Coyoacán, Ciudad de México, 04510, Mexico.
E-mail address: vertebrata.j@ciencias.unam.mx (J.A. Díaz-Cruz).

https://doi.org/10.1016/j.jsames.2021.103492
Received 16 December 2020; Received in revised form 23 July 2021; Accepted 26 July 2021
Available online 29 July 2021

(Mantell, 1822), *E. venator* (Arambourg, 1954), *E. brevis* Chalifa (1989) and *Parenchodus longipterygius* Raab and Chalifa (1987). In the other tendency, the head, trunk, or both were progressively elongated as in *Eurypholis boissieri* Pictet (1850), *Saurorhamphus judeaensis* Chalifa (1985) and *Palaeolycus dreginensis* von der Marck (1863). Díaz-Cruz et al. (2019b), observed that the tendencies of body shape variation in enchodontids show five different patterns: longirostrine head and elongated trunk such as in *Saurorhamphus*; pug-nose head with a noticeably short trunk as *Parenchodus*; pug-nose head and elongate body as *Palaeolycus*; pug-nose and pisciform trunk as in *Enchodus* and *Unicachichthys*; and moderate longirostrine head with a pisciform trunk as *Eurypholis*. All these conditions result in a complex and rich pattern of body shape variation.

The inclusion of the morphological variation displayed by enchodontids in a phylogenetical framework is a challenging task. Fielitz (2004) was the first to propose a phylogenetic hypothesis of the evolutionary relationships of Enchodontidae and other Aulopiform fossils. Later, Silva and Gallo (2011) performed a phylogenetic assay of the fossil forms of the suborder Enchodontoidei *sensu* Nelson (1994). Both analyses recovered Enchodontidae as a natural group but the synapomorphies supporting this clade were different; the first hypothesis proposed that the absence of interopercle and the presence of a single dermopalatine tooth, while in the latter, the presence of dorsal scutes is the single synapomorphy.

The addition of recently discovered taxa into the proposed phylogenetical hypotheses of Enchodontidae has enriched the knowledge of morphology within the group, to such a degree that new hypotheses of primary homology have been added and others reinterpreted. One of the most important changes was made by Holloway et al. (2017) that included characters proposed by Silva and Gallo (2011) in the phylogenetical hypotheses of Fielitz (2004). Soon after this work, it was noticed that some of these characters were, in a certain sense, duplicated of some of the original ones, and a new proposal was made by Díaz-Cruz et al. (2020). One of these characters is related to the shape of the preopercle, a highly variable bone difficult to discretize, which makes it prone to bias. Also, authors of this work, JAO, and JADC noticed that the lower jaw in Enchodontidae displays a highly variable pattern comparable to that of the preopercle which may be important in portraying the taxonomic groups of the family. To characterize the variation of these bones, this paper uses Phylogenetic morphometrics (PM) and Geometric Morphometrics (GM), to assess their relationship among the members of the family and recognize the contribution of the Mexican species to the knowledge of the anatomical morphology of Enchodontidae.

2. Material and methods

2.1. Institutional abbreviations

IHNFG, Instituto de Historia Natural –Fósil, Geográfico–, Museo de Paleontología "Eliseo Palacios Aguilera", Chiapas, México. **MSNT,** Museo Civico di Storia Naturale, Trieste, Italy. **NHMUK**, Natural History Museum, London, United Kingdom. **GMWWU**, Geomuseum der WWU, Münster. **UAHMP,** Museo de Paleontología, Centro de Investigaciones Biológicas, Universidad Autónoma del Estado de Hidalgo.

2.2. Comparative materials examined

The following specimens were studied for comparative purposes. *Cimolichthys lewesiensis* Leidy (1857): NHMUK PV P 5491 from the Cenomanian-Turonian of the English Chalk, England. *Enchodus gracilis* (von der Marck, 1858): GMWWU 8498 from the Upper-Senonian deposits of Sendenhorst, Warendorf, North Rhine-Westphalia, Germany. *Enchodus lewesiensis* (Mantell, 1822): NHMUK P 73992, NHMUK PV OR 4184, and NHMUK PV P 5415 from the Cenomanian-Turonian deposits of Lewes, East Sussex, United Kingdom. *Enchodus marchesettii* (Kramberger, 1895) NHMUK PV OR 4748, from the Cenomanian deposits of Hakel, Lebanon. *Enchodus mecoanalis* Forey et al. (2003): NHMUK PV P.63250 (paratype) from the Middle Cenomanian deposits of Namoura, Lebanon.

Enchodus petrosus (Cope, 1874): NHMUK PV P. 9647 from the Upper Cretaceous deposits of Kansas, United States. *Enchodus zimapanensis* Fielitz and González-Rodríguez (2010): UAHMP 679 (holotype) the Albian-Cenomanian deposits of Zimapán, Hidalgo, Mexico. *Eurypholis boissieri* Pictet (1850): NHMUK PV P.49479, from the Middle Cenomanian deposits of Namoura, Lebanon. *Palaeolycus dreginensis* von der Marck (1863): GMWWU 8438 from the Upper-Senonian deposits of Sendenhorst, Warendorf, North Rhine-Westphalia, Germany. *Saurorhamphus freyeri* Heckel (1850): MSNT 7811 from the Middle-Upper Cenomanian deposits of Komen, Slovenia. *Unicachichthys multidentata* Díaz-Cruz et al. (2016): IHNFG-2988 from the early Cenomanian deposits of the El Chango quarry, Chiapas, Mexico. *Veridagon avendanoi* (Díaz-Cruz et al., 2019a, 2019b, 2019b): IHNFG-5816 (holotype) from the early Cenomanian deposits of the El Chango quarry, Chiapas, Mexico. *Vegrandichthys coitecus* Díaz-Cruz et al. (2020): IHNFG-5927 (holotype) from the early Cenomanian deposits of the El Chango quarry, Chiapas, Mexico. Additionally, other comparative materials reviewed based on their original publications were: *Enchodus brevis* Chalifa (1989) (Chalifa, 1989:359, Fig. 2), *Enchodus faujasi* Agassiz (1843) (Friedman, 2012:127, Fig. 3C), and *Parenchodus longipterygius* Raab and Chalifa (1987) (Raab and Chalifa, 1987:720, 722, Figs. 3 and 4). Lastly, information of *Enchodus dirus* (Leidy, 1857) and *Enchodus gladiolus* (Cope, 1872), was taken from the Oceans of Kansas website (Everhart, 2020).

2.3. Landmark acquisition and digitalization

The structures analyzed were the lower jaw and the preopercle. These structures were either directly photographed or images obtained from their original publication, according to the information mentioned in the previous section. For the preopercle, a total of three landmarks of type II and 17 of type III [see (Palci and Lee, 2019)] were placed, while the lower jaw was represented with tree landmarks of type II and 20 of type III following the element contour. The definition of the semi-landmarks type II and placement of the semi-landmark can be accessed in.Appendix A Line templates were drawn over each photograph/image with the IMP tool MakeFan 8 (Sheets, 2014) to optimize points digitization. The digitalization was performed in tpsDig2 v2.16 (Rohlf, 2010a) using the scale factor tool to set the scale for each image. For the preopercle, a total of three landmarks of type II and 17 of type III were placed, while the lower jaw was represented with three landmark of type II and 20 of type III following the structure contour (see Appendix B). The digitalization procedure was repeated twice by the same observer on different days to evaluate landmark measurement error with the R package geomorph (Adams and Otárola-Castillo, 2013).

2.4. Phylogenetic morphometric (PM) analysis and temporal calibration

The tps files produced in tpsDig2 were imported in TNT 1.5 (Goloboff and Catalano, 2016), merged (see Appendix B), and posteriorly analyzed with the same software to explore the phylogenetic relationships expressed by the two landmarks configurations. Phylogenetic analysis was conducted according to the following parameters: default standardization among configurations (*lmark fact* = *), RFTRA superimposition method for both configurations because this procedure is less prone to the Pinocchio effect, since it does not account for interdependence between landmark displacement, and so, there is no overall change of shapes (Palci and Lee, 2019), using *Cimolichthys* as reference taxon, and modifying the configuration size (lmreal rftra [0]!/0 1). The designated outgroup was *Cimolichthys*, previously considered as close relative of Enchodontidae (Fielitz, 2004; Davis and Fielitz, 2010). The search strategy followed a heuristic (traditional search), using random addition sequences, tree bisection reconnection (TBR) as branch

swapping algorithm, holding one tree per replicate and 1000 runs (mult = ras tbr hold 1 rep 1000). The tree thus obtained was time-calibrated using the R package strap (Bell and Lloyd, 2015) according to the locality ages presented in Table 1 and the International Chronostratigraphic Chart 2019. In addition to the PM morphometrics analysis, the phylogenetic hypothesis of Enchodontidae from Díaz-Cruz et al. (2020) based on discrete characters under the Maximum Parsimony approach was updated incorporating *Enchodus mecoanalis* information. This analysis was performed with the same parameters stated by the authors.

2.5. Geometric Morphometric (GM) analyses

The tps files produced in tpsDig2 were also used to perform GM analyses independently; however, in these analyses *Cimolichthys* was excluded. Each file was loaded in tpsRelw 1.49 (Rohlf, 2010b), and superimposition of landmarks and semi-landmarks conducted through the chord-min d2 slide method. In this software, the Relative Warp score matrix was obtained after performing a Relative Warp analysis. The score matrix was posteriorly loaded in Past 4.03 (Hammer et al., 2001) to display the explanatory method of Principal Component Analysis and visualize the shape variation among superimposed configurations. In the same software, a phenogram employing the clustering method UPGMA (Unweighted Pair Group Method with Arithmetic Mean) was built using the score matrix to assess the morphological similarity of the configurations.

Table 1
Nominal species considered in the phylogenetic analyses performed in this work. The references support the descriptions of the species and/or recent geological studies dating the outcrops.

Taxa	Locality and Age	References
Cimolichthys	Chalk group, England; Cenomanian-Turonian boundary.	Friedman et al., (2015).
Enchodus brevis	Ein-Yabrud, Jerusalem; Lower Cenomanian.	Chalifa, (1989).
E. dirus	Pierre-Shale group, South Dakota; Santonian-Maastrichtian.	Parris et al., (2007).
E. faujasi	Maastricht Formation, ? Maastricht area, the Netherlands	Friedman, (2012).
E. from Gavdos	Gavdos, Greece; Middle to Late Maastrichtian.	Cavin et al., (2012).
E. gladiolus	Pierre-Shale group, South Dakota; Santonian-Maastrichtian.	Parris et al., (2007).
E. gracilis	Sendenhorst, Westphalia, Germany; Upper Campanian.	Fielitz (2004); Dietze (2009).
E. lewesiensis	Chalk group, England; Cenomanian-Turonian boundary.	Friedman et al., (2015).
E. marchesettii	Hakel, Lebanon; Middle Cenomanian.	Goody (1969); Fielitz (2004).
E. mecoanalis	Namoura, Lebanon; Middle Cenomanian.	Forey et al., (2003).
E. petrosus	Pierre-Shale group, South Dakota; Coniacian-Maastrichtian.	Parris et al., (2007).
E. venator	Jbel Tselfat, Morocco; Cenomanian-Turonian boundary.	Khalloufi et al., (2010).
E. zimapanensis	Muhi, Mexico; Albian-Cenomanian.	Fielitz and González-Rodríguez, (2010).
Eurypholis boissieri	Namoura, Hekel and Hajula; Lebanon; Middle Cenomanian.	Goody (1969); Forey et al. (2003).
Palaeolycus dreginensis	Sendenhorst, Westphalia, Germany; Upper Campanian	Fielitz (2004); Dietze (2009); Davis and Fielitz (2010).
Parenchodus longipterygius	Givat-Shaul, Jerusalem; Upper Cenomanian.	Raab and Chalifa, (1987).
Saurorhamphus freyeri	Trieste-Komen, Slovenia; Middle-Late Cenomanian.	Goody (1969); Palci et al. (2008).
Unicachichthys multidentata	El Chango, Chiapas, Mexico; Early Cenomanian.	Díaz-Cruz et al., (2016).
Veridagon avendanoi	El Chango, Chiapas, Mexico; Early Cenomanian.	Díaz-Cruz et al., 2019a, 2019b.
Vegrandichthys coitecus	El Chango, Chiapas, Mexico; Early Cenomanian.	Díaz-Cruz et al., (2020).

3. Results

3.1. Phylogenetic morphometrics

The phylogeny based on the two landmark configurations is shown in Fig. 1, and the best score is 6.31040. In this hypothesis, *Enchodus zimapanensis*, *Vegrandichthys*, and *Saurorhamphus* are placed in the base of the Enchodontidae from which they branch sequentially. The first two species are among the oldest enchodontid species; these taxa possess a shallow and elongated lower jaw and their preopercle ventral limb is slightly expanded anteroposteriorly. Branching immediately after the two species mentioned above is *Saurorhamphus*; this taxon also exhibits an elongated lower jaw and an inverted "T" preopercle. Then, two clades are formed. On one hand, a small clade including *E. gracilis* (*Eurypholis* (*Unicachichthys* + *E. lewesiensis*)), with species that exhibit a true and well-developed posteroventral spine in the preopercle, such as *Eurypholis* and *Unicachichthys*, and those with a moderate expansion of the preopercular ventral limb such as *Enchodus gracilis*; their lower jaw is rather short and shallow. On the other hand, a bigger clade is formed with the remaining *Enchodus* species plus *Palaeolycus*, *Parenchodus*, and *Veridagon*, where, the lower jaw is deeper than previous clades and the preopercle exhibits different grades of ventral limb expansion and dorsal limb curvatures. This hypothesis shows relationships among members of Enchodontidae markedly different from those recovered by discrete morphological data (see Fig. 1). The temporal calibration of the phylogenetic hypothesis shows, at first glance, two enchodontids groups temporally divided. The first group, from the early-Upper Cretaceous, includes those species with temporal range either restricted to the Cenomanian or reaching the Turonian. The species in this group are *Enchodus brevis*, *E. lewesiensis*, *E. marchesettii*, *E. mecoanalis*, *E. venator*, *E. zimapanensis*, *Eurypholis*, *Parenchodus*, *Saurorhamphus*, *Unicachichthys*, *Vegrandichthys*, and *Veridagon*. The second group, placed in the late-Upper Cretaceous section, includes species with temporal ranges enclosed from the Coniacian to the Maastrichtian; in this group we can find six *Enchodus* species plus *Palaeolycus*. Among these, the *Enchodus* species gathers *E. dirus*, *E. faujasi*, *E.* from Gavdos, *E. gladiolus*, *E. gracilis*, and *E. petrosus*.

3.2. Geometric morphometric

The first two principal components of the lower jaw explain 68.26% of the observed variation (Fig. 2A). The first component explains 51.58% and the second component 16.68% of the observed variation. Among the patterns found in the lower jaw, the most noticeable is the relative proximity of members of the subfamily Eurypholinae, which includes *Eurypholis*, *Vegrandichthys*, and *Saurorhamphus*, except *Eurypholis*, these taxa exhibit an expanded and very shallow lower jaw. The proximity of these two taxa is even more evident in the similarity phenogram (Fig. 2B), since they are forming a group. Another clear pattern exposed by this analysis reveals that no lower jaw shape is characteristic of the subfamily Enchodontinae, where it can be described as short but ranging in different deep levels. Consequently, the genera *Palaeolycus*, *Parenchodus* and *Veridagon* are even more closely related to most *Enchodus* species than *E. lewesiensis*. This latter pattern is also displayed by the similarity analysis, which shows *E. lewesiensis* closer to the monospecific genus *Unicachichthys*. On the other hand, the first two components of the preopercle PCA explain 64.57% of the cumulated variation (Fig. 2C). The first component explains 46.55% of the observed

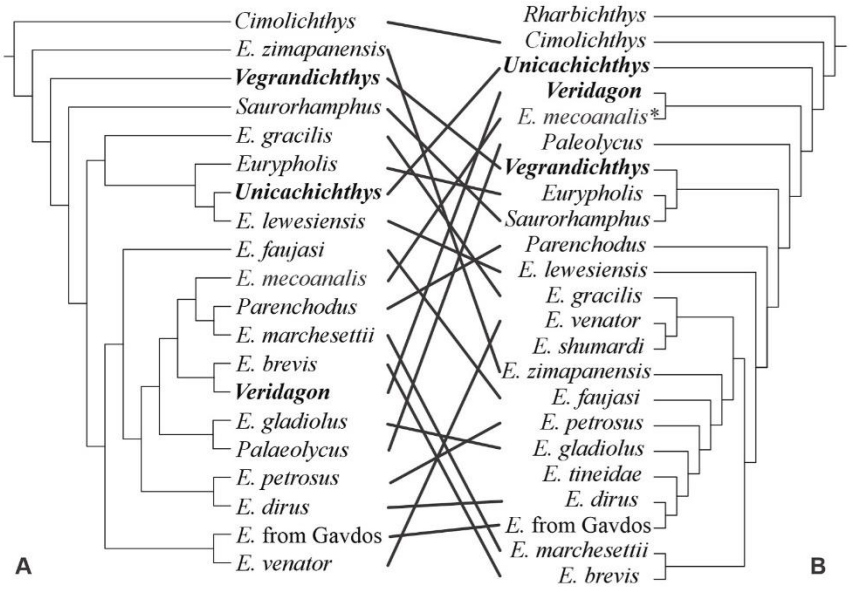

Fig. 1. Tanglegram comparing phylogenetic relationships of Enchodontidae based on two different data sources. A) phylogenetic hypothesis based on two landmark configurations and B) using discrete morphological characters. Mexican species in bold. *A formal analysis of its phylogenetic position is in progress.

variation and 18.02% of observed variation is associated with the second component. The preopercle PCA analysis does not show an evident differentiation pattern in the points cloud, except that the subfamily Enchodontinae, plus *Palaeolycus*, *Veridagon*, and *Vegrandichthys* are closely related on the basis of a preopercle shape with a ventral limb slightly expanded, sometimes exhibiting a small posterior spine of even an entire and straight posterior border. The most differentiated taxa are *Eurypholis*, *Saurorhamphus*, and *Unicachichthys*, all of them display an expanded ventral limb. Likewise, the similarity analysis reveals that *Eurypholis* and *Unicachichthys* are closely related forming a separated group from the rest of the Enchodontidae members, in these taxa the ventral limb expands posteriorly to form a well-developed spine (Fig. 2D). The comparison of the taxa arrangement between the two phenograms is not congruent; each configuration shows different taxa association. One of the most remarkable things observed in both analyses is that certain *Enchodus* species exhibit more similarity with genera as *Palaeolycus* or *Veridagon* than with other species from the same genus.

3.3. Enchodontidae geographical distribution

Based on the two-landmark configuration phylogeny, the early-Upper Cretaceous enchodontid group encloses 12 species, while the late-Upper Cretaceous group encloses only seven species (Fig. 3). In the first group, species such as *Vegrandichthys* and *Enchodus zimapanensis*, placed in the base of the phylogeny, come from the West realm of the Tethys sea. Branching immediately after the species mentioned above is *Saurorhamphus* from the Central realm of the Tethys. Other species from the early group are those of the monophyletic clade composed of *Enchodus brevis* + *Veridagon* and *E. mecoanalis* (*E. marchessettii* + *Parenchodus*), all these species, except *Veridagon* are restricted to the middle or late Cenomanian and are geographically located in the East realm of the Tethys Sea, modern Middle East localities (Fig. 4). Excepting *Eurypholis boissieri*, which comes from the middle Cenomanian of the East realm of the Tethys Sea, and *Unicachicthys* of the early Cenomanian from the West realm, the remaining species of the early-Upper Cretaceous enchodontids, *E. venator* and *E lewesiensis*, come from localities from the Central realm of the Tethys Sea, and phylogenetically they are recovered in different positions. Noticeably, both species reach the Turonian.

The late-Upper Cretaceous enchodontid group gathers fewer species than the early group. However, the temporal range of this group is wider, since species such as *Enchodus petrosus* extends through four different ages. *E.* from Gavdos and its sister group *E. faujasi* are species not closely related to *E. gracilis*, but geographically each of them came from different localities from the Central realm of the Tethys. The clade integrated by *E. dirus* + *E. petrosus* is recovered as the sister group of the clade *E. gladiolus* + *Palaeolycus*. Excepting *Palaeolycus* that comes from the Central realm of the Tethys, the rest of these species come from the West realm, more specifically, from the northern region of the opened Western Interior sea (Fig. 5).

4. Discussion

4.1. Phylogenetic morphometrics

The phylogenetic relationships among enchodontids members recovered by the two landmark configurations are noticeable different from those recovered by discrete morphological data. (Díaz-Cruz et al., 2020:17 Fig. 8A) found that the phylogenetic analysis of the preopercle configuration of Enchodontidae recovers certain relationships also retrieved by discrete data. In this sense, Catalano et al. (2015) stated that landmark data is not always congruent with phylogenies based on another data source, but the increase of the number of characters, landmark configurations, improves the congruence between phylogenies. The addition of the lower jaw landmark configuration to the analysis did not show an increase in the topology congruence among taxa. Reasons for this may be related to the few mandibular characters included in the discrete morphological data set. Another explanation is that phylogenetic morphometric analysis could be reflecting association in functional morphology such as the strength and speed of the jaw

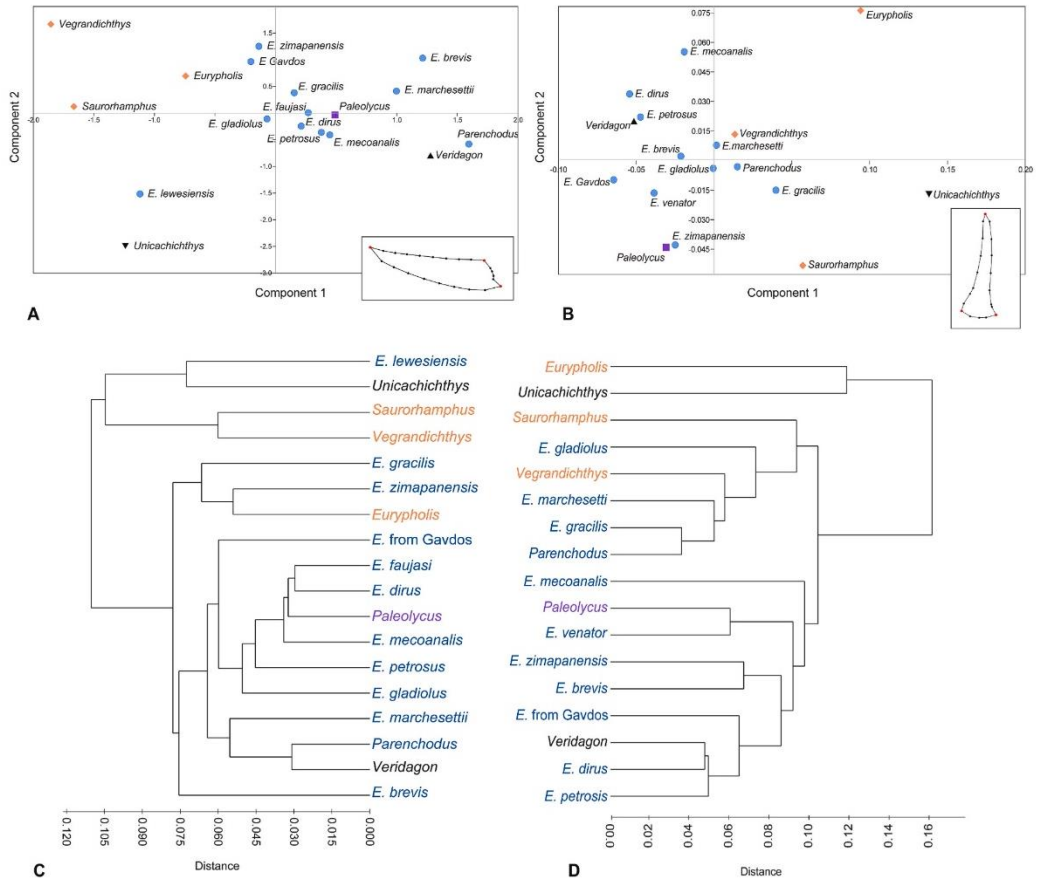

Fig. 2. Assessment of the morphological variation of two landmarks configurations in enchodontid fishes. A) Principal Component Analyses (PCA) of the lower jaw and B) Phenogram showing the lower jaw similarity. C) PCA of the preopercle and D) Phenogram showing the preopercle similarity. Similarity analysis of the species use UPGMA. Members of the subfamily Enchodontinae are in blue dots, while orange diamonds show the Eurypholinae members. Similarity analyses of the species using UPGMA. The colors of terminals in phenograms correspond to those of the PCA diagrams. For practical purposes, only generic names are displayed, except for *Enchodus* species. The extensive species names can be found in Table 1.

closure which has been suggested by landmark based analyses in other fish taxa (Hill et al., 2018). Although discrete and landmarks configuration data are comparable for measuring morphological disparity (Schaeffer et al., 2019), in a phylogenetic framework our data may be reflecting ecomorphology rather than phylogenic signal. In this regard, it seems right to assume variation in the phylogenetic signal contribution according to the landmark configuration being analyzed. Undoubtedly, a deep and thorough study is required.

4.2. Morphological variation in lower jaw and preopercle

Analyzing the lower jaw in members of the subfamily Eurypholinae, we observe that it tends to be expanded and shallow, as in *Saurorhamphus* and *Vegrandichthys*. In *Eurypholis*, this condition is not as clear as the first two taxa, but the anguloarticular posterior edge is leaning forward and the lower jaw is somewhat elongated. Surprisingly, *Enchodus zimapanensis* follows a similar lower jaw shape, the PCA (Fig. 2) suggest this similarity, but it is more evident in the Phylogenetic Morphometric analysis (see Fig. 3), where taxa with an elongated lower jaw are retrieved as sister groups and the basal members of Enchodontidae. The proximity of *Palaeolycus, Parenchodus*, and *Veridagon* with *Enchodus* species revealed by the lower jaw PCA plot and the similarity analysis (Fig. 2A and B) indicates that no particular genus shows a characteristic shape. The similarity of these genera with *Enchodus* is because this genus also contain species with short, and posteriorly deep lower jaw, such as *Enchodus dirus*. This similarity may be attributed to the fact that variation in lower jaw shape is commonly associated with feeding ecology, in this sense, mandibular levers and so mandibular shapes have shown to be extensively convergent in actinopterygians (Westneat, 2004). Generalized features observed in the lower jaw of Enchodontidae are a) the very low or inexistent coronoid process; b) the postarticular process sometimes is either well-developed as displayed by *E. marchesettii* or *E. gladiolus*, or very reduced as *E. brevis* or *Veridagon*; and c) apparently, there is an association between the development of the postarticular process and the modification in the anterior border of the preopercle ventral limb.

The results obtained from the preopercle analysis are quite similar to those of the lower jaw. The preopercle PCA shows the monospecific genera *Palaeolycus*, *Vegrandichthys*, and *Veridagon* as closely related to *Enchodus* species, while the more differentiated taxa are *Unicachichthys*, *Eurypholis*, and *Saurorhamphus* (Fig. 2C and D). The last two genera, although in the points cloud exhibited completely opposed on the basis of a preopercle ventral limb expansion, are recognized as members of Eurypholinae (Fielitz, 2004). The reason why *Eurypholis* and

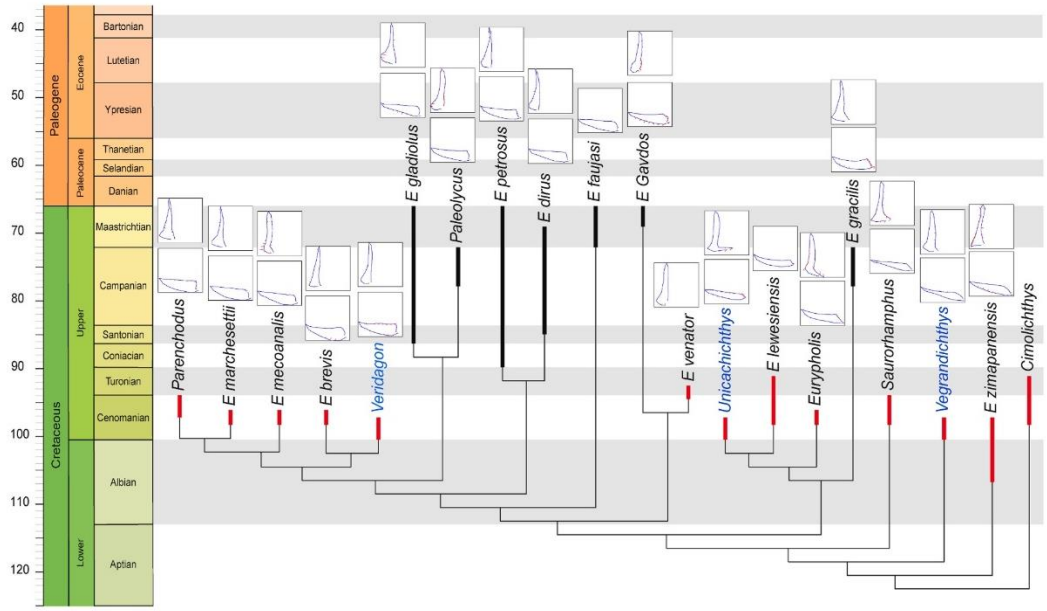

Fig. 3. Time-calibrated phylogenetic relationships among Enchodontidae members using two morphometric configurations. All the terminals correspond to the species named in Table 1. Terminals in blue show the Mexican species. Above terminals, the landmark configurations analyzed by each species are placed. Thick bars exhibit the temporal range per species. Red temporal ranges, except *Cimolichthys*, indicate the early-Upper Cretaceous enchodontid group, while the black temporal range shows the late-Upper Cretaceous enchodontid group.

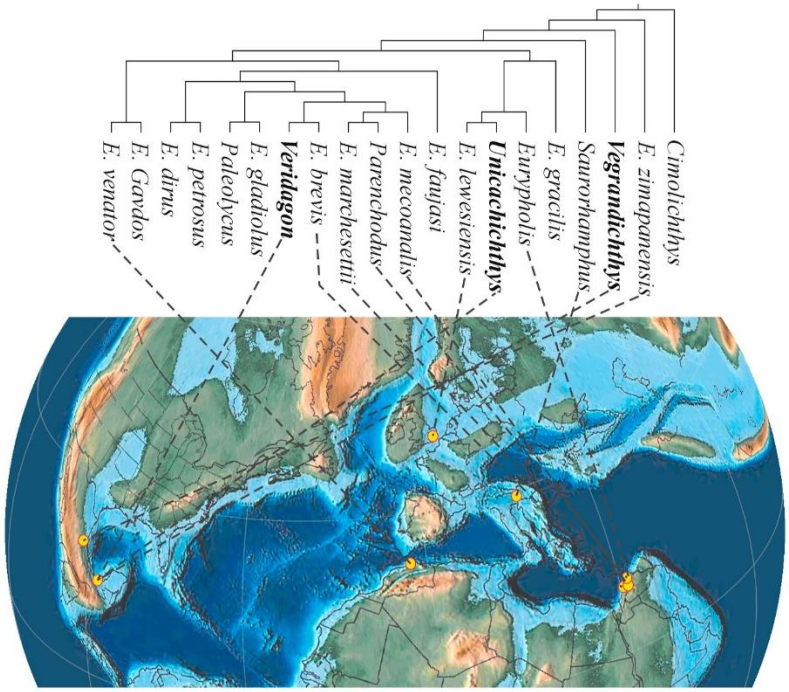

Fig. 4. Geographical localization of the early-Upper Cretaceous enchodontid species. PaleoMap from the Late Cenomanian (96.6 Ma) taken from Scotese and Wright (2018). Cladogram from the analysis of two landmarks configuration herein studied.

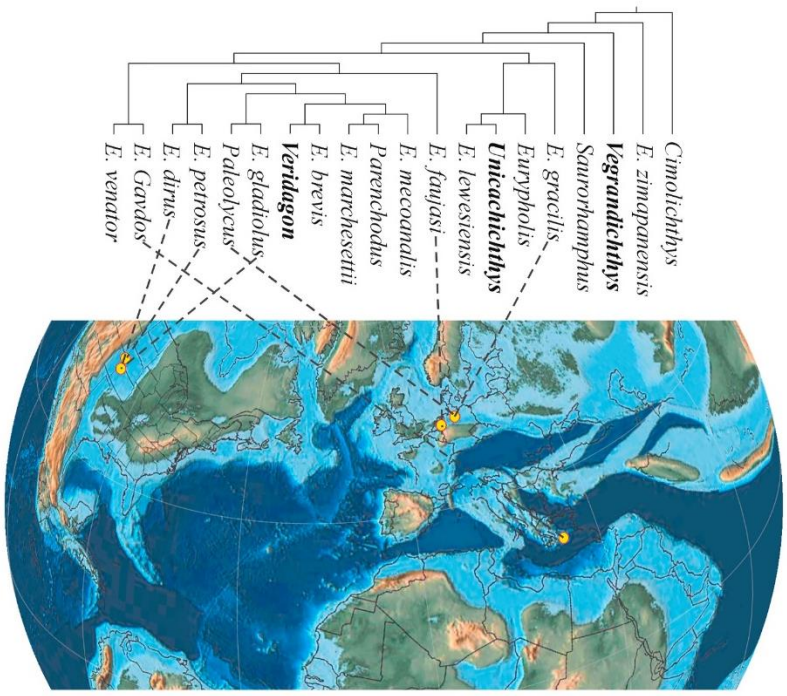

Fig. 5. Geographical localization of the late-Upper Cretaceous enchodontid species. PaleoMap from the Early Campanian (80.3 Ma) taken from Scotese and Wright (2018). Cladogram from the analysis of two landmarks configuration herein studied.

Unicachichthys are closely displayed in the similarity phenogram lays in the "L" shaped preopercle. The similarity of *Unicachichthys* with Eurypholinae was also reported by Díaz-Cruz et al., (2020) based on the phylogenetic analysis of the preopercle landmark configuration. Likewise, as the lower jaw indicated, a particular preopercle shape seems not to depict any specific enchodontid taxon. However, one of the most remarkable facts in the preopercle variation is that the ventral limb displays a very diversified series of shapes. This variation may be associated with a modular variation, presumably correlated to the body or skull shape or the locomotion, but this hypothesis should be formally addressed.

The recent study of the Mexican enchodontid species and its morphology has contributed to the recognition in the western realm of Tethys, with morphologies previously recognized only in the Middle and East realms of Tethys. Simultaneously, this region is creating its own taxonomical identity enriching the morphological variation of Enchodontidae. Examples of the shared morphology include the "L" shape preopercle of *Unicachichthys*, or the spoon-like preopercle of *Veridagon*, and its differentiation starts with the laminar preopercle displaying ventral small spine in *Vegrandichthys* or the uniqueness of the tilted preopercle with a fan-shape ventral limb of *E. zimapanensis*. In the meantime, the immediate challenge is portraying all this variation in phylogenetic analyses being this information as either discrete morphological characters or morphometric configurations.

4.3. Paleobiogeography

The biogeographical hypotheses proposed for Enchodontidae suggest that the group, at least the *Enchodus* genus, arose in actual Middle East localities in the early stage of the Upper Cretaceous (Fielitz, 2004; Cavin et al., 2012). These hypotheses also mention that the characteristic North American *Enchodus* species clade (Fielitz, 2004:630 Fig. 7) might have originated later in that region. To understand these relationships, Cavin et al. (2012) describe vicariant events in each of these periods, involving the regions of Morocco-Italy with North America and Europe with North America. However, recent reports have put on the map the presence of *Enchodus* throughout the Mexican territory, from which new specimens in process of species-level taxonomical determination have been collected from different Cenomanian-Turonian localities (Alvarado-Ortega et al., 2006, 2019, 2020a, 2020b, 2019, 2020b; Porras-Múzquiz et al., 2019). These discoveries may complement or reinterpret the hypotheses about the origin and diversification *Enchodus*.

Seen from a family level, the Mexican portion of the Tethys contains the basal-most and the oldest genera of Enchodontidae (Díaz-Cruz et al., 2016, 2019b, 2020, 2019b), suggesting a Tethys western realm origin for the family. Nevertheless, this is a preliminary statement and the study and description of enchodontids should continue. Contrasting to previous works, our phylogeny, although exploratory since it is based on two landmark configurations only, shows interesting associations among taxa herein studied. For instance, in the early-Upper Cretaceous enchodontid group, the clade composed by *Enchodus mecoanalis*, *E. marchesettii* and *Parenchodus* along with its close relative, *E. brevis* (all of them from East realm Tethys localities possessing similar ages), revealed close relationship on the bases of the preopercle and lower jaw shape. Regarding the late-Upper Cretaceous enchodontid group, our phylogeny also retrieved the North American *Enchodus* species as closely relatives; these species have been recorded in several localities of the Western Interior Sea, extending their distribution up to its most southern edge as well as other regions in the world (McIntosh et al., 2016; Shimada and Everhart, 2003; Parris et al., 2007; Becker et al., 2010; Carbot-Chanona and Than-Marchese, 2013; among others).

Members of Enchodontidae are commonly recognized as good swimmers that inhabited epicontinental seaways (Goody, 1969, 1976, 1976; Cavin et al., 2012), in this regard, the Caribbean region (Hispanic corridor) may have played a critical role in enabling the faunistic marine

interchange of enchodontids between Central and Eastern realms of the Tethys, as noted in other Cretaceous marine taxa (Cavin, 2008; El-Shazly, 2015; Arratia et al., 2018; Alves et al., 2020). Aware of the limitation of our phylogenetic exercise, a comprehensive biogeographical study of Enchodontidae should be carried out considering a more detailed phylogeny, like those based on discrete morphological data or those combining different sources of data. Despite that, our approximation allowed us to analyze the relationship and shape variation in some structures of Enchodontidae taking into account the temporality of the taxa.

4.4. Evolutionary morphological trends in enchodontidae

The time-calibrated phylogeny sheds light on the temporal division of two enchodontid groups. Focusing particularly on the trends of the species herein studied, neither the shortening nor lengthening in the body is typical of any of the temporal groups. Chalifa (1996) also noticed this pattern when stating that body elongation is found in species from the Cenomanian or Santonian ages. Although the body shape variation in enchodontids is better depicted by the five body shape patterns described by Díaz-Cruz et al. (2019b), the recognition of these two trends in body evolution is central, since they lay the basis of the morphological change study in Enchodontidae. Seen from a different perspective, the early-Upper Cretaceous enchodontid group exhibit a rather small body size. Species such as *Parenchodus longipterygius* from the Middle East (Raab and Chalifa, 1987:721), and *Unicachichthys multidentata* (Díaz-Cruz et al., 2016:139), along with *Vegrandichthys coitecus* from southeastern Mexico (Díaz-Cruz et al., 2020:11), are the smallest species in Enchodontidae, presumably not overpassing 110 mm in standard length (SL). In this regard, *Enchodus zimapanensis* deserves special attention since its maximum standard length reaches up to 300 mm (Fielitz and González-Rodríguez, 2010:1345), and temporally is the oldest known species within the family. Its derived phylogenetic position in Enchodontidae decreases the stratigraphic fit of the phylogeny (Díaz-Cruz et al., 2020), leading some authors to suggest the need for ghost lineages addition to better fit its age (Cavin et al., 2012).

Early enchodontids species that may not fit the small body size pattern are *Enchodus venator* and *E. lewesiensis*. The first species has been reported from the Cenomanian-Turonian from Bomba Quarry, Cinto Euganeo, Italy (Amalfitano et al., 2020:293); based on a skull approximately 80 mm in length, and according to Goody (1976:107), who demonstrated that in *Enchodus* species the head length represents about 20% of the standard length, its standard length is approximately 400 mm, resulting in it being even larger than *E. zimapanensis*. However, Arambourg (1954:125) reported some small and middle-sized specimens of *E. venator*, the largest although incomplete measuring 140 mm, from the late Cenomanian-Turonian of Jebel-Tselfat, Morocco. The case of *E. lewesiensis* is not as complex as *E. venator*, the most complete specimen consists of an incomplete skull, with lower jaw of about 40 mm in length, a measurement is similar to that of *E. zimapanensis* specimens. However, a better approximation of this species is required since isolated lower jaws assigned to the species are larger (e.g. NHMUK PV OR 4184 and NHMUK P 73992). Interestingly, *E. venator* and *E. lewesiensis* are species with a temporal range extending up to the Turonian age, which makes the Cenomanian restricted species the smallest in Enchodontidae.

Contrarily, the late-Upper Cretaceous species display large body sizes. Although most of them are incomplete, the measurement of the skull or the lower jaw length indirectly reveals their body size. For instance, *Enchodus faujasi* from the Maastrichtian of the Netherlands whose lower jaw is approximately 140 mm in length (Friedman, 2012:127). Also, the North American species, *Enchodus dirus*, *E. gladiolus*, and *E. petrosus* are large, the latter species reaching up to 767 mm of standard length (Goody, 1976:107). *Palaeolycus dreginensis* exhibit 330 mm in standard length (Chalifa, 1996:363), while *E. gracilis* is 360 mm (Goody, 1976:107); both species are among the smallest in this group, nevertheless their standard length is larger than *E. zimpananesis*. Presumably, *Enchodus* from Gavdos from the Middle-Late Maastrichtian of Gavdos, Greece, is the only species not fitting this pattern, its approximately 60 mm length skull indicates a standard length close to 300 mm. The recent study of the Mexican enchodontids has brought new insights into the knowledge of the group; however, the evolutionary relationships seem to be, as yet, preliminary. The two temporal group delimitation and its correspondence with the body size seem to be clear, even though species are challenging this pattern such as *E. longidens* (Pictet, 1850) from the Upper Santonian of Lebanon (240 mm SL), *E. longipectoralis* from the Turonian of Brazil (>400 mm SL), or *Enchodus* sp. From the early Cenomanian of Southern Mexico (lower jaw ~130 mm). Other species offer evidence supporting our observation such as *Enchodus zinensis* Chalifa (1996) from the Upper Campanian-Lower Maastrichtian of Israel (1722 mm SL).

Seemingly, the general trend in Enchodontidae is that of the progressive increase in body size. This phenomenon, recognized as phyletic size increase or Cope's rule and displayed by many biological groups, indicates the largest representatives are usually geochronologically younger than the smaller ones, being small when the group first appears (Newell, 1949). In fishes, this is a process recurrently identified in different taxa either extinct or extant forms throughout the Phanerozoic (Albert et al., 2009; Albert and Jhonson, 2012). By the end of the Cretaceous period, enchodontids would have reached large sizes, a condition that made them vulnerable to the end-Cretaceous extinction, since extinction selectivity mainly affected large body-sized fishes (Friedman, 2009). This condition in combination with factors such as the abrupt decline in nannoplankton and foraminifera, primary producers and consumers (D'Hondt, 2005), and the strong collapse of mid and upper trophic levels in pelagic food webs in the Tethys (Sibert et al., 2014) might be reasons why the enchodontid fossil record in the Paleogene is rather scarce.

5. Conclusions

Our results show the great diversity that the preopercle shape can display in Enchodontidae and the implicit difficulty translating it to discrete morphological characters. No preopercle shape, except for those in Eurypholinae, is characteristic of a single Enchodontidae genus.

On the other hand, while the jaw diversity may be associated to ecological feeding aspects, this character might be important to differentiate among taxa, especially *Enchodus* species that in general exhibit high levels of similarity among them. Similar to the preopercle, the most differentiated lower jaw shapes correspond to those found in the subfamily Eurypholinae. However, with this structure, it is possible to find similarities in other enchodontid taxa.

The calibrated phylogeny allowed us to study the morphological variation of the analyzed structures regarding their temporality. Besides, it was possible to distinguish to enchodontids groups temporally divided. Either early or late Upper Cretaceous enchodontids species can display any of the five body shape patterns presented in the group. The general trend observed in Enchodontidae seems to relate with that of the body size increase, being the smallest species the oldest, and the larger species restricted to most recent ages. Although there are some special cases, this pattern is confirmed by the recently described Mexican species.

Due to the limitation in specimen representation we only visually inspect patterns rather than test hypotheses of shape differentiation among groups or to determine character states. Nevertheless, this approach depends on the future discovery of more representatives.

The paleobiogeographic associations found in the phylogenetic morphometric analysis are only approximations; however, the Hispanic corridor seems to be relevant for the enchodontid interchange and colonization of the different Tethys realms. A thorough paleobiogeographic hypothesis should be based on a more consistent phylogeny of Enchodontidae.

Funding

This research was supported by the Universidad Nacional Autónoma de México through the grant DGAPA-PAPIIT IN110920; CONACyT provided financial support through the grant number 632640 to JADC.

Declaration of competing interest

The authors declare that they have no known competing financial interests or personal relationships that could have appeared to influence the work reported in this paper.

Acknowledgements

This manuscript represents a partial fulfillment of the requirements to obtain the degree of Doctor in Biological Sciences (Systematics) within the Posgrado en Ciencias Biológicas at Universidad Nacional Autónoma de México for the first author. The authors thank to the staff of the Museum of Paleontology "Eliseo Palacios Aguilera" (MEPA) who is in charge of the "Proyecto de prospección y resguardo del patrimonio paleontológico de Chiapas". Authors are deeply grateful with all the curators of the paleontological collections that kindly allowed us access to review and borrow fossils material herein studied especially to D. Arbulla (Museo Civico di Storia Naturale di Trieste, Italy), G. Carbot-Chanona (MEPA, Chiapas, Mexico), K. González-Rodríguez (Museo de Paleontología, UAEH, Hidalgo, Mexico), and M. Bertling (The Geomuseum der WWU, Münster, Germany). J. Amalfitano kindly provided photographs of *Enchodus venator*. Finally, we thank to two anonymous reviewers for the comments that helped to improve this manuscript.

Appendix A. Supplementary data

Supplementary data to this article can be found online at https://doi.org/10.1016/j.jsames.2021.103492.

Author statement

Jesús Alberto Díaz-Cruz and Jesús Alvarado-Ortega. Both authors contributed equally to this work: conceptualization, methodology, formal analyses, resources, writing the original draft, writing and review-editing. Marcia M. Ramírez-Sánchez: Advised GM analysis, as well as review-editing. Emma Louise Bernard, Lu Allington-Jones, and Mark Graham: Authors were involved in specimen preparation, resources, and reviewing and editing.

References

Adams, D.C., Otárola-Castillo, E., 2013. Geomorph: an r package for the collection and analysis of geometric morphometric shape data. Methods in Ecology and Evolution 4 (4), 393–399. https://doi.org/10.1111/2041-210X.12035.

Agassiz, L., 1843. Recherches sur les Poissons fossils Tome V. Imprimerie de Petitpierre, Neuchâtel.

Albert, J.S., Jhonson, D.K., 2012. Diversity and evolution of body size in fishes. Evol. Biol. 39 (3), 324–340. https://doi.org/10.1007/s11692-011-9149-0.

Albert, J.S., Johnson, D.M., Knouft, J.H., 2009. Fossils provide better estimates of ancestral body size than do extant taxa in fishes. Acta Zool. 90 (Suppl. 1), 357–384. https://doi.org/10.1111/j.1463-6395.2008.00364.x.

Alvarado-Ortega, J., Cantalice, K.M., Barrientos-Lara, J.I., Díaz-Cruz, J.A., Than-Marchese, B.A., 2019. The huehuetla quarry, a turonian deposit of marine vertebrates in the sierra norte of puebla, Central Mexico. Palaeontol. Electron. 22 (1), 1–20. https://doi.org/10.26879/921.

Alvarado-Ortega, J., Cantalice, K.M., Díaz-Cruz, J.A., Castañeda-Posadas, C., Zavaleta-Villareal, V., 2020a. Vertebrate fossils from the San José de Gracia quarry, a new Late Cretaceous marine fossil site in Puebla, Mexico. Boletín de La Sociedad Geológica Mexicana 72 (1), 1–21. https://doi.org/10.18268/BSGM2020v72n1a160819.

Alvarado-Ortega, J., Cantalice, K.M., Martínez-Melo, A., García-Barrera, P., Than-Marchese, B.A., Díaz-Cruz, J.A., Barrientos-Lara, J.I., 2020b. Tzimol, a campanian marine paleontological site of the angostura formation near comitán, chiapas, southeastern Mexico. Cretac. Res. 107, 1–16. https://doi.org/10.1016/j.cretres.2019.104279.

Alvarado-Ortega, J., Garibay-Romero, L.M., Blanco-Piñón, A., González-Barba, G., Vega, F.J., Centeno-García, E., 2006. Los peces fósiles de la formación Mexcala (Cretácico superior) en el Estado de Guerrero, México. Rev. Bras. Palaontol. 9 (3), 261–272.

Alves, Y.M., Alvarado-Ortega, J., Brito, P.M., 2020. †*Epaelops martinezi* gen. and sp. nov. from the Albian limestone deposits of the Tlayúa quarry, Mexico – a new late Mesozoic record of Elopiformes of the western Tethys. Cretac. Res. 110, 104260. https://doi.org/10.1016/j.cretres.2019.104260.

Amalfitano, J., Giusberti, L., Fornaciari, E., Carnevale, G., 2020. Upper cenomanian fishes from the bonarelli level (OAE2) of northeastern Italy. Riv. Ital. Paleontol. Stratigr. 126 (2), 261–314. https://doi.org/10.13130/2039-4942/13224.

Arambourg, C., 1954. Les Poissons crétacés du Jebel tselfat (maroc). Notes et Mémoires Du Service Géologique Du Maroc 118, 1–188.

Arratia, G., González-Rodríguez, K.A., Hernández-Guerrero, C., 2018. A new pachyrhizodontid fish (actinopterygii, teleostei) from the muhi quarry (Albian-Cenomanian), Hidalgo, Mexico. Fossil Record 21 (1), 93–107. https://doi.org/10.5194/fr-21-93-2018.

Becker, M.A., Mallery, C.S., Chamberlain, J.A., 2010. Osteichthyans from an Arkadelphia Formation Midway Group lag deposit (Late Maastrichtian-Paleocene), Hot Spring County, Arkansas, U.S.A. J. Vertebr. Paleontol. 30 (4), 1019–1036. https://doi.org/10.1080/02724634.2010.483603.

Bell, M.A., Lloyd, G.T., 2015. Strap: An R package for plotting phylogenies against stratigraphy and assessing their stratigraphic congruence. Palaeontology 58 (2), 379–389. https://doi.org/10.1111/pala.12142.

Carbot-Chanona, G., Than-Marchese, B.A., 2013. Presencia de *Enchodus* (Osteichthyes: Aulopiformes : Enchodontidae) en el Maastrichtiano (Cretácico Tardío) de Chiapas, México. Palaontol. Mexic. 63, 8–16.

Catalano, S.A., Ercoli, M.D., Prevosti, F.J., 2015. The more, the better: The use of multiple landmark configurations to solve the phylogenetic relationships in Musteloids. Syst. Biol. 64 (2), 294–306. https://doi.org/10.1093/sysbio/syu107.

Cavin, L., 2008. Palaeobiogeography of Cretaceous bony fishes (Actinistia, Dipnoi and Actinopterygii). Geol. Soc. Spec. Publ. 295 (1), 165–183. https://doi.org/10.1144/SP295.11.

Cavin, L., Alexopoulos, A., Piuz, A., 2012. Late Cretaceous (Maastrichtian) ray-finned fishes from the island of Gavdos, southern Greece, with comments on the evolutionary history of the aulopiform teleost Enchodus. Bull. Soc. Geol. Fr. 183 (6), 561–572. https://doi.org/10.2113/gssgfbull.183.6.561.

Chalifa, Y., 1985. Saurorhamphus Judeaensis (salmoniformes: Enchodontidae), a new longirostrine fish from the cenomanian of ein-yabrud, near Jerusalem. J. Vertebr. Paleontol. 5 (3), 181–193. https://doi.org/10.1080/02724634.1985.10011857.

Chalifa, Y., 1989. New species of *Enchodus* (Pisces: Enchodontoidei) from the lower Cenomanian of Ein-Yabrud, Israel. J. Paleontol. 63 (3), 356–364. https://doi.org/10.1017/S0022336000019521.

Chalifa, Y., 1996. New species of *Enchodus* (Aulopiformes: Enchodontidae) from the Northern Negev, Israel, with comments on evolutionary trends in the Enchodontoidei. In: Arratia, G., Viohl, G. (Eds.), Mesozoic Fishes, vol. 1, pp. 349–367.

Coelho, P.M., 2004. Revisão sistemática dos Enchodontidae (Euteleostei : Aulopiformes) do Brasil. https://pantheon.ufrj.br/handle/11422/3048.

Cope, E.D., 1872. On the Families of Fishes of the Cretaceous Formation of Kansas. Proc. Am. Phil. Soc. 12 (86), 327–357.

Cope, E.D., 1874. Review of the Vertebrata of the Cretaceous Period found west of Mississippi River. Bulletin of the U.S. Geological and Geographical Survey,. Territories 1 (2), 3–48.

D'Hondt, S., 2005. Consequences of the cretaceous/paleogene mass extinction for marine ecosystems. Annu. Rev. Ecol. Evol. Syst. 36, 295–317. https://doi.org/10.1146/annurev.ecolsys.35.021103.105715.

Davis, M.P., Fielitz, C., 2010. Estimating divergence times of lizardfishes and their allies (Euteleostei: Aulopiformes) and the timing of deep-sea adaptations. Mol. Phylogenet. Evol. 57 (3), 1194–1208. https://doi.org/10.1016/j.ympev.2010.09.003.

Díaz-Cruz, J.A., Alvarado-Ortega, J., Carbot-Chanona, G., 2016. The Cenomanian short snout enchodontid fishes (Aulopifomes, Enchodontidae) from Sierra Madre Formation, Chiapas, southeastern Mexico. Cretac. Res. 61, 136–150. https://doi.org/10.1016/j.cretres.2015.12.026.

Díaz-Cruz, J.A., Alvarado-Ortega, J., Carbot-Chanona, G., 2019a. Corrigendum to "*Dagon avendanoi* gen. and sp. nov., an Early Cenomanian Enchodontidae (Aulopiformes) fish from the El Chango quarry, Chiapas, southeastern Mexico. J. S. Am. Earth Sci. 91, 272–284. https://doi.org/10.1016/j.jsames.2019.01.014.

Díaz-Cruz, J.A., Alvarado-Ortega, J., Carbot-Chanona, G., 2019b. *Dagon avendanoi* gen. and sp. nov., an Early Cenomanian Enchodontidae (Aulopiformes) fish from the El Chango quarry, Chiapas, southeastern Mexico. J. S. Am. Earth Sci. 91, 272–284. https://doi.org/10.1016/j.jsames.2019.01.014.

Díaz-Cruz, J.A., Alvarado-Ortega, J., Giles, S., 2020. A long snout enchodontid fish (Aulopiformes: Enchodontidae) from the early cretaceous deposits at the el chango quarry, chiapas, southeastern mexico: A multi-approach study. Palaeontol. Electron. 23 (2), 1–27. https://doi.org/10.26879/1065.

Dietze, K., 2009. Morphology and phylogenetic relationships of certain neoteleostean fishes from the Upper Cretaceous of Sendenhorst, Germany. Cretac. Res. 30 (3), 559–574. https://doi.org/10.1016/j.cretres.2008.11.001.

El-Shazly, S., 2015. Cretaceous - Tertiary Hoploparia species: Occurrence, paleobiogeography and predation context. J. Afr. Earth Sci. 112, 299–313. https://doi.org/10.1016/j.jafrearsci.2015.09.014.

Everhart, M.J., 2020, October 13. Enchodus Sp. Retrieved from. http://oceansofkansas.com/Enchodus.html.

Fielitz, C., 2004. The phylogenetic relationships of the †Enchodontidae (Teleostei: Aulopiformes). In: Arratia, G., Wilson, M.V.H., Cloutier, R. (Eds.), Recent Advances

in the Origin and Early Radiation of Vertebrates, pp. 619–634 (Verlag Dr. Friedrich Pfeil).
Fielitz, C., González-Rodríguez, K.A., 2010. A new species of *Enchodus* (Aulopiformes: Enchodontidae) from the Cretaceous (Albian to Cenomanian) of Zimapán, Hidalgo, México. J. Vertebr. Paleontol. 30 (5), 1343–1351. https://doi.org/10.1080/02724634.2010.501438.
Forey, P.L., Yi, L., Patterson, C., Davies, C.E., 2003. Fossil fishes from the cenomanian (Upper Cretaceous) of Namoura, Lebanon. J. Syst. Palaeontol. 1 (4), 227–330. https://doi.org/10.1017/S147720190300107X.
Friedman, M., 2009. Ecomorphological selectivity among marine teleost fishes during the end-Cretaceous extinction. Proc. Natl. Acad. Sci. Unit. States Am. 106 (13), 5218–5223. https://doi.org/10.1073/pnas.0808468106.
Friedman, M., 2012. Ray-finned fishes (Osteichthyes, Actinopterygii) from the type Maastrichtian, the Netherlands and Belgium. In: A, E., Jagt, J.W.M., Donovan, S.K., Yazykova, Jagt (Eds.), Fossils of the Type Maastrichtian (Part 1), Ed, pp. 113–142 (Scripta Geologica Special Issue).
Friedman, M., Beckett, H.T., Close, R.A., Johanson, Z., 2015. The English Chalk and London Clay: two remarkable British bony fish Lagerstätten. Geological Society, London, Special Publications 430 (1), 165–200. https://doi.org/10.1144/SP430.18.
Goloboff, P.A., Catalano, S.A., 2016. TNT version 1.5, including a full implementation of phylogenetic morphometrics. Cladistics 32, 221–238. https://doi.org/10.1111/cla.12160.
Goody, P.C., 1969. The relationships of certain Upper Cretaceous teleosts, with special reference to the myctophoids. Bull. Br. Mus. (Nat. Hist.) Geol. Suppl. 7, 1–255.
Goody, P.C., 1976. *Enchodus* (Teleostei: Enchodontidae) from the Upper Cretaceous Pierre Shale of Wyoming and South Dakota with an evaluation of the North American enchodontid species. Palaeontograph. Abteilung 91–112.
Hammer, Ø., Harper, D.A.T., Ryan, P.D., 2001. Past: Paleontological Statistics Software Package for Education and Data Analysis. Palaeontol. Electron. 4 (1), 1–9. http://palaeo-electronica.org/2001_1/past/issue1_01.htm.
Heckel, J.J., 1850. Beiträge zur Kenntniss der fossilen fische Oesterreiche. Denkschriften, Akademie Der Wissenschaften, Wien 1, 201–242.
Hill, J.J., Puttick, M.N., Stubbs, T.L., Rayfield, E.J., Donoghue, P.C.J., 2018. Evolution of jaw disparity in fishes. Palaeontology 61 (6), 847–854. https://doi.org/10.1111/pala.12371.
Holloway, W.L., Claeson, K.M., Sallam, H.M., El-Sayed, S., Kora, M., Sertich, J.J.-W., O'Connor, P.M., 2017. A new species of the neopterygian fish *Enchodus* from the Duwi Formation, Campanian, Late Cretaceous, Western Desert, central Egypt. Acta Palaeontol. Pol. 62 (3), 603–611. https://doi.org/10.4202/app.00331.2016.
Khalloufi, B., Ouarhache, D., Lelièvre, H., 2010. New paleontological and geological data about Jbel Tselfat (Late Cretaceous of Morocco). Hist. Biol. 22 (1), 57–70. https://doi.org/10.1080/08912961003668756.
Kramberger, D.G., 1895. De piscibus fossilibus Comeni, Mrzleci, Lesinae et M. Libanonis. Djela Jugoslavenska Akademija Znanosti, I Umjetnosti, Zagreb 16, 1–67.
Kriwet, J., 2003. Lancetfish teeth (Neoteleostei, Alepisauroidei) from the Early Cretaceous of Alcaine, NE Spain. Lethaia 36 (4), 323–332. https://doi.org/10.1080/00241160310006484.
Leidy, J., 1857. Notices of some remains of extinct fishes. Proc. Acad. Nat. Sci. Phila. 167–168.
Mantell, G., 1822. The Fossils of the South Downs; or Illustrations of the Geology of Sussex. Lupton Relfe.
McIntosh, A.P., Shimada, K., Everhart, M.J., 2016. Late Cretaceous marine vertebrate fauna from the Fairport Chalk Member of the Carlile Shale in southern Ellis County, Kansas, U.S.A. J. Vertebr. Paleontol. 119 (2), 222–230. https://doi.org/10.1660/062.119.0214.
Nelson, J.S., 1994. Fishes of the World. John Wiley & Sons.
Newell, N.D., 1949. Phyletic Size Increase, An Important Trend Illustrated by Fossil Invertebrates. Evolution 3 (2), 103–124.
Palci, A., Jurkovšek, B., Kolar-Jurkovšek, T., Caldwell, M.W., 2008. New palaeoenvironmental model for the Komen (Slovenia) Cenomanian (Upper Cretaceous) fossil lagerstätte. Cretac. Res. 29 (2), 316–328. https://doi.org/10.1016/j.cretres.2007.05.003.
Palci, A., Lee, M.S.Y., 2019. Geometric morphometrics, homology and cladistics: review and recommendations. Cladistics 35 (2), 230–242. https://doi.org/10.1111/cla.12340.
Parris, D.C., Grandstaff, B.S., Gallagher, W.B., 2007. Fossil fish from the Pierre Shale Group (Late Cretaceous): Clarifying the biostratigraphic record. Geol. Soc. Am. Spec. Pap. 427, 99–109. https://doi.org/10.1130/2007.2427(07).
Pictet, F.J., 1850. Description de quelques poissons fossiles du Mont Liban. Imprimerie de J.-G. Fick.
Porras-Múzquiz, H.G., Díaz-Cruz, J.A., Alvarado-Ortega, J., Cantalice, K.M., 2019. Evidencia de interacción depredador-presa en peces del género Enchodus (Enchodontidae: Aulopiformes) de localidades del Cretácico Superior Coahuila, Norte de México. Palaontol. Mexic. 5, 116.
Raab, M., Chalifa, Y., 1987. A new enchodontid fish genus from the upper Cenomanian of Jerusalem, Israel. J. Paleontol. 30, 717–731.
Rana, R.S., 1990. Palaeontology and palaeoecology of the intertrappean (Cretaceous-Tertiary transition) beds of the peninsular India. J. Palaeontol. Soc. India 35, 105–120.
Rana, R.S., Kumar, K., Singh, H., 2004. Vertebrate fauna from the subsurface Cambay Shale (Lower Eocene), Vastan Lignite Mine, Gujarat, India. Curr. Sci. 87 (12), 1726–1733.
Rohlf, F.J., 2010a. tpsDig2, Digitize Landmarks and Outlines, Version 2.16. Department of Ecology and Evolution. State University of New York at Stony Brook.
Rohlf, F.J., 2010b. tpsRelw v.1.49. Department of Ecology and Evolution. State University of New York at Stony Brook.
Schaeffer, J., Benton, M.J., Rayfield, E.J., Stubbs, T.L., 2019. Morphological disparity in theropod jaws: comparing discrete characters and geometric morphometrics. Palaeontology, November. https://doi.org/10.1111/pala.12455, 0–17.
Scotese, C.R., Wright, N.M., 2018. PALEOMAP Paleodigital Elevation Models (PaleoDEMS) for the Phanerozoic PALEOMAP Project. https://www.earthbyte.org/paleodem-resource-scotese-and-wright-2018/, 1-26.
Sheets, H.D., 2014. Integrated Morphometrics Package (IMP) 8. Canisius College, New York, USA.
Shimada, K., Everhart, M.J., 2003. *Ptychodus mammillaris* (Elasmobranchii) and *Enchodus* cf. *E. shumardi* (Teleostei) from the Fort Hays Limestone Member of the Niobrara Chalk (Upper Cretaceous) in Ellis County, Kansas shumardi (Teleostei) from the Fort Hays Limestone M. Trans. Kans. Acad. Sci. 106 (3), 171–176. https://doi.org/10.1660/0022-8443(2003)106.
Sibert, E.C., Hull, P.M., Norris, R.D., 2014. Resilience of Pacific pelagic fish across the Cretaceous/Palaeogene mass extinction. Nat. Geosci. 7 (9), 667–670. https://doi.org/10.1038/ngeo2227.
Silva, H.M.A., Gallo, V., 2011. Taxonomic review and phylogenetic analysis of Enchodontoidei (Teleostei: Aulopiformes). An. Acad. Bras. Cienc. 83 (2), 483–511. https://doi.org/10.1590/S0001-37652011000200010.
Tewari, V.C., Lokho, K., Kumar, K., Siddaiah, N.S., 2010. Late Cretaceous-Paleogene Basin Architecture and Evolution of the Shillong Shelf Sedimentation, Meghalaya, Northest India. Journal, Indian Geological Congress 2 (November), 61–73.
Vernygora, O., Murray, A.M., Luque, J., Ruge, M.L.P., Fonseca, M.E.P., 2018. A new Cretaceous dercetid fish (Neoteleostei: Aulopiformes) from the Turonian of Colombia. J. Syst. Palaeontol. 16 (12), 1057–1071. https://doi.org/10.1080/14772019.2017.1391884.
von der Marck, W., 1858. Ueber einige Wirbelthiere, Kruster und Cephalopoden der Westfälischen Kreide. Zeitschrift Der Deutschen Geologischen Gesellschaft, Berlin 10, 231–271.
von der Marck, W., 1863. Fossile Fische, Krebse und Pflanzen aus dem Plattenkalk der jüngsten Kreide in Westphalen. Palaeontographica 1846–1933, 1–40.
Westneat, M.W., 2004. Evolution of levers and linkages in the feeding mechanisms of fishes. Integr. Comp. Biol. 44 (5), 378–389. https://doi.org/10.1093/icb/44.5.378.

CAPÍTULO VI: *Apuliadercetis gonzalezae* sp. nov., a North American Campanian dercetid fish (Teleostei, Aulopiformes) from Tzimol, Chiapas, Mexico

Journal Pre-proof

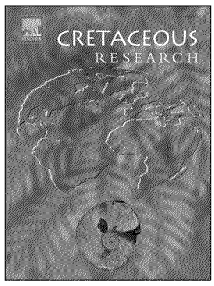

Apuliadercetis gonzalezae sp. nov., a North American Campanian dercetid fish (Teleostei, Aulopiformes) from Tzimol, Chiapas, Mexico

Jesús Alberto Díaz-Cruz, Jesús Alvarado-Ortega, Kleyton Magno Cantalice

PII: S0195-6671(21)00308-6

DOI: https://doi.org/10.1016/j.cretres.2021.105060

Reference: YCRES 105060

To appear in: *Cretaceous Research*

Received Date: 25 May 2021

Revised Date: 2 October 2021

Accepted Date: 3 October 2021

Please cite this article as: Díaz-Cruz, J.A., Alvarado-Ortega, J., Cantalice, K.M., *Apuliadercetis gonzalezae* sp. nov., a North American Campanian dercetid fish (Teleostei, Aulopiformes) from Tzimol, Chiapas, Mexico, *Cretaceous Research*, https://doi.org/10.1016/j.cretres.2021.105060.

Apuliadercetis gonzalezae sp. nov., a North American Campanian dercetid fish (Teleostei, Aulopiformes) from Tzimol, Chiapas, Mexico

Jesús Alberto Díaz-Cruz[a], Jesús Alvarado-Ortega[b,*], Kleyton Magno Cantalice[b]

[a] Posgrado en Ciencias Biológicas, Universidad Nacional Autónoma de Mexico, Circuito de la Investigación S/N, Ciudad Universitaria, Delegación Coyoacán, Ciudad de Mexico, 04510 Mexico.

[b] Instituto de Geología, Universidad Nacional Autónoma de Mexico, Circuito de la Investigación S/N, Ciudad Universitaria, Delegación Coyoacán, Ciudad de Mexico, 04510 Mexico.

*correspondig autor: alvarado@geologia.unam.mx

Keywords: *Apuliadercetis*, Campanian, America, Mexico, Chiapas

A B S T R A C T

A new member of the family Dercetidae is named in this work as *Apuliadercetis gonzalezae* sp. nov., based on specimens from the marine Campanian deposits of the Angostura Formation, exposed in the Tzimol quarry, next to Ochuxhob, Tzimol Municipality, southeastern Chiapas. The osteology of this serpentiform and longirostrine new fish shows a diagnostic character of the order Aulopiformes, the occurrence of epipleurals bones associated with abdominal centra extends up to the centrum 2. This species is a member of the family Dercetidae because it shows the most outstanding characters of this extinct clade, two pairs of triangular and expanded transverse processes in the abdominal centra, the low and elongated neural arches on the abdominal centra bearing short neural spines, and a row of triradiate flank scutes on each side of the body. Additionally, this fish belongs to *Apuliadercetis* because it shares the synapomorphy of this genus, the neural spines of the centra located below the dorsal fin are extremely reduced. This fish represents the third species in the genus and the first from America; such a discovery also shows that this genus had a wide geographical distribution that at least comprised Europe and the far south of North America.

1. Introduction

The genus *Apuliadercetis* Taverne, 2006a, is a teleost marine fish belonging to the extinct family Dercetidae and the order Aulopiformes (Taverne, 2006a, b; Vernygora et al., 2018; Alvarado-Ortega and Díaz-Cruz, 2021). This genus was erected to include *A. tyleri* Taverne, 2006a, from the Campanian-Maastrichtian (ca. 74 m.y.b.p) marine deposits at the Cava, Canale, and Portoselvaggio sites, near Nardó, Province of Lecce, Apulia Region, southeastern Italy. Later, a second species of the genus, *A. indeherbergei* Taverne and Goolaerts, 2015, was discovered in upper Maastrichtian deposits of the Gulpen Formation exploited in the CBR Lische quarry, near Eben-Emael, Belgium. Unfortunately, these species are known by poorly preserved fossils, whose skeletons are incomplete or strongly disarticulated. Recently, Alvarado-Ortega et al. (2020a) reported the discovery of *Apuliadercetis* in Mexico based on well-preserved fossils from the Campanian deposits of the Angostura Formation, exposed in Tzimol, Chiapas. Therefore, the present work aims to provide an accurate description of the *Apuliadercetis* specimens from Tzimol, to support their inclusion into a new species, and to explore its relationships.

The Tzimol locality is a newly paleontological site reported by Alvarado-Ortega et al. (2020a). This consists of numerous small quarries opened on the southwestern side of the Ochuxhob town, which belong to different local families and nearby neighbors. Ochuxhob forms part of the Tzimol Municipality and is located about 12 Km west of the Comitán de Domínguez city, State of Chiapas, southeastern Mexico (Fig. 1). Such quarries are spread between the coordinates 16°12´57.52" and 16°13´49.22" N — 92°15´00" and 92°16´11" W. This site is near to the western edge of a complex tectonic region previously named as the Upland of Chiapas, the Morphotectonic Province of Folded Mountains, and the

66 Reverse-Fault Tectonic Province (e. g. Sánchez Montes de Oca, 1979; Quezada-Muñetón,
67 1987; Ferrusquía-Villafranca, 1996; Consejo de Recursos Minerales, 1999; Menses-Rocha,
68 2001; Omaña and Alencaster, 2019). A lithological sequence of about 15 m thick is
69 exploited in the Tzimol quarries; this sequence consists of centimetric to decimetric layers
70 of yellowish to beige marly limestones interbedded with clays. The bottom and top of this
71 sequence are unknown. These marly strata are millimetric and parallelly laminated, with no
72 paleo-currents or load marks, showing fine textures with no macroscopic clastic
73 components, and no horizontal nor vertical bioturbations except for the abundant
74 compressed coprolites. Also, there are dark-gray colored bands in which the limestone is
75 affected by silicification that are randomly distributed and form vertical and horizontal
76 geometric patterns or alter complete strata.
77 The outcrops exploited in Tzimol belong to the Angostura Formation. Sánchez Montes
78 de Oca (1979) identified and named this marine lithostratigraphic unit of about 1,100 m
79 thick composed of Campanian-Maastrichtian limestones, marls, and fine sands exposed
80 along the Central Depression and Upland regions of Chiapas, which rest discordantly over
81 the Cantelhá Formation (Albian–Cenomanian), as well as, transitionally on the Jolpabuchil
82 Formation (Cenomanian–Maastrichtian). The Angostura Formation is covered concordant
83 and transitionally by the Paleocene deposits of the Tenejapa, Lacandón, and Soyaló
84 formations, as well as the El Bosque Formation of Eocene age (e. g. Quezada-Muñeton,
85 1987, 1990; Ferrusquía-Villafranca et al., 2000; Meneses-Rocha, 2001; Islas-Tenorio et al.,
86 2004; Martínez-Amador et al., 2004; Omaña and Alencáster, 2019). The recent recognition
87 of *Radiolites acutocostata* Adkins, 1930, in Tzimol indicates that the strata exposed in the
88 site correspond to the Campanian (Pons et al., 2010; Alvarado-Ortega et al., 2020a).
89 Until now, the fossil assemblage recovered from Tzimol is rich, diverse, and well-

preserved and includes microfossils as foraminifera and algae, as well as macrofossils of plants, vertebrates, and invertebrates. The plants are represented by possible fruits, leaves, and remains of conifers and palms. The invertebrates include scarce bivalves, gastropods, scaphopods, ostracods, and hemiasterid echinoderms. The vertebrates are mainly different groups of fishes, including *Nursallia* Blot, 1987; *Saurodon* Hays, 1829; and *Enchodus* Agassiz, 1833; as well as mosasaur remains. The UV light reveals the calcium phosphate in Tzimol vertebrates, preserved in bones, teeth, and patches of soft tissues (muscles). The plant remains are extremely scarce and poorly preserved as carbonized impressions (Alvarado-Ortega et al., 2020a).

2. Materials and Methods

Preparation. The fossils herein studied were prepared with both chemical and mechanical methods. The surface of the fossils was exposed using a 5% aqueous solution of acetic acid that was applied with fine brushes to eliminate the calcareous patches. Later, the treated specimens were washed for one hour in freshwater. Also, pin-vises and needles were used under a binocular stereo microscope to remove rock fragments from the fossil surface. A light solution of plexigum P24 into ethyl methacrylate was applied with fine brushes on the dry and clean surfaces to harden the bones and fossil impressions. High-quality photographs of the fossils were taken under different illumination conditions, with white and UV lights, as well as with the fossils uncovered and coated with magnesium smoke.

Anatomical nomenclature. The osteological nomenclature and abbreviations used here follow those of respective similar works (e.g. Goody, 1969; Taverne, 2006a, b; Taverne and Goolaerts, 2015; Vernygora et al., 2018).

Comparative material. The following specimens were studied for comparative purposes. *Hastichthys totonacus* Alvarado-Ortega and Díaz-Cruz, 2021: IGM 7969, holotype as well as IGM 7970 and IGM 11518 to IGM 11530, from the Turonian deposits of the Huehuetla quarry, Puebla, Mexico.

Institutional abbreviations. Fossils from the Tzimol site studied here are deposited and catalogued under the acronym IGM, which corresponds to the Colección Nacional de Paleontología, housed into the Museo María del Carmen Perrilliat at the Instituto de Geología, Universidad Nacional Autónoma de México (UNAM).

3. Results

3.1. Systematic paleontology

Order Aulopiformes Rosen, 1973.

Family Dercetidae Woodward, 1901.

Genus *Apuliadercetis* Taverne, 2006a.

Apuliadercetis gonzalezae sp. nov.

(Figs. 2–10, Table 1)

LSID. urn:lsid:zoobank.org:act:559BE020-1286-414B-96DF-843D44E9C534

Holotype. IGM 11403, complete articulated specimen exposing the left side with 129 mm of SL (Figs. 2, 4) (also see Alvarado-Ortega et al., 2020a, figs. 7A-C).

Paratypes. IGM 12947, head exposing the skull roof and the pectoral girdle (Fig. 3A). IGM 12948, an almost complete specimen with the caudal skeleton disarticulated (Figs. 3B, 6, 7D). IGM 12949, an incomplete specimen with the head bones disarticulated and the anterior part of the trunk (Fig. 5). IGM 12950, an almost complete specimen with bones of

the head and trunk partially disarticulated and scattered (Figs. 7A, 8A-B, 9). IGM 12951, an incomplete specimen with the head bones disarticulated and the abdominal part of the trunk (Fig. 7B). IGM 12952, an incomplete specimen with the head bones disarticulated and the trunk fragmented into three parts (Fig. 7C). IGM 12953, a complete specimen lacking the anterior tip of both jaws (Figs. 8C-D, 10). IGM 12954, an almost complete specimen lacking the caudal fin with the bones of the paired and unpaired fins disarticulated and scattered. IGM 12957, a complete specimen with poorly preserved fins and a strongly twisted body.

Etymology. The species epithet honors our colleague Katia Adriana González Rodríguez, the first woman paleoichthyologists in Mexico, for her valuable contributions to science.

Age and distribution. All specimens come from the laminated, parallel, and centimetric marl strata belonging to the Campanian deposits of the Angostura Formation. Tzimol quarry, Ochuxhob town, Tzimol quarry, Chiapas, southeastern Mexico (Fig. 1).

Diagnosis. Species of the genus *Apuliadercetis* in which the supraoccipital crest is long; the pterotic is broad and short; the parietal does not contact the epioccipital; the anal fin consists of 16 rays; the pectoral fin has 12 rays; there is a long dorsal fin stay; the pelvic fin consists of seven rays; there are 41-42 caudal centra in the vertebral column; the compound caudal centrum includes the fusion of the preural 1, both urals, and all the upper hypurals forming the dorsal hypural plate.

3.2. *Description*

Body shape and general proportions. Table 1 summarizes the measurements and body proportions of the new species. Regarding the head length, the larger specimen is IGM

12951; however, the body of this specimen is segmented and incompletely preserved. Among complete specimens, the holotype is the longest specimen known; its standard length is 128.5 mm (Fig. 2). The trunk is extremely long, it is uniformly high from the occiput to the end of the anal fin and becomes shallower posteriorly. The caudal peduncle is about two-thirds of the maximum body height. The head is longirostrine, its height equals the maximum body height, and its length represents about 30% of the SL (ranging between 28.2 to 29.8). In the head, including the opercular series, the rostrum or preorbital length is between 17 and 18.9% of the SL, and occupies slightly less than two-thirds of the head length; the posterior part of the head length is equally divided among the orbit, the postorbital part of the skull and the opercular bones. The anterior tip of the lower jaw reaches the anterior end of the rostrum. The dorsal fin is triangular, short, and raises just at the beginning of the posterior half of the body; this represents 3.1 to 3.4 and is extended from 53.5-55.2 to 56.6-58.6% of the SL. Unfortunately, in all the specimens referred here, the pelvic girdle is displaced from its original position; however, this could be close or opposed to the dorsal fin. The anal fin is acuminate and comparatively long; this is placed far back and opposed to the dorsoposterior region of the body; the anal fin length represents 8% of the SL and is extended in the last fifth of the body, between 82.3 to 90.3 of the SL. The caudal fin is deeply forked, short, higher than the maximum body height, and consists of two triangular, deep, and equally sized lobes.

Skull. The skull of this longirostrine fish is triangular, very elongated, and anteriorly tapered; this is about 10 times longer than high. Its rostrum is very slender, straight, and ends in an acute tip (Figs. 2–4). The frontals are the largest bones in the skull; these share a straight suture with no interfrontal fenestra and cover about 40% of the skull and the anterior half of the postorbital region of the skull. Each frontal is somewhat triangular,

anteriorly tapered, laterally notched above the orbit, and strongly expanded posteriorly covering part of the lateral surface of the skull. The posterior edge of each frontal overlaps the parietal and pterotic bones; its lateral edge sutures with the pterotic and sphenotic, and its anterior ends join the mesethmoid and lateroethmoid. The frontal surface is smooth and has some longitudinal ridges alongside the lateral edges that enclose the supraorbital sensory canal, which opens through some pores.

The parietals are rectangular, longer than wide, smooth, and located far back on the skull roof, over the posterior half of the skull postorbital region (Fig. 4). These bones are in contact along their middle edges and separate the supraorbital from the frontals. The lateral edge of each parietal sutures the middle edge of the respective pterotic. The pterotic is a large square bone in the dorsal view (Fig. 4). Laterally, the pterotic is somewhat triangular, projected downward along the posterior half of the skull, and roofs the hyomandibular facet. The exoccipital is a roughly rectangular bone, about two times wider than long.

The parasphenoid consists of two sections. The postorbital section is expanded while the orbital section is a straight bar-like structure, smooth and untoothed with an oval anterior expansion (Figs. 4, 5). The postorbital part of the parasphenoid covers the ventral surface and is extended dorsally to cover the basal third of the lateral surface of the skull postorbital region. In IGM 12949, a single and small vomer is present in front of the parasphenoid; this bone seems to have a patch of conic teeth.

The ethmoid skull region shows a large nasal cavity (Fig. 4). The nasal bone is elongated and uniformly high that occupies the nasal capsule. On either side of the skull, this cavity is bordered by the frontal dorsally, the parasphenoid ventrally, and the lateral ethmoid posteriorly. Each lateral ethmoid bone is rectangular, tightly sutured to the ventral surface of the respective frontal bone, and projected downward to reach the parasphenoid. The

mesethmoid is a V-shaped bone located in the anterior end of both frontals; this single bone is deeply forked in its posterior edge and has a sharp anterior tip separating the posterior ends of both premaxillae.

Circumorbital bones. The circumorbital bones are small and flimsy. Probably, five bones form an incomplete series around the orbit, including the ovoid antorbital, three rectangular infraorbitals in the ventral and posterior edge of the orbital, and the triangular dermosphenotic. The sclerotics are wide semicircular bones.

Upper jaw. The upper jaw consists of the premaxilla and maxilla (Figs. 4, 5). This fish has no supramaxilla. The premaxillae are narrow and long bones, which anterior three quarters are semicylindrical and tightly sutured to from the rostrum. The entire rostrum is ornamented with longitudinal, narrow, and straight grooves. The posterior end of the maxilla becomes flat and is laterally extended below the mesethmoid and a small part of the palatine bone. The inter-premaxillary suture is straight in dorsal and ventral views. On the ventral surface, the maxilla has a row of small conical teeth with tips curved posteriorly. These teeth are millimetric, show the same size and shape, and are uniformly separated by empty spaces along the bone.

The maxilla is an elongated, shallow bone, shorter than the orbit, ventrally straight, and with the dorsal border convex and higher in the middle. This bone extends from the posterior orbit to the anterior tip of frontal bones (Figs. 4, 5). The anterior tip of the maxilla contacts the posterior tip of the premaxilla. The maxilla bears a row of numerous small conical teeth, with sharp tips and curved backward. The shape and distribution of these teeth are like those of the premaxilla.

Lower jaw. The lower jaw is an elongate, shallow, and triangular structure that consists of the dentary, anguloarticular, and retroarticular bones (Figs. 4-6). The anterior tip of this jaw

w

234 is anteriorly extended as far as the anterior tip of the rostrum. The articulation between the
235 lower jaw and the quadrate is below the middle of the postorbital region, and therefore, the
236 length of this jaw represents 80% of the skull length. The postarticular process is small and
237 short.

238 The dentary is an elongated triangular bone deeply forked posteriorly with an extremely
239 low symphysis, and a very shallow coronoid process (Figs. 4-6). The dorsal and ventral
240 borders of this bone are straight. The dentary symphysis is long and strong; this occupies
241 the anterior half of the lower jaw and shows a sinuous suture. The alveolar part of the
242 dentary is stout and semicircular and shows a flat dorsal surface that occupies the anterior
243 half of the bone; beyond the dentary, it becomes lateromedially expanded. The dentary
244 alveolar border is extended up to the anterior half of the orbit; it shows a row of small teeth
245 similar in size, shape, and distribution to those of the premaxilla. The size, shape, and
246 distribution of dentary teeth resemble those of the maxilla. The lateral surface of the
247 symphysial region of the dentary shows one or two longitudinal grooves resembling those
248 that ornament the rostrum; however, these surfaces are rather smooth.

249 The anguloarticular is triangular, occupies the posterior third of the lower jaw, and forms
250 a large part of the mandibular postarticular process. The ventrocaudal region of this process
251 includes an elongated and triangular retroarticular bone. The mandibular sensory canal is
252 enclosed along the dentary and anguloarticular bone; this opens only through some pores
253 near the ventral border of the jaw.

254 **Suspensorium and branchial arch.** The hyomandibular is a robust triangular bone with a
255 single and large articular head dorsally tilted, as well as a short shaft vertically oriented
256 (Figs. 4, 5). Its opercular condyle is stout and protrudes backward from the middle of its
257 posterior edge. The quadrate bone is triangular, more expanded anterodorsally, and has a

small rounded articular head somewhat tilted forward. The articulation of the quadrate and lower jaw is laterally exposed. The symplectic bone is obscured below the preopercle in all the specimens studied here. The metapterygoid is roughly subrectangular and broad. The ectopterygoid and endopterygoid are elongated and toothless bones placed below the orbit. The palatine is somewhat rectangular, long, and bears small conic teeth.

Although the dorsal hypohyal is not preserved in the referred specimens; IGM 12952 shows part of the ventral hypohyal, the branchiostegal rays, and the anterior and posterior ceratohyals well preserved (Fig. 7C). The ventral hypohyal seems a small rectangular bone attached to the base of the anterior edge of the anterior ceratohyal. The anterior ceratohyal is a flat and rectangular structure, constrained in the middle and about three times longer than high. The posterior ceratohyal is a flat and semi-oblong bone, with a straight anterior edge and about 1,5 times longer than high. Five progressively longer and thread-like branchiostegal rays are present; three of them join with the lateral surface of the anterior ceratohyal and the other two with the posterior ceratohyal.

Opercular bones. The opercular series is complete and consists of the opercle, subopercle, preopercle, and interopercle (Figs. 4, 5). The opercle is ovoid, flat, and smooth, as well as almost 1.5 times higher than long. The anterior edge of this bone is slightly concave and has the hyomandibular facet near the middle. The subopercle is a long saber-shaped, flat, and smooth bone that possesses a triangular and small anterior ascending process. The subopercle is a strongly curved bone that extends along the entire ventral edge and the basal half of the opercle.

The preopercle is a triangular and curved bone, about 1.5 higher than long, in which the ventral region slightly expands rostrally, the dorsal extension is tapered, and the caudal edge is convex (Figs. 4, 5). This bone has scarce openings of the preopercular sensory canal

on its lateral surface. The interopercle is a triangular bone, about as high as long, located between the preopercle and the subopercle.

Axial skeleton. The axial skeleton consists of 64 total centra, including 41 to 42 abdominals, 22 to 21 caudal centra plus two urals (Figs. 2, 3; Table 1). Among these centra, the preural 1 and both ural centra are fused (Fig. 10). In general, along the vertebral column, the centra are rectangular, somewhat constricted in the middle, and variable in size. The first two centra are hourglass-shaped bones with a strong middle constriction, those are the longest in the series, being about 1.5 times longer than the others. Beyond, along the abdominal and anterior caudal region, the centra are of the same height but become progressively shorter. In the back of the body and behind the anal fin, the first eight preural centra are gradually less high and the first four of these become higher than long.

The preural centra are fused with its respective neural arch (Figs. 2-6). Each neural arch is a shallow rectangular structure, dorsally concave, and slightly longer than its centrum. The anterior end of each neural arch slightly overhangs its centrum forming an anterior projection or prezygapophyses. In the posterior region of all the neural arches, there is a stick-like neural spine, except in those located below the dorsal fin pterygiophores, in which the neural spines are not developed (Figs. 2, 6). In the abdominal and some of the caudal centra, the neural spines are homogeneously sized and shaped; each of these is caudally tilted forming an angle of about 45° regarding the longitudinal body axis; also, they extend over the anterior half, and rest above the prezygapophysis of the subsequent neural arch. In those centra behind the anal fin, the neural spines become shorter, thicker, and tend to be more inclined, except for those less inclined that support the caudal fin.

In the abdominal region, there is a pair of large triangular transverse processes extended laterally and ventrally from each side of the centra (Figs. 2-5). Among these, the anterior

process is larger than the posterior one. Near the caudal region, the anterior transverse processes become smaller, projected more vertically, and probably meet each other medially forming haemal arches, in which small zygapophyses are present. Small and thin ribs articulate with the ventral edge of the anterior transverse processes. In the caudal centra, the arches are progressively smaller and shorter than their respective centra, and the shapes and sizes of the haemal spines resemble those of the opposed neural spines.

In the holotype, the anterior centra are associated with long and thin epineural bones preserved above four centra; however, it is not possible to recognize remains of epipleurals preserved in this specimen (Fig. 4). The long and thin epipleurals are preserved in the specimen IGM 11948 and IGM 12949 (Fig. 5). In the predorsal region and above the vertebral column, there are at least three pairs of predorsal bones, which are about flat, about seven centra long, and evenly wide throughout the length (Fig. 9).

Pectoral girdle and fin. The posttemporal is an oval, flat, and smooth bone that lies above the opercle. This has a rounded dorsoposterior edge and two anterior processes including a thin ventral process and a broader and longer dorsal process (Fig. 4). The supracleithrum is an elongated bone that is slightly tilted downward and covers the dorsal posterior region of the cleithrum.

The cleithrum is J-shaped with limbs forming a 90° angle and united by an internal wing (Fig. 5). In this bone, the horizontal limb is thick, elongated, and shallow. On the contrary, the vertical limb is rather rectangular, laterally expanded, and its height is slightly less than 0.5 of the length of the horizontal limb. The medial surfaces of both cleithra are partially exposed in IGM 12950 (Fig. 8); here, each of these bones borders a large part of the coracoid fossa and has a short process projected from the posterior vertex that sutures with the respective coracoid. There is no poscleithra.

In medial view, the coracoid is a triangular bone dorsally tilted, posteriorly expanded, and anteriorly sharpened (Figs. 8A, 8B). The ventroposterior edge of this bone is straight while its anterior and dorsal edges are somewhat curved and bear small processes, the first has a rectangular process to attach with the vertical limb of the cleithrum and the second shows a shallow process to attach with the scapula diagonally. These processes form the ventral edge of the scapular fossa. The anterior tip of the coracoid is sutured with a caudally extended small posterior process from the posterior vertex of the cleithrum. The coracoid fossa is about two times larger than the scapular fossa; this is bordered mainly by the vertical limb and the ventroposterior process of the cleithrum, as well as by the anterior process and anteroventral edge of the coracoid.

The scapula is a rectangular bone that anteriorly attaches with the vertical limb of the cleithrum, has a semicircular and huge notch that forms the dorsal edge of the scapular fossa (Figs. 8A, 8B). Behind this notch, the ventral edge of the scapula is dorsally tilted and tightly sutured with the coracoid. In this bone, a small posterior part of its ventral edge articulates with the first rays of the pectoral fin; behind, a series of about four pectoral radials articulate the remaining pectoral rays. The pectoral radials are small bones somewhat constrained medially and possess two expanded extremes.

The pectoral fin seems to be triangular, long, and probably its length equals that of three abdominal centra (Figs. 2, 8A-B). In this fin, the articulation between the radials and rays is horizontally oriented and probably was placed in the middle of the trunk, between the abdominal edge and the vertebral column. Al least 12 thin, elongated, and distally branched and segmented rays form this fin.

Pelvic girdle and fin. The pelvic girdle consists of two triangular pelvic bones (Figs. 2, 8C-D). Although these bones are displaced in the large part of the specimens referred here;

these seem to be on the abdominal edge and located in opposition to the dorsal fin base. The pelvic bones are triangular, anteriorly pointed, about 2.5 times longer than wide, and about two abdominal centra long. The posterior edges of these bones have a short and rounded posterior process that joints with the proximal head of at least four pelvic radials, which are small, elongated, constrained in the middle, and with expanded ends bones. The distal heads of these radials joint with the pelvic fin that consists of seven elongated, distally branched, and segmented rays. The pelvic fin seems to be triangular and about four abdominal centra long.

Dorsal fin. The dorsal fin is triangular, short, and high. This fin is placed in the middle region of the trunk extending for two abdominal centra; in the holotype, these are centra 22 and 23, (Figs. 2, 9A, 9C). The fin consists of six to seven thin, elongated, and distally branched and segmented rays that are preceded by one or two little procurrent dorsal rays. The first dorsal ray is the longest in the fin and its length equals those of the five or six abdominal centra that are located below this fin. Posteriorly, the dorsal rays become progressively shorter; the shortest ray is one-half of the length of the first dorsal ray.

The internal support of the dorsal fin consists of six or seven proximal pterygiophores, no medial or distal pterygiophores are present (Figs. 2, 9A, 9C). The dorsal pterygiophore 1 is hypertrophied and the highest in the series; it exhibits a triangular anterior wing that anteriorly ends in a sharp tip and is five abdominal centra long. Posterior dorsal pterygiophores are noticeably shorter than the first one, they become slightly shorter in anteroposterior direction, and have a middle thick bar bordered by two wings, which are cranial and caudally extended from the articular head to the distal tip of the middle bar. These wings contact each other and fill the space between the pterygiophores. The neural spines of the abdominal centra, located below the dorsal pterygiophores, are extremely

reduced and hardly represent a tiny spine. The last posterior dorsal pterygiophore is associated with a thin and long dorsal fin stay that is seven abdominal centra long and distally bifurcated.

Anal fin. This long and acuminate fin is located far back in the trunk, at the beginning of the posterior quarter of the body length, and extends for eight centra, from 45 to 52 (= preurals 21 and 12) (Figs. 9B, 9D). This fin consists of one or two little procurrent rays plus 16 distally segmented and branched rays. Among these, the anal rays 2-4 are the longest and equal the length of five centra, whereas the rest become successively shorter.

The anal fin is internally supported on 16 proximal pterygiophores that include one hypertrophied and fifteen normal stick-shaped pterygiophores, progressively smaller, and have expanded terminal articular heads (Figs. 9B, 9D). These pterygiophores are dorsally extended and occupy the interspaces between the haemal spines of those centra located above the fin. The anteriormost anal pterygiophore is anteriorly projected, in a parallel position to the vertebral column, and below five abdominal centra; this pterygiophore consists of a thick ventral edge and a dorsal wing that tapers anteriorly and ends in a sharp tip. The posterior part of this bone joints the first anal ray and the one or two anterior procurrent rays of this fin. Beyond, the relation of pterygiophores to anal rays articulating is one to one. In the posterior half of this fin, there are some small medial or distal pterygiophores between the proximal pterygiophores (Figs. 7D, 9B, 9D).

Caudal skeleton. The caudal fin consists of two triangular lobes of similar size that are deeply forked (Fig. 3A). This fin consists of 19 procurrent and 17 principal rays ordered following the formula ix+I+7—8+I+x (Fig. 10). The haemal arch of preural 1 is small while the parhypural is a wide and stout structure, which posterior edge is entirely in contact with the ventral hypural plate. The spines of preurals 4 and 5 are relatively thick,

short, and strongly tilted backward and almost lying in parallel to the longitudinal body axis, whereas the haemal and neural spines of the preurals 2-3 are slender, elongated, and about 45° tilted backward reaching and supporting the elements of the caudal fin. The preural 5 is about 1.3 times longer than high; on the contrary, the preurals 1-4 are progressively shorter, and the preural 2 and 3 are rather higher than long.

The caudal skeleton is complex and consists of a compound caudal centrum and two hypural plates (Fig. 10). The dorsal hypural plate is a wide triangular plate that results from the fusion of the dorsal hypurals. A narrow notch is dividing the posterior half of this dorsal plate, which probably was generated due to the incomplete fusion of hypurals 3 and 4. The ventral hypural plate is smaller than the dorsal one; the former results from the fusion of the hypurals 1 and 2 heads; the three posterior quarters of the hypurals form a straight and tight contact. The compound centrum includes the fusion of the dorsal hypural plate with the urals 1 and 2 plus preural 1. There is a deep and narrow caudal diastema between the hypural plates, in which the dorsal and ventral interhypural edges are almost in parallel. Into the space between the dorsal hypural plate and the neural spine of preural 2, there is a single, thick, somewhat curved, and long epural. There is only one uroneural, which is stout, lies on the lateral dorsal region of the compound centrum, and has an expanded anterior edge that does not reach the preural 2.

Scutes. The body is naked except for a row of thick scutes extended on each body flank, which lie slightly above the abdominal centra and over the caudal vertebrae. These scutes are unattached and therefore these are scattered and patchy preserved (Figs. 4, 5, 9). The scutes are triradiate or Y-shaped, flat, and have a horizontal, elongated, and anteriorly forked limb plus two posterior symmetrical limbs, which are shorter than the anterior one, and tilted about 45° downward and upward. The horizontal limb is rostrocaudal perforated

426 by the lateral line. The scutes are similarly shaped and sized along the middle part of the
427 series; however, near the head, these have little posterior limbs while those near the tail
428 become smaller and have a ventral limb that tends to be smaller and disappear in the most
429 posterior scutes. Although these scutes seem to be entirely smooth lateral and medially; the
430 outer surfaces of some of them show a middle longitudinal ridge in front of the posterior
431 bifurcation, which is robust, shallow, and short. The total number of scutes along the body
432 flanks is unknown.
433
434 **4. Discussion**
435
436 *4.1. Comparative remarks*
437
438 Today, the order Aulopiformes is diagnosed with seven features, including 1) the
439 epibranchial 2 has an elongate uncinate process bridging the gap between the
440 posterolaterally displaced pharyngobranchial 2 and the pharyngobranchial 3 (Rosen, 1973);
441 2) the absence of cartilaginous condyle on pharyngobranchial 3 for articulation with
442 epibranchial 2 (Johnson, 1992); 3) the epipleural series is anteriorly developed from at least
443 the abdominal centrum 2 (Patterson and Johnson, 1995); 4) the larvae have peritoneal
444 pigmentation (Johnson, 1982); 5) one or more of the anterior epipleurals are dorsally
445 displaced into the horizontal septum (Patterson and Johnson, 1995); 6) the lack of swim
446 bladder (Johnson, 1982); and 7) the medial processes of the pelvic girdle are joined
447 medially by cartilage (Baldwin and Johnson, 1996). Unfortunately, only the first four of
448 these features are synapomorphies (Baldwin and Johnson, 1996, p. 396). *Apuliadercetis*
449 *gonzalezae* sp. nov. is included in this order because here we observe the presence of

450 character 3. Although epipleurals are particularly scarce in the fossils herein studied, these
451 are present above the centra 2 (Fig. 5).

452 Today, including the species erected here, the family Dercetidae is composed of 16
453 genera and 34 species (Alvarado-Ortega and Díaz-Cruz, 2021). Against their authors,
454 *Robertichthys* Blanco-Piñón and Alvarado-Ortega, 2005, and *Paradercetis* Casier, 1965, do
455 not belong to this family (Taverne, 1976; Giersch, 2014; Díaz-Cruz et al., 2016). Although
456 recently, the monophyly and interrelationships of the family Dercetidae have been
457 discussed through different phylogenetic studies (Chalifa, 1989; Taverne, 1991, 2005a, b;
458 2006b; Silva and Gallo, 2011; Vernygora et al., 2018; Alvarado-Ortega and Díaz-Cruz,
459 2021), the results so far achieved must be considered partial because these only include 13
460 genera and in the case of oligospecific genera, only one or two species are considered (Fig.
461 11). At this moment, these researches show numerous supporting characters of Dercetidae
462 (Taverne, 2006b; Silva and Gallo, 2011; Vernygora et al., 2018), which include (following
463 the above enumeration): 8) the trunk is shallow and long; 9) the head is longirostrine, low,
464 and the orbital and postorbital skull sections are noticeably short; 10) the maxilla has a
465 single row of teeth; 11 and 12) the supraorbital and supramaxilla are not developed; 13) the
466 first two vertebrae are elongated (at least, these are 2.5 times longer than the posteriors);
467 14) the abdominal centra have one or two pairs of transverse processes projected
468 lateroventrally; 15) the neural arches are shallow, elongated, and cover the entire dorsal
469 edge of the centra; 16) the trunk shows one or two rows of triradiate or Y-shape scutes
470 covering the flanks of the trunk; and 17) the abdominal and the anterior caudal centra show
471 neural spines extremely small, lower than the half of the length of the respective centrum.
472 Among these, only the character 17 is a synapomorphy. *Apuliadercetis gonzalezae* sp. nov.
473 unquestionably is a new member of the family Dercetidae because it shows character 17, as

474 well as all these diagnostic features. Although the first two vertebrae of this species are
475 somewhat dissimilar to those of other dercetids (character 13), these are less than 2.5 times
476 longer than the subsequent vertebrae, as it is noticed in the character 3. In this species, such
477 vertebrae are the longest in the vertebral column and are at least 2 times longer than the
478 posteriors (Figs. 4, 5, 6).

479 In the description of *Apuliadercetis tyleri*, Taverne (2006a, p. 24) listed 23 features to
480 highlight the uniqueness and support its inclusion into its own genus. Unfortunately, such
481 features have been revealed as homoplasies in recent phylogenetic studies (Fig. 11) and
482 only six of these require additional commentaries:

483

484 A) According to Taverne (2006a, p.23, ch. 31), *A. tyleri* has two rows of scutes on each side
485 of the body (one on the abdomen and the other above the vertebral column); however, he
486 realized that his fossils have no more than two scale rows exposed; therefore, he
487 suggested that these scutes could be organized only in one row in each side of the trunk.
488 In *A. gonzalezae* sp. nov., there is only one row of scutes in both trunk flanks, which
489 supports Taverne's alternative explanation (Figs. 2, 3).
490 B) Taverne (2006a, p.23, ch. 21) described four series of accessory bones on each side of
491 the vertebral column of *A. tyleri,* which are caudally extended just from behind the skull;
492 in the trunk. His “supraepineurals” are the longest (and probably the widest) of these
493 bones; the epineurals are shorter (and thread-like) and lie just above the centra; the
494 epipleurals are below the centra; his “infraepipleurals” are elongated bones near the
495 ventral body edge. Unfortunately, this author did not provide accurate illustrations of
496 these bones; however, based on his descriptions and his figure 7, we identified these as
497 those described here as predorsals, epipleurals, and probably ribs and epineurals,

498 respectively (Figs. 4, 5). This observation confirms that *Apuliadercetis* species share the
499 occurrence of epipleurals from the most anterior centra, confirming its belonging to
500 Aulopiformes.

501 C) Taverne (2006a, p.23, ch. 23) claimed that the pterygiophore 1 of the dorsal and anal
502 fins in *A. tyleri* have an exceedingly long anterior horizontal process. Although this
503 character has been ignored in the most recent phylogenetic studies, in which this is
504 described as "the different shape of the first dorsal pterygiophore" (Silva and Gallo,
505 2011; Vernygora et al., 2018; Alvarado-Ortega and Díaz-Cruz, 2021). The proximal
506 pterygiophores 1 of anal and dorsal fins is elongated (at least equal to four centra long)
507 in *Apuliadercetis*, *Caudadercetis* Taverne, 2006b, and *Dercetoides* Chalifa, 1989.
508 Besides, in *Hastichthys* Taverne, 1991, only the dorsal proximal pterygiophore 1 is
509 elongated (Chalifa, 1989, fig. 1; Taverne, 2006a, b; Alvarado-Ortega and Díaz-Cruz,
510 2021, fig. 6), while in other dercetids these bones are not distinctively elongated. The
511 distribution of these pterygiophores anteriorly long among dercetids requires additional
512 research because this could be the evolutionary preamble of the development of wings in
513 such pterygiophores, as those seen only in *Apuliadercetis* and *Caudadercetis* (Figs. 7B,
514 9).

515 D) Taverne (2006a, p.23, ch. 20) discovered the presence of extremely reduced neural
516 spines (to petite structures) in those neural arches located below the dorsal
517 pterygophores in *A. tyleri*. Here, this character is confirmed in *A. gonzalezae* sp. nov.
518 (Figs. 9, 7B); no other dercetid shares this feature. The potential autapomorphic value of
519 this diagnostic feature of *Apuliadercetis* is obscured because such neural arches are
520 unknown in *Caudadercetis*, the other genera with the proximal pterygiophore 1
521 hypertrophied (elongated and winged).

E) Taverne (2006a, p. 23, ch. 30) recognized only 17 principal rays in the caudal fin of *A. tyleri*. Again, among dercetids, this character is shared only by *A. gonzalezae* sp. nov. (Fig. 10) and *Caudadercetis* (Taverne, 2006b, fig. 7).

F) Taverne (2006a, p. 23, ch. 19) stated that the pelvic bones of *A. tyleri* are fused into a small single plate, in which the medial caudal processes are lost. This character is also present in *A. indeherbergei* (Taverne and Gooleaerts, 2015, fig. 20); however, *A. gonzalezae* sp. nov. and the dercetids these bones are not fused (Figs. 4, 8C-D).

Into the family, the genus *Apuliadercetis* differs from other dercetids in a combination of three features that includes the presence of a single row of flank scutes plus; the straight contact between the ventral and dorsal hypural plates; and the presence of a long lower jaw (Taverne, 2006b; Silva and Gallo, 2011; Vernygora et al., 2018; and Alvarado-Ortega and Díaz-Cruz, 2021). Recent studies concluded that the presence of a convolute or sinuous suture between the dorsal and ventral hypural plates represents a synapomorphy of most derived dercetids, including *Hastichthys*, *Dercetoides, Rhynchodercetis* Arambourg, 1943, and *Nardodercetis* Taverne, 2005a. On the contrary, in *Apuliadercetis* and *Dercetis* Munster and Agassiz, 1833 (in Agassiz, 1833), these plates display a simple straight contact. The hypural plates are unknown in other dercetids. Although *Caudadercetis* has been indicated as possessing the convolute suture between the hypural plates; we consider that this fish shows a peculiar condition that could have been developed independently, in which the hypural plates are tightly integrated through a deep zigzagging suture.

Besides, *Caudadercetis* shares with *Hastichthys*, *Dercetoides, Nardodercetis*, *Rhynchodercetis*, and *Apuliadercetis* the presence of one row of flank scutes; on the contrary, the body is naked in *Candelarhynchus* Vernygora, Murray, Luque, Parra Ruge,

546 and Páramo, 2018, while there are two scute rows in each flank of the body of *Dercetis*,
547 *Benthesikyme* White and Moy-Thomas, 1940; *Cyranichthys* Taverne, 1987; *Ophiodercetis*
548 Taverne, 2005b; *Brazilodercetis* Figuereido and Gallo, 2006; *Pelargorhynchus* von der
549 Marck, 1858; and *Scandadercetis* Taverne, 2005b.

550 Among dercetids, the length of the lower jaw is variable; this may be as long as the
551 rostrum or shorter. *Apuliadercetis gonzalezae* sp. nov. shares a long jaw that is the most
552 frequent condition found in the family. The lower jaw is short in *Brazilodercetis*,
553 *Candelarhynchus*, *Hastichthys*, *Nardodercetis*, *Rhynchodercetis*, as well as in *Leccedercetis*
554 Taverne 2008. The length of the lower jaw is unknown in *Cyranichthys*.

555 Summarizing the features discussed above, we conclude that *Apuliadercetis* and
556 *Caudadercetis* are close similar. These genera share two features that are absent in other
557 dercetids, the first anal and dorsal proximal pterygiophores are hypertrophied (elongated
558 and winged) and 17 principal caudal-fin rays; and probably these also share the reduction of
559 those neural arches below the dorsal fin. Despite this, the comparison between the nominal
560 species of these genera highlights some peculiar differences (Table 2). Unfortunately, the
561 dorsal view of the head and a large part of the middle part of the trunk are unknown in the
562 single species of *Caudadercetis*, *C. bannikovi* Taverne, 2006b; and at the same time, *A.*
563 *indeherbergei* was described based on a specimen that only preserves part of the dorsal
564 surface of the skull, fragments of both girdles, some vertebrae, and numerous disarticulated
565 scutes. *Caudadercetis bannikovi* has more anal rays (23), which duplicate those of *A. tyleri*
566 (12) and about one-third more than *A. gonzalezae* sp. nov. (16). The pectoral fin of *C.*
567 *bannikovi* shows fewer rays (9) than those exhibit in *A. tyleri* (14-15) and *A. gonzalezae* sp.
568 nov. (12). The vertebral column of *C. bannikovi* consists of approximately 40 abdominal
569 plus 30 caudal centra; these amounts are slightly higher than those observed in *A. tyleri* (38-

35 plus 29-28) but in comparison with *A. gonzalezae* sp. nov., the number of abdominal centra is slightly lower (41-42) and that of the caudal centra is noticeable lower (22-23). Teeth in bones of both jaws and the palatine are irregularly sized in *C. bannikovi* and *A. tyleri,* but in *A. gonzalezae* sp. nov. these are of the same size. The composition of the caudal compound centra is different in all these species; the urals 1 and 2 are fused with the dorsal hypural plate in *A. tyleri*; and the preural 1, urals 1 and 2, the dorsal hypural plate are fused in *A. gonzalezae* sp. nov.; and only the pleural 1 and u1 are fused in *C. bannikovi*. Finally, the most significant difference that supports the separation of these species into two genera is related to the shape of the interhypural suture, which is straight in at least two species of *Apuliadercetis* and is zigzagging in *C. bannikovi*.

The same data set (Table 2) shows that *Apulidaercetis gonzalezae* sp. nov. differs from its allied European species because its pelvic bones are not fused. Additionally, *A. gonzalezae* sp. nov. differs from *A. tyleri* because its jaw and palatine have teeth of regular size, the dorsal fin has a long dorsal stay, the pelvic bones are unfused, and has fewer pectoral rays (12) and more anal rays (16); on the contrary, *A. tyleri* has teeth of irregular size, no dorsal fin stay, fused pelvic bones, more pectoral rays (14-15), and less anal rays (12). Finally, *A. gonzalezae* sp. nov. also differs from *A. indeherbergei* in the presence of a long supraoccipital crest and elongated pterotic bones, and in the lack of contact between the epioccipital (= epiotic in Taverne, 2006, fig. 6) and parietal bones, which are features also present in *A. tyleri.* In contrast, in *A. indeherbergei* the supraoccipital crest and pterotic bone are short, and there is no epioccipital-parietal contact.

4.2. Notes on the biogeography of dercetids

Temporary and geographical distribution of the family Dercetidae is limited to Cenomanian-Danian deposits of Europe, the Middle East, central and northern Africa, North America, and central and northern South America (e.g. Agassiz, 1833; Alvarado-Ortega and Díaz-Cruz, 2021; Alvarado-Ortega et al., 2020a, b; Arambourg, 1954; Dalla Vecchia and Tentor, 2004; Blanco et al., 1998, 2001; Casier, 1965; Davis, 1890; Figueiredo and Gallo, 2006; Forey et al., 2003; Friedman, 2012; Goody, 1969; Marck, 1858; Pictet 1850; Taverne 2006a; Vernygora et al., 2018; Wallaard et al., 2019; Woodward, 1901). The discovery of the fossils in these regions, today widely separated by the Atlantic Ocean, suggests that this family was originated during the early Cenomanian in the shallow marine environments of a relatively smaller region within the realm of the Tethys Sea, survived the Cretaceous-Paleogene Extinction Event, and was finally extinct during the Danian. Apparently, until their extinction, the dercetids inhabited the same marine regions, which were progressively separated during the late Cretaceous due to the opening of the Atlantic Ocean.

Until 1998, the fossil record of this family was limited to the eastern Tethys Sea region. More recently these fishes have been discovered in the deposits of the western region of such a sea, in Mexico, Colombia, and Canada. A single Canadian specimen, probably to be related to the genus *Dercetis*, from the Campanian deposits of the Bearpaw Formation, Alberta, was recently reported by Chida et al. (2020). The single specimen so far known from the Turonian deposits of the San Rafael Formation, Departament of Boyacá, was named *Candelarhynchus padillai* Vernygora, Murray, Luque, Parra Ruge, and Páramo Fonseca, 2018.

In America, the Mexican fossil record of derectids is the most diverse and abundant. Besides the species described in this manuscript; this record includes those fishes from the

Turonian deposits of the Vallecillo quarry, Nuevo León, reported by Blanco et al. (1998) that subsequently were described as *Rhynchodercetis regio* Blanco and Alvarado-Ortega, 2006. Later, *R. regio* was suggested as synonymous junior with *Rynchodercetis yovanovitchi* Arambourg, 1943 (Giersch, 2014) and recently renamed as *Hastichthys regio* by Alvarado-Ortega and Díaz-Cruz (2021). Additional specimens attributable to the genus *Hastichthys* were discovered in the Turonian strata of the Las Bocas quarry, Guerrero (Alvarado-Ortega and Díaz-Cruz, 2021). A second species of this genus, *Hastichthys totonacus* Alvarado-Ortega-Díaz-Cruz, 202, was recently discovered in the Turonian deposits of the Huehuetla quarry, Puebla. Alvarado-Ortega et al. (2020b) reported the presence of an indeterminate specimen of *Dercetis* from the Turonian deposits of the San José de Gracia, Puebla. Moreover, other indeterminate dercetids are present in the Early Cenomanian limestones of the El Chango quarry (Chiapas), the Turonian deposits of Xilitla (San Luis Potosi), and the Campanian deposits of the Tzimol quarry (Chiapas) (Blanco-Piñón et al., 2006; Alvarado-Ortega, pers. obs.).

Today, it is desirable the establishment of a biogeographical hypothesis capable to reveal the processes that drawn the temporal and geographical patterns of the dercetids. To achieve such an objective, some tasks must be solved first including the description and taxonomical determination of a good number of putative dercetids from America, Africa, and the Middle East and the finding of a satisfactory phylogenetic hypothesis of the group. In America, the fossil record of this family seems to be scarce; however, Mexico has an increasing number of representatives of this group.

Although South American dercetids represent the monospecific Turonian genera (*Candelarhynchus* and *Brazilodercetis*), the Mexican dercetids have important biogeographical implications because these reveal two important facts: 1) Since the

642 Cenomanian, the dercetids were widely distributed within the Tethys Sea, from the Middle
643 East to Mexico. 2) Along the Late Cretaceous, the dercetids were active elements in the
644 marine biotic interchange between eastern and western regions of the Tethys Sea, even in
645 the second part of the Late Cretaceous, when the opening of the Atlantic Ocean had already
646 marked considerable distances and deep ocean conditions between the shallow marine
647 environment of America and Europe-Middle East-Africa.

648 The eastern-western marine biotic interchange of the Tethys Sea was established since
649 the Jurassic and continued up to the Cretaceous (e.g. Smith, 1983, Hallam, 1983;
650 Damborenea, 2000; Gasparini and Fernández, 2005; Cavin, 2008). This biotic process
651 involved marine reptiles (ichthyosaurs, metriorhynchids, and pliosaurs) and fishes
652 (lepisosteiforms, macrosemiids, ophiophsids, ichthyodectiforms, ellimmichthyiforms, and
653 enchodontids, among others) recently described from different Mexican Jurassic and Early
654 Cretaceous paleontological sites (e.g. Baños-Rodríguez et al., 2020; Barrientos-Lara et al.,
655 2015, 2016, 2018; Blanco-Piñón, 2003; Brito et al., 2017; Cantalice et al., 2019; Díaz-Cruz
656 et al., 2020; Fielitz and González-Rodríguez, 2010; Giersch, 2014; González-Rodríguez et
657 al., 2004, 2016; Than-Marchese et al., 2020). An important pending task, beyond the scope
658 of the present work, is to carry out a comprehensive biogeographic study to include
659 vertebrate and invertebrate marine taxa with allied species and genera distributed in the
660 western and eastern regions of the Tethys Sea.

661

662 **4. Conclusions**

663

664 The genus *Apuliadercetis* consists of three valid nominal Late Cretaceous species, *A.*
665 *tyleri* and *A. indeherbergei* from European marine deposits, as well as *A. gonzalezae* sp.

666 nov. that from the Campanian marine deposits of the Angostura Formation exploited in the
667 Tzimol quarry, near Ochuxhob, Chiapas, Mexico. The erection of this new species is based
668 on the analysis of 10 relatively well-preserved specimens, including complete skeletons.
669 The features discussed here support the inclusion of these specimens into the order
670 Aulopiformes, family Dercetidae, and genus *Apuliadercetis*. The distinctive characters of *A.*
671 *gonzalezae* sp. nov. were uncovered in a comparative exercise that involves the nominal
672 species of *Apuliadercetis* and *Caudadercetis*.

673 The discovery of *A. gonzalezae* sp. nov. is highly significative because its type series
674 includes specimens comparatively better preserved than those of the other species of
675 *Apuliadercetis*, which enables the record of fine anatomical details for the genus. This
676 achievement also significantly expands the geographical distribution of *Apuliadercetis*
677 during the Late Cretaceous, from the eastern Tethys Sea deposits in Europe to the shallow
678 marine deposits of Mexico that once was the western margin of this Mesozoic Sea.

679

680 **Acknowledgments**

681 We are in debt with the institutions and people that made this research possible. We owe
682 our gratitude to local workers of the Tzimol quarries and our students for their help during
683 the field season. Mr. J.M. Contreras helped us with the photos included in this work. The
684 manuscript was improved with the valuable suggestions provided by Alison Murray and an
685 anonymous reviewer. Financial support for this research was provided by the UNAM
686 (grants DGAPA-PAPIIT IN 209017, and IN 110920). JADC was supported by the
687 CONACyT through the doctoral fellowship 632640.

688

689 **References**

690

691 Adkins,W.S., 1930. New rudistids from the Texas and Mexican Cretaceous. The University
692 of Texas Bulletin 3001: 77-100.

693 Agassiz, L., 1833, Recherches sur les poisons fossils, volume 1 (preface dated in1833):
694 Neuchâtel, Universitat Neuchâtel.
695 https://www.biodiversitylibrary.org/item/23069#page/7/mode/1up

696 Alvarado-Ortega, J., Cantalice, K.M., Martínez-Melo, A., García-Barrera, P., Than-
697 Marchese, B.A., Barrientos-Lara, J.I., Díaz-Cruz, J.A., 2020a. Tzimol, a Campanian
698 marine paleontological site of the Angostura Formation near Comitán, Chiapas,
699 southeastern Mexico. Cretaceous Research 107: 104279.
700 https://doi.org/10.1016/j.cretres.2019.104279.

701 Alvarado-Ortega, J., Cantalice, K.M., Díaz-Cruz, J.A., Castañeda-Posadas, C., Zavaleta-
702 Villareal, V., 2020b. Vertebrate fossils from the San José de Gracia quarry, a new Late
703 Cretaceous marine fossil site in Puebla, Mexico. Boletín de la Sociedad Geológica
704 Mexicana 72, 1-21. https://doi.org/10.18268/BSGM2020v72n1a160819.

705 Alvarado-Ortega, J., Díaz-Cruz, J.A., 2021. *Hastichthys totonacus* sp. nov., a North
706 American Turonian dercetid fish (Teleostei, Aulopiformes) from the Huehuetla quarry,
707 Puebla, Mexico. Journal of South American Earth Sciences 105, 102900.

708 Arambourg, C., 1943. Note préliminaire sur quelques poissons fossiles nouveaux. Bulletin
709 de la Société géologique de France, 5(4-6), 281-288.

710 Arambourg, C., 1954, Les poissons crétacés du Jebel Tselfat (Maroc). Moroc, Éd. du
711 Service géologique du Maroc.

712 Baldwin, C.C., Johnson, G.D., 1996. Interrelationships of Aulopiformes. pp. 255-404 in:
713 Stiassny, M.L., Parenti, L.R., Johnson, G.D. (Eds.), Interrelationships of Fishes.
714 Academic Press.
715 Baños-Rodríguez, R.E., González-Rodríguez, K.A., Wilson, M.V., González-Martínez,
716 J.A., 2020. A new species of *Heckelichthys* from the Muhi Quarry (Albian–
717 Cenomanian) of central Mexico. Cretaceous Research, 110, 104415.
718 Barrientos-Lara, J.I., Alvarado-Ortega, J., Fernández, M.S., 2018. The marine crocodile
719 *Maledictosuchus* (Thalattosuchia, Metriorhynchidae) from the Kimmeridgian deposits of
720 Tlaxiaco, Oaxaca, southern Mexico. Journal of Vertebrate Paleontology 38, 1-14.
721 https://doi.org/10.1080/02724634.2018.1478419
722 Barrientos-Lara, J.I., Fernández, M.S., Alvarado-Ortega, J., 2015. Kimmeridgian
723 pliosaurids (Sauropterygia, Plesiosauria) from Tlaxiaco, Oaxaca, southern
724 Mexico. Revista Mexicana de Ciencias Geológicas 32, 293-304.
725 Barrientos-Lara, J.I., Herrera, L.Y., Fernández, M.S., Alvarado-Ortega, J., 2016.
726 Occurrence of *Torvoneustes* (Crocodylomorpha, Metriorhynchidae) in marine Jurassic
727 deposits of Oaxaca, Mexico. Revista Brasileira de Paleontologia, 19, 415-424. doi:
728 10.4072/rbp.2016.3.07
729 Blanco, A., Alvarado-Ortega, J., 2006. *Rhynchodercetis regio*, sp. nov., a dercetid fish
730 (Teleostei: Aulopiformes) from Vallecillo, Nuevo León State, northeastern
731 Mexico. Journal of Vertebrate Paleontology 26, 552-558. https://doi.org/10.1671/0272-
732 4634(2006)26[552:RRSNAD]2.0.CO;2
733 Blanco, A., López-Oliva J.G., Stinnesbeck, W., Adette, T., Gonzáslez, A., 1998. Vallecillo,
734 Nuevo León: "Fóssil lagerstätte", en el noreste de Mexico. VI Congreso Nacional de

735 Paleontología. Sociedad Mexicana de Paleontología. D.F., Mexico, 11-13 de febrero de
736 1998. Resúmenes, p. 10-11.
737 Blanco, A., Stinnesbeck, W., Oliva, J.G.L., Frey, E., Adatte, T., González, A.H., 2001.
738 Vallecillo, Nuevo León: una nueva localidad fosilífera del Cretácico Tardío en el noreste
739 de México. Revista Mexicana de Ciencias Geológicas 1, 186-199.
740 Blanco Piñón, A., 2003. Peces fósiles de la formación Agua Nueva (Turoniano) en el
741 municipio de Vallecillo, Nuevo León, NE-México. Doctoral dissertation, Universidad
742 Autónoma de Nuevo León, Mexico.
743 Blanco-Piñón, A., Alvarado-Ortega, J., 2005. New dercetid fish (Aulopiformes: Teleostei)
744 from the early Turonian of Vallecillo, NE Mexico, 43-46 pp. in : Poyato-
745 Ariza, J. (Ed.), Fourth International Meeting on Mesozoic Fishes – Systematics,
746 Homology, and Nomenclature, Miraflores de la Sierra, Madrid.
747 Blanco-Piñón, A., Alvarado-Ortega, J., Rojas León, A., Camargo-Cruz, T., 2006. Xilitla,
748 Una asociación fosilífera del Cretácico Superior (Turoniano) de San Luis Postosí,
749 México central. Memorias del X Congreso Nacional de Paleontología, Sociedad
750 Mexicana de Paleontología, Mexico, p. 25.
751 Blot, J., 1987. L'Ordere des Pycnodontiformes. Studi e Ricerche sui Giacimenti Terziari di
752 Bolca, 5, 1-211.
753 Brito, P. M., Alvarado-Ortega, J., Meunier, F. J., 2017. Earliest known lepisosteoid extends
754 the range of anatomically modern gars to the Late Jurassic. Scientific reports 7, 1-8. Doi:
755 10.1038/s41598-017-17984-w
756 Cantalice, K.M., Martínez-Melo, A., Romero-Mayén, V.A., 2019. The paleoichthyofauna
757 housed in the Colección Nacional de Paleontología of Universidad Nacional Autónoma
758 de Mexico. Zoosystematics and Evolution 95, 429. https://doi.org/10.3897/zse.95.35435

759 Casier, E., 1965. Poissons fossiles de la serie du Kwango (Congo). Musee Royal de
760 L'Afrique Centrale, Annales - Serie IN-8 - Sciences Geologiques 50, 1-64.
761 Cavin, L., 2008. Palaeobiogeography of cretaceous bony fishes (Actinistia, Dipnoi and
762 Actinopterygii). Geological Society, London, Special Publications 295, 165-183.
763 Doi: 10.1144/SP295.11
764 Chalifa, Y., 1989. Two new species of longirostrine fishes from the early Cenomanian (late
765 Cretaceous) of Ein-Yabrud, Israel, with comments on the phylogeny of the Dercetidae.
766 Journal of Vertebrate Paleontology 9, 314-328. Doi: 10.1080/02724634.1989.10011765
767 Chida, M., Murray, A.M., Brinkman D.B., Vernygora, O., Kitagawa, H., 2020. A new
768 dercertid fish (Neoteleostei, Aulopiformes) from the Campanian Bearpaw Formation,
769 Alberta, Canada. Proceedings of the 169th Annual Meeting of the Paleontological
770 Society of Japan. General Lecture, p. 35.
771 Consejo de Recursos Minerales, 1999. Monografía Geológico-Minera del Estado de
772 Chiapas. Consejo de Recursos Minerales, Pachuca, Hidalgo, México, 180 p.
773 Dalla Vecchia, F.M., Tentor, M., 2004. Il Carso 85 milioni di anni fa: gli straordinari fossili
774 di Polazzo. Gruppo Speleologico Monfalconense A.d.F, Italy.
775 Damborenea, S.E., 2000. Hispanic Corridor: its evolution and the biogeography of bivalve
776 mollusks. 369-379 p. in: Hall, R.L., Smith, P.L. (Eds.), Advances in Jurassic Research
777 2000. GeoResearch Forum 6. Proceedings of the 5th International Symposium on the
778 Jurassic System, Vancouver, 1998.
779 Davis, J., 1890. On the Fossil Cretaceous Formation of Scandinavia, vol. 4, Scientific
780 Transaction Royal Dublin Society, 2ème série, 391-434 (+ plts. xxxviii-xliv).
781 Díaz-Cruz, J.A., Alvarado-Ortega, J., Carbot-Chanona, G., 2016. The Cenomanian short
782 snout enchodontid fishes (Aulopifomes, Enchodontidae) from Sierra Madre Formation,

783 Chiapas, southeastern Mexico. Cretaceous Research 61, 136–150.
784 https://doi.org/10.1016/j.cretres.2015.12.026
785 Díaz-Cruz, J.A., Alvarado-Ortega, J., Carbot-Chanona, G. 2019. Corrigendum to "Dagon
786 avendanoi gen. and sp. nov., an Early Cenomanian Enchodontidae (Aulopiformes) fish
787 from the El Chango quarry, Chiapas, southeastern Mexico. Journal of South American
788 Earth Sciences 91, 272–284. https://www.sciencedirect.com/science/article/pii/
789 S0895981119304183
790 Díaz-Cruz, J.A., Alvarado-Ortega, J., Giles, S., 2020. A long snout enchodontid fish
791 (Aulopiformes: Enchodontidae) from the Early Cretaceous deposits at the El Chango
792 quarry, Chiapas, southeastern Mexico: A multi-approach study. Palaeontologia
793 Electronica 23(2), a30. https://doi.org/10.26879/1065 palaeo-
794 electronica.org/content/2020/3063-a-long-snout-enchodontid-fish
795 Ferrusquía-Villafranca, I., 1996. Contribución al conocimiento geológico de Chiapas: el
796 área Ixtapa-Soyaló. Boletín del Instituto de Geología 109, 130 p.
797 Ferrusquía-Villafranca, I., Applegate, S.P., Espinosa-Arrubarrena, L., 2000. First Paleogene
798 selachifauna of the middle American-Caribbean Antillean region, La Mesa de Copoya,
799 west-central Chiapas, Mexico -Geologic setting. Revista Mexicana de Ciencias
800 Geológicas 17, 1–23.
801 Fielitz, C., González-Rodríguez, K. A., 2010. A new species of *Enchodus* (Aulopiformes:
802 Enchodontidae) from the Cretaceous (Albian to Cenomanian) of Zimapán, Hidalgo,
803 Mexico. Journal of Vertebrate Paleontology 30, 1343–1351.
804 https://doi.org/10.1080/02724634.2010.501438

Figueiredo, F.J., Gallo, V., 2006. A new dercetid fish (Neoteleostei: Aulopiformes) from the Turonian of the Pelotas Basin, southern Brazil. Palaeontology 49, 445–456. https://doi.org/10.1111/j.1475-4983.2006.00540.x

Forey, P.L., Yi, L., Patterson, C., Davies, C.E., 2003. Fossil fishes from the Cenomanian (Upper Cretaceous) of Namoura, Lebanon. Journal of Systematic Palaeontology 1, 227. Doi: 10.1017/S147720190300107X

Friedman, M., 2012. Ray-finned fishes (Osteichthyes, Actinopterygii) from the type Maastrichtian, the Netherlands and Belgium. Scripta Geologica, Special Issue 8, 113-142.

Gasparini, Z., Fernández, M., 2005. Jurassic marine reptiles of the Neuquén Basin: records, faunas and their palaeobiogeographic significance. Geological Society, London, Special Publications 252, 279-294. https://doi.org/10.1144/GSL.SP.2005.252.01.14

Giersch, S., 2014. Die Knochenfische der Oberkreidezeit in Nordostmexiko: Beschreibung, Systematik, Vergesellschaftung, Paläobiogeographie und Paläoökologie. PhD thesis, Ruprecht-Karls-Universität Heidelberg, 275 p.

González-Rodríguez, K., Applegate, S.P., Espinosa-Arrubarrena, L., 2004. A New World macrosemiid (Pisces: Neopterygii-Halecostomi) from the Albian of Mexico. Journal of Vertebrate Paleontology 24, 281-289. https://doi.org/10.1671/1862

González-Rodríguez, K.A., Fielitz, Ch., Bravo-Cuevas, V.M., Baños-Rodríguez, E., 2016.Cretaceous Osteichthyan fish assemblage from Mexico. In: Khosla, A., Lucas, S.G. (eds.), Cretaceous Period: Biotic Diversity and Biogeography. New Mexico Museum of Natural History and Science Bulletin 71, 107–119.

827 Goody, P.C., 1969. The relationships of certain upper Cretaceous teleosts with special
828 reference to the myctophoids. Bulletin of the British Museum (Natural History) Geology
829 Series, Supplement 7, 1–255.
830 Hallam, A., 1983. Early and Mid-Jurassic molluscan biogeography and the establishment of
831 the central Atlantic seaway. Palaeogeography, Paleoclimatology, Paleoecology 43, 181-
832 193. https://doi.org/10.1016/0031-0182(83)90010-X
833 Hays, I., 1830. Description of a fragment of the head of a new fossil animal, discovered in a
834 marl pit, near Moorestown. New Jersey Transactions of the American Philosophical
835 Society, series 2 (3), 471-477.
836 Islas-Tenorio, J.J., Ramírez-García, M.G., Moreno-Ruiz, J.P, Gómez-Ávilez, J., 2004.
837 Carta Geológica-Minera, Villahermosa, E15-8, 1:250000: Pachuca, Hidalgo, México,
838 Servicio Geológico Mexicano, 1 mapa e informe, 76 p.
839 Martínez-Amador, H., Rosendo-Brito, B., Fitz-Bravo, C., 2004. Carta Geológico-Minera
840 Tuxtla Gutiérrez E15-11 escala 1:250 000. Estados de Chiapas y Oaxaca, Informe
841 Técnico. Pachuca, Hidalgo, México, Consejo de Recursos Minerales, 106 p.
842 Marck, W. von der, 1858. Über einige Wirbeltiere, Kruster und Cephalopoden der
843 westfälischen Kreide. Zeitschrift der deutschen geologischen Gesellschaft 10: 231–271.
844 Meneses-Rocha, J.J., 2001. Tectonic Evolution of the Ixtapa Graben, an Example of a
845 Strike-slip Basin of Southeastern Mexico: Implications for Regional Petroleum Systems.
846 In: Bartolini, C., Buffler, R.T., Cantu-Chapa, A. (eds.), The western Gulf of Mexico
847 Basin: Tectonics, sedimentary basins, and petroleum systems. The American
848 Association of Petroleum Geologists, Memoir 75, 183–216.
849 Omaña, L., Alencáster, G., 2019. Late-latest Maastrichtian foraminiferal assemblage from
850 the Angostura Platform, Chiapas, SE Mexico: Biostratigraphic, paleoenvironmental and

paleobiogeographic significance. Journal of South American Earth Sciences 91, 203–213. https://doi.org/10.1016/j.jsames.2019.02.004

Patterson, C., Johnson, G.D., 1995. The intermuscular bones and ligaments of teleostean fishes Smithsonian Contribution to Zoology 559, 1-85.

Pictet, F.J., 1850. Description de quelques poisons fossiles du Mont Liban. Jules-Guillaume Fick.

Pons, J. M., Vicens, E., Pichardo, Y., Aguilar, J., Ster, G. A., A-barrera, P. G., Pons, J. M., Vicens, E., Pichardo, Y., Aguilar, J., and Garci, P., 2010. A New Early Campanian Rudist Fauna from San Luis Potosi in Mexico and its Taxonomic and Stratigraphic Significance. Journal of Paleontology, 84(5), 974–995.

Quezada-Muñetón, J.M., 1987. El Cretácico medio-Superior y el límite Cretácico Superior-Terciario inferior en la Sierra de Chiapas. Convención Geológica Nacional de la Sociedad Geológica de México 39, 3–98.

Sánchez Montes de Oca, R., 1979. Geología petrolera de la Sierra de Chiapas. Boletín de la Asociación Mexicana de Geólogos Petroleros 31, 67–97.

Silva, H., Gallo, V., 2011. Taxonomic review and phylogenetic analysis of Enchodontoidei (Teleostei: Aulopiformes). Anais da Academia Brasileira de Ciências, 83(2), 483-511.

Smith, P.L., 1983. The Pliensbachian ammonite *Dayiceras dayiceroides* and Early Jurassic paleogeography. Canadian Journal of Earth Sciences 20, 86-91. https://doi.org/10.1139/e83-008

Taverne, L., 1976. Les téléostéens fossiles du Crétacé moyen de Kipala (Kwango, Zaïre). Annales du Musée Royal de l'Afrique Centrale, Série in-8°, Sciences Géologiques 79: I-XI + 1-50.

874 Taverne, L., 1987. Ostéologie de *Cyranichthys ornatissimus* nov. gen. du Cénomanien du
875 Zaire et de *Rhynchodercetis yovanovitchi* du Cénomanien de l'Afrique du Nord. Les
876 relations intergeneriques et la position systématique de la famille neocrétacique marine
877 des Dercetidae (Pisces, Teleostei). Annales du Musée Royal de l'Afrique Centrale,
878 Rapport Annuel, 93-112.
879 Taverne, L., 1991. New considerations on the osteology and phylogeny of the Cretaceous
880 marine teleost family Dercetidae Biologisch Jaarboek Dodonaea, 58, 94-112
881 Taverne, L., 2005a. Les poissons crétacés de Nardo. 22°. *Nardodercetis vandewallei* gen. et
882 sp. nov. (Teleostei, Aulopiformes, Dercetidae). Bollettino del Museo Civico di Storia
883 Naturale di Verona, Geologia Paleontologia Preistoria, 29, 81–93.
884 Taverne, L., 2005b. Les poissons crétacés de Nardò. 21°. *Ophidercetis italiensis* gen. et sp.
885 nov. (Teleostei, Aulopiformes, Dercetidae). Une solution ostéologique au problème des
886 genres *Dercetis* et *Benthesikyme* (= *Leptotrachelus*). Bollettino del Museo Civico di
887 Storia Naturale di Verona, Geologia Paleontologia Preistoria, 29, 55- 79.
888 Taverne, L., 2006a. Les poissons crétacés de Nardò. 23°. *Apuliadercetis tyleri* gen. et sp.
889 nov. (Teleostei, Aulopiformes, Dercetidae). Bollettino del Museo Civico di Storia
890 Naturale di Verona, Geologia Paleontologia Preistoria, 30, 11–26.
891 Taverne, L., 2006b. Les poissons crétacés de Nardo. 24°. *Caudadercetis bannikovi* gen. et
892 sp. nov. (Teleostei, Aulopiformes, Dercetidae). Considérations sur la phylogénie des
893 Dercetidae. Bollettino del Museo Civico di Storia Naturale di Verona, Geologia
894 Paleontologia Preistoria, 30, 29–50.
895 Taverne, L., 2008. Les poissons crétacés de Nardò. 27◦ *Leccedercetis longirostris* gen. et
896 sp. nov. (Teleostei, Aulopiformes, Dercetidae). Bollettino del Museo Civico di Storia
897 Naturale di Verona, Geologia Paleontologia Preistoria, 32, 3–8.

http://www.museostorianaturaleverona.it/media/_Musei/_StoriaNaturale/_Allegati/Biblioteca/Bollettino/Bollettino%2032/Bollettino%2032%20blu/02_Taverne_3-8.pdf

Taverne, L., Goolaerts, S., 2015. The dercetid fishes (Teleostei, Aulopiformes) from the Maastrichtian (Late Cretaceous) of Belgium and The Netherlands. Geologica Belgica18, 21–30. https://popups.uliege.be/1374-8505/index.php?id=4794

Than-Marchese, B.A., Alvarado-Ortega, J., Matamoros, W.A., Velázquez-Velázquez, E., 2020. *Scombroclupea javieri* sp. nov., an enigmatic Cenomanian clupeomorph fish (Teleostei, Clupeomorpha) from the marine deposits of the Cintalapa Formation, Ocozocoautla, Chiapas, southeastern Mexico. Cretaceous Research 112, 104448. https://doi.org/10.1016/j.cretres.2020.104448.

Vernygora, O., Murray, A.M., Luque, J., Ruge, M.L.P., Fonseca, M.E.P., 2018. A new Cretaceous dercetid fish (Neoteleostei: Aulopiformes) from the Turonian of Colombia. Journal of Systematic Palaeontology 16, 1057–1071. https://doi.org/10.1080/14772019.2017.1391884

Wallaard, J.J.W., Fraaije, R.H.B., Diependaal, H.J., Jagt, J.W.M., 2019. A new species of dercetid (Teleostei, Aulopiformes) from the type Maastrichtian of southern Limburg, the Netherlands. Netherlands Journal of Geosciences 98, e2. https://doi.org/10.1017/njg.2019.1

White, E.I., Moy-Thomas, J.A., 1940. Notes on the nomenclature of fossil fishes. Part II. Homonyms DL. Journal of Natural History 6, 98–103.

Woodward, A.S., 1901. Suborder Apodes. Catalogue of the fossil Fishes. British Museum (Natural History), part 4, 337–340.

922 TABLE AND FIGURE CAPTIONS

923

924 **Table 1.** Comparison of the meristic and morphometrics measurements of the *A.*
925 *gonzalezae* specimens recovered in the Tzimol quarry. Lengths are in millimeters.

926

927 **Table 2.** Comparison of the species of the genus *Apuliadercetis*, including *A. gonzalezae*
928 sp. nov. from the Tzimol quarry. Abbreviatures: dhp, dorsal hypural plate; pu, preural; vhp,
929 ventral hypural plate; u, ural.

930

931 **Figure 1**. Geographical location of the Tzimol quarry, near Comitán de Domínguez,
932 Chiapas, southeastern Mexico (based on Alvarado-Ortega et al., 2020a, fig. 1).

933

934 **Figure 2**. Specimen IGM 11403, holotype of *Apuliadercetis gonzalezae* sp. nov. from the
935 Tzimol quarry. A, Photograph under white light. B, Line drawing of the same specimen.

936

937 **Figure 3**. Paratypes of *Apuliadercetis gonzalezae* sp. nov. photographed under UV light. A,
938 IGM 12947. B, IGM 12948.

939

940 **Figure 4**. The head and anterior part of the trunk of IGM 11403, holotype of
941 *Apuliadercetis gonzalezae* sp. nov. from the Tzimol quarry. A, Photograph under white
942 light. B, Line drawing of A. Abbreviations: aa, anguloarticular; cor, coracoid; den, dentary;
943 epi, epioccipital; epl, epipleural; exo, exoccipital; fr, frontal; hym, hyomandubular; io,
944 infraorbital bone; le, lateral ethmoid; mes, mesethmoid; mtp, metapterygoid; mx, maxilla;
945 op, opercle; pa, parietal; pal, palatine; par, parasphenoid; pcfr, pectoral fin rays; pcrad,
946 pectoral radials; pd, predorsal bone; pmx, premaxilla; pto, pterotic; ptt, posttemporal; pv,

pelvic; pvfr, pelvic fin ray; pvrad, pelvic radials; q, quadrate; r, rib; rar, retroarticular; scl, supracleithrum; sc, scutes; sca, scapula; sl, sclerotic; sop (fgr), infraopercle (fragment); sp, autosphenotic; soc, supraoccipital; the numbers indicate the cranio-caudal position of the vertebrae along the vertebral column.

Figure 5. Head and anterior part of the body of the specimen IGM 12949, paratype of *Apuliadercetis gonzalezae* sp. nov. from the Tzimol quarry. A, Photograph under UV light. B, Line drawing of the same specimen. Abbreviations: aa, anguloarticular; atp, anterior transverse process; boc, basioccipital; br, branchostegal rays; cl, cleithrum; cor, coracoid; den, dentary; ect; ectopterygoid; end, endopterygoid; epl, epipleural; epn, epineural; exo, exoccipital; fr, frontal; hym, hyomandubular; ic; intercalar; iop, infraopercle; io, infraorbital bone; le, lateral ethmoid; na, neural arch; mx, maxilla; op, opercle; pal, palatine; par, parasphenoid; pmx, premaxilla; pop, preopercle; pto, pterotic; ptp, posterior transverse process; ptt, posttemporal; q, quadrate; rar, retroarticular; scl, supraleithrum; sl, sclerotic; sop, subopercle; vo, vomer; the numbers indicate the cranio-caudal position of the vertebrae along the vertebral column; the circular line with two arrows indicates the point where the spine was twisted (hence, the anterior vertebrae show the lateral surface while the posterior vertebrae show the ventral surface).

Figure 6. Head of the specimen IGM 12948, paratype of *Apuliadercetis gonzalezae* sp. nov. from the Tzimol quarry. A, Photograph under white light. B, Close up of the anterior part of the ethmoid region showing the palatine teeth and longitudinal grooves ornamenting the dentary (black arrows in B). Abbreviations: den, dentary; fr, frontal; pal, palatine.

971 **Figure 7**. Details of the head and trunk of *Apuliadercetis gonzalezae* sp. nov. from the
972 Tzimol quarry. A, Closeup of the rostrum of IGM 12950 under white light, showing its
973 ornamentation (black arrows). B, Closeup of the abdominal region of the trunk of IGM
974 12951 under white light. C, Closeup of ceratohyals of IGM 12952 under white light. D,
975 Closeup of the anterior part of the anal fin of IGM 12948 under UV light. Abbreviations:
976 aa, anguloarticular; adp, anal distal pterygiophore; afpr, anal fin anterior procurrent ray; afr,
977 anal fin ray; app, proximal anal pterygiophore; atp, anterior transverse process; cha,
978 ceratohyal anterior; chp, ceratohyal posterior; cl, cleithrum; dfr, dorsal fin ray; dfs, dosal fin
979 stay; dpp, dorsal proximal pterygiophore; fr, frontal; hym, hyomandibular; iop,
980 infraopercle; mes, mesethmoid; na+ns, neural arch with neural spine; na-ns, neural arch
981 lacking neural spine; op, epercle; pd, predorsal; pmx, premaxilla; ptp, posterior transverse
982 process; pvf; pelvic fin; r, rib; sl, sclerotic; black arrows in A show the longitudinal and
983 straight grooves that ornament the premaxillae; black arrows in C show the branchiostegal
984 rays.
985
986 **Figure 8**. Paired fins and girdles bones of *Apuliadercetis gonzalezae* sp. nov. from the
987 Tzimol quarry. A, Closeup of the pectoral girdle and fin of the paratype IGM 12950,
988 photographed under white light. B, Line drawing of A. C, Closeup of pelvic girdle and fins
989 of the paratype IGM 12953 photographed under under UV light. D, Idealized drawing of C.
990 Abbreviations: cl, cleithrum; cor, coracoid; pcfr, pectoral fin ray; pcrad, pectoral radials;
991 pv, pelvic bone; pvfr, pelvic fin ray; pvrad, pelvic radial; sca, scapula.
992
993 **Figure 9**. Unpaired fins under white light of IGM 12950, paratype of *Apuliadercetis*
994 *gonzalezae* sp. nov. from the Tzimol quarry. A, Closeup of the dorsal fin photographed

995 under white light. B, Closeup of the anal fin photographed under white light. C, Line
996 drawing of A. D, Line drawing of B. Abbreviations: adp, anal distal pterygiophore; afr, anal
997 fin ray; amp, anal medial pterygiophore; app, proximal anal pterygiophores; dfr, dorsal fin
998 ray; dfs, dorsal fin stay; dpp, dorsal proximal pterygiophore; epn, epineurals; epl,
999 epipleurals; na, neural arch; ns, neural spine; pafr, procurrent anal fin ray; pd, predorsal;
1000 pdfr, procurrent dorsal fin ray; sc, scute; numbers indicate the cranio-caudal position of the
1001 vertebrae along the vertebral column.
1002
1003 **Figure 10**. Caudal fin of the specimen IGM 12953, paratype of *Apuliadercetis gonzalezae*
1004 sp. nov. from the Tzimol quarry. A, Photograph under white light. B, Line drawing of the
1005 same specimen. Abbreviations: cc, compound caudal centhrum; dhp, dorsal hypural plate;
1006 ep, epural; hspu, haemal spine of preural; nspu, neural spine of preural; pu; preural
1007 centhrum; pcfr, procurrent caudal fin ray; php, parhypural; ur, ural; vhp, ventral hypural
1008 plate; I, unbranched and unsegment principal caudal fin ray (in ventral and dorsal lobe); 1-
1009 8, branched and segmented principal caudal fin ray of the dorsal lobe of caudal fin (in
1010 ventral and dorsal lobe).
1011
1012 **Figure 11**. Recent phylogenetic hypotheses of the family Dercetidae showing the position
1013 of the genus *Apuliadercetis*.

	IGM 11403	IGM 12947	IGM 12948	IGM 12949	IGM 12950	IGM 12951	IGM 12952	IGM 12953	IGM 12954	IGM 12955
Standard length	128.5	≈122	118.2	-	≈120	-	≈116	≈122	102.6	≈114.4
Head length	38.4	≈35	33.4	≈41.4	-	-	≈30	-	30	≈30
% SL	29.8	-	28.2	-	-	-	-	-	29.2	-
Preorbital length	24.3	23.2	20	≈24	-	≈25	≈18	-	18.2	-
% SL	18.9	-	17	-	-	-	-	-	17.8	-
Predorsal length	68.8	≈64.7	-	-	-	-	-	-	56.7	-
% SL	53.5	-	-	-	-	-	-	-	55.2	-
Dorsal fin length	4	3.7	-	-	3.6	-	-	-	3.5	-
% SL	3.1	-	-	-	-	-	-	-	3.4	-
Preanal length	105.8	-	-	-	-	-	-	-	85.1	≈94
% SL	82.3	-	-	-	-	-	-	-	82.9	-
Anal fin length	10.2	-	-	-	9	-	-	-	-	-
% SL	7.9	-	-	-	-	-	-	-	-	-
Pectoral fin rays	12	+7	-	-	12	+9	+10	12	+11	-
Pelvic fin rays	7	7	7	-	6	7	-	7	6	-
Dorsal fin rays	ii+6	?+6	-	-	ii+6	7	6	-	-	-
Anal fin rays	?+16	-	ii+(9?)	-	ii+16	-	-	ii+(8?)	i+(11?)	10?
Total vertebrae	64	+50	64	-	64	-	-	64	64	64
Abdominal centra	41	+33	-	-	41	-	-	42	41	40?

1

	Caudadercetis bannikovi (3)	*Apuliadercetis tyleri* (22)	*Apuliadercetis gonzalezae sp. nov.* (10)	*Apuliadercetis indeherbergei* (1)
Supraoccipital crest	-	Long	Long	Short
Pterotic	-	Long	Long	short
Contact epioccipital-parietal	-	Absent	Absent	Present
Pelvic bones	-	Fused	Not fused	Fused
Teeth size	Irregular	Irregular	Regular	-
Dorsal fin rays	-	ii-iii+7	ii+6-7	-
Dorsal fin stay	-	Absent	Present	-
Anal fin rays	iii+23	iii-iv+12	ii+16	-
First anal and dorsal pterygiophores	Elongated and winged	Elongated and winged	Elongated and winged	-
Neural spines below the dorsal pterygiophores	-	Extremely reduced	Extremely reduced	-
Pectoral fin rays	9	14-15	12	-
Pelvic bones	-	Fused	Unfused	Fused
Pelvic fin rays	-	6	6-7	-
Total vertebrae	≈70	63-67	64	-
Abdominal vertebrae	≈40	35-38	41-42	-
Composed caudal centrum	pu1+u1	u1-2+dhp	pu1+u1-2+dhp	-
Suture dhp-vhp	zigzag	straight	straight	-

1

CAPÍTULO VII: DISCUSIÓN GENERAL Y CONCLUSIONES

Diversidad de encodóntidos

Previo a este trabajo, el registro de encodóntidos en México era notablemente limitado. Estos peces fósiles estaban representados en distintos sitios de Chiapas (Matrichthiano), Coahuila (Turoniano), Guerrero (Turoniano), Hidalgo (Albiano-Cenomaniano), Nuevo León (Turoniano), San Luis Potosí (Turoniano) y Tamaulipas (Turoniano); sin embargo, en general, su diversidad e identidad taxonómica aún no se había determinado con precisión (Cuadro 2, Introducción). Aunque la mayoría de estos reportes están basados en material fragmentario, fuertemente desarticulado, o incluso solo por dientes aislados; estos fósiles muestran un patrón general de distribución geográfica y diversidad del grupo en México. Entre estos reportes, destacan por su abundancia y buen estado de preservación, el registro de *Enchodus* cf. *venator* recuperados en estratos Cenomanianos-Turonianos de Vallecillo, Nuevo León (Ifrim et al., 2007; Giersch, 2014), así como, el de *Enchodus zimapanensis*, un encodóntido de los estratos Albianos-Cenomanianos en Muhi, Hidalgo (Fielitz y González-Rodríguez, 2010).

Los descubrimientos recientes de los estratos fosilíferos del Turoniano en canteras de Huehuetla y San José de Gracia, en Puebla, han incrementado el registro de encodóntidos en México (Alvarado-Ortega et al., 2019, 2020a). De igual manera, este registro se ha enriquecido con al menos dos encodontoides descubiertos en los sedimentos Campanianos de la cantera Tzimol, en Chiapas (Alvarado-Ortega et al., 2020b). En la Cantera San José de Gracia se reportó la presencia de *Dercetis* y de *Enchodus.* En Huehuetla, fue descrito el dercétido, *Hastichthys totonacus* y restos muy mal conservados de un posible representante de *Enchodus.* En tanto que, en Tzimol, se describió el primer representante americano del género

Apuliadercetis, *A. gonzalezae*, así como abundantes ejemplares del género *Enchodus*, cuya determinación taxonómica a nivel específico se encuentra en desarrollo.

Si a los registros anteriormente mencionados se adicionan las investigaciones sobre encodóntidos de la cantera el Chango, incluidos los del presente trabajo, notamos que *Unicachichthys multidentata* (Díaz-Cruz et al., 2016), *Veridagon avendanoi* (Díaz-Cruz et al., 2019c, 2019b) y *Vegrandichthys coitecus* (Díaz-Cruz et al., 2020) son representantes distintivos y únicos de esta región geográfica. Estos taxa se suman a la presencia de *Saurorhamphus* sp. y *Enchodus* sp. en este mismo sitio (Alvarado-Ortega et al., 2009; Díaz-Cruz et al., 2016), los cuales también son representantes comunes en el extremo oriental del mar de Tethys (Bannikov and Bacchia, 2005; Cavin et al., 2012). En suma, la riqueza de encodóntidos a nivel genérico en El Chango ha superado a la de otros sitios del Cretácico Tardío del mundo (e.g. cantera Bomba, Cinto Euganeo, Italia; Amalfitano et al., 2020), y comienza a rivalizar directamente con la riqueza encontrada en localidades del Medio Oriente, particularmente con los afloramientos del Cenomaniano Medio de Jerusalén (Chalifa, 1985), en donde la riqueza de encodóntidos es la mayor del planeta. La riqueza de encodóntidos en estas canteras está representada en total por siete géneros (Forey et al., 2003), de los cuales, *Dercetoides* y *Parenchodus* son exclusivos de estos afloramientos, mientras que los registros del Chango incluyen cinco géneros de encodóntidos con tres géneros típicos de la localidad. Actualmente, se han preparado e identificado otros taxa miembros de Enchodontoidei del Chango que aún esperan descripción formal y determinación taxonómica a nivel específico (Díaz-Cruz y Alvarado-Ortega, 2018). Entre estos taxones se identifica preliminarmente a *Apateopholis* sp. con base en varios ejemplares de cuerpo completo (Figura 1). Con este registro, la riqueza genérica y específica de la cantera podría igualar e incluso superar a la

riqueza de las localidades de Jerusalén, y convertirse en el afloramiento con mayor número de encodóntidos en el mundo.

Otros avances en el estudio de los encodóntidos de México están representados por los descubrimientos realizados en diferentes canteras localizadas en las cercanías del municipio de Melchor Múzquiz, Coahuila. Las investigaciones que se conducen en estos afloramientos han documentado una abundante riqueza y diversidad de encodóntidos (Blanco-Piñón et al., 2004) de diferentes edades del Cretácico Tardío. Además, gracias al elevado número y buen estado de preservación de los especímenes rescatados, en algunos de ellos se pueden distinguir aspectos de su ecología trófica y aparente relación taxonómica con especies registradas en la porción superior del Cretácico Tardío de Estados Unidos (Figura 2) (Porras-Múzquiz et al., 2019). Otros ejemplares de las localidades de Múzquiz consisten en morfotipos con las características típicas de los miembros de Enchodontoidei como son: ausencia de escamas en el cuerpo, ornamentación típica en los huesos dérmicos y presencia de escudos dorsales. Sin embargo, en este momento es difícil asignarlos a un taxón reconocido de encodóntidos gracias a su variación morfológica singular, pudiéndolos considerar como potenciales taxones nuevos en espera de su estudio formal (Figura 3).

Figura 1. Encondóntidos de la Cantera el Chango preparados y en espera de descripción formal. A) Ejemplar IHNFG-5815, *Enchodus* sp. y B) IHNFG-5923, *Apateopholis* sp.; imagen reflejada horizontalmente para presentar ambos ejemplares en la misma dirección. Escala igual a 1 cm.

Por otra parte, la mayoría de los afloramientos epicontinentales del Cretácico que cuentan con un trabajo relativamente sistemático de explotación, con registro de algún taxón de Enchodontoidei, han demostrado poseer asociaciones con dos o más miembros del grupo. En México, esto queda ejemplificado en los trabajos conducidos en la cantera Muhi, Zimapán, Hidalgo con la presencia de taxones como *Enchodus* o *Ichthyotringa* (Fielitz y Gonzalez-Rodríguez, 2008; Fielitz y González-Rodríguez, 2010); en Vallecillo, Nuevo León, con reportes de *Enchodus* y *Hastichthys* (antes *Rhynchodercetis*) (Giersch et al., 2008; Giersch, 2014; Alvarado-Ortega y Díaz-Cruz, 2021); Tzimol, Chiapas, con *Apuliadercertis y Enchodus*

(Alvarado-Ortega et al., 2020b). Este mismo fenómeno se puede identificar en afloramientos de otras regiones del mundo como Namoura, Líbano de donde se han reportado *Enchodus*, *Eurypholis*, o *Rhynchodercetis* (Forey et al., 2003) o la cantera Bomba, Cinto Euganeo, Italia con registros de *Enchodus*, *Ichthyotringa*, o *Rhynchodercetis*. La cantera El Chango, Chiapas también exhibe esta condición y, además, como se documenta en la presente investigación, se caracteriza por contener un número relativamente alto de taxa exclusivos.

Los resultados de este trabajo aportan evidencia para asegurar que el extremo Occidental del Mar de Tethys (que más tarde dio origen al proto-Atlántico Norte) fungió como una región clave para la especiación y diversificación de los encodóntidos desde el Cretácico Medio, etapa en la que más de la mitad del territorio mexicano formaba parte de un mar somero (Cao et al., 2017), manteniéndose así en algunas regiones hasta comienzos del Paléogeno (Figura 4A). En este contexto, los afloramientos del Cretácico de México con presencia de encodóntidos corresponden principalmente al Turoniano, aunque se mantiene una representación para todas las edades del Cretácico Tardío, con excepción del Santoniano (Figura 4B). El alcance temporal de las localidades mexicanas comprende prácticamente toda la existencia que los encodóntidos tuvieron en el mundo hasta su extinción a finales del Cretácico (Friedman, 2009). Existen registros en el mundo sobre la presencia de encodóntidos antes y después del Cretácico superior; no obstante, estos corresponden principalmente a dientes aislados y su determinación en ocasiones es incompleta o cuestionable (Rana, 1990; Kriwet, 2003; Coelho, 2004; Rana et al., 2004; Tewari et al., 2010). Dada la elevada cantidad de material, el excelente estado de preservación, y la temporalidad que abarcan los encodóntidos mexicanos, su estudio es crucial para comprender sus tendencias evolutivas y las relaciones que mantuvieron con sus congéneres en otras regiones del mundo.

Figura 2. Ejemplares pertenecientes al género *Enchodus sp* recuperados de la cantera Piedritas, Múzquiz, Coahuila. A) MUZ 3009 ejemplar con neurocráneo desarticulado y pobremente preservado. B) MUZ 574 ejemplar con aletas pectorales alargadas y rastros del contenido estomacal. En esta figura, el esqueleto caudal no está preservado en ninguno de los ejemplares.

Observaciones taxonómicas y filogenéticas en Enchodontoidei

A la fecha, dos propuestas filogenéticas de Enchodontoidei han servido como base para evaluar la posición filogenética de los nuevos taxones que se han descubierto. Por un lado, la hipótesis filogenética de Fielitz (2004) explora las relaciones de parentesco de formas fósiles de la familia Enchodontidae respecto a formas recientes de Aulopiformes. Por el otro, la propuesta de Silva y Gallo (2011) se centra en evaluar las relaciones de Enchodontoidei *sensu* Nelson (1994), en la que se incluyen diferentes familias fósiles, entre ellas Apateopholidae, Dercetidae o Enchodontidae. Considerando estos hechos, el objetivo de cada una de estas

filogenias es diferente y, por lo tanto, las hipótesis de homología primaria también varían entre ellas. A pesar de estas diferencias, es notable cómo la naturalidad de Enchodontidae se recupera en ambos trabajos, aunque es soportada por diferentes caracteres. De acuerdo con los resultados del análisis filogenético de Fielitz (2004:627, Fig. 2), la familia Enchodontidae es monofilética con base a la ausencia del interopérculo y por presentar un solo diente en el hueso dermopalatino. Luego, para completar la diagnosis revisada de la familia, este autor adiciona la longitud del hueso dermopalatino igual o menor respecto al diente único. A su vez, el estudio de Silva y Gallo (2011) tiene como única sinapomorfía de Enchodontidae la presencia de escudos dorsales.

Figura 3. Ejemplares reconocidos como Enchodontoidei y potenciales miembros de Enchodontidae. A) Ejemplar único preservado en parte. En este ejemplar no se preservó el esqueleto ni la aleta caudal, así como la porción posterior del cuerpo. B) Ejemplar preservado en parte y contra parte. Aquí se expone el lado más completo del espécimen, el cual carece de la aleta caudal. Escala igual a 1 cm.

La propuesta de Fielitz (2004) señala que *Rharbichthys*, *Palaeolycus*, *Eurypholis*, *Saurorhamphus*, y *Enchodus* componen a Enchodontidae. El autor sinonimizó a *Parenchodus* con *Enchodus*, tomando como referencia su posición filogenética. Por su parte, la propuesta de Silva y Gallo (2011) también reconoce cinco géneros integrantes de Enchodontidae. No obstante, *Rharbichthys* se excluye de Enchodontidae y se recupera como grupo hermano de Dercetidae. De esta manera, los miembros restantes de Enchodontidae en esta propuesta son los mismos reportados por Fielitz (2004) con la diferencia de que *Parenchodus* se mantiene y se reconoce como una rama independiente de *Enchodus* que se recupera como grupo hermano de *Palaeolycus*.

Indicios de la posición filogenética problemática de *Rharbichthys* se observan en el estudio de Fielitz y González-Rodríguez (2010:1349, Fig.11), trabajo que a su vez se basa en los datos de Fielitz (2004). En sus resultados, estos autores recuperaron a *Rharbichthys* formando una politomía con *Cimolichthys*, y estos en la base de Enchodontidae. No obstante, los autores de este estudio no discutieron las implicaciones de este cambio en la composición de Enchodontidae.

Con el estudio de los taxa descubiertos en la cantera El Chango, *Unicachichthys multidentata* y *Veridagon avendanoi*, las relaciones internas Enchodontidae en la propuesta de Fielitz (2004) no se han visto sustancialmente modificadas, de modo que estos taxa son recuperados en la base de Enchodontidae (ver Díaz-Cruz et al., 2016, 2019c). Los principales cambios luego de la inclusión de estos taxa recaen principalmente en las sinapomorfías que soportan la naturalidad de Enchodontidae. Con la inclusión de *Unicachichthys multidentata*, Enchodontidae se recupera como un grupo monofilétco con base a la ausencia del hueso supraorbital (Díaz-Cruz et al., 2016:146, Fig. 13). En tanto que la inclusión de *Veridagon*

avendanoi en el análisis recupera esta misma sinapomorfía y se adicionan la presencia de una barra de reforzamiento sobre el opérculo y ornamentación en la forma de tubérculos alineados en crestas sobre el opérculo y subopérculo (ver Díaz-Cruz et al., 2019c:280, Fig. 7B). Hasta la fecha, los mayores cambios a las relaciones internas de Enchodontidae están dadas por la integración de *Vegrandichthys coitecus* en el análisis. A diferencia de los taxa previamente mencionados, que se recuperan en posición basal de Enchodontidae, *V. coitecus* se recupera como el grupo hermano del clado formado por *Eurypholis* + *Saurorhamphus*, en la posición basal de Eurypholinae (ver Díaz-Cruz et al. 2020:16, Fig. 7). Respecto a los caracteres que soportan la naturalidad de Enchodontidae, la ausencia del hueso supraorbital y el patrón de ornamentación en los huesos dérmicos también son recuperados como en la propuesta de Díaz-Cruz et al. (2019c). En adición, se recupera la presencia de proyecciones anteroventrales de la mandíbula y la aleta pélvica ubicada en o posterior al nivel de la aleta dorsal (Díaz-Cruz et al., 2020:16, Fi. 7). Respecto a la posición filogenética y reconocimiento del género *Parenchodus* como un taxón distinto de *Enchodus*, los resultados de los estudios aquí realizados no son consistentes en su posición. De esta forma vemos que, con la integración de los encodóntidos de El Chango en los datos propuestos por Fielitz (2004), el género *Parenchodus* ha sido recuperado como integrante de un clado monofilético junto con el resto de las especies de *Enchodus* (Díaz-Cruz et al., 2016:146, Fig.13; Díaz-Cruz et al., 2019b:280, Fig. 7B), pero también como el grupo hermano del clado monofilético formado exclusivamente por las especies de *Enchodus* (Díaz-Cruz et al., 2020:16, Fig. 7).

La inclusión de los encodóntidos mexicanos en la propuesta filogenética de Silva y Gallo (2011) ha resultado más controversial. La reconstrucción filogenética con los datos de estos autores recuperó a *Unicachichthys multidentata* como el grupo basal de Enchodontidae y la

única sinapomorfía que soporta la monofilia del grupo fue la presencia de los escudos dorsales (Díaz-Cruz et al., 2016:146, Fig.13), la misma que fue reportada previo a la inclusión de este taxón. Posteriormente, con la matriz modificada por Alvarado-Ortega y Díaz-Cruz (2021) observaron las mayores modificaciones en la estructura del grupo. Con la adición de *Veridagon* y *Vegrandichthys*, junto con un nuevo taxón Dercetidae, la reconstrucción filogenética resultante presentó una politomía entre *Unicachichthys*, *Parenchodus* y *Enchodus*, de la que ramifican secuencialmente *Palaeolycus* y *Veridagon*, y al final se localiza un clado en politomía conformado por *Vegrandichthys*, *Saurorhamphus* y *Eurypholis*. La sinapomorfía que soporta la naturalidad de Enchodontidae es nuevamente la presencia de los escudos dorsales, pero se adiciona la presencia de dientes con diferente tamaño en la mandíbula superior (Alvarado-Ortega y Díaz-Cruz, 2021, Mat.Sup. C., Fig 1.).

El caso de las relaciones internas de Dercetidae es particularmente interesante. La familia contaba con una reconstrucción filogenética propia (Gallo et al., 2005b), en la que el grupo se recuperaba como monofilético soportado en dos sinapomorfías: espinas neurales reducidas y la ausencia de cresta longitudinal en el opérculo. Posteriormente, Silva y Gallo (2011) seleccionaron algunas hipótesis de homología primaria de Dercetidae de ese estudio y las combinaron con otras provenientes de diferente reconstrucciones filogenéticas con el objetivo de realizar un análisis más incluyente y propio de las formas fósiles de Enchodontoidei. Este trabajo confirma la naturalidad de la familia Dercetidae, así como la presencia de espinas neurales reducidas como su única sinapomorfía. La monofilia de Dercetidae demostró ser consistente luego de la inclusión de *Candelarhynchus padillai* Vernygora et al. 2017, un dercétido de estratos Turonianos de Colombia, en la hipótesis filogenética de Enchodontoidei. Las características que dan soporte a la naturalidad de esta familia incluyen la sinapomorfía

única reportada por Silva y Gallo (2011), espinas neurales reducidas, en conjunto con una cabeza baja, hocico largo, hipurales fusionados y la presencia de escudos tripartitos en los flancos. A pesar de esto, la reconstrucción filogenética de Enchodontoidei colapsó casi completamente con la inclusión de *Hastichthys totonacus* Alvarado-Ortega y Díaz-Cruz 2020, proveniente de estratos Turonianos de Huehuetla, Puebla. El algoritmo de Máxima Parsimonia que resuelve a *H. totonacus* como grupo hermano de *H. gracilis*, también recupera la monofilia de Enchodontidae, aunque el resto de miembros de Enchodontoidei forman, en su mayoría, una politomía (Alvarado-Ortega y Díaz-Cruz, 2021:13, Fig. 11). El reconocimiento de *H. totonacus* como integrante de Dercetidae se fundamenta en que este taxón presenta las sinapomorfías indicadas por Vernygora et al. (2017), mencionadas anteriormente. Esto fue corroborado con el mapeo de las espinas neurales y del contacto entre los hipurales en la reconstrucción filogenética que resolvió las relaciones internas de Dercetidae y que fue obtenida con el algoritmo de Máxima Parsimonia de Pesos Implicados (ver Alvarado-Ortega and Díaz-Cruz, 2021; Mat.Sup. C., Fig. 2). Además, el trabajo de estos autores es importante porque permitió reconocer y reasignar a *Rhynchodercetis regio* Blanco y Alvarado-Ortega 2006 como *Hastichthys regio* con base en características merísticas, morfológicas y morfométricas que revelan mayor afinidad con *Hastichthys* en lugar de *Rhynchodercetis* (ver Alvarado-Ortega y Díaz-Cruz, 2021:12, Cuadro 3).

La existencia de dos propuestas filogenéticas de los encodóntidos ha resultado hasta cierto punto problemática. A pesar de que tanto Dercetidae como Enchodontidae se recuperan normalmente como clados monofiléticos, el estudio de Alvarado-Ortega y Díaz-Cruz (2021) muestra que la reconstrucción filogenética basada en los datos de Silva and Gallo (2011) y empleando el algoritmo de Máxima Parsimonia estándar, no es tan robusta como se creía.

Antes de este descubrimiento, un intento por robustecer la propuesta filogenética de Fielitz (2004) fue ejecutada por Holloway et al. (2017). Estos autores adicionaron algunas de las hipótesis de homología primaria del trabajo de Silva y Gallo (2011) a la matriz de Fielitz (2004). Sin embargo, redundancia de datos fue detectada posteriormente por Díaz-Cruz et al. (2020). Entre los caracteres adicionados, el carácter 56 de Silva y Gallo (2011) hace referencia a la forma del preopérculo. De acuerdo con estos autores, este hueso puede adoptar una forma de "L" [0], triangular [1], forma de luna creciente [2], de bacilo [3], o de pipa [4]. Fielitz (2004) también notó esta variación y su potencial para contener señal filogenética; para él, la información contenida en el preopérculo estaba representada por dos caracteres: 45) la porción ventral del preopéculo: [0] dirigida anteriormente; [1] miembro posterior pequeño; [2] se amplía anterior y posteriormente; y por 46) borde posterior de la porción ventral del preopérculo: [0] redondeado; [1] se estrecha hasta un punto; [2] se estrecha hasta un punto y forma una espina. Ante esta situación, los caracteres arriba mencionados se reformularon en siete nuevas hipótesis de homología primaria. En dichas propuestas se aborda la forma general del preopérculo, pero también se separan elementos que se consideran independientes, tales como las proyecciones anteriores o posteriores de la porción ventral del hueso (ver Díaz-Cruz et al., 2020; M at. sup. II:2). Este ejercicio tomó en consideración las construcciones problemáticas de caracteres para evitarlas y se recurrió al uso de codificación reductiva que apela al "*token*" inaplicable ("-") para no otorgar estados de carácter a los taxones que lógicamente no contienen un valor del rasgo en particular, porque este depende de la presencia de otro carácter (Brazeau, 2011; Simões et al., 2016; Brazeau et al., 2019).

La revisión a detalle de las hipótesis de homología primaria en las reconstrucciones filogenéticas de Enchodontidae, evidenció que, por lo regular, se emplea codificación

compuesta o tradicional (Wilkinson, 1995; Simões et al., 2016). No obstante, en ocasiones, una misma hipótesis de homología primaria evalúa diferentes atributos, con lo que se incumple el prerrequisito de construcción de caracteres para análisis filogenéticos que requiere que los caracteres sean independientes unos de los otros (Farris, 1983). Ante esto, se hace necesaria una urgente reevaluación de todas las hipótesis de homología primaria empleadas para la reconstrucción filogenética de los encodóntidos. Motivos adicionales para realizar dicha evaluación proceden de la necesidad de incluir la variación morfológica exhibida por los taxa mexicanos. Esto implica que las hipótesis de homología primaria planteadas hasta ahora o sus estados de carácter, no reflejen algunos de los atributos morfológicos reconocidos en los nuevos taxones. Ejemplos de esto se pueden observar en el caso de *Vegrandichthys coitecus*, taxón que exhibe múltiples crestas engrosadas corriendo lateralmente el opérculo, preopérculo con un borde posterior tuberculado, y una barra de reforzamiento sobre la superficie externa del cleitro (Díaz-Cruz et al., 2020:9 Fig. 4).

Conscientes del desafío que representa entender y discretizar la variación morfológica en un grupo tan diversificado como los encodóntidos, Díaz-Cruz et al. (2021) presentaron un análisis de morfometría geométrica para algunas de las estructuras más variables en el grupo. Estos autores notaron que el formato del opérculo no es exclusivo de algún género en particular, pudiéndose encontrar la misma forma en diferentes taxones de encodóntidos. Este trabajo procura fundamentar y sentar las bases para futuras propuestas de homología primaria y contrarrestar el bajo soporte que algunos clados presentan en la reconstrucción filogenética de Enchodontidae (ver Fielitz, 2004:630). Alternativamente, se elaboraron reconstrucciones filogenéticas de Enchodontidae con diferentes criterios de optimalidad, pues se ha documentado que, criterios como Inferencia Bayesiana (IB) o Máxima Parsimonia de Pesos

Implicados (MPPI), se desempeñan mejor ante elevados niveles de homoplasia y datos faltantes (O'Reilly et al., 2016; Goloboff et al., 2017; Puttick et al., 2019; Smith, 2019, entre otros). Los diferentes criterios de optimalidad coinciden en recuperar a la familia Enchodontidae como monofilética; sin embargo, bajo IB, las relaciones internas son colapsadas o recuperadas en una organización muy diferente respecto a las relaciones obtenidas con Máxima Parsimonia o Máxima Parsimonia de Pesos Implicados (Díaz-Cruz et al., 2019c, 2020). En este sentido, dicha inconsistencia podría atribuirse a que IB resulta ser más sensible a los niveles de homoplasia y datos faltantes de los datos analizados, pero mayor investigación en este sentido es requerida. Por otra parte, el único clado de Enchodontidae que siempre se ha mantenido constante, sin importar el criterio de optimalidad empleado, es el de la Subfamilia Eurypholinae. Al respecto, se puede asumir que la naturalidad de este grupo está fuertemente apoyada por los datos, y que sus niveles de homoplasia son bajos, dado que conjuntos de datos con baja homoplasia, recuperan las mismas relaciones sin importar el criterio de optimalidad que se emplee para la reconstrucción filogenética (Puttick et al., 2019).

Para el caso particular del análisis de ajuste estratigráfico de la filogenia de Enchodontidae, se pone en evidencia cómo la inclusión de *Enchodus zimapanensis* disminuye el ajuste estratigráfico de la topología (Díaz-Cruz et al., 2020). Este fenómeno puede relacionarse a la falta de inclusión de encodóntidos de otras latitudes (Díaz-Cruz et al., 2019a), a la necesidad de incluir linajes fantasmas que soporten la posición derivada de esta especie (Cavin et al., 2012), de las más antiguas de la familia, y ultimadamente a la necesidad de revisar las homologías primarias propuestas para la reconstrucción filogenética del grupo como discutido anteriormente. Por otro lado, las calibraciones temporales de Enchodontidae aportan evidencia para sugerir que este grupo podría seguir la ley del crecimiento filético del

tamaño corporal o ley de Cope, con base en el registro de las especies de menor tamaño corporal localizadas en el Cretácico Medio, hasta aquellas especies al final del Cretácico que alcanzaron tallas entorno del metro y medio de longitud (Díaz-Cruz et al., 2021); características que los predispusieron a la extinción selectiva del Cretácico/Paleógeno que afectó principalmente a los peces depredadores grandes (Friedman, 2009; Guinot y Cavin, 2016). El empleo de diferentes criterios de optimalidad para la reconstrucción filogenética, el análisis morfométrico de la variación morfológica y la evaluación del ajuste estratigráfico de las filogenias obtenidas en Enchodontidae han revelado y confirmado aspectos evolutivos dentro del grupo de los que apenas se contaba con aproximaciones.

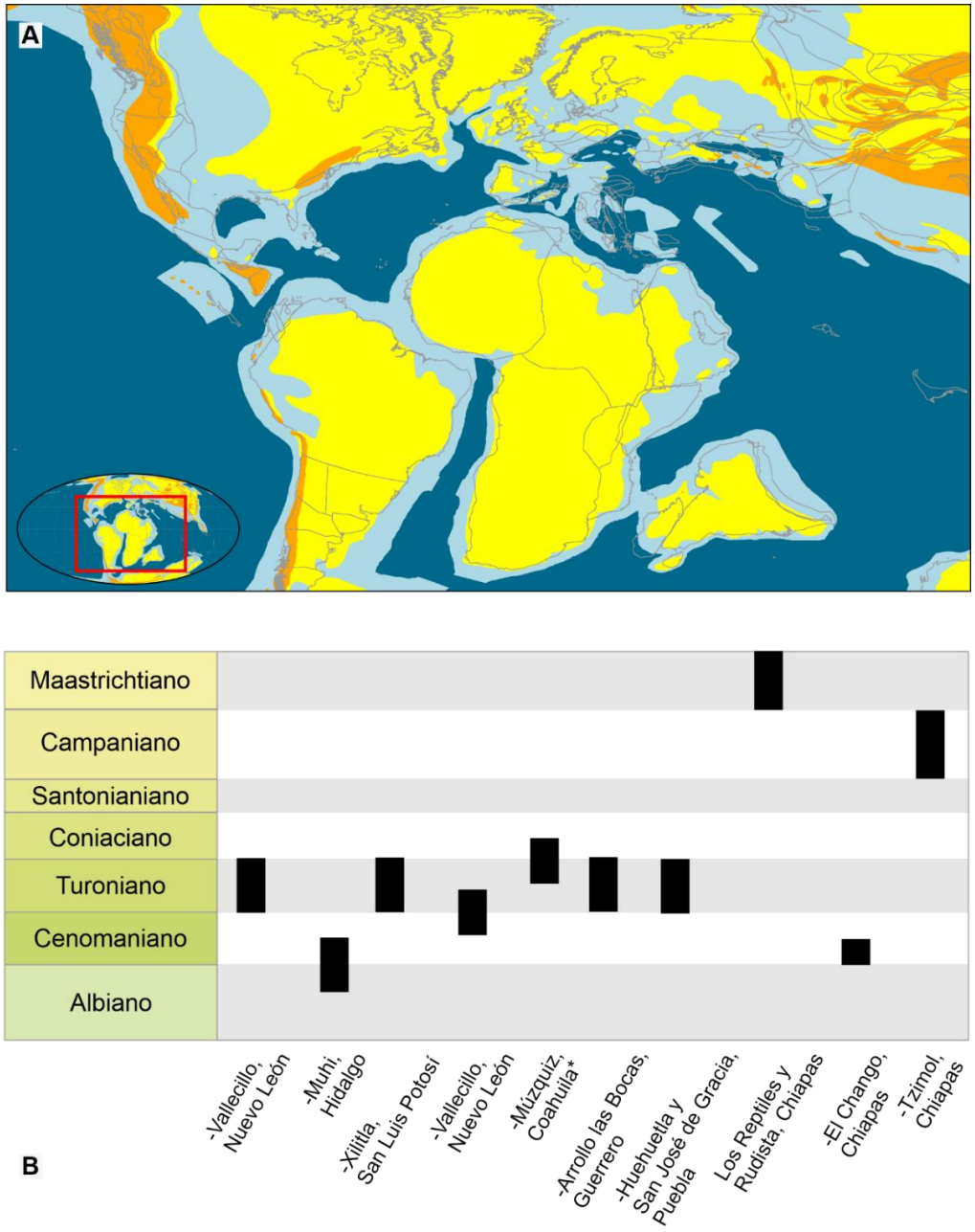

Figura 4. Distribución continental durante el Cretácico Medio en el mundo y temporalidad de los afloramientos mexicanos. A). Los mares epicontinentales durante el Cretácico Medio están indicados por la coloración celeste. Imagen tomada de Cao et al. (2017). B) Calibración temporal de los afloramientos mexicanos que cuentan con registros de encodóntidos.

Implicaciones biogeográficas

Como se indicó en la primera parte de este capítulo, la riqueza de encodontoides a nivel genérico encontrados en la localidad de El Chango ha igualado e incluso superado la riqueza genérica reportada en localidades de edad similar de otras latitudes, incluso de aquellas con una larga historia de trabajo paleontológico y décadas de explotación (Forey et al., 2003). Durante el Cretácico Tardío, el territorio mexicano ocupó un área en la cual los Enchodontoidei encontraron las condiciones ideales para habitar y reproducirse, así lo evidencian los resultados reportados en el presente trabajo. Se observan taxa a nivel genérico que son exclusivos de esta región como *Unicachichthys*, *Veridagon* o *Vegrandichthys*, pero también se reconocen representantes identificados en otras latitudes como los géneros *Apuliadercetis*, *Enchodus*, *Hastichthys* o *Saurorhamphus* de la región de Europa y Medio Oriente (Chalifa, 1985, 1989; Forey et al., 2003; Taverne, 2006).

La similitud de faunas entre distintas localidades Cenomanianas puede ser atribuía a la semejanza de los ambientes de depósito. De esta manera vemos que, los sedimentos cenomanianos de Ein-Yabrud en Israel se depositaron en un ambiente marino, somero, restringido, parcialmente bordeado y en condiciones de baja energía (Chalifa, 1985). A su vez, los sedimentos cenomanianos de Namoura en Líbano, que contienen peces, fueron depositados en pequeñas cuencas interpretados como dolinas formadas por la actividad tectónica del piso marino en el margen exterior de una plataforma continental; en estos sedimentos se han observado, además de peces, crustáceos, equinoideos, reptiles marinos e incluso plantas terrestres (Forey et al., 2003). De manera similar en El Chango, localidad del Cenomaniano temprano, donde se han reportado especies animales marinas y vegetales tanto de origen continental como marino y cuyos depósitos se han relacionado a un estuario o laguna poco

profunda y marginal con base a su proximidad geográfica a la localidad Aptiana de El Espinal (Vega et al., 2006; González-Ramírez et al., 2013; Huerta-Vergara et al., 2013; Moreno-Bedmar et al., 2014; Heard et al., 2020; Bruce et al., 2021).

Si bien es cierto que localidades cretácicas con ambientes similares compartieron taxones, estas regiones se ubicaban geográficamente distantes en la conformación del antiguo mar de Tethys para el Cretácico Tardío. Es este contexto, aunque los encodóntidos son abundantes en el Cretácico, poco se ha estudiado desde el punto de vista paleobiogeográfico, y los estudios que existen a la fecha se basan principalmente en datos obtenidos de afloramientos cretácicos de América del Norte (Estados Unidos principalmente), Europa o Medio Oriente. Forey et al. (2003), en una comparación entre faunas de diversas localidades tethyanas, notaron que los Aulopiformes (Enchodontoidei) a nivel genérico y específico son el grupo más abundante en Jerusalén; aunque este trabajo no analiza específicamente la distribución del grupo, representa una aproximación a su estudio en un nivel geográfico más incluyente.

Posteriormente, en la propuesta filogenética de Enchodontidae elaborada por Fielitz (2004; 630. fig 7), se distinguió una relación entre especies de *Enchodus* del Tethys central con especies del Tethys occidental. Este autor observó que algunas de las especies más primitivas de *Enchodus* + *Parenchodus* se localizaban en Medio Oriente, y que las formas derivadas se encontraban en Europa y América del Norte, situación que lo llevó a sugerir que el género *Enchodus* surgió en el Tethys central o actual Medio Oriente y posteriormente se originó un grupo de especies de *Enchodus* norteamericanas. Adicional a esto, Silva y Gallo (2007) distinguen dos áreas de endemismo para los miembros de Enchodontoidei durante el Cenomaniano; una de ellas comprendida por los territorios que hoy conforman por Marruecos

y el sureste de Italia, mientras que la segunda se integra por territorios actuales del Líbano e Israel.

Un enfoque alternativo para el estudio de la distribución de los encodóntidos fue propuesto por Cavin (2008) con base en los trabajos filogenéticos publicados por Fielitz (2004) para encodóntiodos y de Gallo et al. (2005) y Taverne (2005a y b) para dercétidos. De acuerdo a este autor, existió un evento vicariante en el Cretácico Medio que involucra a *Enchodus venator* del Norte de África con *E. shumardi* de América del Norte. Este mismo autor reconoce para el Cretácico Tardío dos eventos vicariantes adicionales; el primero de ellos entre Europa y América del Norte, representado por *Enchodus gracilis* y un clado de formas derivadas de *Enchodus*. El segundo evento vicariante del Cretácico Tardío ocurre entre las mismas regiones, pero corresponde a las dos especies reconocidas de *Cimolichthys.* Adicionalmente, se identifica un evento de radiación para la familia Dercertidae. Más tarde, Cavin et al. (2012) ratifican la propuesta de vicarianza del Cretácico Medio, con la inclusión de la región de Italia; se reinterpreta el evento vicariante de *E. gracilis* de Europa, pero esta vez con respecto a *E. pretrosus* de América del Norte en el Cretácico Tardío e indican un evento vicariante adicional. Este último establecido entre las especies de *Enchodus* de Gavdos, Grecia, con *E. dirus* que tiene presencia en el margen occidental del Tethys (proto Atlántico Norte) y en el Mar Interior de Norte América, confirmando un vínculo entre las especies de encodóntidos de Europa con las de América de Norte.

Recientemente, Silva y Gallo (2016) identificaron un trazo generalizado de encodóntidos para el Cenomaniano que vincula la región del Noreste de África con Italia, a la que le asociaron corrientes oceánicas. En tanto que, para las asociaciones paleoictiológicas del Cretácico Medio (Albiano-Cenomaniano), Amalfitano et al. (2020) notaron un patrón de relación Oriente-

Occidente involucrando a África y América del Sur, así como los dominios central y occidental del Tethys, en acuerdo con la apertura del Océano Atlántico en dirección sur a norte (Cavin, 2008).

Los trabajos arriba citados coinciden en señalar que, la actual región del Medio Oriente es una zona rica y diversa en cuanto a la presencia de encodóntidos. También, es notable la relación encontrada entre algunas de estas regiones con áreas de Europa, como Inglaterra o Italia, o incluso con América del Norte. Esta última merece ser especialmente destacada, ya que nos sugiere una conexión próxima entre la región central del Tethys con su extremo occidental o proto-Atlántico Norte. Esta conexión sugiere la existencia de eventos vicariantes y/o de migración de ictiofaunas en dirección Este-Oeste. Este fenómeno ha sido documentado para el Cretácico Temprano y Cretácico Medio con belemnites y bivalvos que migraron desde la porción central del Tethys (actual medio Oriente) y Tethys europeo hasta el extremo occidental del proto Océano Atlántico Norte por medio del corredor Hispánico (Zell et al., 2013; Radulović et al., 2019). De la misma forma, el empleo de esta ruta de migración está documentada para diversos grupos de peces fósiles, por ejemplo Elopiformes o Gonorynchiformes durante el Cretácico Medio (Amaral y Brito, 2012; Alves et al., 2020). La formación de este corredor pudo haber desempeñado un papel preponderante para que las especies de encodontoides de Medio Oriente y de Europa originaran a los taxa de América, tal como ha sido sugerido por varios autores (Fielitz, 2004; Cavin, 2008; Cavin et al., 2012). Contrario a esta propuesta, los resultados del presente trabajo señalan que el origen de Enchodontidae pudo haberse localizado en el extremo occidental del mar de Tethys. De esta forma, vemos que los géneros *Unicachichthys* y *Veridagon* se reconocen como los grupos más basales de Enchodontidae en repetidas reconstrucciones filogenéticas (Díaz-Cruz et al., 2016, 2019c, 2020). De manera similar,

Vegrandichthys es recuperado como el miembro basal de la subfamilia Eurypholinae (Díaz-Cruz et al., 2020). La temporalidad de los estos taxones también apoya esta hipótesis, puesto que esos taxa han sido rescatados de sedimentos del Cenomaniano Temprano, de los más jóvenes entre todos los miembros de la familia (Díaz-Cruz et al., 2021). Asimismo, el reporte de *Enchodus zimapanensis* de estratos Albianos-Cenomanianos en el territorio mexicano extiende el registro formal del género *Enchodus* para finales del Cretácico Inferior (Fielitz y González-Rodríguez, 2010); aunque debe considerarse con reserva dada su posición derivada en la filogenia. Del mismo modo, los reportes del género *Saurorhamphus* de la localidad Aptiana de El Espinal, en Chiapas, que extienden la temporalidad del género al Cretácico Inferior (Alvarado-Ortega et al., 2009; Heard et al., 2020). La distinción de algunos de los encodóntidos más antiguos en el extremo occidental del Tethys junto con su posición basal en reconstrucciones filogenéticas no parece ser un caso aislado de este grupo. Este patrón también es documentado por otros taxa de peces primitivos y antiguos, tal es el caso de algunos Crossognathiformes (Arratia et al., 2018) o Acantomorfos como *Zoqueichthys carolinae* miembro Lampripterygii o *Choichix alvaradoi*, integrante de Acanthopterygii (Alvarado-Ortega y Than-Marchese, 2012; Cantalice et al., 2021). Lejos de identificar y confirmar un patrón de migración de las asociaciones paleoictiológicas en un solo sentido, nuestros datos se suman a propuestas previas (ver Arratia et al., 2004) para indicar que el corredor Hispánico desempeñó un papel clave en el intercambio de faunas entre los diferentes dominios del Tethys. Particularmente, considerando la temporalidad y los resultados de las reconstrucciones filogenéticas de la familia Enchodontidae, es posible sugerir que ésta pudo tener origen en el extremo occidental del Tethys, desde donde se dispersó a otras latitudes. El buen estado de preservación, la alta riqueza genérica y específica, así como la

temporalidad de los encodóntidos mexicanos, representan elementos esenciales para entender mejor las adaptaciones, relaciones evolutivas y biogeográficas que estos taxones desarrollaron.

LITERATURA CITADA

Alvarado-Ortega, J., Cantalice, K.M.C., Díaz-Cruz, J.A., Castañeda-Posadas, C., Zavaleta-Villareal, V. (2020a). Vertebrate fossils from the San José de Gracia quarry, a new Late Cretaceous marine fossil site in Puebla, Mexico. *Boletín de La Sociedad Geológica Mexicana*, 72(1), 1–21. https://doi.org/10.18268/BSGM2020v72n1a160819

Alvarado-Ortega, J., Cantalice, K.M.C., Martínez-Melo, A., García-Barrera, P., Than-Marchese, B.A., Díaz-Cruz, J.A., Barrientos-Lara, J.I. (2020b). Tzimol, a Campanian marine paleontological site of the Angostura Formation near Comitán, Chiapas, southeastern Mexico. *Cretaceous Research*, 107, 1–16. https://doi.org/10.1016/j.cretres.2019.104279

Alvarado-Ortega, J., Díaz-Cruz, J. A. (2021). *Hastichthys totonacus* sp. nov., a North American Turonian dercetid fish (Teleostei, Aulopiformes) from the Huehuetla quarry, Puebla, Mexico. *Journal of South American Earth Sciences*. https://doi.org/10.1016/j.jsames.2020.102900

Alvarado-Ortega, J., Than-Marchese, B. A. (2012). A Cenomanian aipichthyoid fish (Teleostei, Acanthomorpha) from America, *Zoqueichthys carolinae* gen. and sp. nov. from El Chango quarry (Cintalapa Member, Sierra Madre Formation), Chiapas, Mexico. *Revista mexicana de ciencias geológicas*, *29*(3), 735-748.

Alvarado-Ortega, J., Ovalles-Damián, E., Blanco-Piñón, A. (2009). *The fossil fishes from the Sierra Madre Formation, Ocozocoautla, Chiapas, Southern Mexico*. 12(2), 4A:22p. http://palaeo-electronica.org/2009_2/168/abstracts.html

Alvarado-Ortega, J., Cantalice, K.M.C., Barrientos-Lara, J. I., Díaz-Cruz, J. A., Than-Marchese, B.A. (2019). The huehuetla quarry, a Turonian deposit of marine vertebrates in the sierra norte of puebla, Central Mexico. *Palaeontologia Electronica*, 22(1). https://doi.org/10.26879/921

Alves, Y. M., Alvarado-Ortega, J., Brito, P. M. (2020). †*Epaelops martinezi* gen. and sp. nov. from the Albian limestone deposits of the Tlayúa quarry, Mexico – A new late Mesozoic record of Elopiformes of the western Tethys. *Cretaceous Research*, 110, 104260. https://doi.org/10.1016/j.cretres.2019.104260

Amalfitano, J., Giusberti, L., Fornaciari, E., Carnevale, G. (2020). Upper cenomanian fishes from the bonarelli level (OAE2) of northeastern Italy. *Rivista Italiana Di Paleontologia e Stratigrafia*, 126(2), 261–314. https://doi.org/10.13130/2039-4942/13224

Amaral, C.R.L., Brito, P.M. (2012). A new chanidae (Ostariophysii: Gonorynchiformes) from the cretaceous of Brazil with affinities to Laurasian gonorynchiforms from Spain. *PLoS ONE*, 7(5), 1–9. https://doi.org/10.1371/journal.pone.0037247

Arratia, G., González-Rodríguez, K.A., Hernández-Guerrero, C. (2018). A new pachyrhizodontid fish (Actinopterygii, Teleostei) from the Muhi Quarry (Albian-Cenomanian), Hidalgo, Mexico. *Fossil Record*, 21(1), 93–107.

Arratia, G., Scasso, R.A., Kiessling, W. (2004). Late Jurassic Fishes from Longing Gap, Antarctic Peninsula. *Journal of Vertebrate Paleontology*, 24(1), 41–55.

Bannikov, A.F., Bacchia, F. (2005). New species of the Cenomanian Eurypterygii (Pisces,

Teleostei) from Lebanon. *Paleontological Journal*, 39(5), 514–522.

Blanco-Piñón, A., Porras-Múzquiz, H., Vega, F., González-Rodríguez, K.A. Alvarado-Ortega, J. (2004). Múzquiz, Coahuila: a new fossiliferous locality, northern Mexico. *IX Congreso Nacional de Paleontología, Tuxtla Gutiérrez, Chiapas: Sociedad Mexicana de Paleontología*, 23.

Blanco, A., Alvarado-Ortega, J. (2006). *Rhynchodercetis regio* sp. nov., A new decertid fish (Teleosteir: Aulopuformes) from Vallecillo, Nuevo León state, Northeastern Mexico. *Jornal of Vertebrate Paleontology*, 26(3), 552–558.

Brazeau, M. D. (2011). Problematic character coding methods in morphology and their effects. *Biological Journal of the Linnean Society*, 104(3), 489–498.

Brazeau, M. D., Guillerme, T., Smith, M. R. (2019). An algorithm for Morphological Phylogenetic Analysis with Inapplicable Data. *Systematic Biology*, 68(4), 619–631. https://doi.org/10.1093/sysbio/syy083

Bruce, N. L., Serrano-Sánchez, M.L., Carbot-Chanona, G., Vega, F. J. (2021). New species of fossil Cirolanidae (Isopoda, Cymothoida) from the Lower Cretaceous (Aptian) Sierra Madre Formation plattenkalk dolomites of El Espinal quarries, Chiapas, SE Mexico. *Journal of South American Earth Sciences*, 104743. https://doi.org/10.1016/j.jsames.2021.103285

Cantalice, K. M., Than-Marchese, B. A., Villalobos-Segura, E. (2021). A new Cenomanian acanthomorph fish from the El Chango quarry (Chiapas, south-eastern Mexico) and its implications for the early diversification and evolutionary trends of acanthopterygians. *Papers in Palaeontology*, 1–28. https://doi.org/10.1002/spp2.1359

Cao, W., Zahirovic, S., Flament, N., Williams, S., Golonka, J., Dietmar Müller, R. (2017). Improving global paleogeography since the late Paleozoic using paleobiology. *Biogeosciences*, 14(23), 5425–5439. https://doi.org/10.5194/bg-14-5425-2017

Cavin, L. (2008). Palaeobiogeography of Cretaceous bony fishes (Actinistia, Dipnoi and Actinopterygii). In L. Cavin, A. Longbottom, & M. Ritcher (Eds.), *Fishes and the Break-up of Pangea* (Vol. 295, pp. 165–183). London, Special Publications. https://doi.org/http://dx.doi.org/10.1144/SP295.11

Cavin, L., Alexopoulos, A., Piuz, A. (2012). Late Cretaceous (Maastrichtian) ray-finned fishes from the island of Gavdos, southern Greece, with comments on the evolutionary history of the aulopiform teleost *Enchodus*. *Bulletin de La Société Géologique de France*, 183(6), 561–572. https://doi.org/10.2113/gssgfbull.183.6.561

Chalifa, Y. (1985). *Saurorhamphus judeaensis* (Salmoniformes: Enchodontidae), a new longirostrine fish from the cenomanian of Ein-Yabrud, near Jerusalem. *Journal of Vertebrate Paleontology*, 5(3), 181–193. https://doi.org/10.1080/02724634.1985.10011857

Chalifa, Y. (1989). New species of *Enchodus* (Pisces: Enchodontoidei) from the lower Cenomanian of Ein-Yabrud, Israel. *Journal of Paleontology*, 63(3), 356–364. https://doi.org/10.1017/S0022336000019521

Coelho, P. M. (2004). *Revisão sistemática dos Enchodontidae (Euteleostei: Aulopiformes) do*

Brasil. Universidade Federal do Rio de Janeiro.

Davis, M.P., Fielitz, C. (2010). Estimating divergence times of lizardfishes and their allies (Euteleostei: Aulopiformes) and the timing of deep-sea adaptations. *Molecular Phylogenetics and Evolution*, 57(3), 1194–1208. https://doi.org/10.1016/j.ympev.2010.09.003

Díaz-Cruz, J. A., Alvarado-Ortega, J. (2018). A new enchodontid fish *Enchodus*-like from Cenomanian deposits from the El Chango quarry (Cintalapa member, Sierra Madre formation), Chiapas, Mexico. *78th Annual Meeting, Society of Vertebrate Paleontology*, 116.

Díaz-Cruz, J. A., Alvarado-Ortega, J., Bernard, E. (2019a). Phylogenetic implications of two enchodontids species (Enchodontidae: Aulopiformes) from the Middle East: Researching on the global evolutive patterns of the enchodontid fishes. *Paleontología Mexicana*, 5, 24.

Díaz-Cruz, J. A., Alvarado-Ortega, J., Carbot-Chanona, G. (2016). The Cenomanian short snout enchodontid fishes (Aulopifomes, Enchodontidae) from Sierra Madre Formation, Chiapas, southeastern Mexico. *Cretaceous Research*, 61, 136–150. https://doi.org/10.1016/j.cretres.2015.12.026

Díaz-Cruz, J. A., Alvarado-Ortega, J., Carbot-Chanona, G. (2019b). Corrigendum to "*Dagon avendanoi* gen. and sp. nov., an Early Cenomanian Enchodontidae (Aulopiformes) fish from the El Chango quarry, Chiapas, southeastern Mexico." *Journal of South American Earth Sciences*, 91, 272–284. https://doi.org/10.1016/j.jsames.2019.102314

Díaz-Cruz, J. A., Alvarado-Ortega, J., Carbot-Chanona, G. (2019c). *Dagon avendanoi* gen. and sp. nov., an Early Cenomanian Enchodontidae (Aulopiformes) fish from the El Chango quarry, Chiapas, southeastern Mexico. *Journal of South American Earth Sciences*, 91, 272–284. https://doi.org/10.1016/j.jsames.2019.01.014

Díaz-Cruz, J. A., Alvarado-Ortega, J., Giles, S. (2020). A long snout enchodontid fish (Aulopiformes: Enchodontidae) from the early cretaceous deposits at the el chango quarry, chiapas, southeastern mexico: A multi-approach study. *Palaeontologia Electronica*, 23(2), 1–27. https://doi.org/10.26879/1065

Díaz-Cruz, J. A., Alvarado-Ortega, J., Ramírez-Sánchez, M. M., Allington-Jones, L., Graham, M. (2021). Phylogenetic Morphometrics , Geometric Morphometrics and the Mexican fossils to understand evolutionary trends of Enchodontid fishes [Manuscrito sometido para publicación]. *Journal of South American Earth Sciences*.

Farris, J. S. (1983). The logical basis of phylogenetic analysis. *Advances in Cladistics*, 1–36. http://www.reocities.com/Hollywood/makeup/5023/Farris1983.pdf

Fielitz, C. (2004). The phylogenetic relationships of the †Enchodontidae (Teleostei: Aulopiformes). In G. Arratia, M. V. H. Wilson, & R. Cloutier (Eds.), *Recent Advances in the Origin and Early Radiation of Vertebrates* (pp. 619–634).

Fielitz, C., Gonzalez-Rodríguez, K. (2008). A new species of *Ichthyotringa* from the El Doctor Formation (Cretaceous), Hidalgo, Mexico. In G. Arratia, H.-P. Schultze, & M. V. H. Wilson (Eds.), *Mesozoic Fishes 4 - Homology and Phylogeny* (pp. 373–388).

Fielitz, C., González-Rodríguez, K. A. (2010). A new species of *Enchodus* (Aulopiformes: Enchodontidae) from the Cretaceous (Albian to Cenomanian) of Zimapán, Hidalgo, México. *Journal of Vertebrate Paleontology*, 30(5), 1343–1351. https://doi.org/10.1080/02724634.2010.501438

Forey, P. L., Yi, L., Patterson, C., Davies, C. E. (2003). Fossil fishes from the cenomanian (Upper Cretaceous) of Namoura, Lebanon. *Journal of Systematic Palaeontology*, 1(4), 227–330. https://doi.org/10.1017/S147720190300107X

Friedman, M. (2009). Ecomorphological selectivity among marine teleost fishes during the end-Cretaceous extinction. *Proceedings of the National Academy of Sciences*, 106(13), 5218–5223. https://doi.org/10.1073/pnas.0808468106

Gallo, V., Silva, H.M.A., Figueiredo, F.J. (2005a). The interrelationships of Dercetidae (Neotelesostei, Aulopiformes). In F. J. Poyato-Ariza (Ed.), *Fourth Internacional Meeting on Mesozoic Fishes – Systematics, Homology, and Nomenclature, Extended Abstracts, Miraflores de la Sierra, Madrid* (pp. 101–104).

Gallo, V., Figueiredo, F. J.., Silva, H.M.A. (2005b). Análise Filogenética Dos Dercetidae. *Arquivos Do Museu Nacional, Rio de Janeiro*, 63(2), 329–333.

Giersch, S. (2014). *Die Knochenfische der Oberkreidezeit in Nordostmexiko: Paläobiogeographie und Paläoökologie INAUGURAL – DISSERTATION Diplom-Geoökologe Samuel Giersch*.

Giersch, S., Frey, E., Stinnesbeck, W., González-González, A. H. (2008). Fossil fish assemblages of northeastern Mexico: New evidence of mid Cretaceous actinopterygian radiation. *6th Meeting of the European Association of Vertebrate Palaeontologists*, 43–45.

Goloboff, P. A., Torres, A., Arias, J. S. (2017). Weighted parsimony outperforms other methods of phylogenetic inference under models appropriate for morphology. *Cladistics*, 34(4), 407–437. https://doi.org/10.1111/cla.12205

González-Ramírez, I., Calvillo-Canadell, L., Cevallos-Ferriz, S. R. S. (2013). Coníferas curpresáceas fósiles de “El Chango”, Chiapas (Aptiano). *Paleontologia Mexicana*, 63, 24–31.

Guinot, G., Cavin, L. (2016). ‘Fish’ (Actinopterygii and Elasmobranchii) diversification patterns through deep time. *Biological Reviews*, 91(4), 950–981. https://doi.org/10.1111/brv.12203

Heard, R. W., Morales-Núñez, A. G., de Lourdes Serrano-Sánchez, M., Coutiño, M. A., Barragán, R., Vega, F. J. (2020). A new family, genus and species of Tanaidacea (Crustacea; Apseudomorpha) from the Lower Cretaceous (Aptian) of Chiapas, Mexico: Systematic revisions, including designation of two new Paleozoic families, and paleoenvironmental observations. *Journal of South American Earth Sciences*, 102(April), 102609. https://doi.org/10.1016/j.jsames.2020.102609

Holloway, W. L., Claeson, K. M., Sallam, H. M., El-Sayed, S., Kora, M., Sertich, J. J.-W., O’Connor, P. M. (2017). A new species of the neopterygian fish *Enchodus* from the Duwi Formation, Campanian, Late Cretaceous, Western Desert, central Egypt. *Acta Palaeontologica Polonica*, 62(3), 603–611. https://doi.org/10.4202/app.00331.2016

Huerta-Vergara, A. R., Calvillo-Canadell, L., Cevallos-Ferriz, S. R. S., Silva-Pineda, A. (2013). Pinaceae en el Cretácico del norte y sur de México: complemento a su escaso registro fósil. *Paleontología Mexicana*, 63, 66–78. http://www.ojs-igl.unam.mx/index.php/Paleontologia/article/view/158

Ifrim, C., Stinnesbeck, W., Frey, E. (2007). Upper cretaceous (Cenomanian-Turonian and Turonian-Coniacian) open marine plattenkalk deposits in NE Mexico. *Neues Jahrbuch Fur Geologie Und Palaontologie - Abhandlungen*, 245(1), 71–81. https://doi.org/10.1127/0077-7749/2007/0245-0071

Kriwet, J. (2003). Lancetfish teeth (Neoteleostei, Alepisauroidei) from the Early Cretaceous of Alcaine, NE Spain. *Lethaia*, 36(4), 323–332. https://doi.org/10.1080/00241160310006484

Moreno-Bedmar, J. A., Latil, J. L., Villanueva-Amadoz, U., Calvillo-Canadell, L., Cevallos-Ferriz, S. R. S. (2014). Ammonite age-calibration of the EL Chango Fossil-Lagerstätte, Chiapas state (SE Mexico). *Journal of South American Earth Sciences*, 56, 447–453. https://doi.org/10.1016/j.jsames.2014.09.022

Nelson, J. S. (1994). *Fishes of the world*. John Wiley & Sons.

O'Reilly, J. E., Puttick, M. N., Parry, L., Tanner, A. R., Tarver, J. E., Fleming, J., Pisani, D., Donoghue, P. C. J. (2016). Bayesian methods outperform parsimony but at the expense of precision in the estimation of phylogeny from discrete morphological data. *Biology Letters*, 12(6). https://doi.org/10.1098/rsbl.2016.0081

Porras-Múzquiz, H. G., Díaz-Cruz, J. A., Alvarado-Ortega, J., Cantalice, K. M. (2019). Evidencia de interacción depredador-presa en peces del género Enchodus (Enchodontidae: Aulopiformes) de localidades del Cretácico Superior Coahuila, Norte de México. *Paleontología Mexicana*, 5, 116.

Puttick, M. N., O'Reilly, J. E., Pisani, D., Donoghue, P. C. J. (2019). Probabilistic methods outperform parsimony in the phylogenetic analysis of data simulated without a probabilistic model. *Palaeontology*, 62(1), 1–17. https://doi.org/10.1111/pala.12388

Radulović, B. V., Ayoub-Hannaa, W., Fürsich, F. T., Bogićević, K., Nenadić, D., Jovanović, D. (2019). Taxonomy and palaeobiogeography of the early and middle Albian (Early Cretaceous) bivalves and brachiopods from central Serbia (Topola, Oplenac Hill). *Cretaceous Research*, 104. https://doi.org/10.1016/j.cretres.2019.07.005

Rana, R. S. (1990). Palaeontology and palaeoecology of the intertrappean (Cretaceous-Tertiary transition) beds of the peninsular India. *Journal of the Palaeontological Society of India*, 35, 105–120.

Rana, R. S., Kumar, K., Singh, H. (2004). Vertebrate fauna from the subsurface Cambay Shale (Lower Eocene), Vastan Lignite Mine, Gujarat, India. *Current Science*, 87(12), 1726–1733.

Silva, H. M. A., Gallo, V. (2007). Parsimony analysis of endemicity of enchodontoid fishes from the Cenomanian. *Carnets de Geologie*, 01, 1–8. https://doi.org/10.4267/2042/7146

Silva, H. M. A., Gallo, V. (2011). Taxonomic review and phylogenetic analysis of enchodontoidei (Teleostei: Aulopiformes). *Anais Da Academia Brasileira de Ciências*,

83(2), 483–511. https://doi.org/10.1590/s0001-37652011000200010

Silva, H. M. A., Gallo, V. (2016). Distributional patterns of enchodontoid fishes in the Late Cretaceous. *Cretaceous Research*, 65, 223–231. https://doi.org/10.1016/j.cretres.2016.03.009

Simões, T. R., Caldwell, M. W., Palci, A., Nydam, R. L. (2016). Giant taxon-character matrices: Quality of character constructions remains critical regardless of size. *Cladistics*, 33(2), 198–219. https://doi.org/10.1111/cla.12163

Smith, M. R. (2019). Bayesian and parsimony approaches reconstruct informative trees from simulated morphological datasets. *Biology Letters*, 15(2). https://doi.org/10.1098/rsbl.2018.0632

Taverne, L. (2005a). Les poissons crétacés de Nardo. 21. *Ophidercetis italiensis* gen. et sp. nov. (Teleostei, Aulopiformes, Dercetidae). Une solution ostéologique au probleme des genres *Dercetis* et *Benthesikyme* (= *Leptotrachelus*). *Bollettino Del Museo Civico Di Storia Naturale Di Verona*, 29, 55–79.

Taverne, L. (2005b). Les poissons crétacés de Nardo. 22. *Nardodercetis vandewallei* gen. et sp. nov. (Teleostei, Aulopiformes, Dercetidae). *Bollettino Del Museo Civico Di Storia Naturale Di Verona*, 29, 91–93.

Taverne L., (2006). Les poissons crétacés de Nardò. 24°. *Caudadercetis bannikovi* gen. et sp. nov. (Teleostei, Aulopiformes, Dercetidae). Considérations sur la phylogénie des Dercetidae. *Bolletino del Museo Civivo di Storia Naturale di Verona. Geologia Paleontogia Preistoria* 30: 27–48.

Tewari, V. C., Lokho, K., Kumar, K., Siddaiah, N.S. (2010). Late Cretaceous-Paleogene Basin Architecture and Evolution of the Shillong Shelf Sedimentation, Meghalaya, Northest India. *Journal, Indian Geological Congress*, 2(November), 61–73.

Vega, F. J., García-barrera, P., Perrilliat, C., Coutiño, M. A., Mariño-Pérez, R. (2006). *El Espinal , a new plattenkalk facies locality from the Lower Cretaceous Sierra Madre Formation , Chiapas , southeastern Mexico*. 323–333.

Vernygora, O., Murray, A. M., Luque, J., Ruge, M. L. P., Fonseca, M. E. P. (2018). A new Cretaceous dercetid fish (Neoteleostei: Aulopiformes) from the Turonian of Colombia. *Journal of Systematic Palaeontology*, 16(12), 1057–1071. https://doi.org/10.1080/14772019.2017.1391884

Wilkinson, M. (1995). A comparison of two methods of character construction. *Cladistics*, 11, 297–308.

Zell, P., Beckmann, S., Stinnesbeck, W., Flores-Ventura, J. (2013). First record of Duvalia ex. gr. Lata (Cephalopoda, coleoidea) from Mexico. *Boletin de La Sociedad Geologica Mexicana*, 65(3), 527–531. https://doi.org/10.18268/BSGM2013v65n3a7